Repurposing Matrine for the Treatment of Non-Alcoholic Fatty Liver Disease

A thesis submitted in fulfillment of the requirements for the degree of

Doctor of Philosophy

Ali Moosa Mahzari

Master of Laboratory Medicine, RMIT University, 2010

Bachelor of Laboratory Medicine, King Saud University, 2005

School of Health and Biomedical Sciences

College of Science, Engineering and Health

RMIT University

August 2018

DECLARATIONS

I certify that, except where due acknowledgement has been made, the work is that of the author alone; the work has not been submitted previously, in whole or in part, to qualify for any other academic award; the content of the thesis is the result of work that has been carried out since the official commencement date of the approved research programme; any editorial work, paid or unpaid, carried out by a third party is acknowledged; and, ethics procedures and guidelines have been followed.

Name: Ali Moosa Mahzari

Date: 23 August 2018

PUBLICATIONS

Publications/Manuscripts that have arisen as a direct result of this thesis:

1. **Ali Mahzari**, Xiao-Yi Zeng, Xiu Zhou, Songpei Li, Jun Xu, Wen Tan, Ross Vlahos, Stephen R Robinson & Ji-Ming Ye. Repurposing matrine for the treatment of hepatosteatosis and associated disorders in glucose homeostasis in mice. Acta Pharmacologica Sinica, 2018 Jul 6.doi: 10.1038/s41401-018-0016-8.

2. **Ali Mahzari**, Songpei Li, Xiao-Yi Zeng, Sherouk Fouda, Xiu Zhou, Dongli Li, Majid Alhomrani, Stephen R Robinson & Ji-Ming Ye. Matrine alleviates MCD-induced steatohepatitis associated with induction of heat shock proteins and inhibition of mTOR differently from metformin (submitted: JEP_2018_1927).

Publications/conference abstracts that have arisen in conjunction with this thesis:

A. Oral presentation conferences:

1. **Ali Mahzari**, Xiao-Yi Zeng, Xiu Zhou, Songpei Li, Jun Xu, Wen Tan, Ross Vlahos, Stephen R Robinson & Ji-Ming Ye. Matrine eliminates hepatosteatosis and glucose intolerance in high fructose-fed mice by suppressing ER stress associated *de novo* lipogenesis in the liver. 3rd World Congress on Hepatitis and Liver Diseases conference was held in Dubai (2016) 10-12 Oct.

2. **Ali Mahzari**, Songpei Li, Xiao-Yi Zeng, Sherouk Fouda, Xiu Zhou, Dongli Li, Majid Alhomrani, Stephen R Robinson & Ji-Ming Ye. The therapeutic effects of matrine for MCD-induced NASH are associated with upregulation of HSP72 and suppression of mTOR. 2nd International Conference on Obesity & Diabetes in Melbourne (2018) 14 – 15 May.

3. **Ali Mahzari**, Songpei Li, Xiao-Yi Zeng, Sherouk Fouda, Xiu Zhou, Dongli Li, Majid Alhomrani, Stephen R Robinson & Ji-Ming Ye. The therapeutic effects of matrine for MCD-induced NASH are associated with upregulation of HSP72 and suppression of mTOR. 2nd World Congress on Gastroenterology (2018) 23-25 July.

B. Poster presentation conferences:

1. **Ali Mahzari**, Xiao-Yi Zeng, Xiu Zhou, Songpei Li, Jun Xu, Wen Tan, Ross Vlahos, Stephen R Robinson & Ji-Ming Ye. Matrine eliminates hepatosteatosis and glucose intolerance in high fructose-fed mice by suppressing ER stress associated *de novo* lipogenesis in the liver. ADS Annual Scientific in Gold Coast (2016) 24-26 Aug.

2. **Ali Mahzari**, Xiao-Yi Zeng, Xiu Zhou, Songpei Li, Jun Xu, Wen Tan, Ross Vlahos, Stephen R Robinson & Ji-Ming Ye. Matrine eliminates hepatosteatosis and glucose intolerance in high fructose-fed mice by suppressing ER stress associated *de novo* lipogenesis in the liver. Biomed Link Conference in Melbourne (2016) 4th Nov.

3. Sherouk Fouda, Anwar Khan, **Ali Mahzari**, Stanley Chen, Ross Vlahos and Ji-Ming Ye. Does cigarette smoking exacerbate high fat induced hepatosteatosis?. 2nd World Congress on Gastroenterology (2018) 23-25 July.

4. Anwar Khan, Sherouk Fouda, **Ali Mahzari**, Stanley Chen, Ross Vlahos and Ji-Ming Ye. Cigarette exposure on exacerbates muscle insulin resistance in mice induced by high fat feeding. Australasian Diabetes Society in Adelaide (2018) 22-24 August.

ACKNOWLEDGEMENTS

First of all, I would like to express my gratitude to everybody at Lipid Biology and Metabolic Disease Laboratory Group. I have enjoyed the last 4 years of my life just working with all of them, without whom this thesis would not have been possible. Their support and friendship have made my life during this process much enjoyable. Appreciation words will not be enough for you guys, but my sincere gratitute goes to Prof. Jiming Ye, who has been there for every step of the way. His enthusiasm in science inspires me, and his insightful advice that made this work worthwhile. I also really appreciate Prof. Stephen Robinson, who has advised and encouraged me. From him, I see a great scientist role model, in the aspects of not only scientific achievements but also personality.

I would like to appreciate the intellectual input from my previous Associate Supervisor Dr. Leanne Stokes. Similarly, I have met a number of wonderful people in the lab, who made my research life at/outside the university full of joy: Dr. Xiaoyi Zeng, Dr. Xiu Zhou, Dr. Hao Wang, Dr. Summer, Dr. Songpei Li, Dr. Mary Zhang, Dr. Wala Alzharani, Sherouk Fouda and Anwar Khan. Dr Stanley Chan for blessing me with his true friendship. To Abdullah Hamadi, Gasim Dobie, Teerousha Mootin, Dr. Dawn Wong (to name a few) who were always supportive and who saved no effort in helping me out.

Many thanks to the School of Health and Biomedical Sciences for all the support provided during my PhD study. Also, I will always be indebted to my family, my mum and brothers and my lovely sister. Without them, I would not have been able to achieve anything I achieved today. Finally, I dedicate this thesis to the soul of my father (Moosa Mahzari), may Allah forgive and grant him paradise.

ABBREVIATIONS

AASLD: American Association for the Study of Liver Diseases

ACC: Acetyl-CoA carboxylase

ALT: Alanine transaminase

AMPK: AMP-activated protein kinase

Akt/PKB: Protein kinase B

AST: Aspartate transaminase

AUC: Area under the curve

BW: Body weight

CCl_4: Carbon tetrachloride

cDNA: Complementary DNA

ChREBP: Carbohydrate-responsive element binding protein

CPT: Carnitine palmitoyltransferase

DNL: *De novo* lipogenesis

DTT: DL-dithiothreitol

FAS: Fatty acid synthase

FAs: Fatty acids

GTT: Glucose tolerance test

H&E: Hematoxylin and eosin

HDL: High-density lipoprotein

HFD: High-fat diet

HFC: High-fat high-cholesterol diet

HSF1: Heat shock factor 1

HSP72: Heat shock protein 72

HSP90: Heat shock protein 90

iAUC: Incremental area under the curve

IKKβ: IκB kinase β

IR: Insulin receptor

IRS: Insulin receptor substrates

LPS: Lipopolysaccharide

LCFA: Long chain fatty acid

MCD: Methionine Choline-Deficient

Met: Metformin

Mtr: Matrine

NAFLD: Non-alcoholic fatty liver disease

NASH: Non-alcoholic steatohepatitis

NFκB: Nuclear factor kappa-light-chain enhancer of activated B cells

PPARs: Peroxisome proliferator-activated receptors

RT-PCR: Real-time polymerase chain reaction

SCD: Stearoyl-CoA desaturase

SDS: Sodium dodecyl sulphate

SREBP1c: Sterol regulatory element binding protein 1c

STZ: Streptozotocin

T2D: Type 2 diabetes

TG: Triglyceride

TNFα: Tumor necrosis factor α

VLDL: very low-density lipoprotein

WHO: World Health Organization

TABLE OF CONTENTS

LIST OF FIGURES

LIST OF TABLES

Abstract

Non-alcoholic fatty liver disease (NAFLD) is a manifestation of metabolic syndrome in the liver. It is the most common chronic liver disease with fast-growing prevalence worldwide that parallels the obesity epidemic and type 2 diabetes (T2D). NAFLD ranges from simple hepatosteatosis to non-alcoholic steatohepatitis (NASH) and may finally leads to liver cirrhosis and failure. NASH is the critical stage in the progression from reversible and asymptomatic hepatosteatosis towards irreversible liver disease with significantly worsen prognosis. However, there is no effective drug for treatment of NASH.

Matrine (Mtr) is a small molecule (MW: 248) originally isolated from plants and it has been used as a hepatoprotective drug in humans with few reported adverse effects. Several lines of evidence suggest that Mtr may be repurposed for the treatment of NASH, including a previous study of this laboratory showing its ability to reduce hepatosteatosis in high fat diet (HFD)-fed mice. However, a single HFD rodent model only replicates simple hepatosteatosis due to increased exogenous lipid overload. Therefore, the overall aim of this thesis was to characterise the therapeutic properties of Mtr for NASH treatment and investigate the underlying mechanism/s. The hypothesis addressed in this study was that Mtr has therapeutic properties for the treatment of NASH by ameliorating hepatic steatosis and inflammation as well as associated metabolic risk factors. These therapeutic effects were examined in three mouse models mimicking different characteristics of NASH.

The first aim was to examine the therapeutic effects of Mtr on hepatosteatosis and glucose intolerance induced by an over consumption of carbohydrates. This was assessed in high fructose (HFru) fed mice, a well-characterised model of hepatosteatosis causing an increased in hepatic *de novo* lipogenesis (DNL) pathway. This study (Chapter 3) showed that treatment with Mtr markedly ameliorates hepatosteatosis (reduced triglyceride content) and glucose intolerance in HFru-fed mice. Further studies revealed that the reduced hepatosteatosis by Mtr is due to its inhibition of hepatic DNL involving the blocking of the endoplasmic reticulum (ER) stress pathway. These effects are associated with an upregulation of heat shock protein 72 (HSP72), the chaperone protein which is known to be protective against metabolic diseases and inflammation. A separate aim was to evaluate the potential efficacy of Mtr in the treatment for hyperglycaemia as hepatosteatosis is an important contributor to hepatic insulin resistance leading to hyperglycaemia. In this study, the antisteatotic effects of Mtr on hyperglycaemia were investigated in a mouse model where type 2 diabetes is induced by HFD in combination with low doses of *streptozotocin* (HFD-STZ). The results showed that oral administration of Mtr to HFD-STZ mice reverses hyperglycaemia and hepatosteatosis. These findings support the use of Mtr to treat hepatosteatosis and associated disorders in glucose homeostasis.

The second aim of this thesis (Chapter 4) was to examine the therapeutic efficacy of Mtr for hepatic inflammation and fibrosis. This was investigated in mice fed a methionine choline-deficient (MCD) diet, a well-established mouse model which shares pathologic features of severe NASH in humans, in particular hepatic inflammation and fibrosis. The study showed that Mtr treatment suppresses the increases in TNFα, CD68, MCP-1, NLRP3, and hepatic fibrosis markers (TGFβ and Smad3) induced by MCD

diet. Along with these effects, Mtr inhibits mTOR activation and upregulates HSP72 expression, suggesting a likely role of mTOR-HSP72 pathway in coordinating the therapeutic effects of Mtr for NASH.

The final aim further investigated cellular mechanisms underlying the effects of Mtr on the inflammatory pathway. This was conducted using cultured J774A cells, a macrophage cell line rused here as a model for Kupffer cells believed to be a major source of inflammatory cytokines in the liver. Incubation of J774A cells with LPS stimulated the production of TNFα and increased NLRP3, CD68 and TGFβ expression. Treatment with Mtr also upregulated HSP72, inhibiting inflammation and fibrosis induced by LPS (Chapter 5). Additionally, Mtr suppressed the level of mTOR. These results provide further evidence that Mtr may exert its effect against NASH through the mTOR-HSP72 pathway.

In summary, this thesis employed three different animal models to characterise a wide range of therapeutic effects of Mtr on NASH. Findings from these studies led to the following conclusions. Firstly, Mtr is a promising therapy for hepatosteatosis and associated glucose disorders. Secondly, Mtr can attenuate NASH-associated inflammation and fibrosis. Finally, mTOR-HSP72 may play an important role in mediating the therapeutic effects of Mtr on NASH. Overall, these findings provide strong pre-clinical evidence to support the repurposing of Mtr as a promising new drug for the treatment of NAFLD, particularly on the progression towards NASH.

Chapter 1 Introduction and Literature Review

1.1 Introduction

Non-alcoholic fatty liver disease (NAFLD) is the accumulation of lipid in the liver that is not due to alcoholic consumption or viral liver infection. Development of NAFLD is generally associated with metabolic disease, and is identified as a hepatic manifestation of the metabolic syndrome. Globally, NAFLD is the most common chronic liver disease. NAFLD includes simple steatosis, non-alcoholic steatohepatitis (NASH), NASH-related cirrhosis and end-stage liver disease. NASH is considered a critical stage in the transition of simple steatosis to life-threatening cirrhosis. In addition to obstacles in understanding NASH pathogenesis, no effective treatment has yet been approved for the treatment of NASH with existing hepatic inflammation and fibrosis. This literature review focuses on relevant research to provide (1) the general background of NAFLD, including its stages and complications; (2) current treatments and newly developed drugs for NAFLD; (3) the rationale behind repurposing matrine (Mtr) for the treatment of advanced NAFLD; and (4) cellular targets, pathways and animal models for the investigation of new therapeutics for NAFLD. From this review of the literature, gaps in the current knowledge are identified and hypotheses/approaches are developed to guide the research presented in this thesis.

1.2 Fatty liver disease

Fatty liver is the accumulation of triglycerides (TG) in the liver and within liver cells (hepatocytes). Although the liver normally contains fat, when the percentage of this fat deposition exceeds 5% of liver tissue weight, it is characterised as fatty liver disease

[1]. This generally occurs when the amount of synthesis and delivery of fatty acids (FAs) exceeds the amount that is excreted and eliminated [2].

FAs are derived from diet, lipolysis in adipose tissue *de novo* lipogenesis (DNL) and through the uptake of intestinally derived chylomicron remnants. Increase FAs the major cause of hepatic lipid accumulation, where saturated FAs (SFA), such as palmitic and stearic acids, are the most abundant circulating free FAs [3]. In contrast, supplementation with polyunsaturated FAs (PUFA) can improve lipid metabolism in NAFLD patients [4]. In addition, an imbalance between energy intake and consumption may cause a defect in FA metabolism and eventually fatty liver.

Fatty liver disease may be broadly classified into two types: alcoholic and non-alcoholic [5]. Alcoholic fatty liver (AFL) is hepatic steatosis caused by the excessive consumption of alcohol. NAFLD is a spectrum of diseases that ranges from steatosis to steatohepatitis. Conversely, AFL is caused by the production of toxic metabolites following excessive alcohol intake and is primarily treated by stopping alcohol consumption. The root cause of NAFLD remains unclear and an effective cure has yet to be developed. Less common causes of fatty liver disease include medications—for example, amiodarone, methotrexate and tamoxifen [6]—and chronic diseases such as HIV, hepatitis C virus (HCV) and autoimmune conditions [7]. Fatty liver disease may also occasionally occur during pregnancy and is associated with significant morbidity and mortality rates [8].

Because NAFLD has long been a serious health concern worldwide, it is of great interest in a broad range of medical fields. The past 30 years have seen increasingly

rapid advances in the field of NAFLD research. However, there remains insufficient understanding of NAFLD molecular mechanisms and treatments. Although the underlying mechanisms of NAFLD have been explored in depth in several studies [6, 9], there remains an urgent need to address effective treatment modalities for NAFLD. To date, no reliable drug has been developed towards this end. Hence, this thesis will focus on NAFLD rather than other types of fatty liver disease and intends to explore an appropriate drug for treatment.

1.3 Non-alcoholic fatty liver disease (NAFLD)

NAFLD is a metabolic disease characterised by the accumulation of lipid in the liver in the absence of alcohol abuse or hepatic infectious disease [6, 10]. It ranges from simple hepatosteatosis to steatohepatitis and cirrhosis. In humans, an NAFLD patient is diagnosed when deposition of fat exceeds 5% of liver weight based on clinical history, clinical examination and non-invasive laboratory tests [1]. It is now globally recognised as the most common chronic liver disease in developed countries including Australia, the United Kingdom and the United States [6, 11].

NAFLD prevalence has doubled over the past two decades compared with other chronic liver diseases, which have remained relatively stable [12]. NAFLD is closely associated with metabolic disorders and abnormal liver physiology. According to the American Association for the Study of Liver Diseases (AASLD), even though NAFLD presents as hepatosteatosis correlated with dyslipidaemia, obesity and type 2 diabetes (T2D), its underlying mechanisms are still not fully understood [10, 13].

There are two forms of NAFLD: simple fatty liver and NASH. Simple fatty liver (hepatosteatosis) is defined as an accumulation of lipid unrelated to alcohol consumption or viral hepatitis [10]. It is chiefly caused by excessive deposition of fat in liver cells (hepatocytes) in the absence of inflammation, fibrosis and hepatocyte injury [6]. It has been observed that hepatosteatosis usually presents with high serum TG level without any indication of inflammation, hepatocellular injury or liver injury in NAFLD patients and mice [14].

NASH is a critical and severe stage of NAFLD, defined as the presence of hepatosteatosis and inflammation with or without fibrosis [15]. Unlike liver disease due to viral infections such as hepatitis C, NASH is characterised by steatosis, hepatocyte damage, hepatic inflammation and fibrosis [6, 10]. As shown in **Table 1.1**, NAFLD can be classified into two major stages: hepatosteatosis and NASH, where NASH is the critical form of the disease because of its potential for progressing to cirrhosis, hepatocellular carcinoma (HCC) and liver failure.

Table 1.1 Classifications and grades of NAFLD

NAFLD stages	Grades	Remarks
Hepatosteatosis	Mild	Increased TG
NASH without fibrosis	Moderate	Increased TG + inflammation
NASH with fibrosis	Severe	Increased TG + inflammation (varying degrees of fibrosis)
NASH-related cirrhosis	End stage (irreversible)	Scar tissue (fibrotic connective tissue) + liver failure

As shown in **Figure 1.1**, NAFLD usually starts with simple fat accumulation within hepatocytes. Under certain conditions, this can progress to hepatic tissue inflammation and fibrosis, causing NASH and finally cirrhosis and even liver cancer (HCC).

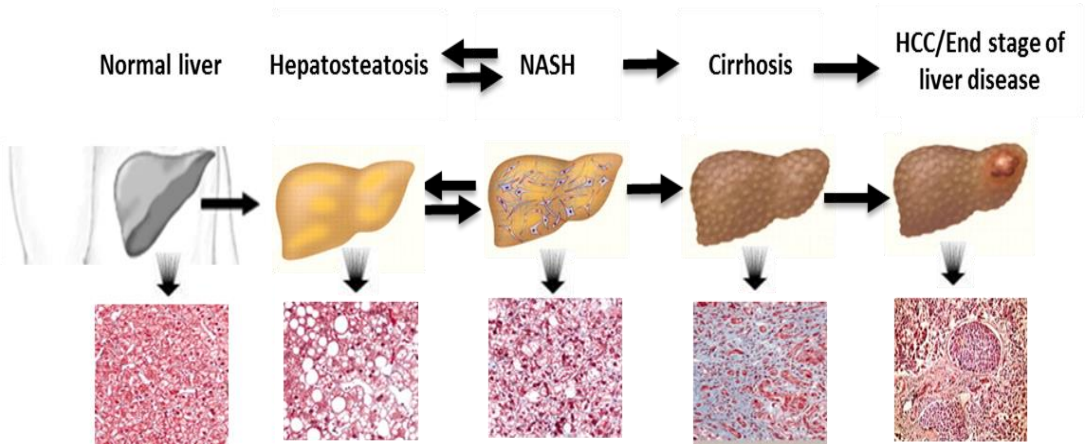

Figure 1.1 Schematic illustration of NAFLD progression presents a spectrum of liver disease.

The progression of fatty liver from healthy liver to end-stage liver disease is illustrated. The first stage starts with excess fat deposits within hepatocytes causing hepatosteatosis. Then, an increase in inflammatory cytokines causing NASH with or without fibrosis occurs. This leads to an irreversible stage and scar tissue formation in cirrhosis, which leads to the end stage of liver disease. Histological sections are shown as the healthy normal liver progresses through these stages. Based on Cohen *et al*. [1].

Indeed, the pathogenic components of NAFLD are complex and a multitude of factors contribute to the development of this disease. Hepatosteatosis appears to be the first stage of NAFLD development, and the progression of NASH appears linked to hepatic inflammation.

1.3.1 Prevalence of NAFLD

NAFLD is becoming increasingly widespread as a result of modern sedentary lifestyles and the increased incidence worldwide of related metabolic diseases including obesity, T2D and insulin resistance [16]. Obesity and T2D are the major risk factors for NAFLD as reviewed in detail in **Section 1.3.2**. In addition, NAFLD patients are highly vulnerable to other metabolic diseases and liver-related morbidity and mortality. The overall prevalence of NAFLD has risen significantly over the last two decades along with increased prevalences of T2D and obesity [17, 18].

Several studies have been conducted to estimate the prevalence of NAFLD. Generally, it has been reported that the prevalence of NAFLD is around 30% in the adult population, and that the prevalence of NASH is almost 3% in most Western populations [5]. The prevalence of NAFLD is markedly increased in obese individuals (more than 25%) [5, 6]. In the United States, approximately 90% obese and 75% diabetic individuals have NAFLD, and this may explain the close relationship between NAFLD and metabolic diseases [5]. As shown in **Table 1.2**, metabolic diseases especially obesity and diabetes are major factors that seem to determine the prevalence of NAFLD.

Table 1.2 The prevalence of NAFLD in different countries

Region/Country	% in general population	% in population with obesity	% in population with T2D	Reference
Africa	9	10	5	[5]
Australia	30	76	50	[19]
China	25–31	70–78	20–32	[20, 21]
Europe/Italy	20–25	80–90	95	[22]
Iran	34	50–70	15–30	[23]
India	9–32	61	25	[24]
Japan	30	80	20–25	[5]
Korea	38	50	40	[5]
Northern Africa	17	30–83	60–98	[5]
Middle East	30–60	68	34	[5]
USA	>30	80–90	45–75	[5, 25, 26]

According to the Gastroenterological Society of Australia and the Australian Liver Association, NAFLD was the most common liver disease, affecting an estimated 5.5 million Australians, in 2012. The number of estimated deaths from NAFLD correlated to the prevalence rate of NAFLD was 2,264 deaths. In 2008, the Australian Bureau of Statistics expected that the prevalence and mortality rates could increase to 7.7 and 4.5, respectively [19] (**Table 1.3**). Further, in the United States, NASH is expected to be the leading cause of liver transplant procedures by 2020 [27].

Table 1.3 Prevalence of NAFLD and mortality in Australia in 2012

	Male	Female	Total
Prevalence	2,713,372	2,825,305	5,538,677
Mortality	1,154	1,110	2,264

Data adapted from the Gastroenterological Society of Australia and the Australian Liver Association in 2012 [19].

Multiple confounding factors affect the prevalence estimation of NAFLD in the general population. These factors include the rapid development of NAFLD and the rather vague classification of the disease stages; in addition, the lack of specific NAFLD markers is an important factor that can lead to further variations. Despite a lack of standard diagnostic tools, and diversity in sample population culture, age, ethnicity and gender, an abundance of studies have reported the incidence of NAFLD linked to these factors [28]. For example, the incidence of simple hepatosteatosis differs in gender and culture and is significantly higher in Hispanic, male and aged populations [5]. It also seems that high prevalence of NAFLD in developed countries may be at least in part due to dietary factors.

The significance of obesity and T2D in the prevalence of NAFLD has been globally recognised [5], and these are strong predictors for this pathological condition in the liver. It has been reported that the incidences of NAFLD in patients with obesity (BMI >30) and T2D are about 90% and 75%, respectively [5, 25]. Further, the increased incidence of progression from hepatosteatosis to NASH is associated with the ongoing epidemic of obesity and diabetes [6]. In addition, the different degrees of NAFLD associated with metabolic syndrome can affect the estimate of NASH. Numbers of patients with mild hepatosteatosis associated with the metabolic syndrome are

significantly high compared with patients without the metabolic syndrome. Moreover, the selection between stages of NASH and different diagnostic criteria between countries affects the estimated prevalence of NAFLD.

1.3.2 Relationship between non-alcoholic fatty liver disease and the metabolic syndrome

NAFLD is regarded as a manifestation of the metabolic syndrome in the liver [29], and is highly prevalent in patients with the metabolic syndrome [30]. This is clearly seen in NAFLD patients with hepatic insulin resistance despite the presence of normoglycaemia and mild increased body weight [31]. Further, NAFLD has been associated with not only poor glycaemic control but also hypertriglyceridaemia, low plasma high-density lipoprotein (HDL)-cholesterol levels, increased waist circumference and high blood pressure (**Figure 1.2**).

The presence of NAFLD is associated with increased risk of obesity, insulin resistance and cardiovascular diseases [29, 32], and its development is accompanied by lipid metabolism alterations [6, 29]. In addition, the ailment goes beyond mere liver disease to become an underlying cause of metabolic syndrome related to failure of other organs in the body. It has been discussed that insulin can inhibit lipolysis and increase TG synthesis in adipocytes and hepatocytes, respectively [33]. Accordingly, excess hepatic fat can induce impairment of glucose and lipid metabolism [31, 34]. This indicates that obesity and insulin resistance are associated with abnormalities in lipid metabolism associated with NAFLD. It has also been reported that the metabolic syndrome is associated with a higher risk of NASH developing in patients [29].

Mechanisms of NAFLD development can be seen by dissecting the metabolic and nutritional pathways involving FAs and glucose sensors [6]. In humans, NAFLD is significantly increased among patients with T2D or hyperlipidaemia compared with non-diabetic or non-obese patients [25, 29]. It has been reported that NAFLD patients have high fasting plasma glucose levels with early metabolic derangement compared with healthy populations [35]. Conversely, the reversal of hepatosteatosis by reduction in hepatic TG content increases insulin sensitivity and glucose metabolism [36]. In further studies, various animal models often exhibit similar pathological features of NAFLD and associated metabolic diseases [37, 38]. Therefore, animal species and strains may be a major factor that influences the development of NAFLD and its association with metabolic syndrome in non-human models [39].

NAFLD is also linked to increased cardiovascular disease, which is a leading cause of death worldwide [40]. Progression of NASH increases the risk of cardiovascular complications and may be related to increased mortality [15]. A recent study has revealed that patients with NAFLD are more likely to have greater myocardial dysfunction than are those without NAFLD [41]. Higher incidences of metabolic syndrome complications including hypertension, hypertriglyceridaemia, hypercholesterolaemia and atherosclerosis have been seen in NAFLD patients with higher BMI [32]. Further, individuals with NAFLD are generally accepted as surrogates for the risk of developing nephropathy and retinopathy [42]. Therefore, NAFLD is increasingly found associated with a more severe adverse outcome and the reversal of NAFLD in the early stages can often alleviate these chronic conditions.

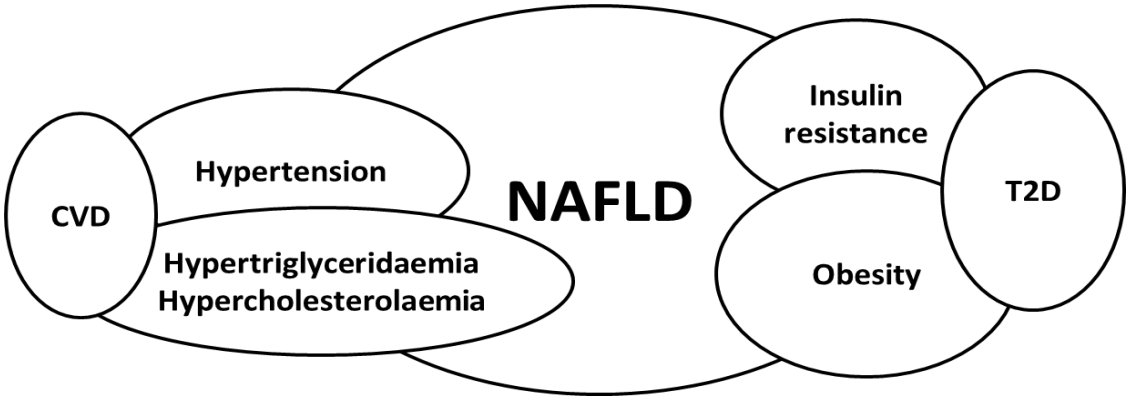

Figure 1.2 NAFLD and NAFLD-associated metabolic syndrome.

NAFLD is likely a key indicator of chronic diseases associated with obesity, T2D and insulin resistance. Further, NAFLD is usually associated with increased risk of cardiovascular complications including hypertension, hypertriglyceridaemia and hypercholesterolaemia.

The impact of dietary factors and nutritional differences in NAFLD-associated metabolic syndrome has been widely studied using animal studies. An increase in free FAs due to dietary overconsumption can result in TG accumulation in the liver and therapeutic hepatosteatosis [2]. A study conducted in rats has clearly indicated that there is a strong relationship between NAFLD and metabolic syndrome [43]. Rats fed a high-fat diet (HFD), high-fructose (HFru) diet or both have induced hyperglycaemia, hyperinsulinaemia and hypertriglyceridaemia associated with hepatosteatosis. The impact of diet on hepatosteatosis and insulin resistance has been demonstrated by Ren and colleagues [44], who have shown that mice fed a HFD or HFru diet have increased hepatosteatosis-induced glucose intolerance. Dietary fructose is almost entirely metabolised via the liver in its first pass, mainly as a substrate for DNL in both animals

[45-47] and humans [48-51]. In contrast, dietary fat directly provides FAs to produce hepatosteatosis.

1.3.3 Pathogenesis of NAFLD

The study of pathogenesis of NAFLD is complicated due to the spectrum of diseases arising from various cellular interactions within the disorder [6]. The first stage is a hepatic manifestation of the metabolic syndrome represented by hepatosteatosis. NASH is a critical and advanced form of NAFLD characterised by hepatocyte damage, release of inflammatory cytokines, and various degrees of fibrosis secondary to hepatosteatosis [1]. Due to the multiple pathways involved in this disease, there are no approved and effective treatments for patients with NAFLD. A better understanding of the complex pathogenesis of NAFLD will help to identify an effective treatment that prevents or helps to delay the development of NAFLD and the progression of NASH.

NASH pathogenesis has been established in literature by the two hit hypothesis [52]. According to Day *et al*, the first hit primarily manifests as an excessive TG accumulation in the hepatocytes and promotion of hepatosteatosis. As shown in **Figure 1.3**, the second hit has been suggested to be the main reason for the progression from hepatosteatosis to steatohepatitis. This hit may be caused by inflammatory, endoplasmic reticulum (ER) and cell injury mediators directly related to activation of inflammation, oxidative stress and apoptosis, respectively. Progression of NASH could irreversible depending on the severity of the disease [6, 52]. The exact mechanism behind NASH causation is multifactorial and its understanding is still incomplete [53]. During the progression of NAFLD, interaction of different pathways such as oxidative

stress, inflammatory cytokines, lipid peroxidation and mitochondrial dysfunction may be able to induce steatohepatitis [15, 44]. It has been claimed that the activation of inflammatory cytokines in hepatic kupffer cells (KCs) plays an important role in NASH development [6].

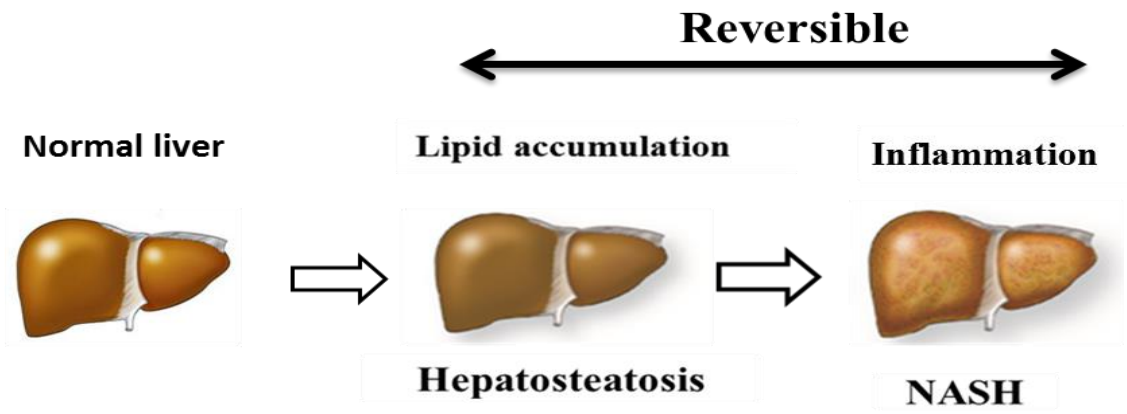

Figure 1.3 The hallmark of NASH and the two-hit hypothesis.

The first hit is caused by TG accumulation in the hepatocytes and promotion of hepatosteatosis. The second hit has been suggested to result from the activation of distinct pathways leading to simple steatosis and NASH, respectively [1].

In current literature, different pathways potentially involved in the pathogenesis of NASH have been investigated. One of the proposed mechanisms is the chronic stimulation of inflammatory cytokines, mainly tumour necrosis factor-α (TNFα) and interleukin 6 (IL-6). The activation of inflammatory mediators aggravates liver cell injury via pro-fibrogenic transforming growth factor beta (TGFβ), IL-6, intercellular adhesion molecule 1 (ICAM-1), monocyte chemoattractant protein 1 (MCP-1) and TNFα [54] (**Figure 1.4**). From this pathway, it appears that inflammation is a dominant

factor involved in the process of the progression of NASH; this will be discussed in detail in **Section 1.6.4**.

Another important factor claimed to be involved in the pathogenesis of NAFLD is oxidative stress [54]. In general, excessive TG accumulation in the liver causes metabolic stress on the mitochondria and ER and the release of reactive oxygen species (ROS). It has been reported that there is a significant increase in the products of lipid peroxidation among NAFLD patients compared with healthy controls [55]. Increased hepatic oxidative stress markers have also been found in severe inflammation in NASH induced in mice by feeding them methionine and choline-deficient (MCD) diet [56]. Further, several studies have reported that ER stress may be an essential factor in both the development of hepatosteatosis and the progression to NASH [57-59]. Indeed, it has been shown that attenuation of ER stress prevents the development of hepatosteatosis and progression of NASH in vivo and in vitro [60, 61].

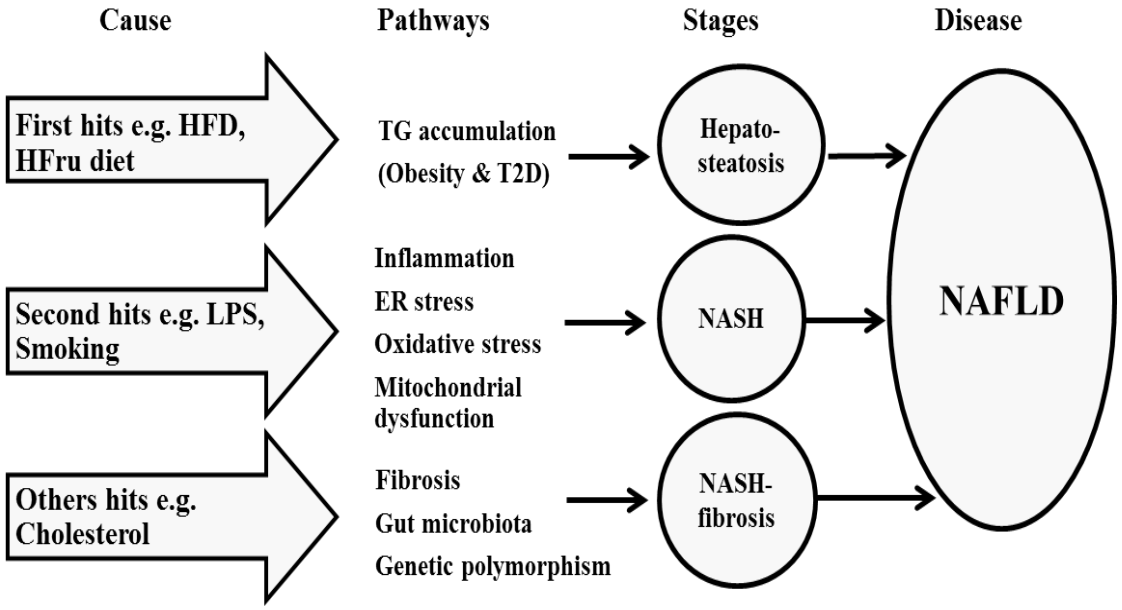

Figure 1.4 Proposed 'multiple hits' in the pathogenesis of NASH.

The initial hit is through increased production of free FAs and hepatic fat deposition, usually due to the metabolic syndrome, resulting in hepatosteatosis. Second hits such as inflammation, oxidative stress and ER stress are involved in the progression of steatosis to NASH. Such multiple factors may include oxidative damage, increased inflammation and fibrosis leading to NASH [62].

To date, several studies have highlighted the multiple-hit theory that is associated with the development of NAFLD. Recent evidence suggests that gut-derived bacterial lipopolysaccharide (LPS) plays a key role in the development and progression of NASH [63]. It has been observed that there is an increase in the growth of LPS bacteria in patients with NASH compared with controls. Several studies in rodents have shown that LPS/toll-like receptor 4 (LPS/TLR4) and LPS-induced TNFα production are involved in the progression of NASH in rats and mice, respectively [64, 65]. Further, LPS stimulation with high caloric intake leads to hepatic inflammation and progression of NASH in C57BL/6 mice [66]. Interestingly, therapeutics that target LPS elevation such as Mtr might ameliorate diet-induced steatohepatitis, particularly fibrosis progression [67]. Gut microbiota-triggered LPS-induced hepatic inflammation and NASH are vital regulators of NAFLD pathogenesis.

Understanding these NAFLD progression mechanisms will help to develop drugs that target hepatosteatosis and NASH that arise along these pathogenesis pathways. Further studies may be beneficial to not only dissect these pathways but also present potential new therapeutic agents that resolve NAFLD. New approaches have been explored to develop appropriate therapeutics that target various elements in the pathogenesis of NAFLD and progression of NASH [68]. There is great interest in identifying molecular targets for the treatment of this condition, making the outlook of NASH therapy more

optimistic. The use of treatments that target predictive risk factors such as obesity and T2D has become prominent, but is insufficient [68]. Current medications targeting these pathways will be discussed in detail in **Section 1.9**.

1.4 Economic burden of NAFLD

The burden of NAFLD is associated with tremendous clinical, economic and health-related quality-of-life costs. The increased prevalence of this disease has led to greater analysis of the quantifications of clinical and economic burdens of this condition [69]. NAFLD has a high financial cost, which affects the patient's health and treatment system, and the overall economy, and needs to be addressed through healthcare and prevention policies. The disease's progression and related illnesses put a strain on national medical services. Hence, estimating economic costs and health burden of fatty liver disease is extremely important in monitoring the incidence of NAFLD and other related health problems. It is also essential to provide standard classifications in outlining the burden of fatty liver, morbidity and deaths affecting individuals and the society. This is aggravated by the limited availability of non-invasive and accurate diagnostic tools—one of the greatest challenges in NAFLD diagnosis [6].

There are currently insufficient data available on the cost-effectiveness of prevention and treatment of this disease [70]. Data reveal that pharmacological treatments in addition to standard lifestyle modifications in NASH patients with advanced fibrosis is likely more cost-effective than in NASH patients without advanced fibrosis. Another study has reported a total cost of 2,521 purchasing power parity (PPP) for each urban NAFLD patient per year including health services, diagnosis and drug treatment [5].

Despite the short-term follow-up, including minimum cost and narrow spectrum of healthcare cost, the study reports that the total cost of NAFLD in Iran is 1 billion PPP yearly.

The economic burden of NAFLD including diagnosis and treatment is extremely high worldwide. Statistics show that NAFLD is the most prevalent liver disease in Australia, with an estimated 5.5 million people affected, including 40% of all adults aged 50 years and over [19]. NAFLD is also associated with the highest number of deaths, with an estimated 2,264 in 2012. According to the same report by the Gastroenterological Society of Australia, the Australian government has spent around $5.44 billion on patients with liver diseases [19]. The prevalence rate of NAFLD continues to rise significantly worldwide including Australia. It is projected that NAFLD will affect more than 7 million Australians in 2030 [19]. A recent study has shown that the high prevalence of NAFLD has a marked effect on the economy of both the United States and Europe, outlining a comprehensive model estimating the clinical and economic burdens of NAFLD [69]. From the data reported in the study, the number of NAFLD patients in the United States and Europe is 60 million and 50 million patients with an annual cost of about $103 billion and €35 billion, respectively.

The enormous economic burdens associated with NAFLD will continue to increase as its prevalence rises. Indeed, it is time to improve awareness of NAFLD at a social level and give more consideration to NAFLD in health policies worldwide to secure a better future for coming generations. Formal cost–benefit analyses in the context of NAFLD are needed for better management and treatment. Clearly, defining the natural history of NAFLD would be beneficial for the early detection and prevention of NAFLD

progression and complications. In turn, the effect of novel treatments on decision-making may be beneficial to avoid high future healthcare costs related to progression of NAFLD.

It is worthwhile to note that lack of awareness of the economic burden of NAFLD among hepatologists and non-hepatologists is putting individuals and society at elevated risk. This is likely due to underestimated prevalence of NAFLD and its implications. One of the most effective ways to monitor development and progression of NAFLD is to estimate the economic burden of this disease. Undertaking a study of the economic burden of NAFLD has been highly recommended by hepatologists and hepatic clinical practitioners to develop a comprehensive understanding of the liability of this disease.

1.5 Hepatosteatosis

Hepatosteatosis (also called fatty liver) is defined as the accumulation of TG in the liver, where the risk of progression to fibrosis and liver failure in the absence of additional insults is relatively small [10]. It is considered a benign stage of NAFLD but a primary mediator of most common fatty liver diseases [6] because of excessive lipid accumulation in the liver both directly and indirectly through liver-related diseases such as obesity and T2D. Simple hepatosteatosis is characterised by a hepatic TG content greater than 5% of liver weight in the absence of liver injury, inflammation and fibrosis (**Figure 1.6**). When left untreated, hepatosteatosis may progress to NASH, where the risk of fibrosis and cirrhosis is dramatically increased [69].

There are four major causes of hepatosteatosis, including increased dietary fat (exogenous fat), increased DNL (endogenous fat synthesised in the liver), reduced fat oxidation and impaired fat export out of the liver [2, 71]. Indeed, dysfunction of the liver may cause improper trafficking of lipids, resulting in a higher rate of TG synthesis than TG secretion [6]. This prolonged impairment of hepatic TG secretion promotes inflammation, oxidative stress and fibrosis in the liver to form NASH.

Table 1.4 Major features differences between simple hepatosteatosis and NASH

Feature	Hepatosteatosis	NASH
Lipid accumulation	✓	✓
Liver injury	✗	✓
Hepatic inflammation	✗	✓
Hepatic fibrosis	✗	✓
Risk of cirrhosis	Minimal risk (cirrhosis <0.7%)	High risk (cirrhosis >12%)
Mortality	Lower mortality (20%)	Higher mortality (42%)

FAs can also be generated from carbohydrates through DNL, a process initiated by the carboxylation of actyl-CoA that is catalysed by acetyl-coA carboxylase (ACC) [6]. It has been shown that DNL is promoted by hyperinsulinemia or high consumption of carbohydrates [72, 73]. Previous studies also showed DNL is increased in the liver of high-fructose fed mice [45].

FAs are the precursor of TG and play an important role in the development of hepatosteatosis. Several mechanisms contribute to increased FAs subsequently causing hepatosteatosis. It has been shown that several putative signalling mechanisms, including inflammatory cytokines, ER stress and oxidative stress, are activated as a result of excessive FAs supply [6]. Regulation of FAs pathways in both adipose tissue

and the liver are essential to maintain TG synthesis and secretion, which is essential for lipid metabolism in relation to hepatosteatosis [9].

1.5.1 Hepatic lipid metabolism

Liver TG is formed from FAs and glycerol via hepatocellular long-chain FAs bound to coenzyme A to form fatty acyl coenzyme A (acyl-CoA) [35]. FAs are generally derived from circulating free FAs, DNL, lipoprotein uptake and TG breakdown [6]. Of the TG present in the liver, approximately 59% comes from circulating free FAs, 26% from DNL and 15% from the diet [2]. Thus, hepatosteatosis can be considered a heterogeneous condition. Our laboratory and others have found that excessive DNL represents a key feature of fatty liver from high-carbohydrate diet [6]. These sources contribute towards TG synthesis, which is stored and metabolised within the liver then exported and stored in adipose tissue.

Dysregulation of lipid metabolism in the liver is strongly correlated with TG accumulation within hepatocytes, causing hepatosteatosis [15]. As indicated previously, an imbalance between free FA formation and utilisation (lipid synthesis and oxidation) can lead to an increase in hepatic free FA concentration, resulting in hepatosteatosis [35].

One important cause of increased fat uptake is excess FA intake, such as with a Western diet or HFD, directly leading to excessive accumulation of fat in the liver and eventually hepatosteatosis [44, 74]. A possible explanation for this connection may be

that circulating FAs mainly derive from digested dietary fat and adipose tissue lipolysis, leading to increased lipid deposits in the liver [6].

Another possibility is that insulin resistance in muscle due to impaired insulin-mediated glucose uptake leads to deviation of glucose to the liver for DNL [75]. Conversely, increased synthesis of TG through non-esterified FAs (NEFAs) and DNL promotes lipid droplets in circulation and in the liver, respectively [6]. During TG lipolysis, NEFAs are transported from adipose tissue to the liver and re-esterified with glycerol to form TG. The other cause of increased fat synthesis through the highly regulated DNL pathway will be discussed in **Section 1.5.2**.

Dysregulation of FA metabolism is likely caused by FA oxidation-reduction [76]. In this pathway, mitochondrial regulated FA oxidation through carnitine palmitoyltransferase 1 (CPT1), which is the key enzyme in FA β-oxidation, facilitates the transport of acyl-CoA into mitochondria. It has been shown that an increase in CPT1 alleviates HFD-induced lipid metabolism disorders in a genetic obesity rat model [77]. Indeed, prevention of free FA-induced hepatosteatosis increased mitochondrial β-oxidation in HepG2 cells and in MCD rats with a carnitine-supplemented diet [78]. In contrast, it has been suggested that overexpression of enzymes such as CPT1 increases FA oxidation and alleviates HFD-induced hepatosteatosis and inflammation [76].

Another factor that contributes to the aggravation of NAFLD is mitochondrial dysfunction. For example, a decrease in the regulator of mitochondrial biogenesis, peroxisome proliferator-activated receptor gamma coactivator 1 alpha (PGC1α), results in impaired lipid metabolism and hepatosteatosis development [79]. Dysregulated

mitochondrial metabolism involved in oxidative stress, ER stress and inflammation constitutes risk factors that progress NASH in humans and rodents [80, 81]. Hence, developing drugs that increase mitochondrial function could ameliorate NASH [82]. This indicates that mitochondrial dysfunction has an essential contribution to the development of NASH.

Very low density lipoprotein (VLDL) secretion, which is a mechanism of TG removal from the liver, is another mechanism of hepatosteatosis [83]. Inhibition of VLDL secretion induces hepatosteatosis, suggesting that VLDL production plays a significant role in hepatic lipid metabolism and hyperlipidaemia [83]. It has been suggested that VLDL secretion deficiency can promote NAFLD progression [6]. Impaired VLDL export in a genetic NASH mice model exhibits excessive hepatic TG and increased expression of inflammatory markers [84]. In Zucker rats, increased TG secretion from the liver by circulation has been shown to prevent the development of hepatosteatosis [85]. Impairment of TG export and deficiency in VLDL synthesis leads to TG accumulation in liver cells, which may lead to hepatosteatosis. The TG exported from the liver is packed into VLDL and released into the blood stream, which is a mechanism of hyperlipidaemia [6]. The main cause of reduction in VLDL secretion in the liver is lack of microsomal TG transfer protein (MTTP), which plays a vital role in the synthesis of apolipoprotein B in VLDL formation. Deficiency of these proteins results in hepatosteatosis and NASH exacerbation in mice [86] and humans [87].

Hyperinsulinaemia has been associated with an increase in lipid synthesis to result in hepatosteatosis. Forkhead box protein O1 (FoxO1) is a key mediator in the insulin signalling pathway, and acts as a master transcription factor regulating hepatic DNL

and gluconeogenesis [88]. Prolonged insulin stimulation restores FoxO1 expression, while insulin receptor substrate 2 (IRS-2) is involved in the inhibitory effects of insulin on FoxO1 [89, 90]. The expression of FoxO1 regulates lipid metabolism through reduced transcriptional activity of sterol regulatory element-binding protein 1c (SREBP1c) in vivo and in vitro [91].

Mitochondria play an essential role in hepatic lipid metabolism and are affected by upstream signalling pathways involved in hepatosteatosis [92]. FA oxidation is a process to shorten FAs into acetyl-CoA and plays a vital role in hepatosteatosis and lipid metabolism. Impairment in FA oxidation and lipid export can increase hepatic DNL and thereby trigger hepatosteatosis. It has been suggested that stimulation of mitochondrial FA oxidation in the liver may ameliorate hepatosteatosis, inflammation and fibrosis and protect against hepatosteatosis [81, 93]. It seems that mild reduction in the rate of FA oxidation induces hepatosteatosis and significant reduction of FA oxidation exacerbates NASH.

1.5.2 *De novo* lipogenesis

The liver is a major metabolic organ responsible for the homeostasis of lipids in the whole body. DNL is a metabolic process for the conversion of an excess of carbohydrates into FAs, which are ultimately esterified with glycerol 3-phosphate to form TG [89]. DNL is thought to contribute to the development of NAFLD and related metabolic diseases [2]. Excess intake of carbohydrates especially fructose that exceeds liver utilisation capacity stimulates the lipogenic pathways and the production of DNL, lipids by disposing of glucose and calories [94]. The conversion of excess

carbohydrates regulated by the DNL pathway is a critical mechanism involved in lipid homeostasis in the liver [1]. Elevated DNL is one important source of hepatic lipid accumulation and the development of hepatosteatosis [6].

Fructose contributes to lipid synthesis via the influx of fructose carbons into lipogenic precursors. The role of dietary fructose has been implicated as an important risk factor for DNL promotion and NAFLD progression [95]. SREBP1c expression in rodents caused by fructose feeding promotes hepatic lipid synthesis [96]. Hepatic lipogenesis is affected by multiple factors including liver X receptor (LXR) and peroxisome proliferator-activated receptor-α (PPARα) [97, 98]. These elements play a vital role in regulating lipid metabolism by reducing the clearance of FAs through oxidation, consequently further increasing fat accumulation in hepatocytes [6]. The major transcriptional regulators and enzymes involved in hepatic DNL, including SREBP1c, carbohydrate-responsive element-binding protein (ChREBP), fatty acid synthase (FAS), ACC and stearoyl-coenzyme A desaturase-1 (SCD1), have garnered significant attention over recent years [95].

SREBP1c and ChREBP are two master transcriptional regulators that are widely expressed in the liver and drive DNL [89, 99]. Both these DNL transcriptional regulators are elevated in the liver during over consumption of fructose [100, 101]. Consumption of fructose has distinct effects on the expression of these lipogenic transcription factors (ChREBP and SREBP1c) and has been associated with poor metabolic outcomes, compared with glucose-fed mice [102].

ChREBP is one of the major regulators of DNL in adipose tissue implicated in hepatosteatosis and insulin resistance [103]. It can be activated by high glucose levels and inhibited by cAMP [71]. It is a key determinant of lipid synthesis as a glucose-responsive transcription factor in the liver [103]. Deficiency of ChREBP in the liver of genetically obese *ob/ob* mice markedly improves insulin resistance and hepatosteatosis [99]. Rodents fed HFru diet display a significant increase in ChREBP expression [104].

SREBP1c regulates the expression of genes encoding enzymes responsible for DNL, such as FAS [89]. A strong relation between the increased levels of nuclear SREBP1c and the elevation rates of hepatic FA synthesis has been previously reported [105]. In other words, elevated levels of hepatic SREBP1c lead to increased expression of genes for the synthesis of FAs, which in turn is associated with the development of hepatosteatosis.

It has been shown that increased SREBP1c expression contributes to the development of hyperglycaemia and hepatic steatosis in diabetic mice [105]. As the activation of SREBP1c expression is not accompanied by lipogenic gene upregulation in adipocytes [106], this transcriptional factor seems to be a dominant regulator of DNL particularly in the liver. The expression of SREBP1c can be stimulated by fructose, glucose, insulin and ER stress [89]. Inhibition of SREBP1c levels by reducing ER stress decreases hepatic lipogenesis and markedly improves hepatosteatosis and insulin sensitivity in obese rodents [107].

Downstream of the enzymes SREBP1c and ChREBP in the lipogenic pathway for hepatic lipogenesis are ACC, SCD1 and FAS [71, 108]. These key lipogenic enzymes

can be targeted for the treatment of NAFLD. For example, mutant mice lacking ACC1 are protected against hepatosteatosis [109]. Additionally, ACC inhibitors reverse hepatosteatosis in rats with diet-induced NAFLD [110]. Further, mice with liver-specific SCD1 knockout are protected against hepatosteatosis induced by high-carbohydrate diet [111], and FAS inhibition leads to a significant reduction in liver TG levels and improved insulin sensitivity in *db/db* mice fed HFru diet [112].

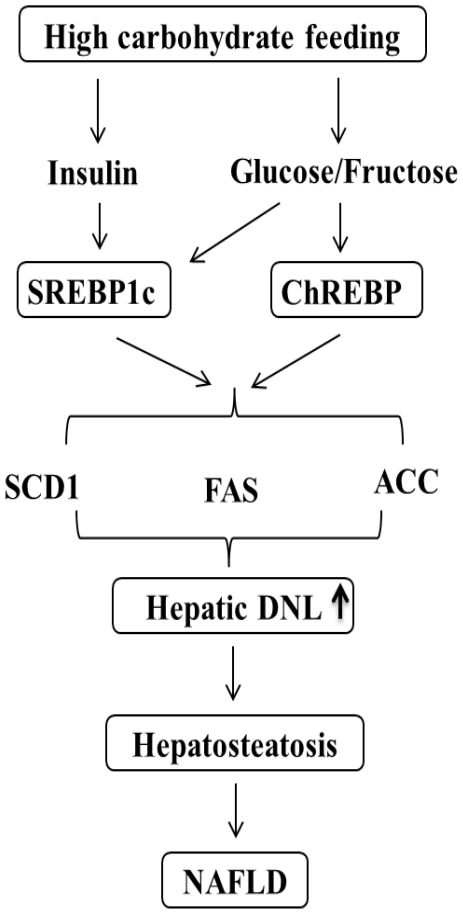

Figure 1.5 Effect of carbohydrate overfeeding on DNL-induced hepatosteatosis.

The conversion of glucose into FAs through DNL is nutritionally regulated by glucose and insulin signalling pathways, which induce lipogenic gene expression. Glucose activates the transcription factor ChREBP, which is required for the transcriptional induction of FAS and ACC. Insulin activates the transcription factor SREBP1c, which is required for the transcriptional induction of FAS and SCD1. Activation of lipogenic enzyme causes dysregulation of lipid metabolism, leading to hepatosteatosis and ultimately NAFLD development.

The activity of the lipogenic pathway is dependent upon nutritional conditions [95]. A diet rich in carbohydrates, mainly fructose, stimulates the lipogenic pathway in the liver, where fructose is cleared from the blood [101]. Several studies have suggested that HFru diet may increase DNL, which contributes to the pathogenesis of NAFLD

[100-102]. The transcription of lipogenic enzymes is regulated by insulin and glucose. Carbohydrate feeding promotes DNL, as summarised in **Figure 1.5**.

Hepatic ER stress pathways have been implicated in the development of hepatosteatosis during HFru feeding in mice [46]. It has been reported that ER stress can lead to hepatosteatosis associated with glucose homeostasis by upregulation of SREBP1c, ACC, FAS and SCD1 [45]. Alleviating ER stress and inhibiting DNL has a significant impact on improving hepatosteatosis involved in NAFLD [57]. Studies in rodents suggest that alleviating ER stress protects against an increase in hepatic lipogenesis and hepatosteatosis [57, 107]. Thus, targeting ER stress might be a good candidate for NAFLD or NASH treatment.

1.5.3 Non-alcoholic fatty liver disease and hyperglycaemia

Data from several human studies suggest that the presence of NAFLD promotes the consecutive development of T2D and is a strong predictor of the metabolic syndrome [35]. T2D and obesity are closely associated with increased delivery of FAs to the liver and hence are the most common risk factors for the development of NAFLD. They have been proposed as major risk factors in T2D with a twofold to fivefold increased risk of developing NAFLD [113]. Factors associated with hepatosteatosis, including glucose intolerance and insulin resistance, can aggravate to severe NASH [6].

The liver is largely involved in whole-body insulin resistance and fasting hyperglycaemia in T2D [35]. Excessive TG accumulation in the liver may be associated with hyperinsulinaemia and dyslipidaemia and can contribute to elevated lipogenesis in

obesity and NAFLD [6]. In addition to the liver, adipose tissue plays an important role in NAFLD development and is associated with higher risk of mortality. A link between intestinal microbiota and development of obesity with its metabolic consequences including T2D has been suggested to be involved in NAFLD progression [63].

Dietary factors significantly contribute to hepatic TG accumulation and hyperglycaemia associated with NAFLD. In NAFLD patients with or without obesity or insulin resistance, roughly 15% of hepatic FAs originate from diet. During dietary over consumption of fructose, hepatosteatosis and insulin resistance occur at a very early stage [48, 114]. Dietary fructose in particular has been shown to have a distinct tendency to induce hepatosteatosis and insulin resistance in experimental animals. For instance, HFru feeding results in hepatosteatosis and insulin resistance induced by excessive DNL [44]. The study also suggested that activation of ER stress pathways may play an important role in DNL and subsequent hepatosteatosis.

Interestingly, reduction of hepatosteatosis in diabetic patients has been shown to markedly improve glycaemia control and insulin sensitivity [36]. The reversal of hepatosteatosis and hyperglycaemia via lifestyle modification may be beneficial for the prevention of NAFLD and its associated metabolic diseases. For example, a study in experimental animals has indicated that improvement in hypertriglyceridaemia and insulin resistance induced by fructose protects against developing NAFLD [115]. It has been reported that PUFAs ameliorate many of the adverse changes in lipid and glucose metabolism responsible for NAFLD development [4].

As previously mentioned, hepatic lipogenesis represents a critical mechanism for hepatosteatosis associated with glucose homeostasis [44]. An important reason for the activation of this lipogenic pathway in the liver is a diet rich in carbohydrates. Post-translational and transcriptional mechanisms control the activities of hepatic lipogenic enzymes. The transcription of lipogenic enzymes is regulated by insulin and glucose as shown in **Figure 1.5**.

There is clear evidence suggesting a strong relationship between hepatosteatosis and insulin resistance in the presence or absence of obesity. Because NAFLD and T2D share some common pathological features, most therapeutic approaches for NAFLD target the major pathways thought to be essential in the metabolic syndrome [35]. Among various stages in the progression of NAFLD, there is increasing interest in the prevention of NASH development as it is crucial for the control of fibrosis and disease prognosis.

There are many different anti-diabetic drugs that act on the same mechanism in increasing insulin sensitivity and decreasing hepatic glucose production. Although metformin is one of these drugs because of its efficacy in T2D [116], it is necessary to develop an efficient therapy for fighting or preventing NAFLD.

1.6 Non-alcoholic steatohepatitis (NASH)

NASH is a severe and progressive stage of NAFLD, in which hepatocyte damage, inflammation and fibrosis are present [10]. Unlike simple hepatosteatosis, NASH may

become a more prominent public health issue in the near future with the potential of becoming the second most common indication for liver transplantation [6].

The pathogenesis of the transition from hepatosteatosis to NASH is complicated and, although it has been extensively studied in humans and animals, it remains unclear. It has been proposed that inflammation, ER stress, oxidative stress and mitochondrial dysfunction may be the dominant mechanisms in this disease [6]. Histologically, prolonged inflammation associated with ballooning degeneration of hepatocytes is a strong feature for defining NASH [54]. Other signs such as collagen deposition contribute to the severity of the disease.

Numerous indications characterise the pathogenesis of NASH but these signs may vary considerably in most cases. For example, TG level and plasma levels of liver enzymes (aspartate aminotransferase [AST] and alanine aminotransferase [ALT]) have been used as markers for diagnosis of NASH [117]. Other markers proposed by Walenbergh *et al*. indicate that oxidised low-density lipoprotein (oxLDL) is a substantial risk factor for NASH [118]. It seems that dysfunctional hepatic lipid metabolism may be a key factor in progression to NASH [119]. However, it is generally agreed that abnormal lipid metabolism alone is insufficient to cause liver injury and NASH [10, 80].

On the basis of the two-hit hypothesis of NAFLD pathogenesis, hepatosteatosis is classified as a first hit but a second hit is required to advance it to NASH [52]. Although it is not well understood how NASH occurs, several factors that seem to contribute to the progression of NASH have been reported in a number of studies [6]. These factors—cell injury, inflammation, ER stress, oxidative stress and mitochondrial dysfunction—are associated with the severity of NASH and progression to NASH with

fibrosis, while other factors yet to be identified contribute to the progression to severe fibrosis. Despite the difficulty in determining NASH due to the lack of definite pathogenesis, animal studies have been used to identify the factors critically involved in the progression of NASH [120, 121]. NASH characterisations according to the AASLD will be discussed in the following sections.

1.6.1 Steatosis

Hepatosteatosis is the hallmark of NAFLD resulting from excessive accumulation of lipids in hepatocytes, which can result from increased DNL, reduced utilisation of lipids or inhibited export of lipids from hepatocytes [6]. The amount of TG accumulated in the liver and other lipids such as FAs, diacylglycerols, phospholipids, sphingolipids and cholesterol is influenced by diet, physical activity, age and ethnicity. Thus, hepatosteatosis has heterogeneous causes, which are obvious risk factors for NASH [122, 123].

The two-hit hypothesis considers steatosis a first hit to the liver in NASH pathogenesis; however, not all patients with steatosis develop NASH: approximately only one-third will develop NASH [6]. In animals, a diet rich in fat, carbohydrate or both has been shown to cause simple hepatosteatosis [120]. Animal models and diets will be discussed in **Section 1.8**.

Understanding the mechanism involved in the progression of hepatosteatosis to NASH is important for the prevention of NASH that can lead to cirrhosis or cancer. According to AASLD guidelines, hepatosteatosis does not require pharmacological treatments

[10]. However, hepatosteatosis should not be neglected because it is a risk in the pathogenesis of NASH.

1.6.2 Cell damage

Hepatocytes are the most predominant cells in the liver and account for 70–80% of healthy liver mass. Hepatocytes are the major storage site for excessive TG accumulation in the highly metabolised liver cell [124]. Hepatocyte injury is a key feature that distinguishes hepatosteatosis from NASH [6]. It is strongly linked to the pathogenesis of NASH because of the ability of hepatocytes to release factors that promote inflammation and fibrosis in the liver (**Figure 1.6**).

It has been suggested that repetitive or chronic liver injury may cause dysregulation in wound-healing response, promoting progressive hepatic cell damage, which leads to cirrhosis [6]. In humans, there exist highly significant correlations between the hepatocyte damage and the severity of NASH [125]. Mice fed with special diets such as choline-deficient L-amino acid-deficient (CDAA) or MCD show liver injury and display more pronounced features of NASH [120].

Hepatocyte damage induces several factors that activate signalling cascades that result in cell death and aggravate NASH development. Fat deposition, ER stress, apoptosis and inflammation in the liver are directly or indirectly caused by cell injury. These factors associated with cell damage induce signalling pathways that contribute to the pathogenesis of NASH. It has been shown that excess lipid in mouse and human hepatocytes induces liver injury, inflammation and fibrosis with NASH [126].

Increased lipid droplets cause hepatic inflammation via cholesterol loading of macrophages in the liver [127].

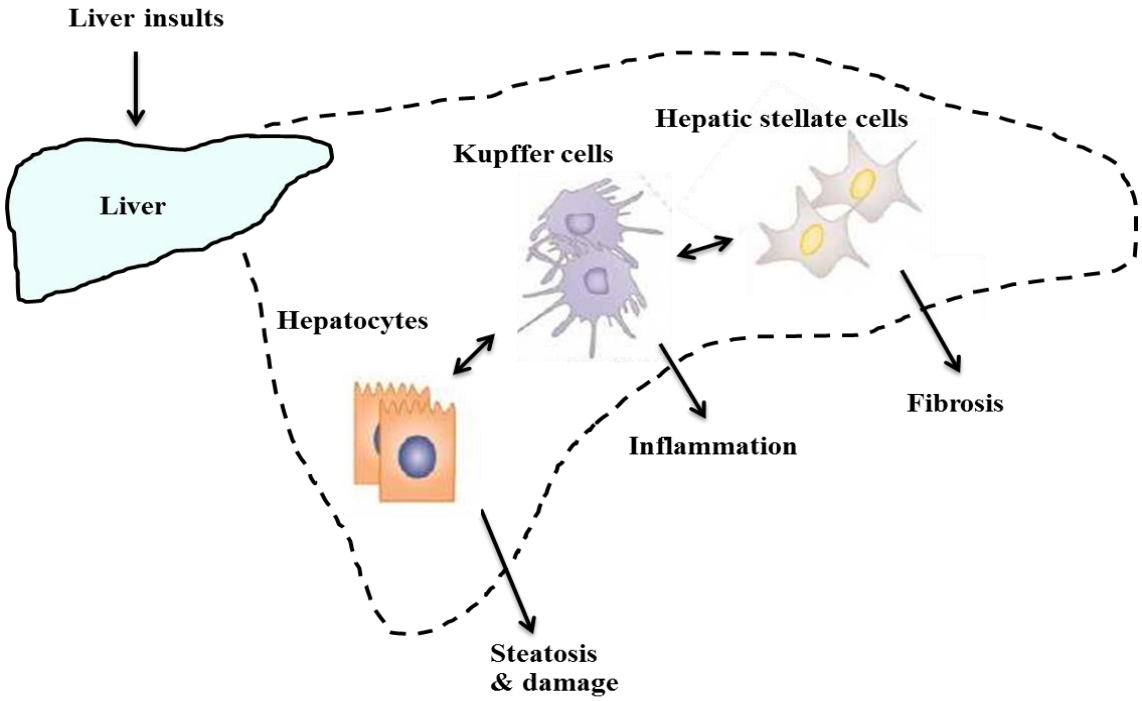

Figure 1.6 Major cell types involved in the pathogenesis of NASH.

Hepatocytes are the most predominant cells in the liver and play a vital role in liver injury. KCs are macrophages present in liver responsible for the release of inflammatory cytokines. HSCs are considered a major source of liver fibrogenic cells.

1.6.3 Macrophages activation and infiltration

Macrophages are a main component of the innate and adaptive immune systems present in all living tissues. It has been shown that KCs in NASH are associated with stimulation of the immune and inflammatory systems to detect and protect against the

disease [6, 128]. Activation of KCs and infiltration of macrophages from the blood circulation have been proposed to be essential in NASH and NASH with fibrosis [129].

Activation of KCs has been identified as a critical factor in NASH pathogenesis, mediating inflammation and exacerbating fibrosis (**Figure 1.7**). It has been found to be increased in both humans and animals with NASH [129]. Secretion of inflammatory cytokines by activated KCs is a key event in the initiation of NASH [130, 131]. It also plays a pivotal role in activation of hepatic stellate cells (HSCs) towards hepatic fibrosis and NASH-related fibrosis. It has been reported that targeted deletion of KCs completely prevents TNFα production and TGFβ mRNA expression in MCD diet-fed mice [131].

Polarisation of KCs has been demonstrated in prevention of the progression of NASH [130]. KCs are classified as M1 when responsible for releasing inflammatory properties and M2 when releasing anti-inflammatory properties. Chronic HFD feeding increases KCs with M1 phenotype, hence increasing inflammatory cytokines, while KCs polarisation switch from M1 to M2 leads to prevention of the development of NAFLD in HFD mice [132]. These studies suggest that pharmacological interventions targeting M2 KCs polarisation may provide an effective therapy in the prevention of inflammatory hepatic injury and hepatic fibrosis in NASH.

1.6.4 Inflammation

Hepatic inflammation plays a critical role in the development of NAFLD and a crucial aspect in NASH pathogenesis [15, 133]. It has been reported that macrophage

activation causing inflammation leads to NASH in mice [134]. LPS has been shown to promote the progression of NASH because of stimulation of inflammatory gene expression [135]. Alternatively, inhibition of inflammation by drugs may improve diet-induced NASH [136, 137].

Activation of KCs induces the production of inflammatory cytokines generated by LPS-induced signalling that is dependent on macrophage activation [138]. Inflammatory cytokines have two roles: first, to increase the recruitment of inflammatory cells and, second, to exacerbate the progression of NASH. The balance between pro- and anti-inflammatory acting cytokines is an acknowledged regulator of liver diseases including NASH [54].

The major inflammatory cytokine TNFα plays diverse roles in the pathogenesis of NASH [15]. The expression levels of TNFα and IL-6, two important inflammatory cytokines, are hugely increased in the liver of NASH subjects [139, 140]. Crespo *et al*. report increased hepatic expression of TNFα and tumour necrosis factor receptor 2 (TNFR2) in patients with NASH compared with healthy people [139]. In NASH patients, more advanced fibrosis is also accompanied by increased hepatic expression of TNFα. In line with these results, TNFα plasma levels have been shown to correlate positively with the grade of liver fibrosis assessed by ultrasound-guided liver biopsy in patients with advanced stages of NAFLD.

The release of numerous inflammatory cytokines, including TNFα, mediates inflammatory production and liver cell death—inflammation and cell damage are known to be involved in the pathogenesis of NASH. An earlier study has revealed that

overexpression of TNFα induces elevation of inflammatory and fibrotic signalling pathways in patients with more advanced NASH [139]. On the contrary, there are no significant differences in the levels of TNFα in NASH patients compared with simple hepatosteatosis [141]. However, it is generally agreed that inflammation plays a major role in the progression of this disease [133].

Recently, reduction of TNFα has been shown as an independent predictor for positive NASH prognosis [139]. Anti-inflammatory drugs can decrease the activity of this cytokine, and thus prevent NASH [67, 142]. In humans, such therapies represent an improvement in histological features of this disease through reduction in hepatosteatosis and inflammation [143, 144]. The anti-inflammatory effects of pentoxifylline reduce the increase in TNFα-induced NASH-like phenotype in mice fed HFD with cholesterol or MCD diet [145].

Activation of inflammatory cytokines also drives activation of inflammasome, which contributes to steatohepatitis [146]. Inflammasome and interleukin 1 beta (IL-1β) activation are required for the pathogenesis of NASH [147, 148]. Identification of the inhibitors of NOD-like receptor family pyrin domain-containing 3 (NLRP3) inflammasome is an important step in the process of developing effective drugs for the treatment of NASH in which inflammation is a known component [149, 150]. It has been reported that the inhibition of NLRP3 inflammasome activation reduces liver injury, inflammation and fibrosis in MCD diet-induced steatohepatitis and in *foz/foz* mice with NASH [149].

Another factor contributing to inflammation of the liver involved in the progression of this disease is iron accumulation. Hepatic iron deposition is strongly associated with hepatocyte injury and inflammation in NASH patients [151]. It has been found in one-third to half of patients with NAFLD and ranges from mild elevations to about 1000–1500 ng/mL accumulated within hepatocytes. Accumulation of iron has been also seen in KCs, which increases inflammatory and fibrotic cytokines [152]. The mild degree of body iron excess compared with markedly raised serum ferritin concentrations suggests that iron overload in patients with NAFLD results from a combination of alimentary and inflammatory-driven iron loading and retention [153, 154]. This is in line with the current evidence that NAFLD is both a metabolic and an inflammatory disease. Indeed, iron depletion is effective in the treatment of NASH, including improving hepatic enzymes and steatosis and reducing inflammation and oxidative stress [154].

1.6.5 Fibrosis

Liver fibrosis is a complicated pathological process that leads to the destruction of hepatocytes and impairment of liver functions, and it is strongly associated with all-cause or liver-related mortality in NASH [155]. It is another hallmark of advanced NASH where KCs induce inflammatory responses for the subsequent steps towards fibrosis. It has been shown that inflammatory cytokines secreted by KCs play a key role in fibrogenesis [156]. In fact, several drugs targeting ER stress, inflammation, oxidative stress and apoptosis may cause activated HSCs [6, 157].

At the cellular level, progression to NASH is associated with activated HSCs, the primary cells that drive the fibrogenic process [15]. Activation of HSCs leads to

increased secretion of fibrotic proteins, including TGFβ, collagen 1, alpha smooth muscle actin (α-SMA) and Smad signalling, and other extracellular matrix proteins causing the formation of scar tissue and fibrosis in the liver [158]. Several studies have shown that diet-induced HSCs activation increases these fibrotic cytokines, promoting the development of NASH fibrosis [159, 160].

The most commonly used model of liver fibrosis in experimental rodents is MCD diet [161]. The MCD mouse model represents the progression of NASH and the development of liver fibrosis. Rodents fed an MCD diet have significantly increased TG and ALT levels, indicators of steatosis and liver injury, respectively [120, 162]. TGFβ-1, α-SMA and type 1 collagen expression levels also increase among mice fed MCD diet for 8 weeks [14, 159].

Advanced fibrosis has become a central focus in clinical studies that address fibrosis and liver-related clinical endpoints in NASH, but the treatment remains the main challenge for scientists [155]. The only treatment available for NASH patients with fibrosis is liver transplantation—commonly used but unsatisfactory because of increased risk of disease recurrence after transplantation [163]. An antifibrotic drug that is safe, potent, bioavailable and specific to the liver is not yet available. Currently, several therapies are being scanned for their efficacy in the treatment of liver fibrosis via regulation of the activity of collagen deposition and HSCs in humans and animals [67, 157, 164].

1.7 Cirrhosis and liver cancer

NASH is a complex pattern of fatty liver disease in the absence of alcohol intake. It is one of the highest liver morbidity and mortality diseases worldwide with poor prognosis and progression of irreversible diseases such as HCC [165]. NASH is now recognised as the most common cause of cirrhosis and may progress to liver cancer [166]. Cirrhosis and liver cancer are characterised by the replacement of healthy liver tissue by scar tissue or cancer cells, respectively. The severity of the disease in humans differs depending on the liver biopsy and clinical and pathological severity. The recent increase in NASH and its impact on liver cirrhosis incidence highlight the need for effective screening and the development of drugs to halt liver disease progression in persons with NASH. A statistical study has revealed that approximately 10% to 29% of NASH advances to cirrhosis within 10 years [1]. In addition, it has been suggested that NASH significantly increases the incidence rate of HCC. A previous report has shown that patients with NASH cirrhosis are at roughly 2.6% increased risk of HCC [167].

NASH is significantly involved in the progression of cirrhosis and primary liver cancer [6]. Some patients suffer NASH-related cirrhosis and liver-related death [168]. Mice fed CDAA with carbon tetrachloride (CCl_4) have been developed to help understand mechanisms of carcinogenesis in NASH [169]. It has been suggested that cirrhosis and cancer represent a late complication of NASH-related fibrosis because progressive fibrosis increases the risk of cirrhosis and HCC [6].

1.8 Non-alcoholic steatohepatitis animal models

Animal models of NASH have been used extensively and discussed in several reviews [120]. The ideal model of NASH should mimic the aetiology and histopathology of NASH in humans. However, there is no single animal model that can completely replicate this disease in humans. It is important to develop an animal model that mimics human disease with respect to disease pathogenesis. It has been recommended that at least two individual NASH models should be used for the assessment of anti-NASH drugs [170].

Hepatosteatosis and NASH stages have distinct histopathological features that differ from each other. For example, the hallmark of hepatosteatosis is an increase in fat droplets within hepatocytes without any damage to hepatocytes. The degree of steatosis varies, with mild (≤30%), moderate (31–60%) and severe (≥61%) in humans [10]. Conversely, liver NASH shows hepatocellular ballooning, with or without Mallory-Denk bodies, accompanied by inflammation in the presence of macrosteatosis [6].

An NAFLD animal model has been a hot topic for scientists interested in NAFLD pathogenesis and treatment. Each of the NAFLD stages has distinctive histopathological features [6]. As mentioned earlier, hepatosteatosis is characterised histologically by excessive fat droplets within hepatocytes. As steatosis progresses to NASH, hepatocyte injury (ballooning and Mallory bodies), inflammation and collagen depositions develop. Thus, metabolic with inflammatory NASH models are highly applicable for preclinical drug testing in NASH [120].

These two features are not always present in one animal model of NASH—that is, the presence of the metabolic syndrome features, including central obesity, hyperglycaemia, insulin resistance and hypertriglyceridaemia, together with the features of hepatic inflammation with or without fibrosis. Apparently, the selection of appropriate animal models is challenging because no rodent displays these features [120].

Some animal models currently used for NAFLD/NASH present only one stage, either hepatosteatosis or NASH. For example, HFD, high-fat high-carbohydrate (HFHC) and HFru-fed animal models are widely used to produce steatosis, as they have the hallmark features observed in humans with NAFLD, including obesity and insulin resistance. Other animal models have been developed for studying NASH pathogenesis, such as the MCD, CDAA and CCl_4 models.

The following section summarises currently used and recently developed animal models for NASH.

HFD represents the modern Western diets, which directly lead to NAFLD and obesity. This can be replicated in animals fed HFD (containing approximately 45–75% fat, 47% carbohydrates and 18% protein) ad libitum. In HFD rat models, a diet of increased FAs (composed of more than 71% fat) caused hepatosteatosis-associated increased insulin level [121]. However, these animals do not usually show a significant increase in plasma level of ALT [80]. Hepatosteatosis, obesity, hyperglycaemia, insulin resistance and mitochondrial changes are also present in C57BL/6 mice fed HFD [171]. Similarly, male C57BL/6 mice fed HFD (45% fat, 35% carbohydrates and 20% protein) for 10 weeks develop steatosis with minimal increases in gene expression levels of

inflammatory cytokines [172]. However, the degree of NASH appears to depend on the rodent strain and duration of HFD. Overall, HFD animal models represent hepatosteatosis related to the metabolic syndrome and hepatosteatosis. However, the inflammatory and fibrotic features are not displayed in most HFD animals; therefore, they are not considered a typical model of NASH.

Food containing high levels of cholesterol is a major risk factor in the development of hepatic inflammation and progression of NASH in animals and humans. Several studies have suggested that dietary cholesterol increases lipid accumulation and inflammation in the liver of HFD-fed mice [80]. It has been suggested that addition of cholesterol (0.2%; #C75209, Sigma-Aldrich) to HFD can produce the NASH phenotype [173]. Similarly, rats fed the same diet do not show severe inflammation and fibrosis [174]. Atherogenic HFD accelerates the development of steatosis and inflammation after chronic feeding for 24 weeks [62]. Hepatosteatosis and liver injury (minimal fibrosis) may develop in mice fed a diet enriched with high-fructose corn syrup (HFHC-fed mice) [175].

One animal model of T2D has been fed HFD with a low dose of streptozotocin (STZ) injections for 5 consecutive days to partially damage the pancreatic β-cells [176-178]. T2D (HFD-STZ) mice display a significant increase in hyperglycaemia and TG content in the liver [88]. However, the HFD-STZ model of T2D only develops metabolic-related NAFLD, not full-blown NASH. Most rodents fed HFD, HFru and HFHC represent hepatosteatosis [120]. However, inflammatory and fibrotic features are not displayed in most HFD animals; therefore, they are not considered typical models of NASH.

MCD diet is commonly used to produce NASH in animals. The diet is deficient in methionine and choline, which are essential proteins in regulating lipid secretion in the liver [162]. Mice fed MCD diet mimic the pathophysiology of NASH in humans but without the phenotype of metabolic syndrome [161]. The development of fibrosis may occur within 3 weeks of MCD feeding. MCD-induced inflammation is usually associated with an elevated plasma level of ALT [162]. Importantly, animals fed MCD diet do not develop obesity or insulin resistance, as in the metabolic profile of NASH in humans. However, it has been reported that mice lacking either leptin (*ob/ob*) or the long form of the leptin receptor (*db/db*) fed MCD exhibit NASH associated with metabolic abnormalities [123], and that HFD promotes NASH in these genetic animal models [120].

Genetic animal models have been widely used in the study of NAFLD/NASH and to identify novel drugs. Genetic models are associated with minor or major contexts of the metabolic syndrome. Animals with a spontaneous truncating mutation, such as acyl-CoA oxidase null (ACOX−/−), methionine adenosyltransferase (MAT)-1A knockout (MATO mice) and liver-specific *pten* deletion, exhibit severe steatosis associated with inflammatory infiltration. However, these mice do not show features of the metabolic syndrome. Conversely, *ob/ob* or *db/db* mice are steatotic and morbidly obese because of hyperphagia but do not display typical characteristics of NASH. Secondary insults such as LPS and MCD may induce steatohepatitis with severe fibrosis, but this depends on mice strain. The liver of HFD-fed *foz/foz* C57BL6/J mice shows severe inflammation and fibrosis compared with non-diabetic *foz/foz* BALB/c mice [179]. Another genetic model used for lipodystrophy-associated steatohepatitis is called

SREBP1c transgenic mouse [120]. This model develops steatosis, inflammation and fibrosis where serum leptin levels are usually increased.

A number of environmental factors promote the pathogenesis of NASH. As mentioned earlier, excess exogenous fat, increased endogenous fat and decreased lipid secretion are the main sources of hepatic lipid accumulation. Animal models produced by these three components generally resemble human NAFLD. Firstly, mice fed HFD represent hepatosteatosis related to obesity. Secondly, increased endogenous fat defined as DNL is observed in mice fed HFru diet, as previously explained in **Section 1.6.2**. However, these two models do not exhibit severe inflammation, hepatocyte injury and fibrosis, as occur in humans. Finally, mice fed MCD diet exhibit decreased lipid secretion and impaired TG excretion. These mice have become the most commonly used model for NASH despite the lack of the phenotype of the metabolic syndrome.

Prevention or treatment of NASH in humans remains a big challenge. Dedicated efforts are necessary to develop an appropriate treatment that is able to improve NASH with hepatoprotective and metabolically favourable advantages. Animal models that recapitulate NASH in humans are important for the evaluation of potential therapeutic agents for the treatment of NASH.

In summary, there is no optimal NASH animal model at present. To determine pathogenic mechanisms of the transition from hepatosteatosis to steatohepatitis, different animal models are required. The table summarises rodent models for NAFLD and NASH reported in the literature (**Table 1.5**).

Table 1.5 Current rodent models of NASH

Manipulation	Model	Metabolic syndrome	Steatosis	NASH	Fibrosis	Characteristics
Dietary	High-fat diet (HFD)	Yes	Yes	Yes	No	Modern Western diet, depends on rodent strain and feeding duration, long-term feeding, not considered a NASH model
	HF + cholesterol	Yes	Yes	Yes	No	Atherogenic diet, depends on the amount of cholesterol and cholate, insulin sensitive, no significant fibrosis
	HFD + streptozotocin (HFD-STZ)	Yes	Yes	No	No	Type 2 diabetes model, does not induce inflammatory NASH
	High-fructose (HFru) diet	Yes	Yes	No	No	Liver injury may develop, no inflammation, not good model for NASH
	Methionine- and choline-deficient (MCD) diet	No	Yes	Yes	Yes	Mimics pathological NASH in humans, appropriate model for studying inflammation and fibrosis in NASH, no metabolic profile of NASH in humans
	Choline-deficient diet (CDD)	No	No	Yes	Yes	Depends on time of feeding, metabolic alterations in Wistar rats
	Carbon tetrachloride (CCl_4)	No	Yes	Yes	Yes	Short-term fibrosis, toxic and high mortality
Genetic	*ob/ob*, *db/db* mice	Yes	Yes	Yes	No	*db/db* mice have a defect in leptin signalling, *ob/ob* mice have a non-functional leptin gene, good models for NAFLD, human metabolic syndrome features, poor models for NASH

Manipulation	Model	Metabolic Syndrome	Steatosis	NASH	Fibrosis	Characteristics
	foz/foz mice	Yes	Yes	Yes	No	*Alms1* gene mutation, metabolic syndrome profile, poor model for NASH
	SREBP1c transgenic mice	Yes	Yes	Yes	Yes	Congenital lipodystrophy mouse model, long-term feeding to develop NASH, severe IR, decreased adiposity
	KK-A^y mice	Yes	Yes	No	No	Loss of melanocortin, MCD diet is a second hit required to develop NASH
	PPARα knockout mice	No	Yes	No	No	PPARα gene homozygous mutation, steatosis in starved state
	ACOX null mice	No	Yes	Yes	No	Defective peroxisomal β-oxidation of LCFAs, mice develop HCC
	Zucker fatty rats	Yes	Yes	Yes	No	Do not spontaneously develop steatohepatitis, resistant to liver fibrosis
	Otsuka Long-Evans Tokushima fatty rats	Yes	Yes	No	No	A model for the metabolic syndrome with diabetes, not a suitable model for NASH
	Prague hereditary hypercholesterolaemic rats	Yes	Yes	No	No	A model for polygenic hypercholesterolaemia, comparable to human disease
	MAT-1A null (MATO) mice	No	Yes	Yes	Yes	Methionine adenosyltransferase-1A mutation, no metabolic syndrome (rare IR)

NASH, non-alcoholic steatohepatitis; IR, insulin resistance; HCC, hepatocellular carcinoma. Based on Lau JK. *et al*, Journal of Pathology, 2017 [179]. Santhekadur PK. *et al*, Journal of Hepatology, 2018 [120].

1.9 Current treatments of NASH

NAFLD is the most common liver disease in developed countries, leading to an emerging public health crisis that may progress to a more serious situation. Persistent NASH leads to cirrhosis or HCC and is a leading cause of liver transplantation. While NASH is reversible, untreated NASH and transition to advanced stages of cirrhosis are difficult to reverse in most cases. Therefore, NASH is a critical stage in NAFLD broad spectrum of diseases and effective treatment that may halt its transition will be of great benefit for the control of fatty liver disease.

To date, there is no approved specific drug for NAFLD or NASH. There is rapid progress in identification of new therapies, and the development of NASH repurposing of currently available drugs is an effective means for the development of new drugs for NASH. Treatment of NAFLD is especially important because this can prevent the progression to NASH.

Patients with NAFLD and NASH need an effective treatment that can reverse hepatosteatosis development and prevent the progression of NASH. Unfortunately, treatments of the metabolic syndrome are not effective for the treatment of NASH [67]. The lack of non-invasive markers to assess steatosis, liver damage, inflammation and fibrosis is also a barrier for developing effective treatments [180]. As NASH results from complex pathophysiological processes, therapeutic treatments are likely to include a wide array of drugs targeting different mechanisms. **Figure 1.7** illustrates the major approaches for these mechanisms. Current treatments for NAFLD include reducing the risk factors that may cause the disease, such as obesity, prediabetes or diabetes and high

cholesterol or TG. Multiple pharmacological agents have been investigated in several studies for the treatment of this disease.

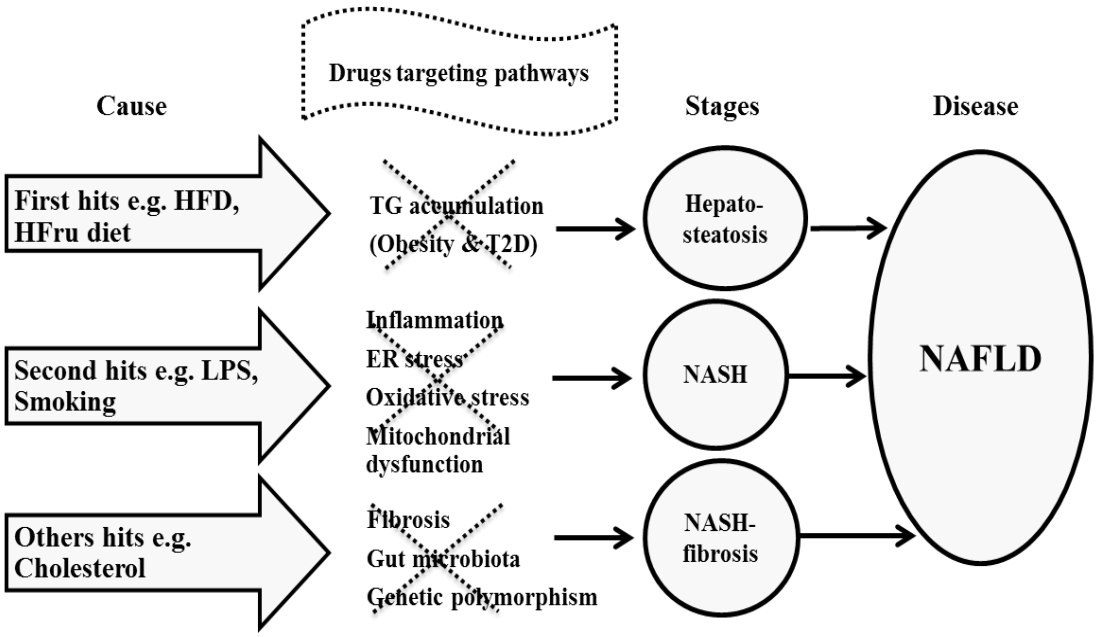

Figure 1.7 Pathways representing possible targets for the treatment of NAFLD.

Understanding the pathogenesis of NAFLD and progression of NASH helps develop effective treatments that target different pathological pathways leading to different stages of NAFLD.

The current management of NAFLD includes lifestyle interventions and drug therapy. Introduction of lifestyle changes including dietary intervention, increased physical activity and reduced weight is usually recommended first for the management of NAFLD. However, it is intended to support the treatment of not only NAFLD but also diseases associated with obesity, insulin resistance, diabetes and dyslipidaemia.

Apart from the above-mentioned lifestyle interventions, some drugs have been considered, including those listed in **Table 1.6**. These include insulin sensitisers (metformin, troglitazone, rosiglitazone and pioglitazone), lipid-lowering agents (statins), antioxidants (Vitamin E and C), hepatoprotective agents (betaine, ursodeoxycholic acid and pentoxifylline) and angiotensin-converting enzyme inhibitors. However, none of these drugs is effective for NASH. Therefore, this thesis aims to investigate the potential use of Mtr for the treatment of NASH.

Table 1.6 Summary of currently drugs used for the treatments of NAFLD/NASH

Target/Mode of action	Example of drugs	Hepatosteatosis	Inflammation	Fibrosis	Adverse events and concerns
Weight loss therapies	Loss of body weight	Yes	No	No	Hard to achieve and poor compliance Liver histology remains unknown
Anti-metabolic	Metformin	Yes	No	No	No effect on liver histology
	Rosiglitazone and Pioglitazone	Yes	No	No	Weight gain, heart disease No effect on inflammation and fibrosis
	Ursodeoxycholic Acid	Yes	No	No	No effect on inflammation and fibrosis
Antioxidant	Vitamin E	Yes	Yes	No	No effect on hepatic fibrosis Prostate cancer
Anti-inflammatory	Pentoxifylline	No	Yes	No	No effect on lipid profile
	Amlexanox	No	Yes	No	Safety but require more data
	Cenicriviroc	No	Yes	No	Insufficient data for safety and efficacy
Antifibrotic	Galectin-3 inhibitor	No	Yes	Yes	Require long-term outcomes
	Simtuzumab	No	Yes	Yes	Ineffective in reducing fibrosis
	Selonsertib	No	Yes	Yes	Require long-term outcomes

Based on Sanyal, A. J. *et al,* The New England Journal of Medicine, 2010 [181] and Sumida, Y. *et al*, Journal of Gastroenterology, 2018 [67].

Despite increasing development of new drugs to keep up with the increasing incidence of NAFLD, there remains an urgent need to identify novel drugs with improved efficacy and fewer side effects for the treatment of NASH.

1.10 Identification of matrine as a potential new drug for non-alcoholic steatohepatitis

In searching for a new therapeutic treatment for NASH, we have taken the approach of repurposing existing drugs for this condition [182]. The main advantage of drug repurposing is safety in humans because these existing drugs have been used without major side effects [182]. A second important advantage is reduction of the duration, risk and cost involved in the drug development pipeline to the clinic and the drug regimens [183].

Several lines of evidence suggest that Mtr may be repurposed for the treatment of NASH. Mtr is a small molecule (**Figure 1.8**), easy to absorb orally and can be scaled up. As reviewed by Liu *et al*., Mtr is a safe drug for the treatment of chronic viral infections and tumours in the liver [184]. Another study has shown that high concentrations of Mtr may lead to cytotoxicity of human hepatocytes; however, low concentrations of Mtr have no severe side effects [185]. Moreover, Mtr may prevent progression of HCC via inhibiting overexpression of MMP-9 by reduction of the nuclear factor kappa beta (NF-κB) signalling pathways [186]. Mtr has a different chemical structure and plasma protein binding from other drugs including metformin, which has no effects on TG level, glucose tolerance, lipogenic protein levels (ACC and

FAS), and protein expression or activity of energy metabolism markers. Recently, Zeng and colleagues have found that Mtr is able to reduce hepatosteatosis and glucose intolerance in HFD-fed mice. This study has also revealed that the antisteatotic effect of Mtr is associated with upregulation of HSP72 in the liver, suggesting a unique mechanism underlying Mtr's effect [172].

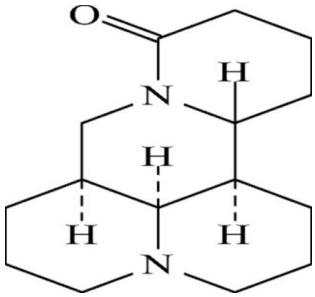

Figure 1.8 The chemical structure of matrine.

Mtr is likely to work at different mechanistic levels to reduce hepatosteatosis and reverse metabolic dysfunction. It is noteworthy to study the benefits of Mtr in the reversal of hepatic fibrosis and reduction in the progression of NASH.

1.10.1 Reported effects of matrine on inflammation

As reviewed previously, hepatic inflammation is one of the major hallmarks of NASH. An early study has shown that Mtr suppresses LPS-induced production of inflammatory cytokines, suggesting Mtr might be an anti-inflammatory drug [187]. Mtr has been shown to inhibit TNFα, IL-6 and NF-κB activation in vivo and in vitro. Consistent with the anti-inflammatory effects of Mtr in BALB/c mice, Mtr significantly reduces the inflammatory gene expression levels in the liver of HFD C57BL/6J mice [172]. Mtr treatment has also been shown to decrease virus-induced TNFα expression and the nuclear translocation of p65 NFκB [188].

1.10.2 Reported effects of matrine on fibrosis

Liver fibrosis leads to the destruction of hepatocytes and impairment of liver functions and is strongly associated with all-cause or liver-related mortality in NASH [155]. Mtr has been shown to inhibit the activation of HSCs, which play a central role in liver fibrogenesis [189]. The antifibrotic effect of Mtr has been proven in CCL_4-induced fibrosis in a rat model by attenuating TGFβ and collagen synthesis.

1.10.3 Heat shock protein as putative targets for matrine

Heat shock proteins (HSPs) are chaperone proteins modified by heat shock response (HSR) to protect the organism against physiological and environmental stresses [190]. HSPs are known to prevent protein aggregation and refolding of damaged proteins through proteasomes, autophagy or protein degradation [191]. HSP90 HSF1 and HSP70 (stress inducible form is HSP72) have been suggested to modulate inflammation [192]. Physiological stress and heat shock activate HSF1 by dissociating it from HSP90 [193]. This allows HSF1 to translocate into the nucleus and transactivate the expression of HSP72. HSP72 is highly inducible and its upregulation has been shown to correlate with attenuation of diabetes, obesity and NAFLD [194]. We have chosen to focus on HSPs because they are ubiquitous chaperone proteins existing in prokaryotes and eukaryotes and they play a major role in inflammatory diseases.

HSP72 is abundantly expressed in the liver under normal conditions [195]. A reduction in HSP72 has been seen in the muscle of T2D patients [192]. It has also been demonstrated that loss of function of anti-inflammatory HSP70 may increase the

progressive liver inflammation influence of NASH [194]. It is possible that HSP72 expression has a critical role in blocking hepatic inflammation and KCs activation.

The correlation between the progression of NASH and expression of HSPs in the liver has been clearly demonstrated [194]. It has been revealed that activation of KCs and production of inflammatory cytokines may result in downregulated expression of HSP72. In contrast, upregulation of HSP72 improves insulin sensitivity and inflammation contributing to insulin resistance and obesity [196]. In humans, there is a significant reduction in HSP72 in the liver paralleled by inflammatory cells that promote NAFLD development and the progression of NASH [194]. Overexpression of HSP72 in mice prevents HFD-induced JNK phosphorylation and impaired insulin signalling [196]. Consistent with this, another study has suggested that increased hepatic HSP72 results in reductions in glucose intolerance and plasma insulin level, hepatic TG content and adiposity in HFD-induced hepatosteatosis mice [172].

The anti-inflammatory HSP72 pathway has been revealed in many cellular activities and is expressed at low level under metabolic disease states [197]. Overexpression of HSPs is sufficient to inhibit LPS-induced TNFα, IL-1β, IL-6 and IL-12 response in the liver [198]. Overexpression of HSP90, a negative regulator of HSP72, increases the activity of hepatitis B virus [192]. Interestingly, HSP72 is involved in the pathogenesis of NASH. Reduction of HSP72 paralleled by similar reductions in HSF1 in KCs may contribute to NAFLD progression and associated ballooned hepatocytes in NASH [194, 199]. Studying the link between compounds and HSP72 is essential to understand how this association can prevent inflammation. Importantly, docking simulation technique has confirmed that there is a strong association between Mtr and HSP72. Further study

suggests that Mtr treatment improves HFD-induced hepatosteatosis in mice, at least in part by upregulating the expression of HSP72 in the liver [172].

As discussed in **Section 1.6.4**, Mtr is one of the oldest drugs used to treat inflammation, and has been proposed as a possible anti-inflammatory drug [182]. This proof-of-principle study reports the potential efficacy of Mtr for the treatment of hepatic inflammation [200] via HSP72 [172, 201].

1.11 Summary, study aims and hypothesis

This review was conducted to identify gaps in the current literature and the aims of this thesis were suggested. Subsequent studies were dedicated to investigate the therapeutic efficacy and underlying molecular mechanisms of Mtr in this disease.

NAFLD is the most common chronic liver disease, affecting one-third of people globally (**Section 1.3.1**) with a high rate of progression to NASH (**Section 1.6**) and serious complications (**Section 1.7**). Although in vitro and animal models have been developed, and may be appropriate as preclinical models of NASH, there is no single animal model that can fully resemble metabolic NASH in humans (**Section 1.8**). Different animal models are therefore needed for the proper evaluation of new therapeutics for NASH. While several drugs have been considered for the control of NAFLD and the progression of NASH (**Section 1.9**), none of them satisfy the requirements for the treatment of this serious condition. In the quest to find an effective and safe treatment for NAFLD and its progressive form, Mtr was selected for the

investigation in this thesis on the basis of its reported pharmacological properties and safety.

Therefore, the overall purpose of this thesis was to investigate the therapeutic effects and mechanisms of Mtr for the treatment of NAFLD and NASH. To address this objective, three specific aims were designed as follows:

Aim 1: To investigate the effects of Mtr on lipogenesis-induced hepatosteatosis and associated disorders in glucose homeostasis (Chapter 3).

Aim 2: To investigate the effects of Mtr on NASH associated with inflammation and fibrosis in MCD-fed mice (Chapter 4).

Aim 3: To investigate the mechanisms involved in the therapeutic effect of Mtr in NAFLD/NASH (Chapters 3 and 4) including HSP72 and the role of macrophages in LPS-stimulated inflammation (Chapter 5).

The working hypothesis was as follows: Mtr can alleviate hepatic steatosis, inflammation, injury and fibrosis by mechanisms involving HSP72 and the inhibition of inflammation.

The overall design of the studies for these aims is illustrated below. The results from these studies are likely to provide new insight into the therapeutic effects of Mtr in the development of NAFLD and progression of NASH. The findings may help decide

whether Mtr is a promising new drug for the treatment of NAFLD, particularly of NASH.

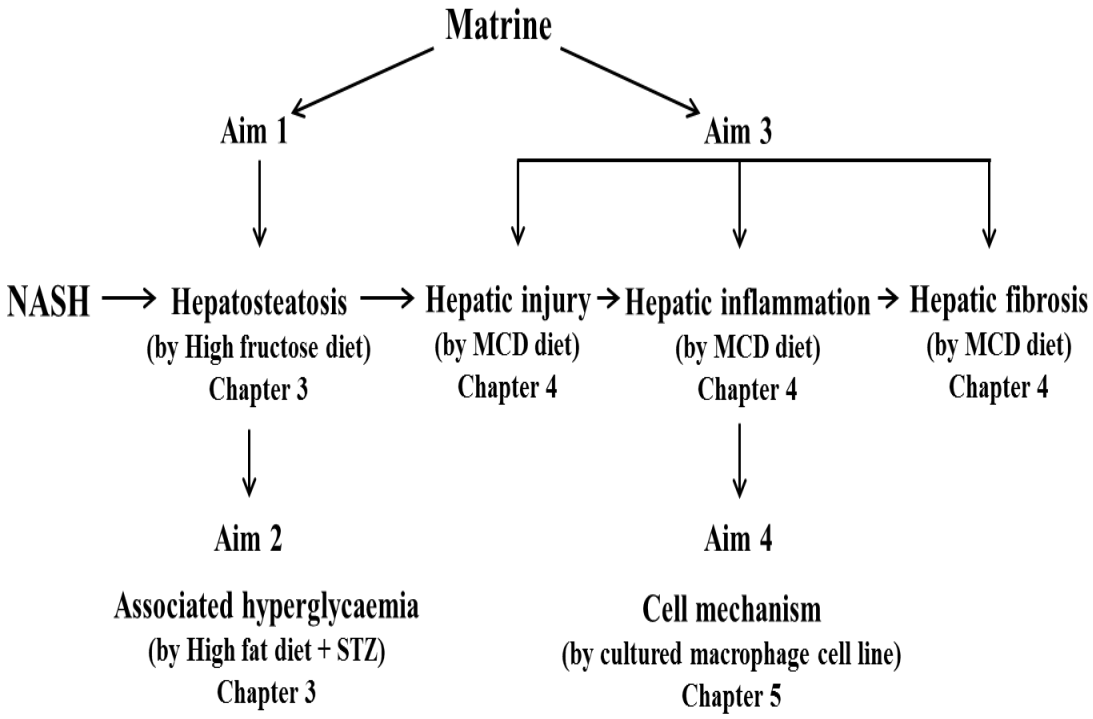

Figure 1.9 Schematic view of the research aims.

Chapter 2 Research Design and Methodology

2.1 Introduction

This section presents all the common methods and techniques used for the studies presented in Chapters 3, 4 and5. Special methods and techniques for a particular study are described separately in corresponding Chapters.

2.2 Rodent models

The Animal Ethics Committee of RMIT University approved all experimental procedures (AEC #1012 and #1415) in accordance with the National Health and Medical Research Council of Australia Guidelines on Animal Experimentation [202, 203].

All animal studies were conducted in male C57BL/6J mice (10 week old and weight 22-25 g) that were purchased from the Animal Resources Centre (Perth, Australia). The animals were kept in a temperature-controlled room (22 ± 1°C) on a 12-h light/dark cycle. Before any procedure was performed, mice were first allowed to acclimatize for at least one week while they were fed *ad libitum* with a standard normal chow diet. The standard chow diet (CH; Meat Mouse Diet) was purchased from Specialty Feeds, Western Australia. It contains 12% calories from fat, 23% from protein, and 65% from carbohydrate. The digestible energy in this diet is 3.34 kcal/kg.

The study animal models were undertaken separately for each animal model Chapter. The number, group and statistical analysis were determined for each model to address the specific

research questions on the hypotheses. Three animal models design including high fructose, HFD-STZ and MCD mice models were demonstrated in Chapter 3 and 4 respectively.

2.3 Measurement of plasma and tissue parameters

Blood samples were collected using heparinized capillary tubes (SteriHealth Laboratory Products, Australia) to prevent clotting. Blood samples were collected from the tail tip and then immediately mixed with the same volume of saline and stored on ice. Plasma separated by centrifugation (13,000 RPM for 1 min) was transferred to a new Eppendorf tube and stored at -80°C for subsequent measurements.

Mice were killed by cervical dislocation and liver samples were immediately freeze-clamped and stored in -80°C. Next, freeze-clamped liver tissue were weighed and placed in different sets of Eppendorf tubes depend on the experimental requirements; such as western blotting set for 30 and 20 mg of liver tissue for western blotting and RT-PCR technique, respectively.

2.4 Glucose determination

The body weight of mice was measured in the afternoon one day before the glucose tolerance test (GTT) for the calculation of glucose loads. On the day of GTT, food removed from mice cages for 5-7 hours before glucose was injected i.p. at a dose indicated in each study. Blood glucose levels were analysed at described time (0, 15, 30, 60 and 90 min) points for the

measurement of blood glucose using an Accu-Chek glucometer (Roche Diagnostics, Australia). The absolute volumes used were depended on the experimental requirements.

2.5 Extraction and determination of tissue triglyceride

The triglyceride level in plasma and liver extracts were determined by a Peridochrom triglyceride GPO-PAP kit (Roche Diagnostics), according to the manufacturer's instructions (Roche Diagnostic, Australia). Triglyceride reagent (300 µl) added to all plasma samples (5 µl), and then incubated at 37°C for 10 min. A FlexStation microplate reader (Molecular Devices, USA) was used for reading the absorbance on microtiter plate at 485 nm. A standard curve was created using internal standards (glycerol solution, 0.21 mg/ml, Roche, Catalogue No.166588).

With regard to measuring liver triglyceride, liver samples were immediately freeze-clamped and stored in -80°C after mice were killed by cervical dislocation. Triglyceride extraction started with a pre-weighed sample of tissue (30 mg liver). Liver tissue was homogenised in 2 ml of chloroform/methanol (2:1) using a glass homogeniser. After transferring the homogenate to a clean 15 ml tube, the homogeniser was rinsed with another 2 ml of chloroform/methanol (2:1) and added to the homogenate. To ensure the complete solubilisation of the triglyceride, the tubes were tightly capped and rotated at room temperature overnight. A sodium chloride (0.6% NaCl, 2 ml) was added to the tubes followed by centrifugation at 2,000 RPM for 10 min to separate the aqueous from the organic phases. The lower chloroform layer contained triglycerides was carefully extracted and then

transferred into a glass vial and dried completely under air at 45°C. An absolute ethanol (500 µl) dissolved in the extract and then triglyceride concentration was determined by a Peridochrom triglyceride GPO-PAP reagent (Roche Diagnostics, Catalogue No. 11730711).

2.6 Protein quantification

Protein concentrations were determined through use of commercially available colorimetric bicinchoninic acid (BCA) protein kit (Sigma-Aldrich, #B9643). Usually, 1 µl tissue lysate was added to 19 µl dH2O to dilute lysate, then 200 µl BCA reagent mix (50 parts reagent A to 1 parts reagent B) was added to detect concentration of protein in the each sample. Solutions were mixed and incubated at 37°C for 30 mins prior to the determination of absorbance by spectrophotometry at 562 nm using a Polarstar Optima microplate reader (BMG Lab Technologies, Germany). In every BCA assay, varying dilutions of BSA protein were included to create a standard curve between the ranges of 0 µg/ml to 2.0 µg/ml

2.7 Western Blotting

2.7.1 Reagents / Buffers

The table below showed the main buffers and solution used in western blotting technique.

Table 2.1 The preparation of western blotting reagents and buffers

Name	Preparation
RIPA buffer	65 mM Trizma® base (Tris, Sigma-Aldrich, #T1503), 150 mM NaCl, 5mM EDTA, 1% Nonide-P 40 Substitute (NP-40, Sigma-Aldrich, #74385), 0.05% Sodium-deoxycholate (Sigma-Aldrich, #D6750), 0.1% (w/v) Sodium dodecyl sulphate (SDS, Sigma-Aldrich, #L4390), 10% Glycerol (Sigma-Aldrich, #49770), pH 7.5 and stored at 4°C
Lysis buffer	10 mM Sodium fluoride (NaF, Sigma-Aldrich, #S7920), 1 mM Sodium orthovanadate (Na3VO4, Sigma-Aldrich, #S6508), 1 mM Phenylmethanesulfonyl fluoride (PMSF, dissolved in 100% Ethanol, Sigma-Aldrich, #78830), and 10 µl/ml Protease/Phosphatase inhibitor (Sigma-Aldrich, #P5726) in RIPA buffer
4xLaemmli's buffer (100ml)	8.2 g SDS, 40ml Glycerol, 50 ml 0.5 M Tris, 500 µl 1% Bromo-phenol blue (Sigma-Aldrich, #114391) in dH2O, pH 6.8 and stored at -20°C. Before use, added 6.2 mg DL-Dithiothreitol (DTT, Sigma-Aldrich, #D9779)

Name	Preparation
Running gel	1.5 M Tris Buffer (pH 8.8), 30% Acrylamide/Bis-acrylamide (Sigma-Aldrich, #A3574), 10% (w/v) SDS, dH2O, 10% Ammonium persulfate (APS, Sigma-Aldrich, #A9164), Tetramethylethylene diamine (TEMED, Sigma-Aldrich, #T9281)
Stacking gel	0.5 M Tris Buffer (pH 6.8), 30% Acrylamide/Bis-acrylamide, 10% (w/v) SDS, dH2O, 10% APS and TEMED
10x Running buffer (1L)	30 g Tris, 144 g Glycine (Sigma-Aldrich, #G8898) and 10 g SDS in dH2O, pH 8.8 and stored at room temperature
10x Transfer buffer (1L)	30 g Tris, 144 g Glycine in dH2O and stored at room temperature
10x TBS (1L)	24.2 g Tris and 80 g NaCl in dH2O, pH 7.6 and stored at room temperature
1x TBS-Tween (TBST, 1L)	100 ml 10x TBS buffer and 500 µl Tween® 20 (Sigma-Aldrich, #P9416) in 900 ml dH2O and stored at room temperature
Blocking buffer	3% (g/100ml) Bovine Serum Albumin (BSA, Sigma-Aldrich, #A9418) in 1x TBST and stored at 4°C
Stripping buffer (1L)	6.25% 1 M Tris-HCl (pH 6.7), 10% (w/v) 20% SDS in dH2O and stored at room temperature. Added 100 mM 2-Mercaptoethanol (Sigma-Aldrich, #M7154) before use

2.7.2 Sample preparation

Tissue samples were homogenized with a pestle mixer in an ice-cold RIPA buffer containing 10 μL/mL protease inhibitor cocktail (Sigma-Aldrich, #9599), 10 μL/mL phosphatase inhibitor cocktail (Sigma-Aldrich, #P5726), 10 mM NaF (Sigma-Aldrich, #S7920), 1 mM Na3VO4 (Sigma-Aldrich, #450243) and 1 mM phenylmethanesulfonyl fluoride (Sigma-Aldrich, #78830). Tissue lysates were then centrifuged at a speed of 20,000 × g for 15 minutes at 4°C. The protein concentrations in the supernatant were determined by bicinchoninic acid assay (Sigma-Aldrich, #B9643). Protein samples were then diluted with water and mixed with 4× Laemmli buffer together with 1 mM DTT. Finally, samples were boiled at 95°C for 5 minutes to denature the protein.

2.7.3 PAGE gels preparation

Sodium Dodecyl Sulfate PolyAcrylamide Gel Electrophoresis (SDS-PAGE) is a standard technique used for separating proteins according to their molecular weight.

Table 2.2 Recommended Polyacrylamide % for Separation in Denaturing Gels

Protein size (kDa)	Gel percentage (%)
25-200	8%
15-100	10%
10-70	12%
4-50	14%

Table 2.3 Composition of running gel and stacking gel

	Running Gel (in ml) (for two gels)				
#	**Solution**	**8%**	**10%**	**12%**	**14%**
1	1.5M Tris Buffer, pH 8.8	5	5	5	5
2	30% Acrylamide/Bis-acrylamide	5.3	6.7	8.0	9.3
3	10% SDS	0.2	0.2	0.2	0.2
4	dH_2O	9.5	8.1	6.8	5.5
5	10% APS	0.2	0.2	0.2	0.2
6	TEMED	0.02	0.02	0.02	0.02

	Stacking Gel (for two gels)	**ml**
1	0.5M Tris Buffer, pH 6.8	1.25
2	30% Acrylamide/Bis-acrylamide	1.7
3	10% SDS	0.1
4	dH_2O	7.0
5	10% APS	0.1
6	TEMED	0.02

2.7.4 Immunoblotting

Following the gel preparation, the denatured protein samples (20 μg/well) and standard protein ladders (5 μL/well, Bio-Rad, #161-0374) were loaded to the gel and separated at 120 V until the protein ladder above or below the protein of interest were well separated. Subsequently, proteins in the gel were transferred to the PVDF membrane

(Bio-Rad, #162-0177) in a transfer buffer at 100 V for 2 h. The PVDF membrane was incubated in 3% BSA (in TBST buffer, Sigma-Aldrich, #A9418) at room temperature for 1 h to block the non-specific binding and then incubated with the primary antibody overnight at 4ºC. After 1 h of wash in TBST, the membrane was incubated in the horseradish peroxidase conjugate secondary antibody (Santa Cruz, #sc-2004 for rabbit, #sc-2005 for mouse) and followed by 1 h of wash in TBST. Enhanced chemilumescent (Perkin Elmer, #NEL113001EA) was used for the detection. Densitometric analysis was performed using Image Lab software 5.0 (Bio-Rad Laboratories). The primary antibodies are listed in **Table 2.4**. Antibodies from Cell Signaling and Abcam were diluted 1:1000 and these from Santa Cruz were diluted 1:500, with a TBST buffer containing 1% BSA, 0.02% sodium azide (Sigma-Aldrich, #71289) and 0.0025% phenol red (Sigma-Aldrich, #32661). The bound antibody was detected using a chemiluminescence system with western lighting ultra solution (Perkin Elmer, #NEL113001EA). The membranes were exposed in a ChemiDoc (Bio-Rad LaboratoriesInc., USA) for images capturing for a sufficient time. Densitometry analysis was performed using Image Lab (version 4.1; Bio-Rad Laboratories, Hercules, CA, USA) [45, 88].

2.7.5 Antibody list

Table 2.4 list of common antibodies

Pathway	Name	Supplier	Catalogue No.
Lipolysis	SREBP1c		
	ChEBP		
	ACC	Cell signaling	3662
	SCD1		
	FAS		
ER stress	eIF2α	Cell signaling	9722
	CHOP	Santa cruz	sc-793
	IRE1	Abcam	ab37073
Inflammation	NLRP3	AdipoGen	20B-0006-C100
	MCP-1	Cell signaling	2027
Fibrosi	TGFβ		3709
	Smad3	Cell signaling	5678
	Caspase-1	Santa cruz	G2914
Loading control	GAPDH	Cell signaling	2118
	Tubulin		3873

2.8 Real-time quantitative reverse transcription polymerase chain reaction (qRT-PCR)

2.8.1 Isolation of RNA from mice

Liver tissues (20-30mg) were homogenised in 1 ml TRIZOL® reagent (Invitrogen, Catalogue No.15596026). The homogenate was mixed with 200 µl of Chloroform

(VWR, Catalogue No.22711324) by inverting several times, and incubated at room temperature for 5 min. The homogenates were subsequently centrifuged at 13,000 rpm for 15 min at 4°C. The upper aqueous phase containing RNA was collected and mixed with 500 µl of isopropanol (Sigma-Aldrich, Catalogue No.I9516). After another centrifugation at 13,000 rpm for 20 min at 4°C, the supernatant was removed. The remaining RNA precipitate was washed twice with 500 µl 75% ethanol with vortex. The ethanol was removed by centrifugation at 13,000 rpm for 5 min at 4°C. The air-dried RNA pellet was dissolved in 100 µl of DEPC-treated water (Invitrogen, Catalogue No.AM9916) for the measurement of RNA concentration.

2.8.2 Measurement of RNA concentration

The liver RNA purity and concentrations were assessed using a NanoDrop Spectrophotometer (Eppendorf Thermo Scientific, Australia) at the absorbance of 260 and 280 nm, with DEPC water as a blank. Each RNA sample (1.0 µl) was loaded onto the sampling platform for the measurement of RNA concentration. The absorption ratio of 260/280 nm is used to assess the purity of RNA samples (Ratio should be between 1.8 and 2.0).

2.8.3 Complimentary DNA synthesis by reverse transcription

Complimentary DNA synthesis by reverse transcription Purified RNA with known concentrations was used to generate the complementary DNA (cDNA) using a Reverse Transcription System (Bio-Rad Laboratories Inc., USA) with random primers according to the manufacturer's instructions. The RNA concentration of each sample

was normalised to 1 µg/8 µl with DEPC water on ice. To remove DNA contamination, 1 µg of RNA was mixed with 2 µl of DNase I (Invitrogen, Catalogue No.18068-015), and incubated at room temperature for 15 min. After the removal of DNA, 1 µl of 25 mM EDTA was added and incubated for 10 min at 65°C to inactivate DNase I. The purified RNA (2 µl) was reverse transcribed using a high capacity cDNA reverse transcription kit (Life Technologies, Catalogue No. 4374967) (2 µl of reverse transcription buffer, 0.8 µl of dNTP mix, 2 µl of random primers, 1 µl of reverse transcriptase and 12.2 µl of DEPC water). Reverse transcription polymerase chain reaction was carried out using the following steps: equilibrated at 25°C for 10 min, 37°C for 2 hr, 85°C for 5 sec, and finally maintained at 4°C. The cDNA products from reverse transcription reactions were stored at 4°C to use for RT-PCR analysis.

2.8.4 Real-time polymerase chain reaction

The cDNA samples were analysed for genes of interest by RT-PCR using the SYBR Green RT-PCR system (Bio-Rad Laboratories Inc., USA). A reaction master mixture (1x IQ SYBR Green Supermix (Bio-Rad Laboratories Inc., USA; Catalogue No.170-8882), 500 nM forward primers and 500 nM reverse primers, DEPC water to a final volume of 24 µl) for each gene of interest was prepared and added to each 1 µl cDNA sample in a sterile 96-well plate. The plate was placed in a controlled-temperature heat block equilibrated at 50°C for 2 min, 95°C for 3 min and 40-50 cycles of 95°C for 15 seconds, 72°C for 30 seconds. The gene expression from each sample was analysed in duplicates and normalised against the ribosomal housekeeper gene 18S (GeneWorks, Australia). All reactions were performed on the iQ™ 5 RT-PCR Detection System

(Bio-Rad Laboratories Inc., USA). The results are expressed as relative gene expression using the ΔCt method. Primers used for specific genes are in **Table 2.5**.

Table 2.5 Primer sequences for measurements of gene expressions

Gene	Primer Sequences
18S	Forward: 5'-CGCCGCTAGAGGTGAAATTCT-3'
	Reversed: 5'-CGAACCTCCGACTTTCGTTCT-3'
TNFα	Forward: 5'-CACAAGATGCTGGGACAGTGA-3'
	Reversed: 5'-TCCTTGATGGTGGTGCATGA-3'
IL1β	Forward: 5'-GACGGCACACCCACCCT-3'
	Reversed: 5'-AAACCGTTTTTCCATCTTCTTT-3'
IL6	Forward: 5'-ATTCCAGAAACCGCTATGAAGTTC-3'
	Reversed: 5'-GTCACCAGCATCAGTCCCAA-3'
CD68	Forward: 5'-TGACCTGCTCTCTCTAAGGCTACA-3'
	Reversed: 5'-TCACGGTTGCAAGAGAAACAT G-3'
Collagen 1	Forward: 5'-CTGCTGGTGAGAGAGGTGAAC-3
	Reversed: 5'-ACCAAGGTCTCCAGGAACAC-3

Each Chapter has designed with measuring specific and interest gene for diagnosis.

2.9 Statistical analysis

Throughout the thesis, results are presented as means ± SEM. For the comparison of only two groups, a Student's t test was used. One-way analysis of variance was used to assess the statistical significance across all groups. When significant differences were found, the Tukey-Kramer multiple comparisons post-hoc test was used to establish differences between groups. Differences at $P \leq 0.05$ were considered to be statistically significant and $P \leq 0.01$ were considered to be highly significant.

Chapter 3Effects of Matrine on Hepatosteatosis and Associated Disorders in Glucose Homeostasis

3.1 Introduction

The liver plays an important role in regulating whole-body lipid metabolism and glucose homeostasis. Excess accumulation of lipids (namely hepatosteatosis), either from endogenous DNL and/or influx of exogenous FAs, can disturb glucose homeostasis, increasing the risk of type 2 diabetes (T2D) [16, 113]. Although the degree of hepatosteatosis and T2D are not necessarily tightly coupled [204], inhibition of excess hepatic DNL has been shown to ameliorate hepatosteatosis and associated glucose intolerance [112]. Shulman and colleagues have also demonstrated that correction of hepatosteatosis in patients with T2D is important for hyperglycaemia control [36]. In a search for new therapeutic agents for the treatment of hepatic steatosis from DNL, we have taken the approach of repurposing existing drugs for these conditions [182, 205]. One main advantage of this approach is most existing drugs are well-known safety and pharmacokinetic profiles.

Mtr is a small molecule (M_W: 248) found in Sophora and is structurally different from the drugs currently used to treat T2D [7, 172, 184]. Mtr has been used clinically as a hepatoprotective drug for the treatment of tumors and viral hepatitis [184], where DNL is often increased [206]. A recent study from our laboratory found that Mtr is able to reduce hepatosteatosis, fasting blood glucose and glucose intolerance in high fat (HF)-fed mice [172]. However, the HF model does not exhibit the characteristics of DNL-induced hepatosteatosis and glucose intolerance because the accumulation of triglyceride (TG) in the liver is due to a direct influx of lipids into the liver from the HF diet [44, 45].

The liver is a major site of DNL production from carbohydrates [44] and interestingly the inhibition of hepatic DNL reduces hepatosteatosis and hyperglycaemia [112, 207]. It has been suggested that an increase in DNL is the second major source of lipid accumulation in the liver after circulating FFAs and contributes about 26% of patients with hepatosteatosis [2]. In mice, a high-fructose (HFru) diet induces hepatosteatosis as early as one day [46] prior to the development of glucose intolerance [44, 48, 114]. Dietary fructose is almost entirely metabolised in the liver in its first pass, and serves mainly as a substrate for DNL in both animals [46, 47] and humans [48-51] . HFru diets increase the expression of lipogenic transcription factors, sterol regulatory element binding protein (SREBP1c) and carbohydrate response element binding protein (ChREBP) which upregulate lipogenic genes. Upregulation of these lipogenic transcription factors can result in hepatosteatosis and glucose intolerance via promoting DNL [99, 105]. Notably, HFru-stimulated hepatic DNL via SREBP1c is dependent on the activation of the ER stress pathway [44].

The primary aim of the present study was to investigate whether the hepatoprotective drug Mtr can limit hepatosteatosis and the associated glucose intolerance that usually results from increased DNL in HFru-fed mice. If established, the second aim was to investigate whether the action of Mtr is mediated via the ER stress pathway. Finally, we also evaluated whether Mtr assists glycemic control in a T2D mouse model generated by a combination of HF and streptozotocin (STZ) where an increased DNL via SREBP1c is also involved [88, 176].

3.2 Materials and methods

3.2.1 Animals and diets

The experiments described in this study were approved by the Animal Ethics Committee of RMIT University (Application ID: 1012) and conducted in compliance with the guidelines of the National Health and Medical Research Council of Australia for Animal Experimentation. C57BL/6J mice aged 10-12 weeks and weighing 21-24 g were obtained from the Animal Resource Centre Pty. Ltd. (Perth, Australia). The animals were housed in a temperature-controlled room (22 ± 1˚C) on a 12-h light/dark cycle with free access to food and water. Mice were fed ad libitum for 1 week on a normal chow diet (~70% calories from starch, ~10% calories from fat, and ~20% calories from protein; Gordon's Specialty Stock Feeds, Yanderra, Australia). Mtr (≥ 98% by HPLC) was purchased from Sigma Aldrich.

Two sets of animal experiments were performed. In the first set of experiments, mice were fed a HFru diet (35% fructose, 35% starch, ~10% fat and ~20% protein) to generate hepatosteatosis. Mice were fed for 8 weeks with or without Mtr at a dose of 100 mg/kg every day as a food additive in the last 4 weeks as described previously [7, 172]. Body weight gain and food intake were measured twice a week. For blood glucose levels, blood samples were collected from the tail tip and measured using a glucometer (AccuCheck II; Roche, New South Wales, Castle Hill, Australia) after 2 weeks of Mtr treatment. In the second set of experiments, the effects of Mtr on hepatosteatosis and hyperglycaemia were examined in a T2D model induced by HF feeding in combination with low doses of STZ as previously reported [88, 208, 209].

Briefly, mice were fed a HF diet (45% calorie from lard, 20% calories from protein and 35% calories from carbohydrate) for 14 weeks to induce insulin resistance. After 8 weeks of HF feeding, mice were injected with STZ at a low dose (40 mg/kg per day, ip) for 5 consecutive days to reduce the level of plasma insulin by ~50% [88, 208, 209]. One week after the last injection of STZ, fasting blood glucose was usually increased by 50-100% (Hyperglycaemia, defined as T2D). The T2D mice were then divided into 2 groups: one group receiving Mtr added in the HF diet (100 mg/kg/day) for 4 weeks (T2D-Mtr) whereas the other group was fed HF alone (T2D-Con) for the same period of time. During the period of Mtr treatment, fasting blood glucose was monitored once a week. A normal control group of mice (CH-Con) was included for the same period. At the end of both sets of experiments, mice were killed by cervical dislocation and liver tissues were collected and freeze-clamped immediately for further analysis.

3.2.2 Assessment of the effect on hepatosteatosis

Hepatosteatosis was assessed by measuring TG content in the liver. Mice were fasted for 5-7 h before being killed; the liver was collected and freeze-clamped immediately. As described previously [45, 88] plasma and liver TG levels were determined with a Peridochrom triglyceride GPO-PAP biochemical kit (Roche diagnostics). The method of lipid extraction from liver with chloroform/methanol has been described previously [46].

3.2.3 Assessment of the effect on hepatic FA oxidation

FA oxidation was assessed in fresh liver tissue *ex vivo* as described [44, 45]. Briefly, fresh liver samples were homogenised in an isolating medium which contained 100 mM sucrose, 50 mM Tris, 100 mM KCl, 1 mM KH_2PO_4 and 0.1 mM EGTA, 0.2% FA-free BSA at pH 7.0. The liver homogenate was incubated with [^{14}C]-palmitate and [^{14}C]-CO_2 produced from the incubation was collected in 1 M sodium hydroxide. Palmitate oxidation rates were determined by counting the ^{14}C radioactivity of captured CO_2 and acid-soluble metabolites and oxidation rate were expressed as nanomoles of CO_2 per gram of wet weight per hour [44].

3.2.4 Assessment of the effects on DNL and ER stress

DNL and ER stress were assessed by immunoblotting with specific anti-bodies for the key proteins in the DNL, ER stress and heat shock protein (HSP) pathways based on our recent work [7, 44-46, 172]. Briefly, freeze-clamped liver was homogenized in ice-cold lysis buffer supplemented with fresh protease inhibitor and phosphatase inhibitor (Sigma Aldrich). The key proteins in the DNL pathway included SREBP-1 (Santa Cruz), ChREBP (Abcam), acetyl-CoA carboxylase (ACC, Upstate), fatty acid synthase (FAS, Abcam) and stearoyl-CoA desaturase 1 (SCD-1, Cell Signaling). The key proteins measured in the ER stress pathway included inositol-requiring kinase 1 (IRE1, Abcam), eukaryotic translation initiation factor 2α (eIF2α, Cell Signaling) and CHOP (Santa Cruz). The effect on the HSP pathway was assessed by heat shock protein 72 (HSP72, Abcam) based on our recent work [7, 172]. Proteins were quantified using a

ChemiDoc and densitometry analysis was performed using Image Lab software (Bio-Rad Laboratories, USA).

3.2.5 Statistical analysis

As described in **Chapter 2 Section 2.9**.

3.3 Results

3.3.1 Effects on body weight, adiposity, hepatosteatosis and glucose tolerance in HFru-fed mice

HFru feeding is a well-defined model of hepatosteatosis, visceral adiposity and glucose intolerance resulting from increased DNL in the liver [44]. As expected, HFru feeding moderately increased the mass of epididymal fat (by 40%, $P < 0.01$) without altering body weight or food intake ($P > 0.05$) (Figure 3.1A-C). The TG content (indicative of hepatosteatosis) was increased dramatically in the liver (by 3 fold) but only moderately in muscle (~35%) (Both $P < 0.01$; Figure 1D). As shown in Figure 3.1E, HFru-fed mice also showed moderate in glucose intolerance.

Administration of Mtr prevented the moderate body weight gain (8-10%) in HFru-fed mice during this period of time (Figure 1A). It corrected HFru-induced increases in epididymal fat, liver TG content and glucose intolerance (all, $P < 0.01$ vs untreated HFru-fed mice) to the levels similar to CH-fed normal mice (Figure 1B-E). Although

not significantly reduced, muscle TG content in Mtr-treated HFru-fed mice was no longer different from the value of CH-fed normal mice (Figure 3.1D).

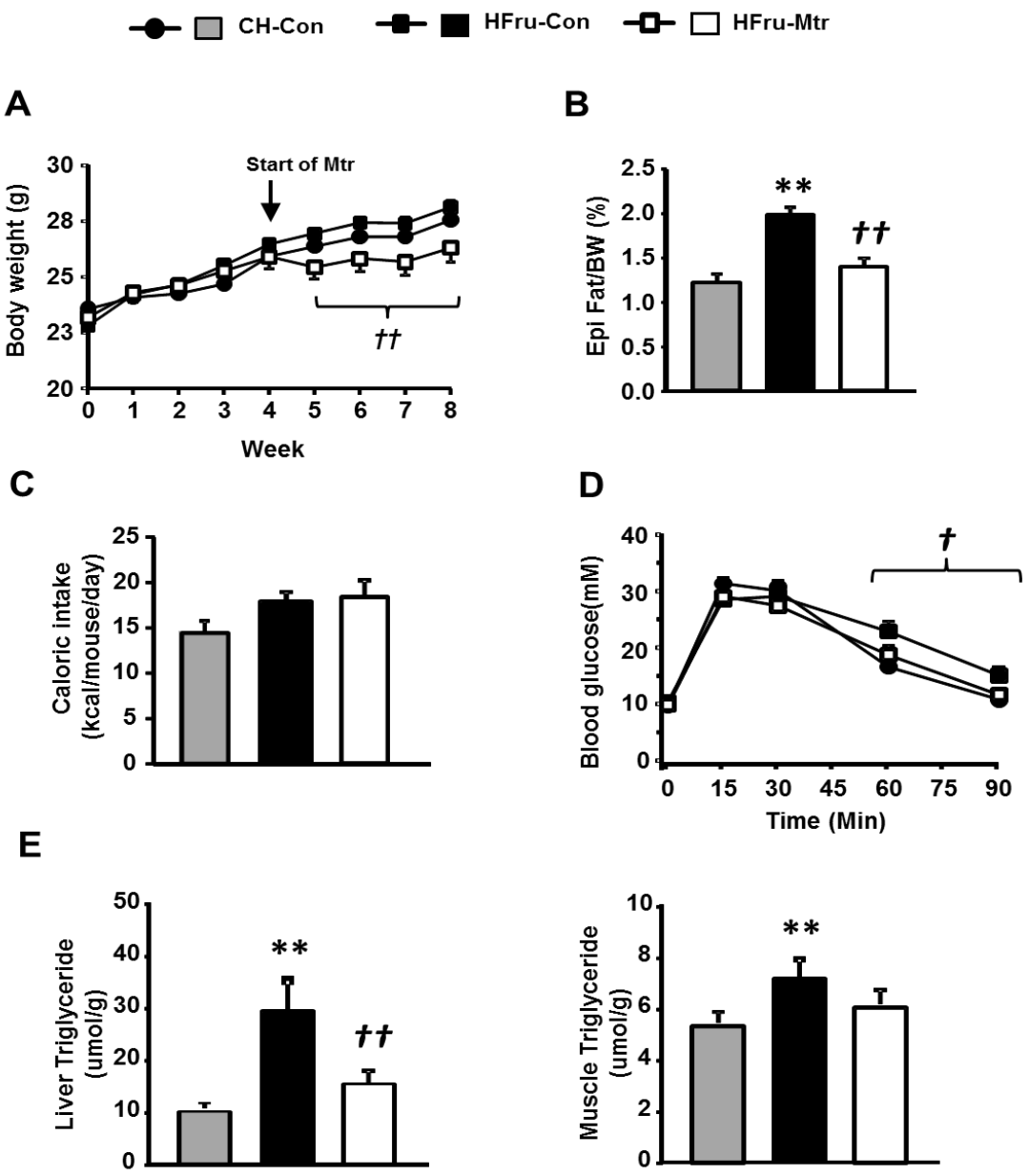

Figure 3.1 Effects of Mtr on body weight gain, visceral adiposity, hepatosteatosis and glucose tolerance in HFru-fed mice.

Mice were fed a high-fructose (HFru) diet for 8 weeks and matrine (Mtr, 100 mg/kg per day in diet) was administered in the last 4 weeks. A glucose tolerance test (GTT at 3g

glucose/kg BW, ip) was conducted after 2 weeks of treatment with Mtr. Epididymal (Epi) fat weight and liver TG content were determined at the end of the study. (A) Body weight gain, (B) Epididymal fat weight as a percentage of body weight, (C) Caloric intake, (D) Glucose tolerance and (E) TG content in liver and muscle. $^{**}P < 0.01$ vs CH; $^{\dagger}P < 0.05$, $^{\dagger\dagger}P < 0.01$ vs HFru (n=7-8 mice/group).

3.3.2 Effects on FA oxidation and DNL in the liver of HFru-fed mice.

We first examined whether Mtr treatment may promote FA oxidation in the liver of HFru-fed mice. As shown in **Figure 3.2A**, palmitate oxidation by the liver homogenates was not affected by the treatment with Mtr, suggesting that the reduced hepatosteatosis by Mtr is not likely to be due to an increased FA oxidation in the liver. We next examined the DNL pathway because HFru-induced hepatosteatosis is believed to result from the stimulation to this pathway in the liver [45-47]. As expected, HFru-fed mice exhibited dramatic increases in DNL proteins in the liver (**Figure 3.2B-E**), including SREBP-1c (by 2-fold), ChREBP (by 33%) ACC (by 3-fold), FAS (by 3.4 fold) and SCD-1 (by 4-fold) (all $P < 0.05$). Interestingly, these lipogenic proteins except for ACC were significantly reduced by the treatment with Mtr, including SREBP-1c (by 45%, $P < 0.01$), ChREBP (by 33%, $P < 0.05$), SCD-1 (by 32%, $P < 0.01$) and FAS (by 24%, $P < 0.05$). These results suggest that the reduced TG content in the liver by Mtr can be attributed to its inhibitory effect on HFru-induced increase in hepatic DNL.

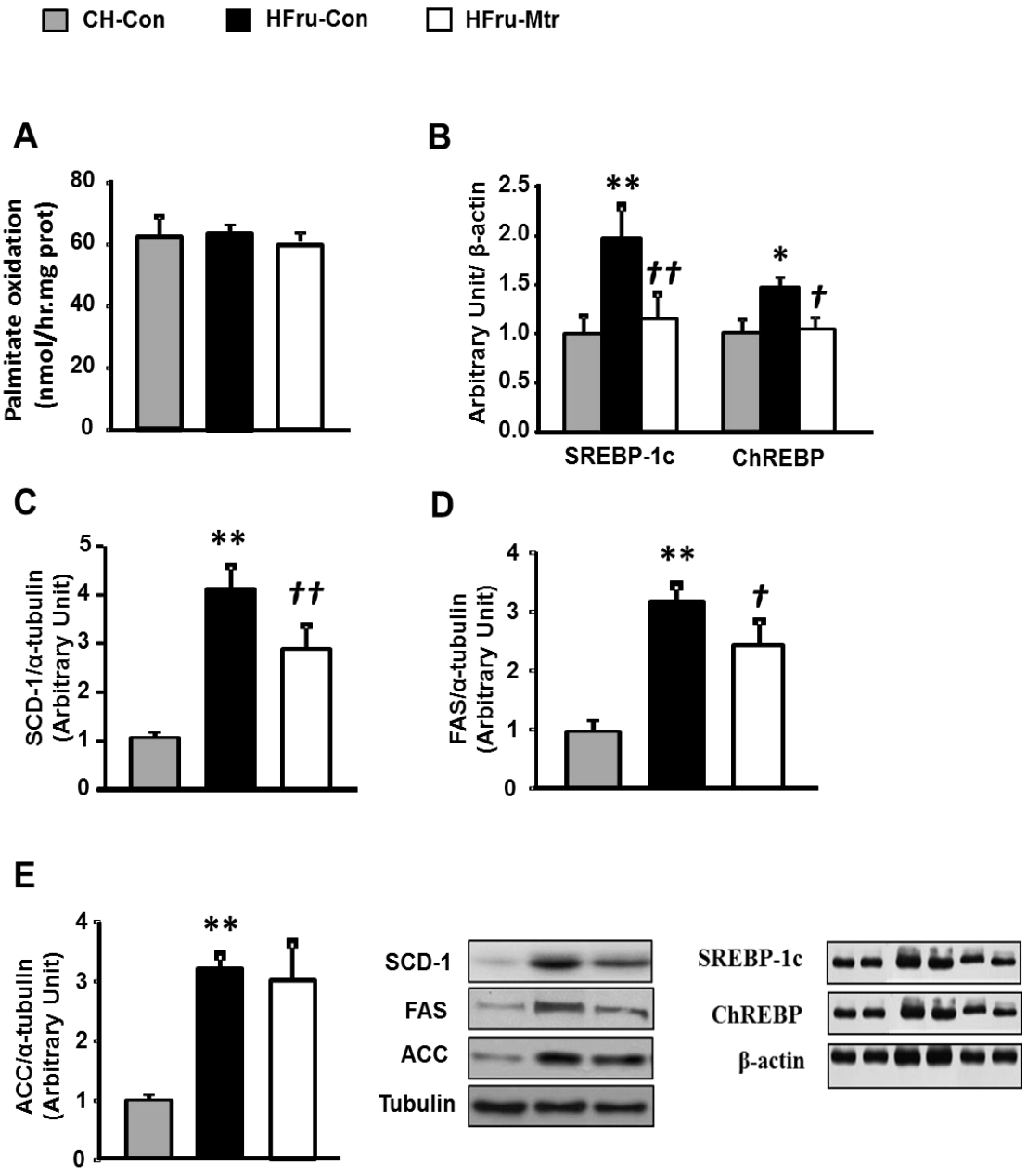

Figure 3.2 Effects of Mtr on FA oxidation and DNL pathways in the liver of HFru-fed mice.

FA oxidation was detected by incubating fresh liver homogenates with [14C]–palmitate and DNL was assessed by the protein expression of palmitate in this pathway. (A). Liver lyzates from mice were immunoblotted with the mature form of SREBP-1c and ChREBP (B), SCD-1 (C), FAS (D) and ACC (E) and then quantified for statistical

analysis. *P < 0.05, **P < 0.01 versus CH-Con; †P < 0.05, ††P < 0.01 versus HFru-Con, n = 7-8 mice per group.

3.3.3 Effects on ER stress and HSP72 in the liver of HFru-fed mice

By promoting DNL in the liver, the activation of ER stress represents a key step in the pathogenesis of hepatosteatosis [44, 59, 210]. As shown in Figure 3.3A, HFru-fed mice exhibited significant increases of the mature form of eIF2α (by 2-fold), CHOP (by 2.3-fold) and IRE1 (by 2-fold) along with the upregulation of the DNL pathway in the liver. Treatment with Mtr markedly reduced the protein levels of these hepatic ER markers towards the levels seen in CH fed mice. These results indicate that Mtr induced-suppression of ER markers may be associated with the improvement in lipogenesis, which could account for its beneficial effects on hepatosteatosis. Recent studies indicate that HSP72 is likely to mediate the effect of Mtr on hepatosteatosis and glucose intolerance [172, 192, 196]. As shown in Figure 3B, there was ~50% suppression of HSP72 (P < 0.05 vs CH fed mice) in the liver of HFru-fed mice and this reduction was reversed following treatment with Mtr (P < 0.05 vs untreated HFru-fed mice).

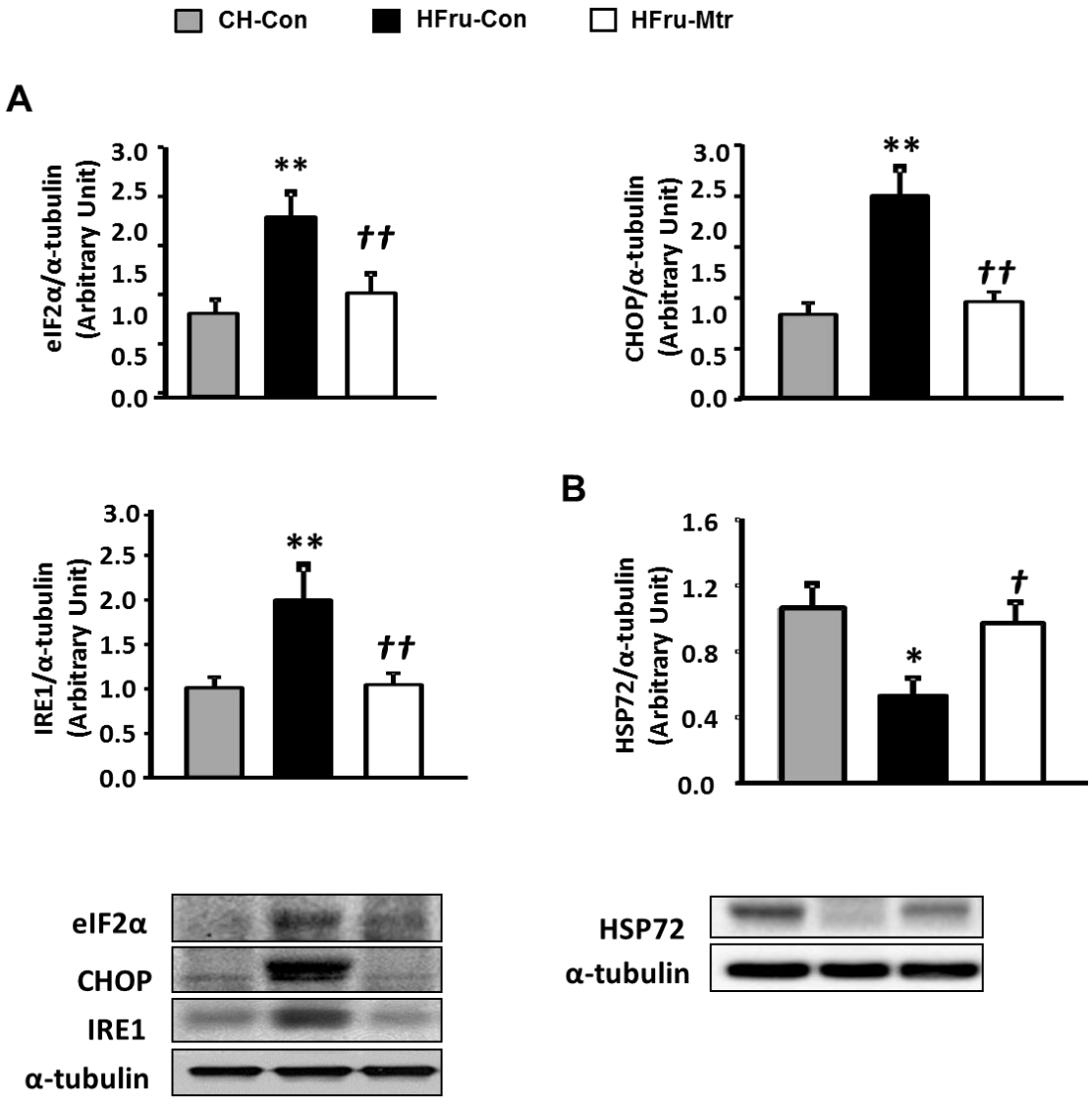

Figure 3.3 Effects on ER stress and HSP72 in the liver of HFru-fed mice.

Liver lyzates from mice were immunoblotted for (A) eIF2α, CHOP and IRE1 and (B) HSP72 and quantified for statistical analysis. **P* < 0.05, ***P* < 0.01 versus CH-Con; †*P* < 0.05, ††*P* < 0.01 versus HFru-Con, n = 7-8 mice per group.

3.3.4 Effects on hyperglycaemia in T2D mice

To investigate the relationship of the effect on hepatosteatosis with glycemic control, we examined the metabolic effects of Mtr in T2D mice generated by a HF diet in combination with low doses of STZ [88, 172, 176]. The body weight was reduced in HFD-STZ-induced T2D mice (by ~15%) and treatment with Mtr had no effect on the body weight (Figure 3.4A), while visceral adiposity remained unchanged in T2D-Con mice compared to CH-fed mice Mtr significantly reduced epididymal fat in T2D mice ($P < 0.05$, Figure 3.4B). T2D-Con mice displayed typical fasting hyperglycaemia and Mtr treatment significantly reduced the degree of the hyperglycaemia over the period of 4 weeks (by 20-30%, Figure 3.4C). As expected, HFD-STZ-induced T2D showed severe glucose intolerance but this was not attenuated by the treatment with Mtr (Figure AD).

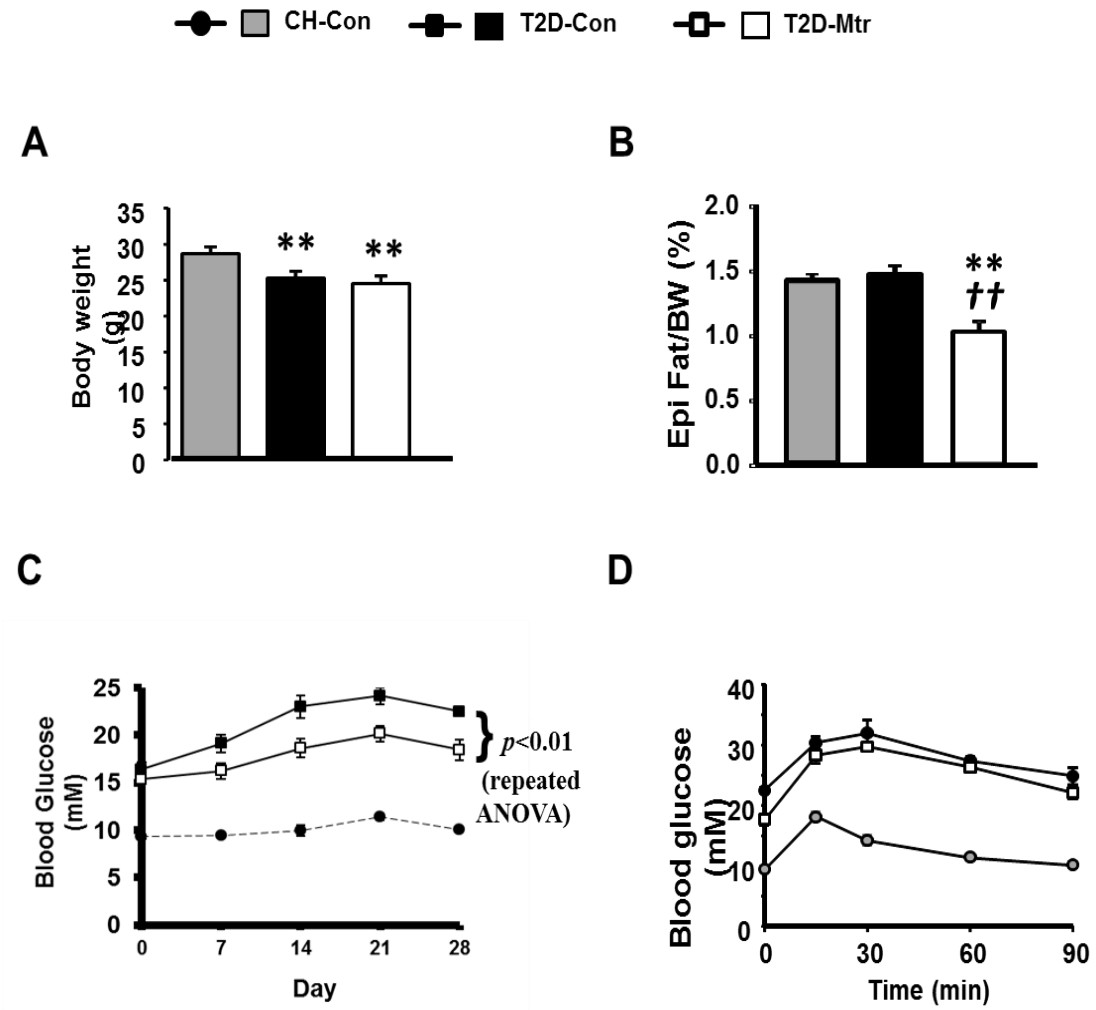

Figure 3.4 Effects of Mtr on body weight, visceral adiposity, blood glucose and glucose tolerance in T2D mice.

T2D was generated by a high-fat (HF) diet plus low-dose of STZ injections. After the development of hyperglycaemia, Mtr (100mg/kg per day in diet) was administered to diabetic mice for 4 weeks. Body weight at the end of the study (A).Epididymal (Epi) fat weight (B). Blood glucose levels (after 5-7 h of fasting) (C) were monitored once a week. An ipGTT (1.0g glucose/g body weight) was performed after 2 weeks of treatment with Mtr (D). ***P* < 0.01 vs CH-Con; ††*P* < 0.01 vs T2D-Con (n=7-8 mice/group).

3.3.5 Effect on TG levels in T2D mice

Recent studies indicate that hepatosteatosis can contribute to hyperglycaemia and hepatic insulin resistance [30, 44]. To determine whether the reduced hepatosteatosis by resulting from Mtr treatment is associated with the control of hyperglycaemia in T2D mice, we measured the TG content in the liver. As shown in Figure 3.5A and B, T2D mice exhibited hypertriglyceridemia and hepatosteatosis; however Mtr significantly reduced these conditions ($P < 0.05$). Together, these results clearly indicate that Mtr reduces the T2D-induced hepatosteatosis that is associated with hyperglycaemia and this could account for its beneficial effects on the regulation of lipid metabolism.

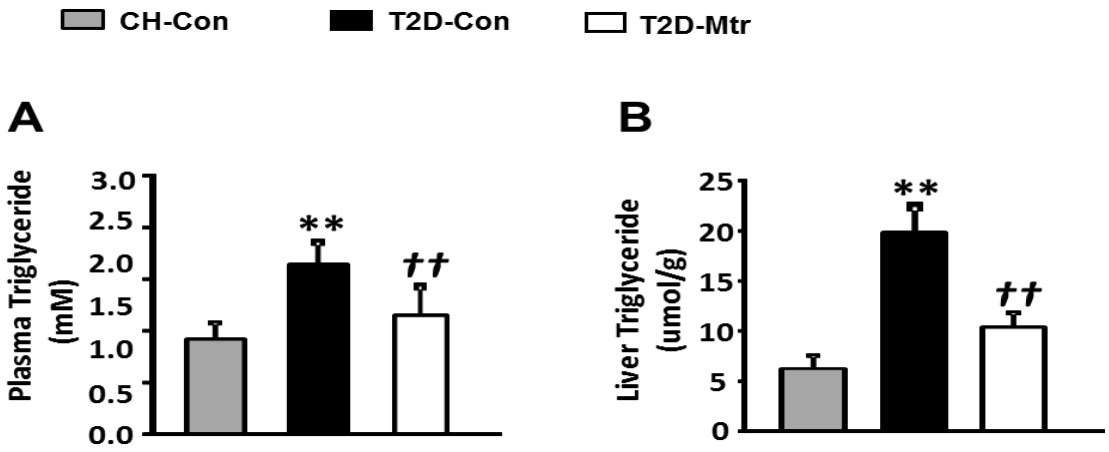

Figure 3.5 Effects of Mtr on TG level in the plasma and livers of T2D mice.

Plasma levels of TG were measured from blood samples collected in week 2 of the treatment (A). Liver TG content was determined from freeze-clamped samples obtained at the end of the study (B). $^{**}P < 0.01$ vs CH-Con; $\dagger\dagger P < 0.01$ vs T2D-Con (n=7-8 mice/group).

3.4 Discussion

The present study investigated whether the hepatoprotective drug Mtr can treat the hepatosteatosis and associated glucose intolerance in HFru-fed mice resulting from increased DNL. Consistent with previous studies from our laboratory [45, 46, 211], HFru-fed mice developed hepatosteatosis and glucose intolerance by promoting ER stress-associated DNL. Treatment of these mice with Mtr ameliorated hepatosteatosis and glucose intolerance. Within the liver, Mtr decreased the protein expression of DNL enzymes concomitant with reduced ER stress. This study further examined the effects of Mtr on hepatosteatosis in relation to glycemic control in T2D mice, which display a phenotype of hyperglycaemia and hepatosteatosis associated with increased DNL [88, 176]. The results showed that Mtr treatment reduced hepatosteatosis and improved hyperglycaemia. Collectively, these findings suggest that Mtr has the potential to be repurposed for the treatment of hepatosteatosis resulting from increased DNL and associated disorders in glucose metabolism.

Overconsumption of dietary fructose can lead to DNL and hepatosteatosis [44, 95], which in turn can result in glucose intolerance and contribute to hyperglycaemia [48, 75]. Therefore, correction of hepatosteatosis is beneficial for improving glucose homeostasis in the metabolic syndrome. For example, in obese patients with T2D, a reversal of hepatosteatosis can improve hepatic insulin action and glycemic control [36]. This study has investigated drugs that have previously been used for the treatment of liver conditions, in order to determine whether they can be repurposed to treat hepatosteatosis [182]. One such candidate is Mtr chosen because liver has been shown to be the major target site of Mtr [212, 213]. Indeed, the study from our laboratory has

demonstrated that Mtr is able to attenuate the increased fasting blood glucose and improve glucose tolerance in insulin resistant mice induced by a HF diet [172]. The same study found that these anti-diabetic effects of Mtr appears to result from its effect in reducing hepatosteatosis without affecting HF diet induced lipid accumulation in muscle.

Mtr is clinically used for treatment of chronic liver conditions including hepatocellular carcinoma and viral hepatitis with minimal adverse effects [172, 182, 184]. Interestingly, both hepatocellular carcinoma and viral hepatitis are associated with an increase in DNL [7, 214, 215]. Indeed, previous findings in 3T3L1 adipocytes have shown that Mtr can reduce DNL and lipid accumulation within the cells [216]. Although recent results from our group [172] have shown that Mtr is able to reduce hepatosteatosis and glucose intolerance in mice that have been fed a HF diet, the source of hepatosteatosis in this mouse model is from the exogenous FA due to the intake of dietary fat rather than endogenous FA from an increased DNL. Therefore, it is not clear yet whether Mtr is effective for metabolic disorders by that involve an increased hepatic DNL [44].

Several studies have demonstrated that DNL enzymes are over-expressed during the development of hepatosteatosis [71, 105]. HFru-fed mice are a well-defined animal model of DNL-induced hepatosteatosis and insulin resistance [44, 45], and DNL-induced hepatosteatosis can be observed as early as one day after HFru feeding [211]. Indeed, the present study showed that chronic HFru feeding resulted in hepatosteatosis (increased TG level) by promoting DNL (indicated by SREBP1c, ChREBP, acetyl-CoA carboxylase (ACC) and fatty acid synthase (FAS) and stearoyl-CoA desaturase-1

(SCD-1)) without affecting FA oxidation, as indicated by unchanged levels of [^{14}C]–palmitate in the liver. However, reduced hepatic FA oxidation and mitochondrial enzyme activity has been demonstrated to occur prior to the appearance of hepatosteatosis, it has been shown that DNL is a primary cause of the development of hepatosteatosis [44, 77]. As expected, treatment with Mtr significantly reduced steatosis in the liver but not in muscle because of the high distribution of Mtr in the liver after oral administration [213]) and the associated glucose intolerance in these mice. Levels of key lipogenic enzymes were then measured and it was found that SREBP1c, ChREBP, SCD-1 and FAS in the liver were all reduced in HFru-fed mice treated with Mtr. These results suggest that Mtr is likely to reduce hepatosteatosis via inhibition of the DNL pathway.

As an increase in FA oxidation can also attenuate hepatosteatosis [217], this study next examined whether the reduction of hepatosteatosis caused by Mtr in HFru-fed mice results from an increase in liver FA oxidation. However, Mtr did not increase oxidation of ^{14}C-palmitate in the liver, indicating that the FA oxidation pathway was not activated in HFru-fed mice. These findings add further support to our interpretation that Mtr reduces hepatosteatosis and glucose intolerance in HFru-fed mice by inhibiting DNL rather than by stimulating FA oxidation in the liver.

It has been shown that the ER stress pathway plays a critical role in HFru-induced DNL and hepatosteatosis [59, 211]. For example, in *ob/ob* mice hepatosteatosis is largely due to increased DNL as a result of hyperphagia in an ER stress-dependent manner [107]. The same study also showed that alleviation of hepatic ER stress by overexpression of GRP78 reduces hepatosteatosis and insulin resistance by inhibiting DNL. Similarly, in

HFru-fed mice, inhibition of ER stress by tauroursodeoxycholic acid (TUDCA) and Betulin suppress DNL and improve insulin signalling in the liver [45-47]. To investigate whether the inhibition of hepatic DNL by Mtr involves the ER stress pathway, the major ER stress markers in response to HFru-induced DNL was examined. Interestingly, the results showed that HFru-induced ER stress (indicated by eIF2α, CHOP and IRE1) were all inhibited by Mtr. These findings suggest that attenuation of ER stress may be a novel mode of action for the inhibitory effect of Mtr on DNL and the resultant hepatosteatosis.

In terms of the possible cellular target of Mtr, published studies from our laboratory suggested that a downregulation of HSP72 contributes to lipid accumulation *in vivo* [172], and *in vitro* [216]. Indeed, Mtr is able to increase HSP72 expression and protect against lipid accumulation and glucose intolerance in the liver. Consistent with this observation, the present study found that liver tissue from HFru-fed mice had significantly lower concentrations of HSP72 protein, and this reduction was prevented by Mtr treatment. HSPs have been implicated in the regulation of diverse metabolic disorders including hepatosteatosis (the major metabolic defect of non-alcoholic fatty liver disease) and insulin resistance (the major metabolic defect of T2D) [194, 196, 218]. It has been reported that an enhanced expression of HSP72 can block the activation of the stress kinase JNK by TNFα [219]. Collectively, the data from this study suggest that Mtr may inhibit the ER-DNL axis by up-regulating HSP72 to reduce hepatosteatosis and the associated glucose intolerance.

Hepatic DNL and hepatosteatosis also occur in transgenic diabetic mice such as *db/db* [105]. Therefore, the present study explored whether Mtr is able to reduce

hepatosteatosis in a mouse model of T2D induced by HFD-STZ [88, 176]. Results from previous studies showed that Mtr reduced epididymal fat and lowered hyperglycaemia, indicating that Mtr may have the potential to control hyperglycaemia in T2D. Although Mtr showed no effect on normal fasting blood glucose, glucose tolerance or liver TG content in chow-fed mice [172], the anti-diabetic effects of Mtr could be attributed to its effect in reducing hepatosteatosis.

In summary, this thesis reports a potential novel application of the hepatoprotective drug Mtr for the treatment of hepatosteatosis and associated abnormal glucose homeostasis. This study is the first to evaluate the effect of Mtr on hepatosteatosis induced by the ER stress-DNL signalling pathway in HFru-fed mice. As suppression of ER stress can reduce hepatosteatosis by inhibiting DNL [2, 211], it is likely that Mtr may exert these beneficial effects by suppressing ER stress-induced increase in hepatic DNL. This study hypothesises that the upregulation of the chaperon protein HSP72 may play a critical role in suppressing ER stress (as illustrated in **Figure 3.6**) but this hypothesis requires validation by further studies using HSP72 knock-down animal model. Together with recent findings in HFD-fed mice [172], results from this Chapter suggest that Mtr may be repurposed for the treatment of hepatosteatosis and associated disorders in glucose homeostasis including T2D.

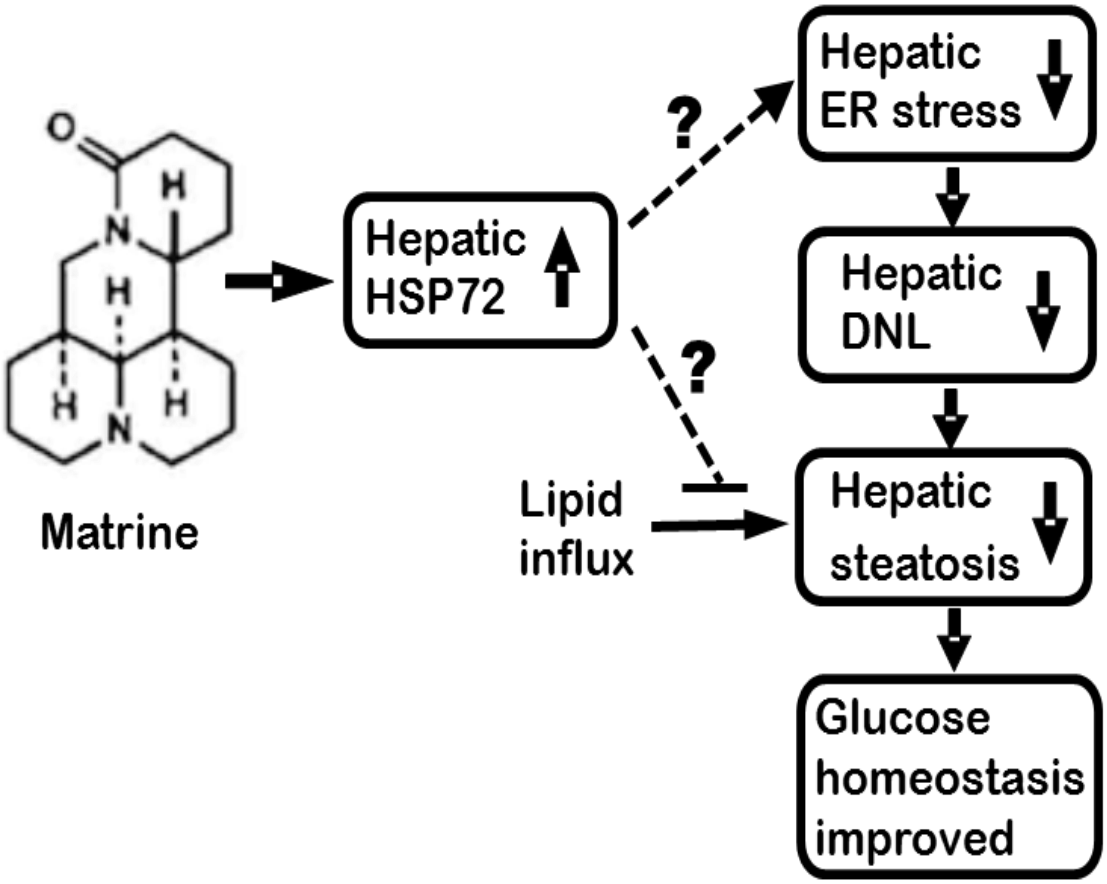

Figure 3.6 Proposed mechanisms underlying the therapeutic effects of Mtr for hepatosteatosis and associated disorders in glucose homeostasis.

Chapter 4 Effects of Matrine on Methionine and Choline-Deficient Diet-Induced Non-Alcoholic Steatohepatitis Associated with Inflammation and Fibrosis

4.1 Introduction

As described in **Section 1.9**, treatments for NASH fail to improve all aspects of this disease because of its diversity and the risks of available drugs. Alternatively, with its predictable efficacy in hepatosteatosis-associated disorders in glucose homeostasis (Chapter 3) and safety profile raises an attractive possibility that this hepatoprotective drug may have therapeutic potential for NASH.

NASH is a severe condition of NAFLD, the most common chronic liver disease. It is characterised by liver damage, inflammation and variable degrees of fibrosis, which may lead to cirrhosis and HCC [6]. The inflammatory component of NASH may induce hepatic fibrosis, which aggravates the progression of this disease [15]. To date, there is no drug approved specifically for the treatment of NASH [220].

As described in Chapters 1 and 3, Mtr has several well-recognised pharmacological effects targeting the liver, including anti-inflammatory, anti-tumour and antiviral activities [184, 221]. One of the well-characterised anti-inflammatory effects of Mtr is inhibition of the inflammatory cytokine production such as TNFα; a key player in the pathogenesis of NASH [143]. Moreover, Mtr treatment significantly inhibits inflammation upon challenge with LPS in vivo and in vitro [187, 222] and improves liver damage due to reperfusion injury in rats [200]. Recently, it has been found that treatment with Mtr attenuates hepatosteatosis and glucose intolerance induced by HFD in mice [172]. Further, the results in Chapter 3 show that Mtr is therapeutically effective in reducing HFru-induced hepatosteatosis.

However, mice fed with either HFD or HFru diet do not exhibit the inflammation and fibrosis in characteristic of NASH. Although MCD diet does not induce the metabolic syndrome as commonly seen in humans, this diet is still considered the most reliable candidate for diet-induced model of NASH in rodents, with liver damage, inflammation and fibrosis—a spectrum of changes that mimic the hepatic pathology of NASH [220, 223].

The results presented in this Chapter demonstrate the therapeutic efficacy of Mtr in the treatment of NASH, which was accompanied by a significant improvement in inflammation and fibrosis—major NASH components. In this study, we investigated the effect of treatment with Mtr on MCD diet-induced NASH in mice. In addition, metformin which has been suggested to be useful for the treatment of NASH [136, 224], was used in this study for comparison.

4.2 Materials and methods

4.2.1 Animal care, diets and experimental design

Male C57BL/6J mice (10 weeks old) were purchased and acclimatised for at least 1 week. Mice were randomly assigned to four groups: feeding ad libitum with a standard chow diet (CH-Con; Gordon's Specialty Stock Feeds, Yanderra, NSW, Australia); MCD alone (MCD-Con); MCD with Mtr treatment as a food additive (MCD-Mtr; Mtr: 100 mg/kg/day); and MCD with metformin treatment as a food additive (MCD-Met; Met: 250 mg/kg/day) for 6 weeks, as indicated in **Figure 4.1**. Body weight and food

intake were monitored daily throughout the experiment. Before the start of the study and at 5 weeks, following 5–7 h of food removal, tail vein blood was collected for glucose measurement with a glucometer (AccuCheck II; Roche, Castle Hill, Perth, Australia). Before the start of the study and at the end of the study, plasma was collected and stored at −80°C for subsequent biochemical testing. Mice were anaesthetised with a ketamine/xylazine mixture (up to 100 mg/kg body weight ketamine and 20 mg/kg body weight xylazine) was administered via intraperitoneal injection. Mice fixation was then performed via transcardial perfusion with heparinised phosphate buffered saline (PBS; 10–20 mL/mouse) followed by 4% paraformaldehyde (PFA; 10–20 mL/mouse; #C007, ProSciTech). At the completion of the PFA perfusion, the right lobe of the liver was dissected and immersed in 4% PFA-filled glass scintillation vials for further analysis.

All experiments were approved by the Animal Ethics Committee of RMIT University (#1415) in accordance with the guidelines of the National Health and Medical Research Council of Australia. Mtr (purity >99.5%) was a gift from Professor Li-Hong Hu from the Shanghai Institute of Materia Medica; metformin was purchased from Sigma-Aldrich.

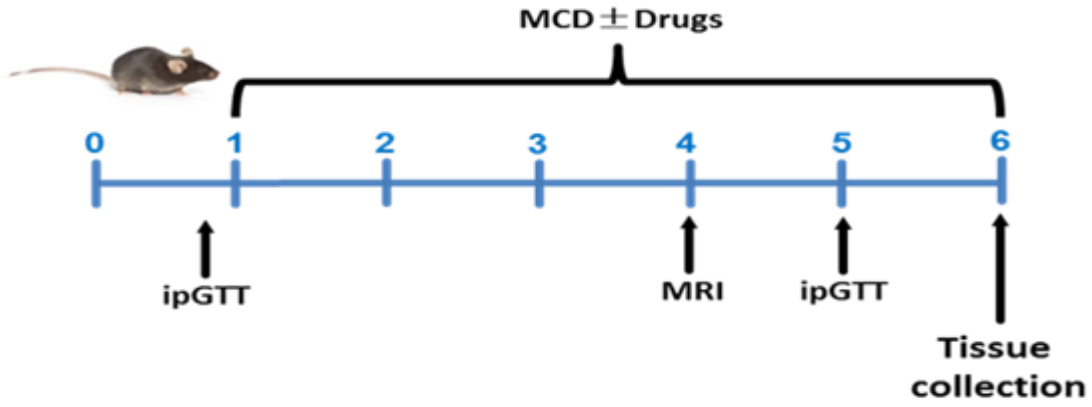

Figure 4.1 Schematic diagram of the experimental plan for studies in MCD diet-fed mice.

Male C57BL/6J mice were fed a chow (CH-Con) or MCD diet for 6 weeks. The MCD diet-fed mice were assigned into three groups: MCD diet-fed mice without treatment (MCD-Con); MCD diet-fed mice with Mtr (100 mg/kg/day) (MCD-Mtr); and MCD diet-fed mice with metformin (250 mg/kg/day) (MCD-Met). ipGTT: intraperitoneal glucose tolerance test; MRI: magnetic resonance imaging.

4.2.2 Assessment of the effect on hepatic steatosis

Hepatosteatosis was assessed by measuring TG contents in the liver using the method of Folch and a colorimetric assay kit (Triglyceride GPO-PAP; Roche, Castle Hill, NSW, Australia), as described previously [44].

4.2.3 Evaluation of total body fat content

Total body fat content in mice was evaluated using the EchoMRI™-100H body composition analyser (EchoMRI). Mice were restrained live inside a tube during this harmless and non-invasive analysis. The principle of measuring the whole-body fat

composition using the EchoMRI™-100H was based on the magnetic resonance imaging (MRI) technique measuring live body composition such as fat tissue, lean tissue and free fluid.

4.2.4 Assessment of the effect on liver damage

To examine the effects of Mtr on liver damage, the second component of NASH, plasma ALT and AST were measured at baseline and at Week 6 using commercial kits (ALT/SGPT Liqui-UV; Australia) [80]. Food was removed from mice cages for 5–7 h, and blood was collected from the tail vein (50 μL blood + 50 μL saline; fast spin for 1 min), and then mixed with 200 μL reagent (R1:R2 = 5:1, as described in the manufacturer instructions). The absorbance was measured at 340 nm using a FlexStation (Molecular Devices, Australia).

4.2.5 Quantitation of total and non-heme iron

The total iron, and heme and non-heme iron, contents of liver samples were determined colorimetrically [225] because iron deposition is also regarded as a characteristic of NASH [226, 227]. As described previously [228], the fixated liver tissue (50–60 mg) was homogenised with 50 mM NaOH (using suitable volume to provide uniform homogenisation). The sample was incubated overnight at 75–80°C, and then separated into two aliquots for determination of the total and non-heme iron contents. The total iron was determined by adding reagent A (a freshly mixed solution of equal volumes of 1.4 M HCl, 4.5% (w/v) $KMnO_4$ and 40% TCA in H_2O), and the non-heme iron was

determined by adding reagent B (same as reagent A without $KMnO_4$), to the sample [229].

The iron content of the sample was calculated by comparing its absorbance to that of a range of standard concentrations of equal volume. Standards (five diluted standards) were prepared as a mixture of $FeCl_3$ in 10 mM HCl and 50 mM NaOH. The standard value was measured using lysis reagent that either contained or lacked permanganate [229]. The mixture was transferred into 96-well plates and its absorbance was measured at 550 nm.

4.2.6 Real-time polymerase chain reaction of liver RNA

Total RNA was isolated from mouse liver using TRIzol reagent (Invitrogen, #15596026) as previously described [88]. Reverse-transcription polymerase chain reaction (RT-PCR) was carried out using the IQ SYBR Green Supermix (Bio-Rad Laboratories, USA) for interest genes and analysed by real-time PCR using specific primer sets. Target gene expression levels were normalised to a housekeeping gene (18s). Primer sequences are listed in **Table 4.1**.

Table 4.1 Primers used in quantitative RT-PCR

Gene	Primer sequences
18S	Forward: 5′-CGCCGCTAGAGGTGAAATTCT-3′
	Reverse: 5′-CGAACCTCCGACTTTCGTTCT-3′
TNFα	Forward: 5′-CACAAGATGCTGGGACAGTGA-3′
	Reverse: 5′-TCCTTGATGGTGGTGCATGA-3′
IL-1β	Forward: 5′-GACGGCACACCCACCCT-3′
	Reverse: 5′-AAACCGTTTTTCCATCTTCTTT-3′
CD68	Forward: 5′-TGACCTGCTCTCTCTAAGGCTACA-3′
	Reverse: 5′-TCACGGTTGCAAGAGAAACATG-3′
Collagen 1	Forward: 5′-CTGCTGGTGAGAGAGGTGAAC-3′
	Reverse: 5′-ACCAAGGTCTCCAGGAACAC-3′

4.2.7 Western blotting

Liver lysates were resolved by SDS-PAGE and immunoblotted with specific antibodies [45]. Antibodies listed in **Table 4.2** were diluted 1:1000 with a TBST buffer containing 1% bovine serum albumin (BSA), 0.02% sodium azide (Sigma-Aldrich, #71289) and 0.0025% phenol red (Sigma-Aldrich, #32661). Ponceau Red ensured equal loading of blots staining (Roth). Proteins were quantified using a ChemiDoc, and densitometry analysis of bands was performed using Image Lab software (Bio-Rad Laboratories, USA).

Table 4.2 List of antibodies used in western blotting

Pathway	Antibody	Supplier	Catalogue no.
Inflammation	MCP-1	Cell Signaling	2027
	NLRP3	AdipoGen	20B-0006-C100
	HSF1	Cell Signaling	4356
	HSP72	Enzo Life Sciences	C92F3A-5
	HSP90	Enzo Life Sciences	ADI-SPA-840HRP
Fibrosis	TGFβ	Cell Signaling	3709
	Smad3	Cell Signaling	9523
Autophagy	mTOR	Cell Signaling	2983
Loading control	Tubulin	Cell Signaling	3873
	GAPDH	Cell Signaling	2118
Secondary antibody	Goat anti-mouse	Santa Cruz	sc-2005
	Goat anti-rabbit	Santa Cruz	sc-2004
	Goat anti-rat	Santa Cruz	Sc-2065

4.2.8 Histopathological examination

The liver samples were perfused using PFA and sliced into 5 μm sections. Free-floating sections were stained with picrosirius red for liver fibrosis, and then quantified in five non-overlapping fields of view per animal by using an Olympus BX41 microscope with a 20× objective lens and an Olympus DP72 digital camera (Olympus, Australia) [80, 230]. The mean value was calculated for each experimental group using the threshold function in the ImageJ software package (NIH, Bethesda, MD, USA). Data are represented as percentage (%) of positive area per field. To obtain statistical significance, at least five random-field images were taken per slide, and at least seven mice per group were scored ($n = 7$).

4.2.9 Statistical analysis

The statistical analysis was carried out as described in Chapter 2, **Section 2.9**.

4.3 Results

4.3.1 Effects on adiposity, hepatosteatosis and plasma glucose

MCD diet feeding is a common nutritional model of NASH despite lack of the metabolic phenotype [162]. As expected, MCD diet-fed mice showed reduced body weight and body weight gain but no significant changes in food intake, calorie intake and blood glucose level. As shown in **Table 4.3**, the TG content (indicative of hepatosteatosis) was increased dramatically in the liver of MCD-Con compared with CH-Con mice (by 1.5 fold, $P < 0.01$). The difference in weight gain between chow, MCD alone and MCD with treatments was maintained throughout the treatment period of 6 weeks.

Mtr had no effect on body weight gain and calorie intake in MCD diet-fed mice. Consistent with previous studies [161, 231], MCD diet-fed mice did not show any glucose intolerance or metabolic abnormality. Glucose levels in Mtr-treated MCD diet-fed mice did not differ from the value of CH-fed mice. Associated with these effects, Mtr had no effect in reducing hepatic TG content in MCD diet-fed mice (**Table 4.3**). Similarly, metformin did not show any effect on any of these parameters in MCD diet-fed mice.

Table 4.3 Effects of Mtr and metformin on body weight, total food intake and liver triglyceride

	CH-Con	MCD-Con	MCD-Mtr	MCD-Met
Body weight (g)	24.3 ± 0.2	23.5 ± 0.2**	22.6 ± 0.1††	22.7 ± 0.1††
Body weight gain (g)	2.0 ± 0.2	0.4 ± 0.2**	0.3 ± 0.2	0.7 ± 0.1
Food intake (g/kg/day)	80.5 ± 2.3	85.6 ± 2.3	86.5 ± 2.5	85.6 ± 3.0
Caloric intake (kcal/kg/day)	268.2 ± 7.5	313.7 ± 9.0	319.7 ± 10.0	334.8 ± 18.4
Fasting blood glucose (mM)	8.0 ± 0.5	7.4 ± 0.4	6.3 ± 0.4	6.4 ± 0.5
Liver TG (mmol/g)	13.8 ± 4.2	31.6 ± 3.3**	28.2 ± 2.5	31.2 ± 3.1

Mice were fed a chow (CH-Con), MCD alone (MCD-Con), MCD treated with matrine 100 mg/kg/day (MCD-Mtr) or MCD treated with metformin 250 mg/kg/day (MCD-Met). Body weight and food intake were measured twice a week. Blood glucose measurement was performed at Week 5. Plasma was collected before tissue collection at Week 6 for subsequent analysis of ALT and AST. ***P* < 0.01 vs. CH-Con; ††*P* < 0.01 vs. MCD-Con (n = 8 mice/group).

4.3.2 Effects on body composition using magnetic resonance imaging

MCD diet feeding resulted in a lack of metabolic phenotype possibly because of significantly decreased body weight (**Figure 4.2A**). Total body fat content using the EchoMRI analyser was measured in all mice. As illustrated in **Figure 4.2B**, in spite of the reduction in body weight by MCD diet feeding, there was a significant increase in fat mass in MCD diet-fed mice compared with the chow-fed group. MRI analysis also revealed that MCD diet-fed mice and mice treated with either Mtr or metformin had a significant decrease in lean mass compared with the chow group (**Figure 4.2C**). However, Mtr and metformin had no effect on fat mass.

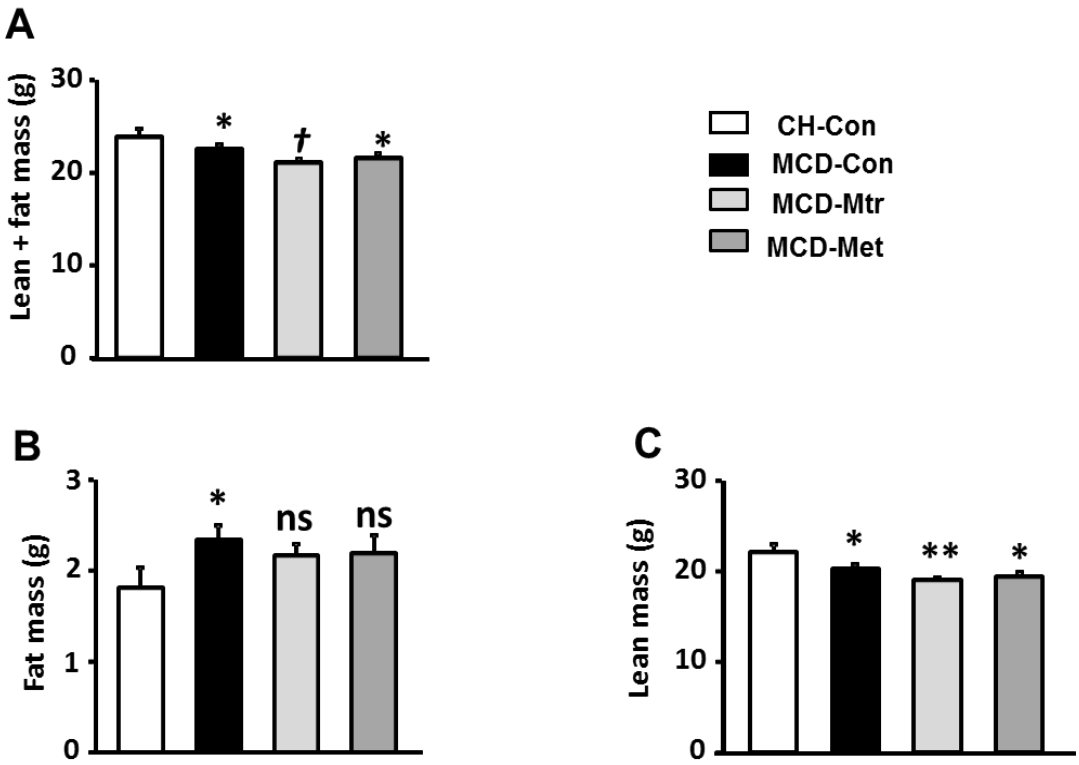

Figure 4.2 Effects of Mtr on body composition in MCD mice.

The body composition of CH-Con, MCD-Con, MCD-Mtr and MCD-Met was determined by EchoMRI analyser at Week 4. (A) Lean + fat mass; (B) Fat mass; (C) Lean mass. *P < 0.05, **P < 0.01 vs. CH-Con; †P < 0.05 vs. MCD-Con; ns: not significant (n = 8 mice/group).

4.3.3 Effects on plasma levels of liver enzymes and iron deposition

Liver damage has been suggested as an important factor that distinguishes NASH from hepatosteatosis [129]. The present study examined whether Mtr treatment might inhibit liver damage of MCD diet-fed mice. As shown in **Figure 4.3A and B**, along with the increase of hepatosteatosis in the liver, MCD-fed mice exhibited marked increases in ALT (by 68%, P < 0.01) and AST (by 40%, P < 0.05) levels, resulting from liver

damage. Treatment with Mtr or metformin markedly decreased ALT levels (±80% and 25%, respectively). In addition, Mtr treatment but not metformin, further decreased AST levels ($P < 0.05$) in MCD diet-fed mice, indicating Mtr may reduce liver damage, a hallmark in the progression of NASH. We further examined the effects of Mtr on iron levels in the liver of MCD-fed mice. Neither Mtr nor metformin treatment altered the accumulation of heme and non-heme iron induced by MCD diet (**Figure 4.3C and D**). This was likely due to an excessive overload of iron in the liver among mice fed MCD diet.

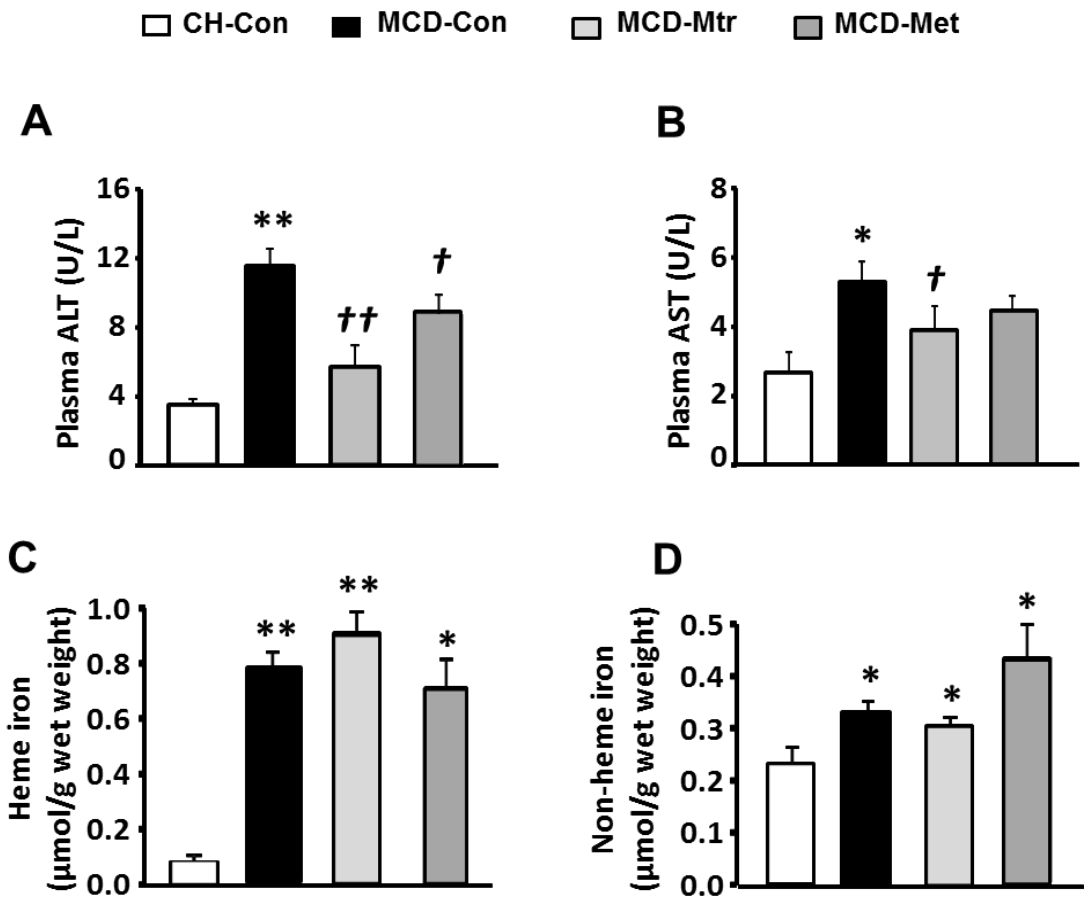

Figure 4.3 Effects of Mtr on liver damage and iron level.

After 6 weeks of feeding and drug treatment, blood samples were collected for the measurement of (A) ALT and (B) AST levels. Liver tissue was collected for iron measurement (C) heme iron and (D) non-heme iron. *P < 0.05, **P < 0.05 vs. CH-Con; †P < 0.05, ††P < 0.01 vs. MCD-Con (n = 7–8 mice/group).

4.3.4 Effects on hepatic inflammation

An important pathological characteristic of NASH is hepatic inflammation, and MCD diet has previously been shown to cause marked hepatic inflammation [10, 120]. Key inflammatory proteins, including TNFα, IL-1β, MCP-1, cluster of differentiation 68 (CD68) and NLRP3 inflammasome, are particularly associated with liver inflammation and the progression of NASH [53, 232]. To examine the anti-inflammatory effects of Mtr in MCD diet-fed mice, the protein expression levels of these inflammatory markers was measured. Consistent with other studies [56, 149, 162], MCD feeding resulted in a marked inflammatory response in the liver as evidenced by increased expression levels of TNFα and CD68 (±50% and 80%, respectively; both P < 0.05), an indicator of KCs activation [233]. Further, livers of MCD-Con mice with NASH exhibited a substantial increase in MCP-1 and NLRP3 expression (both 38% vs. CH-Con). Mtr treatment normalised the expression levels of TNFα, CD68 (both P < 0.05 vs. MCD-Con) and MCP-1 (P < 0.01 vs. MCD-Con), as shown in **Figure 4.4A, B and D**. However, no significant differences were detected in the expression of IL-1β among the experimental groups (**Figure 4.4C**). It has been suggested that NLRP3 blockade reverses advanced stage liver inflammation and fibrosis in MCD diet-induced NASH [149]. Consistent with the previous study, there was ±65% reduction in NLRP3 inflammasome expression (P < 0.05 vs. CH-Con) (**Figure 4.4E**). In contrast to Mtr, metformin had no

effect on the expression levels of inflammatory markers including TNFα, CD68, MCP-1 and NLRP3 (**Figures 4.4A-E**).

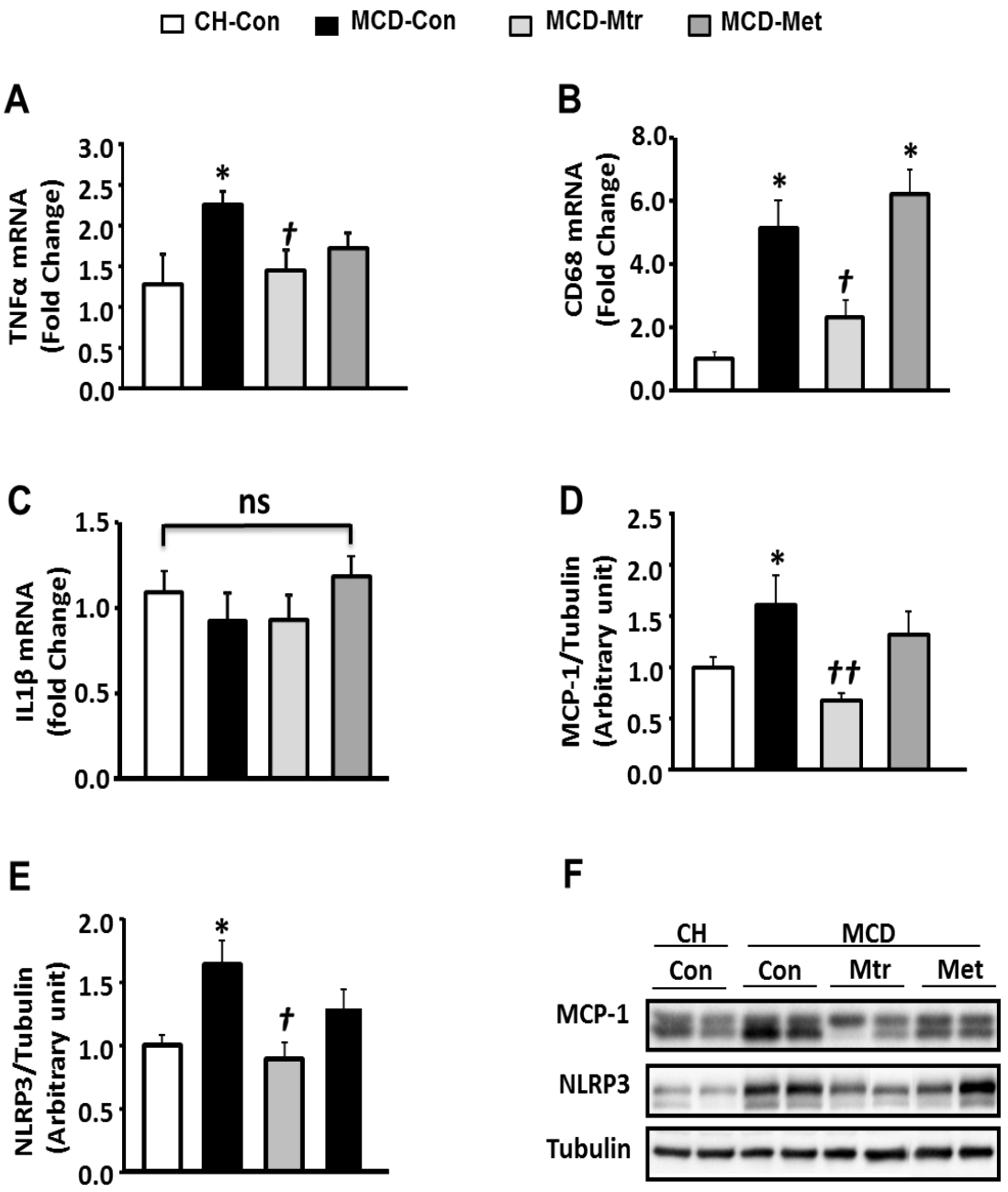

Figure 4.4 Effects of Mtr on hepatic inflammation in MCD diet-fed mice.

(A) TNFα mRNA, (B) CD68 mRNA, (C) IL1β mRNA, (D) MCP-1 (E) NLRP3 and (F) representative western blot images. *P < 0.05 vs. CH-Con; †P < 0.01, ††P < 0.01 vs. MCD-Con; ns: not significant (n = 7–8 mice/group).

4.3.5 Effects on expression of genes involved in hepatic fibrosis

Liver fibrosis is another hallmark of advanced NASH [15]. An ideal anti-inflammatory approach to NASH treatment would not only abolish inflammation but also reverse established liver fibrosis. Therefore, the effect of Mtr on hepatic fibrosis was examined. As shown in **Figure 4.5A-C**, MCD diet-fed mice exhibited marked increases in the expression of key proteins of the pro-fibrotic pathway in the liver, namely collagen 1, TGFβ and Smad3 (all P < 0.05 vs. CH-Con), and these results were consistent with others [14, 149]. Treatment of MCD diet-fed mice with Mtr inhibited hepatic expression of these proteins (±55%, 65% and 45%, respectively) towards the levels seen in CH-Con mice. In contrast, metformin treatment had no effect on MCD diet-induced liver fibrosis. There were no significant changes in caspase-1 protein expression between groups (**Figure 4.5D**). These results revealed that treatment with Mtr attenuated MCD diet-induced fibrosis in the liver, which may support its beneficial effects in NASH with fibrosis.

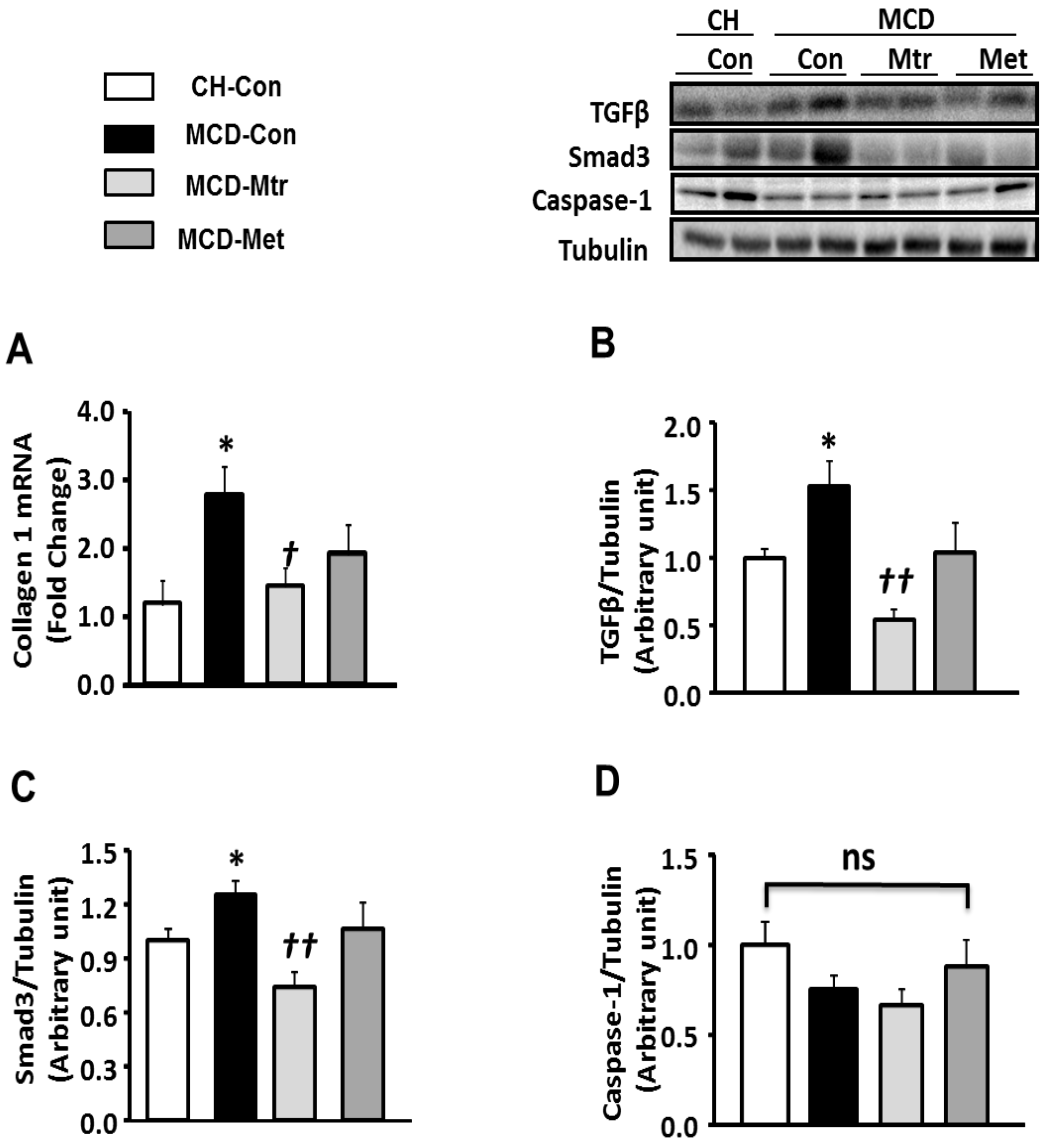

Figure 4.5 Effects of Mtr on hepatic fibrosis in MCD-fed mice.

(A) A hepatic fibrosis gene of collagen 1 was determined by quantitative RT-PCR analysis. Liver lysates from mice were immunoblotted for (B) TGFβ, (C) Smad3 and (D) caspase-1 and quantified for statistical analysis. **P* < 0.05 vs. CH-Con; *†P* < 0.05, *††P* < 0.01 vs. MCD-Con; ns: not significant (n = 7–8 mice/group).

4.3.6 Effects on liver fibrosis using picrosirius red stained liver sections

MCD diet caused extensive fibrosis at 6 weeks, evidenced by collagen accumulation combined with thickened hepatocytes cell membranes (**Figure 4.6A**). Picrosirius red staining of the liver sections for collagen confirmed the beneficial effects of Mtr treatment on hepatic fibrosis. In agreement with the gene expression and western blot data, treatment with Mtr resulted in a robust reduction in collagen accumulation As shown in **Figure 4.6B**, there was an increase in liver fibrosis of ±83% ($P < 0.01$ vs. CH-Con) in the liver of MCD-fed mice and this increase was reversed following treatment with Mtr (reduction of ±66%, $P < 0.01$ vs. MCD-Con). In comparison, no obvious hepatic fibrosis changes were observed in mice fed MCD diet with metformin treatment.

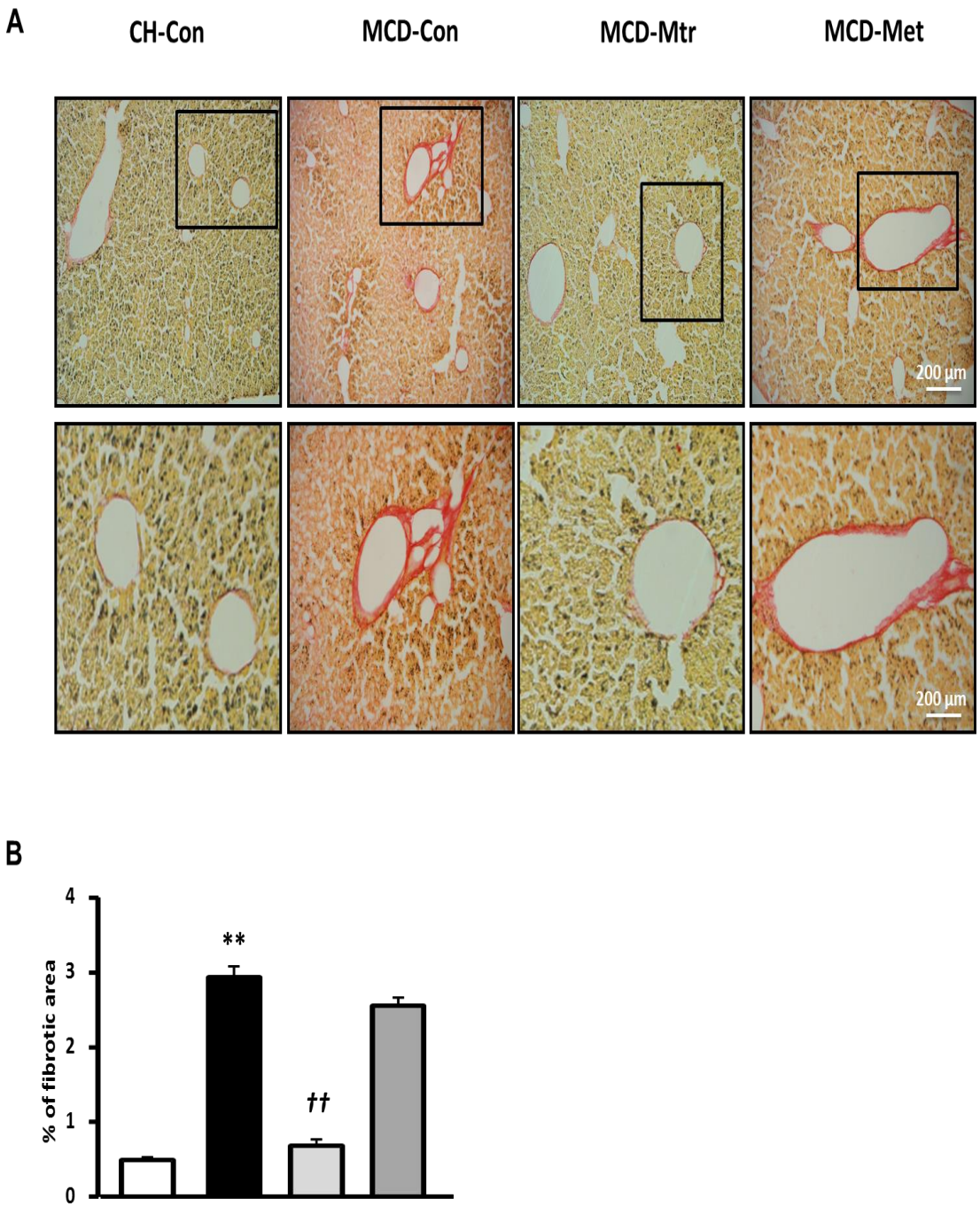

Figure 4.6 Effects on extent of liver fibrosis stained with picrosirius red.

(A) Representative images showing collagen staining with picrosirius red in liver sections from CH-Con, MCD alone and MCD treated groups (scale bar = 200 μm (top set) and 50 μm (below set), 10× magnification). (B) Mtr-treated mice had significantly reduced fibrosis area compared with MCD diet-fed mice. $^{**}P < 0.01$ vs. CH-Con; $\dagger\dagger P < 0.01$ vs. MCD-Con (n = 7–8 mice/group).

4.3.7 Effects on hepatic mTOR and heat shock protein expression

Dysregulation of mTOR signalling has been implicated in fatty liver diseases [234]. Inhibition of mTOR has previously been shown to be efficacious in improvement of NASH-induced by MCD diet [235-237]. It has been reported that Mtr treatment inhibits autophagy in cell lines by impairing the activity of lysosomal proteases [238]. To elucidate the mechanism underlying mTOR inhibition-induced by Mtr, protein expression using western blotting was performed to evaluate whether mTOR contributes to hepatocyte damage, inflammation, and fibrosis in NASH. Interestingly, treatment with Mtr normalised the protein level of mTOR ($P < 0.01$ vs. MCD-Con) towards the levels seen in CH-Con mice (**Figure 4.7A**). These results revealed that treatment with Mtr inhibited MCD diet-induced hepatic mTOR expression.

A recent study has examined the effects of Mtr on the expression of HSP72 [172]. This study has shown that the antisteatotic effect of Mtr is associated with the upregulation of HSP72 in the liver of HFD-fed mice. To determine whether Mtr treatment is associated with the upregulation of HSP-induced improvement in NASH, HSP90, HSF1 and HSP72 expression was measured in the liver. As shown in **Figure 4.7B-D**, HSP90 and HSP72 expression levels were blunted (50% reduction vs. CH-Con, $P < 0.05$) by MCD diet feeding, but there was no significant effect on the protein levels of HSF1. Treatment with Mtr upregulated hepatic HSP72 and HSF1 expression levels ($P < 0.01$ vs. MCD-Con) in MCD diet-fed mice, but had no significant effect on HSP90 expression. Therefore, these results indicated that the beneficial effect of Mtr on the development of MCD diet-induced NASH might be associated with its ability to limit

mTOR and upregulate HSPs. In comparison, metformin treatment significantly rescued HSF1 but had no significant effect on the expression of HSP72 and HSP90.

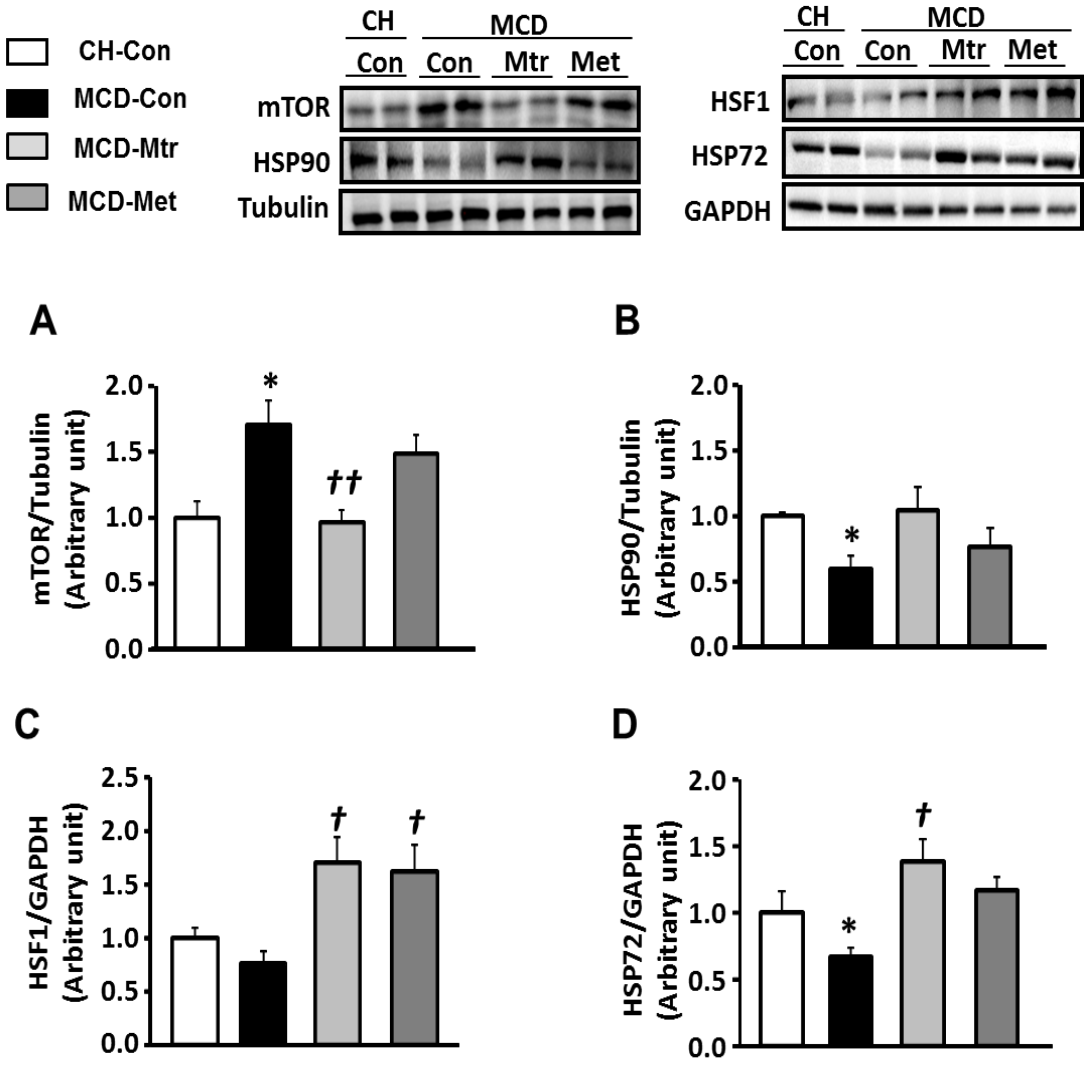

Figure 4.7 Effects of Mtr on mTOR, HSF1, HSP90 and HSP72 in MCD-fed mice.

Liver lysates from mice were immunoblotted for (A) mTOR, (B) HSP90, (C) HSF1 and (D) HSP72 and quantified for statistical analysis. **P* < 0.05 vs. CH-Con; *†P* < 0.05, *††P* < 0.01 vs. MCD-Con (n = 7–8 mice/group).

4.4 Discussion

This study found that Mtr markedly ameliorated MCD diet-induced NASH by suppressing key regulators of hepatic damage, inflammation and fibrosis. Results of this Chapter showed that Mtr treatment was therapeutically effective for the treatment of NASH compared with metformin in MCD diet-fed mice. These effects were associated with an inhibition of mTOR and upregulation of HSPs, suggesting Mtr might be repurposed for the treatment of NASH by a novel mechanism different from those recognised at the present time [67].

Previous studies have reported a potential effect of Mtr in ameliorating hepatosteatosis, fasting blood glucose and glucose intolerance in HFD-fed mice [172]. In addition, Mtr treatment is effective at reversing hepatosteatosis and glucose intolerance, probably via reduced ER stress associated with decreased hepatic lipogenesis in mice fed HFru diet. Despite the possible benefits of Mtr for the treatment of NAFLD-associated glucose intolerance, the therapeutic effects in NASH are not clear because of the absence of NASH features in these mouse models. Therefore, the studies described in Chapter 4 particularly examined the protective effect of Mtr against MCD diet-induced NASH in mice.

MCD diet feeding is a well-recognised model of NASH and rapidly induces steatohepatitis in mice [120, 161]. Although MCD-fed mice do not exhibit metabolic abnormalities such as insulin resistance and hyperglycaemia; MCD diet feeding is a frequently used dietary model because it causes severe NASH with hepatic steatosis, damage, inflammation and fibrosis [162]. This study showed that 6-week Mtr treatment

significantly ameliorated liver damage, inflammation and fibrosis, albeit not hepatosteatosis.

The degree of hepatosteatosis may predict the severity of NAFLD and vary among NASH patients [28]. MCD diet has been shown to induce higher levels of TG in the liver compared with normal chow diet [145]. To investigate the antisteatotic effects of Mtr in the liver, hepatic TG content was measured in MCD diet-fed mice. Treatment of these mice with Mtr or metformin did not change hepatosteatosis in relation to body weight and glucose level in MCD mice. This might be due to the lack of metabolic abnormalities in MCD diet-induced NASH. Secondly, Mtr treatment exerts its beneficial effects on NASH independent of an improvement in hepatosteatosis.

It is suggested that elevations of liver enzymes and hepatic iron levels are strongly associated with hepatocyte injury and liver damage [239]. ALT is used as a marker of liver damage in fatty liver including NASH [240]. Consistent with these reports, feeding mice MCD diet produces a significant increase in ALT levels in the mouse MCD diet model of NASH [241]. Mtr showed a beneficial effect in the inhibition of MCD diet-induced increases in plasma ALT and AST; this indicates that Mtr can attenuate the liver damage without changes in body composition in mice. Conversely, metformin had moderate effect on ALT levels, but did not change AST levels; therefore, it is not strongly recommended for NASH treatment [10, 242, 243].

The activation of inflammatory cytokines plays a vital role in the progression of NASH [244]. The increase in inflammatory cytokines production, in particular TNFα by KCs, resident hepatic macrophages, was suggested to be the key mediator of the progression

of NASH [245]. In line with increased TNFα production, increased CD68 and MCP-1 are associated with the severity of NASH [80, 231]. Alternatively, inhibition of TNFα activity using anti-inflammatory drugs improves liver damage, inflammation and NASH [145, 246]. It is generally believed that the anti-inflammatory activities of Mtr are largely due to its ability to inhibit hepatic inflammation [200, 222].

Iron overload plays a role in liver damage where simple uncomplicated steatosis progresses to fibrotic NASH [153, 154]. It has been suggested that iron overload exacerbates inflammation and fibrosis-induced steatohepatitis in humans [151, 227] and in animals [226, 247]. Further, iron accumulation in tissue is positively correlated with the severity of NASH manifestations in the Tsumura Suzuki obese diabetes (TSOD) mouse model [248]. It appears that reduced iron overload may prevent development and progression of NASH. Despite the inhibitory effects of Mtr on liver enzymes, the elevation of heme and non-heme iron did not change during the treatment period with Mtr or metformin. These findings together raise the possibility that Mtr might offer additional therapeutic effects on manifestations of NASH through reduction of liver enzymes.

Results in this Chapter revealed that Mtr prevented NASH-associated hepatic inflammation and fibrosis after 6 weeks of treatment. Mtr suppressed the increases in TNFα, CD68 and MCP-1, major inflammatory markers in NASH. Another central participator in the development of NASH is the activation of NLRP3 inflammasome [147, 249]. It has been recently reported that blockage of NLRP3 activation reduces liver inflammation and fibrosis in MCD-fed mice [149]. Consistent with the anti-inflammatory effects, a similar reduction in NLRP3 expression in the liver was

observed compared with CH-Con mice. The results support Mtr may reduce NASH via inhibition of inflammatory pathways.

Hepatic fibrosis is known as another hallmark feature of NASH after inflammation, which can cause scaring, resulting in liver cirrhosis and cancer [15, 240]. Because of its severe impact on the prognosis of NASH, the control of hepatic fibrosis is regarded as a key criterion in the treatment of NASH [6]. Although Mtr has been reported to prevent liver fibrosis (TGFβ and collagen synthesis) induced by CCl_4 in rats [189], whether Mtr inhibits fibrosis in MCD-induced NASH remains unclear. To investigate whether the inhibition of hepatic inflammation by Mtr involves the inhibition of fibrosis pathways [147], this study examined the effect of Mtr on the major fibrotic markers in response to MCD diet-induced NASH. Consistent with the reduction in inflammation, our data indicated that Mtr inhibited the activation of fibrosis by suppression of TGFβ, Smad3 and collagen synthesis in the liver of MCD diet-fed mice. These results provide further support for the idea that Mtr might provide a possible mechanism for the inhibition of fibrosis because of its antifibrotic effects. Indeed, this is the first experimental evidence that Mtr can prevent and ameliorate the progression of NASH of not only inflammation but also fibrosis in the liver of a NASH model.

In terms of possible cellular targets of Mtr, a critical role of the activated mTOR pathway in the severity and progression of NASH has become a focus for research [234, 250, 251]. The involvement of the mTOR pathway in MCD-induced advanced NASH has been explored [237]. Recently, Mtr has shown beneficial effects in the inhibition of mTOR in cell lines and primary cells of acute myeloid leukaemia [252]. Mtr treatment decreased the expression of mTOR in the liver of MCD diet-fed mice. In

particular, Mtr may provide a protective effect against the progression of NASH through mTOR inhibition.

Another interesting finding presented in this Chapter was that Mtr is able to modulate HSP expression levels. It has been reported that overexpression of HSP72 may attenuate inflammation and restore homeostasis even in the face of metabolic insult [196], which may likely be attributed to its ability to suppress the production of inflammatory cytokines [253]. A previous study from our laboratory has suggested that upregulation of HSP72 may contribute to hepatosteatosis induced by HFD or HFru feeding in mice [172]. Consistent with this observation, the present study found that liver tissue from MCD diet-fed mice had significantly lower levels of HSP72 and HSP90, and this reduction was rescued by Mtr treatment. It is noteworthy that upregulation of HSPs by Mtr treatment has been associated with the improvement of NASH. Importantly, Mtr exerts these effects through a distinct pathway different from that of metformin without any significant change in mTOR or HSP72. These data suggest that the therapeutic effects of Mtr in treating NASH may involve dysregulation of mTOR or HSPs.

This studies reported in this chapter have provided direct support for our hypothesis that Mtr treatment markedly ameliorates NASH via inhibiting the inflammatory and fibrotic pathways. Therefore, Mtr has the potential to be a therapeutic drug for the treatment of NASH, possibly by inhibiting mTOR expression and upregulating HSP72. Importantly, anti-inflammatory and antifibrotic effects of Mtr are related to the inhibition of key aspects of NASH (**Figure 4.8**).

In summary, the study in this Chapter demonstrated that Mtr may be useful as an effective drug to prevent NASH-associated inflammation and fibrosis. It is possible that the improvement of inflammation and fibrosis by Mtr treatment occurs via the inhibition of mTOR, which appears associated with the upregulation of HSP72. Compared with metformin, Mtr demonstrates clear superiority for the treatment of NASH. Further works are needed to explore whether the anti-inflammatory and antifibrotic effects of Mtr result directly from its effects on the hepatic mTOR-HSP72 pathway, given that previous studies from our laboratory have excluded the commonly recognised mechanisms.

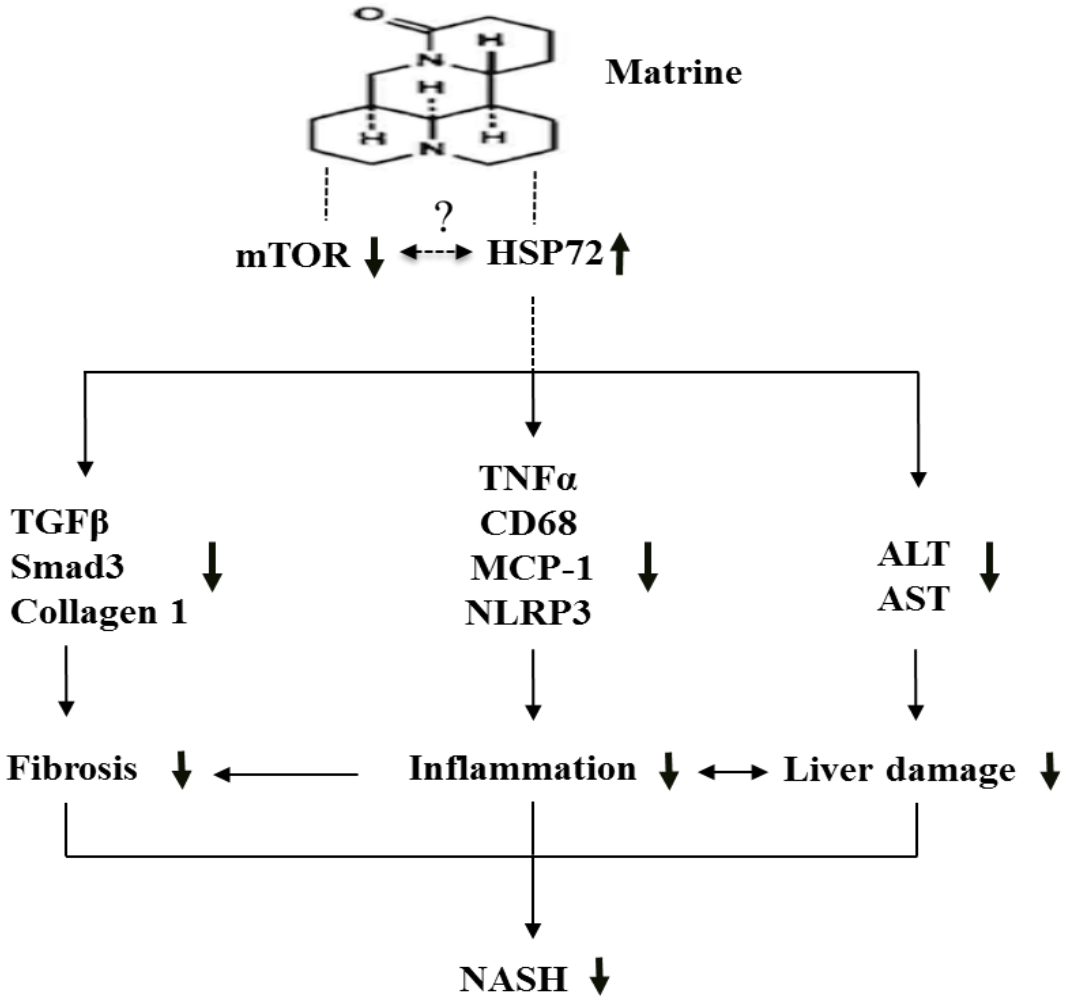

Figure 4.8 Schematic diagram illustrating the proposed mechanism underlying the effects of Mtr against MCD diet-induced NASH.

Chapter 5 Effects of Matrine on Lipopolysaccharide-Stimulated Inflammation in Macrophage Cells

5.1 Introduction

As reviewed in Chapter 1, macrophages including hepatic KCs play an important role in perpetuating the inflammatory phase of NASH by the release of inflammatory and fibrogenic mediators [130, 254]. It has been shown that LPS stimulates the inflammatory activation of KCs, which contributes to NASH [255]. Because macrophages are critical in initiating liver damage and inflammation, targeting macrophages activation may guide the development of effective treatment for the inflammation in NASH [129]. For example, mice with lack of hepatic TLR4 stimulated with LPS are protected from hepatosteatosis and inflammation via impaired hepatocytes and activated KCs [256]. J774A.1 is a macrophage-like cell line that is used as a model for KCs in the liver and the macrophages in the circulation. Activation of J774A.1 by LPS produces inflammatory cytokines and promotes the fibrogenic process [257].

LPS or endotoxin comprises a major portion of the cell wall of gram-negative bacteria and is a potent inducer of the inflammatory response in macrophages via its receptor the CD14/TLR4 complex [258]. It has been proposed that LPS may be a 'second hit', which contributes to the progression of simple hepatosteatosis to NASH [54]. Activation of macrophages by LPS induces the expression of TLR4, which mediates the secretion of inflammatory cytokines such as TNFα [138, 259]. The release of TNFα can cause severe liver inflammation and contribute to pro-fibrotic activity and eventually NASH [129]. An increase in the synthesis of inflammatory cytokines including TNFα has been reported in patients [129, 131, 139] and rodents [142, 245]

with NAFLD/NASH. Indeed, inhibition of LPS-induced TNFα production reduces inflammatory cytokine activation and decreases inflammation [260].

The studies reported in Chapter 4 revealed that Mtr treatment inhibits the elevated expression of TNFα and related inflammatory and fibrotic signals in the liver. Chapters 3 and 4 have described the ability of Mtr to reduce lipid accumulation, inflammation and fibrosis in the liver. However, the underlying cellular mechanisms of the effects of Mtr in these conditions are not clear because of multiple interactions among different cells in the organ. As cell lines are homogenous, and are easily manipulated and propagated for the study of signalling pathways, they can be used to provide a clearer understanding of the cellular mechanisms of Mtr on specific cell types for NASH. This Chapter investigates the cellular mechanisms underlying the effects of Mtr on inflammatory and fibrogenic pathways in a cell line that represents the major cell type responsible for the inflammatory cytokines in NASH.

5.2 Materials and Methods

5.2.1 Cell Culture

J774A.1 a murine reticulocyte sarcoma cell line derived from a female BALB/c mouse, was purchaesed ATCC® TIB-67™ and maintained in RPMI (Gibco/Invitrogen, Carlsbad, CA, USA) supplemented with 2 mM L-glutamine, 100 U/mL penicillin, 100 μg/mL streptomycin and 10% (v/v) heat-inactivated foetal bovine serum in a humidified 5% CO_2 atmosphere at 37°C. Cell culture medium was changed every two

or three days and used at passages numbers 6–15 for all experiments. Briefly, cells were subcultured at 1 in 10 dilutions when cells reached 80–90% confluence. Subculture was formulated by rinsing the cells first with warm 1× PBS, and then adding 2–3 mL 1× trypsin-EDTA solution to detach the cells from the T75 flask. Cells were then centrifuged at 100 × g for 5 min and re-suspended in ±10 mL fresh growth medium, and the desired amount of cells was transferred into a new T75 flask containing fresh RPMI growth medium.

5.2.2 Chemicals and drugs

LPS was purchased from Sigma-Aldrich (O127:B8; Australia). It was dissolved in water to obtain a stock concentration of 10 mg/mL. Mtr (≥98% by high performance liquid chromatography) was purchased from Sigma-Aldrich. Mtr (purity >99.5%) was a gift from Professor Li-Hong Hu from the Shanghai Institute of Materia Medica. Quercetin was purchased from Sigma-Aldrich (Q4951; Australia), dissolved in dimethyl sulfoxide (0.1% DMSO) and stored at −20°C. Bay 11-7082 was purchased from Sigma-Aldrich (B5556; Australia).

5.2.3 Treatments of J774A.1 macrophage cell line

To induce inflammation in J774A.1 cells, a serial dilution of LPS was prepared and 1 mg/mL stock LPS solution was kept at −80°C for further experiments. On the day before testing, the cultured cells were confirmed as having a confluence of >90% and cell viability of >90% by microscopic examination and LDH release cytotoxicity assay, respectively (**Section 5.2.5**). Medium was aspirated from the cell culture flask and

10 mL fresh RPMI medium added to the flask. Cells were removed using a cell scraper and 0.5 (× 2) mL was used to start a new passage, while the remaining 9 mL was placed into a 15-mL conical tube. Cells were counted using trypan blue at a 1:10 dilution. The desired volume of the cell-containing medium (at a density of 2×10^5 cells per well) was transferred into a 24-well culture plate with fresh growth medium. Two hours prior to inflammatory stimulation, each prepared drug was added to the appropriate well at a indicated concentration. The plate was then returned to the incubator for the indicated periods of time. Then, LPS was added to appropriate wells to induce inflammation. After 2 h of incubation, the cell supernatant was collected in 1.5-mL Eppendorf tubes for enzyme‐linked immunosorbent assay (ELISA). Cell lysates were harvested after washing with cold PBS and kept at −80°C for further analysis.

5.2.4 Determination of TNFα, IL-1β and IL-6 production

The production of the inflammatory cytokines, TNFα, IL-1β and IL-6, in the culture medium of J774A.1 was determined using commercially available ELISA kits (BD Biosciences) according to the manufacturer protocol. The experimental design is illustrated in **Figure 5.1**.

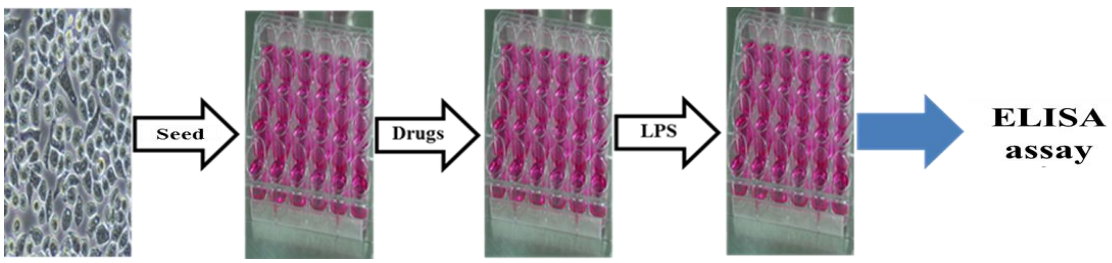

Figure 5.1 Schematic diagram of the *in vitro* experimental protocol.

Cells were harvested and seeded at 2×10^5 cells/mL per well into 96-well plates. After cells were treated with selected compounds, followed by incubation with or without 3 ng/mL LPS at 37°C for 2 h, the culture supernatants were collected into microfuge tubes and centrifuged at 10,000 rpm for 2–3 min at 4°C. J774A.1 cells were lysed after washing with ice-cold 1× PBS buffer.

5.2.5 Determination of lactate dehydrogenase release

The cytotoxicity was assessed by measuring the activity of released lactate dehydrogenase (LDH) in the medium. The enzyme activity in the whole cell lysate and medium was determined using a CytoTox 96® Non-Radioactive Cytotoxicity Assay kit (#G1780; Promega) according to the manufacturer protocol. Briefly, 50 µL diluted cell medium (1:5) or cell lysate (1:10) was transferred into a 96-well plate before the addition of 50 µL reconstituted substrate mixture. The plate was then covered with foil and incubated at room temperature for 30 min; subsequently, 50 µL stop solution was added to each well before measuring absorbance. The absorbance was read at 490 nm using a POLARstar OPTIMA microplate reader (BMG Lab Technologies, Germany). The LDH released into the medium (a measure of cells viability) was expressed as a percentage of the total LDH activity (ratio of LDH in lysate and in the medium) [216].

5.2.6 Determination of protein concentration

As described in **Section 2.6,** protein concentration in J774A.1 cells was measured through the use of a colorimetric bi-cinchoninic acid (BCA) protein kit (#B9643; Sigma-Aldrich). First, 1 µL diluted tissue lysate (1 part lysate to 9 µL dH_2O) was added to 200 µL BCA reagent mix (50 parts reagent A to 1 part reagent B). Solutions were

then mixed and incubated at 37°C for 30 min prior to the determination of absorbance at 562 nm using a POLARstar OPTIMA microplate reader (BMG Lab Technologies, Germany). In each BCA assay, varying dilutions of BSA protein were included to create a standard curve in the range of 0–2.0 μg/mL.

5.2.7 Other methods

Other methods used in this study are as described in Chapter 2.

5.3 Results

5.3.1 Inflammatory response of J774A.1 cells to the stimulation of LPS

We firstly determined the effective concentration of LPS (1–100 ng/mL) to induce inflammatory cytokines in J774A.1 cells. As shown by the inflammatory cytokines in cell culture media, at 1 ng/mL, LPS had no effect on the production of TNFα, whereas at 3–100 ng/mL LPS increased TNFα production in a concentration-dependent manner (**Figure 5.2A**). As shown in **Figure 5.2B and C**, however, there was no significant difference between vehicle and LPS-treated J774A.1 in the production of IL-1β and IL-6 at this range of concentrations. On the basis of these results, 3 ng/mL LPS was used in further experiments and TNFα was used as the readout of cell inflammation.

To determine the optimal Mtr concentration, cells were treated with different concentrations of Mtr in the absence of LPS. Mtr had no effect on the basal production

of TNFα (**Figure 5.2D**). In contrast, in the presence of LPS, Mtr (1–50 μM) significantly reduced LPS-induced increase in TNFα production in a concentration-dependent manner (**Figure 5.2E**). The minimum inhibitory concentration of Mtr to suppress LPS-induced TNFα production in J774A.1 macrophages was 1 μM. Its efficacy was similar to that of the well-known inflammatory inhibitor Bay 11-7082 at its maximum concentration (15 μM).

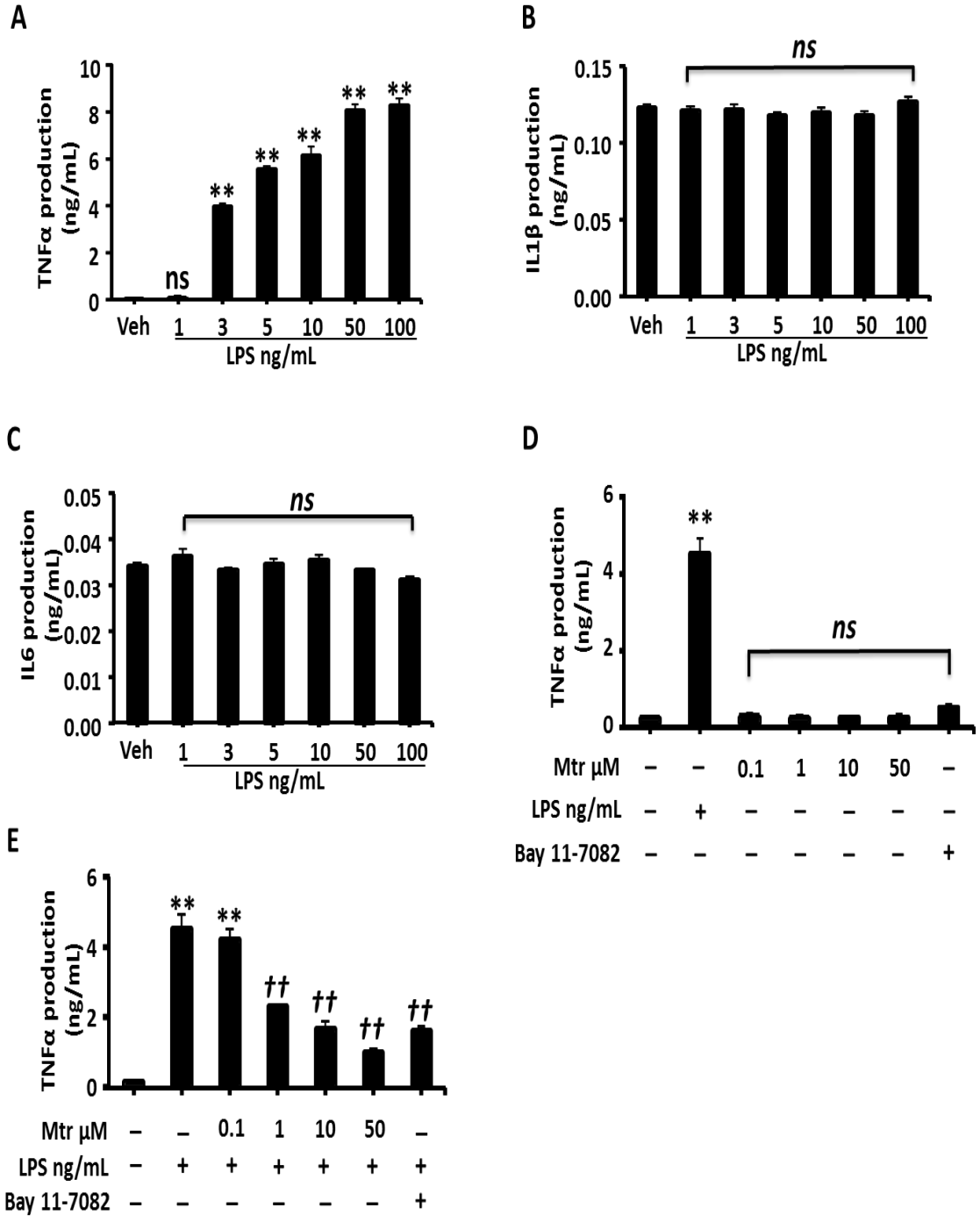

Figure 5.2 Effects of Mtr on LPS-induced production of inflammatory cytokines in J774A.1 cells.

J774A.1 cells (2 $\times 10^5$ cells/mL) were treated with 1–100 ng/mL LPS for 2 h to stimulate the production of inflammatory cytokines. Levels of (A) TNFα, (B) IL-1β and (C) IL-6 in culture media were determined by ELISA. Cells were pretreated with

different concentrations of Mtr (0.1, 1, 10 and 50 μM) and 15 μM Bay 11-7082 for 2 h, and then treated (D) without or (E) with 3 ng/mL LPS for 2 h. At the end of treatment, each cell culture medium was collected and the production of TNFα was determined by ELISA as described in **Section 5.2.4**. Results are expressed as ±SEM and represent at least three independent experiments. $^{**}P < 0.01$ vs. Veh; ††$P < 0.01$ vs. LPS-untreated group; ns: not significant. Veh: vehicle.

5.3.2 Effects on the viability of J774A.1 macrophages

To exclude a possibility that the inhibition of inflammation by Mtr resulted from cytotoxic effects, we determined LDH activity in the culture medium as an indicator of cell damage. As shown in **Figure 5.3A**, LPS and Mtr caused no significant elevation in LDH level at 3 ng/mL and 1 μM, respectively, compared with the positive control causing elevation of LDH activity. Consistent with the negative results of LDH release, the cells displayed normal morphology in response to these treatments. Similarly, cells treated with Mtr or LPS remained similar to the vehicle without cell damage observed (**Figure 5.3B**).

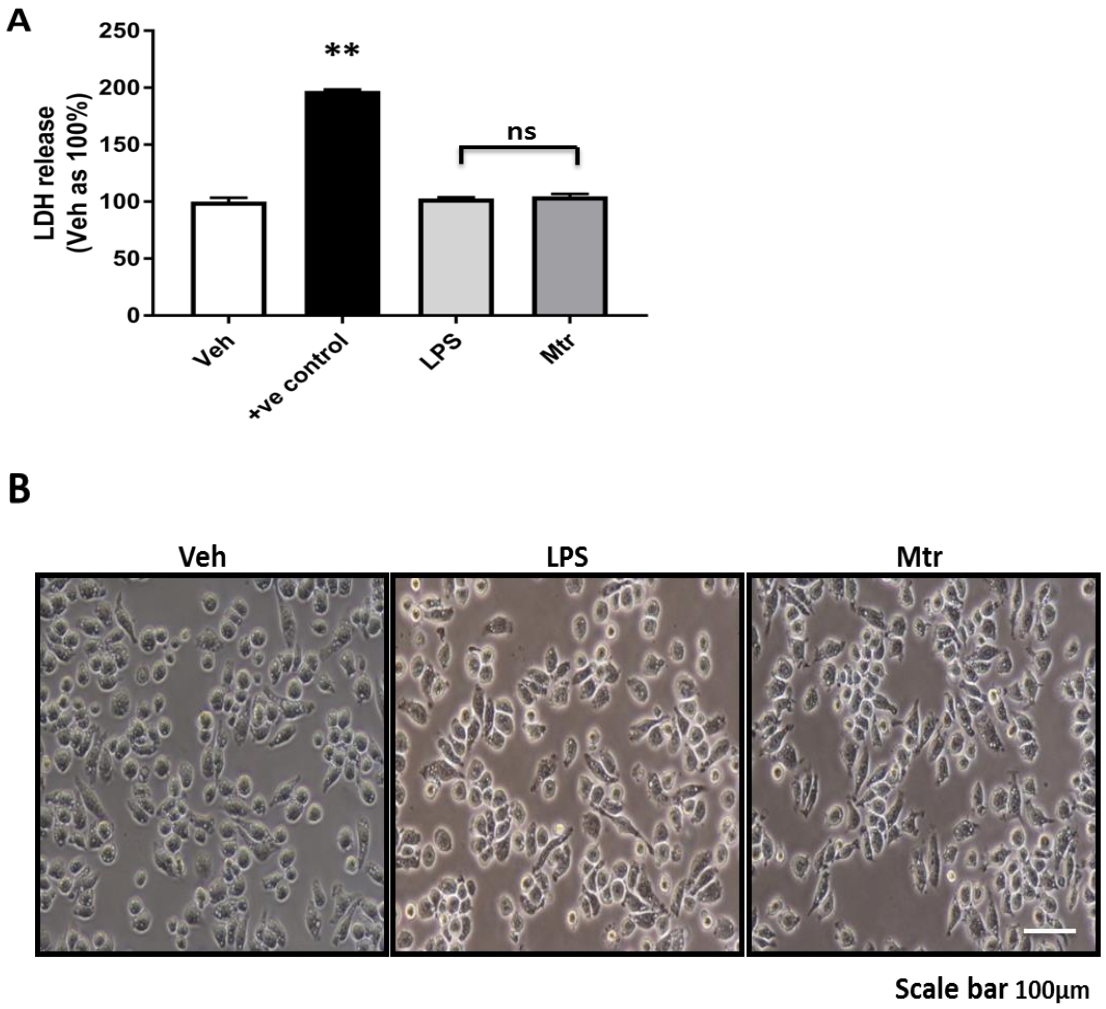

Figure 5.3 Effects of Mtr on cell viability and morphology in J774A.1 cells.

(A) J774A.1 cells (2×10^5 cells/mL) were treated with 3 ng/mL LPS or 1 μM Mtr for 2 h, and cell viability was determined by LDH assay in the cultured medium. (B) Cells were examined under a light microscope (magnification, ×100). Results are expressed as ±SEM and represent at least three independent experiments. $^{**}P < 0.01$ vs. Veh; ns: not significant. Veh: vehicle.

5.3.3 Changes in mTOR and heat shock proteins

As shown in Chapters 3 and 4, the anti-inflammatory effects of Mtr are associated with the downregulation of mTOR and upregulation of HSP72. To assess the potential involvement of mTOR and HSPs in the effects of Mtr in LPS-activated J774A.1 macrophages, we measured the mTOR, HSP72, HSF1 and HSP90 expression levels in the cell lysate using western blotting. Consistent with the results from the previous Chapters, treatment with Mtr reversed the increased protein level of mTOR ($P < 0.01$ vs. LPS) to normal levels as seen in the vehicle (**Figure 5.4A**).

Interestingly, HSP72 expression was significantly suppressed (40% reduction vs. vehicle, $P < 0.01$) following stimulation with LPS with a trend to reduce HSF1. However, HSP90 was not affected. Pretreatment with Mtr upregulated HSP72 and blocked the suppression of LPS on HSF1 protein expression with no significant effect on HSP90 expression (**Figure 5.4B-D**).

To elucidate the potential mechanism by which Mtr upregulates HSP72 in LPS-activated J774A.1 macrophages, the HSP72 inhibitor quercetin was examined for comparison in this Chapter. Cells were pretreated with quercetin (50 μM) for 2 h, and then treated with LPS (3 ng/mL) for 2 h. Interestingly, quercetin significantly increased mTOR expression in the presence of LPS compared with the vehicle (**Figure 5.4A**). As expected, quercetin significantly decreased HSP72 ($P < 0.01$ vs. vehicle) expression in the presence of LPS (**Figure 5.4B**), whereas there were no significant changes in HSF1 and HSP90 expression levels (**Figure 5.4C-D**). These data suggest that the reversal of LPS-induced upregulation of mTOR may be dependent on an upregulation of HSP72.

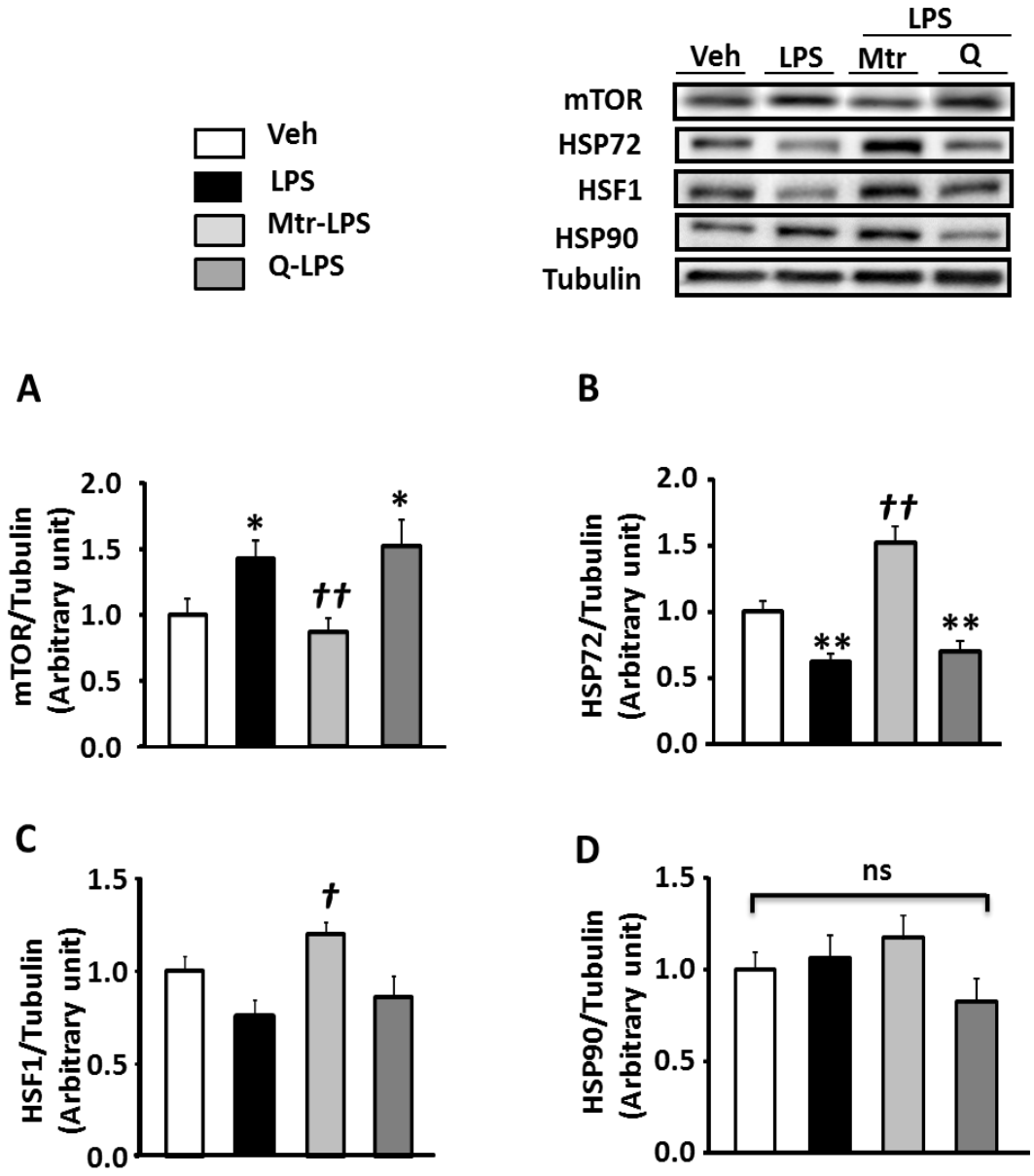

Figure 5.4 Changes in mTOR, HSF1, HSP90 and HSP72 in J774A.1 macrophage cells. Cells (2×10^5 cells/well) were pretreated with 1 μM Mtr or 50 μM quercetin for 2 h, and then treated with 3 ng/mL LPS for 2 h. Cell lysates were immunoblotted for (A) mTOR, (B) HSP72, (C) HSF1 and (D) HSP90 and quantified for statistical analysis. Results are expressed as ±SEM and represent at least three independent experiments. *$P < 0.05$, **$P < 0.01$ vs. Veh; †$P < 0.05$, ††$P < 0.01$ vs. LPS; ns: not significant. Veh: vehicle; Q: quercetin.

5.3.4 Effects of matrine on lipopolysaccharide-induced changes in inflammatory markers

The anti-inflammatory effect of Mtr was previously explored by measuring secretion of TNFα in the cell culture medium. In line with this, the effect of Mtr on CD68 mRNA expression was examined by quantitative RT-PCR and the protein expression levels of MCP-1 and NLRP3 inflammasome were detected by western blotting. As shown in **Figure 5.5A-C**, LPS at 3 ng/mL significantly increased the levels of these inflammatory markers in cell lysate (all $P < 0.05$ vs. vehicle). As expected, Mtr completely reversed all of these increases induced by LPS. In contrast, treatment with the HSP72 inhibitor quercetin in the presence of LPS did not show any significant reduction in any of these inflammatory markers.

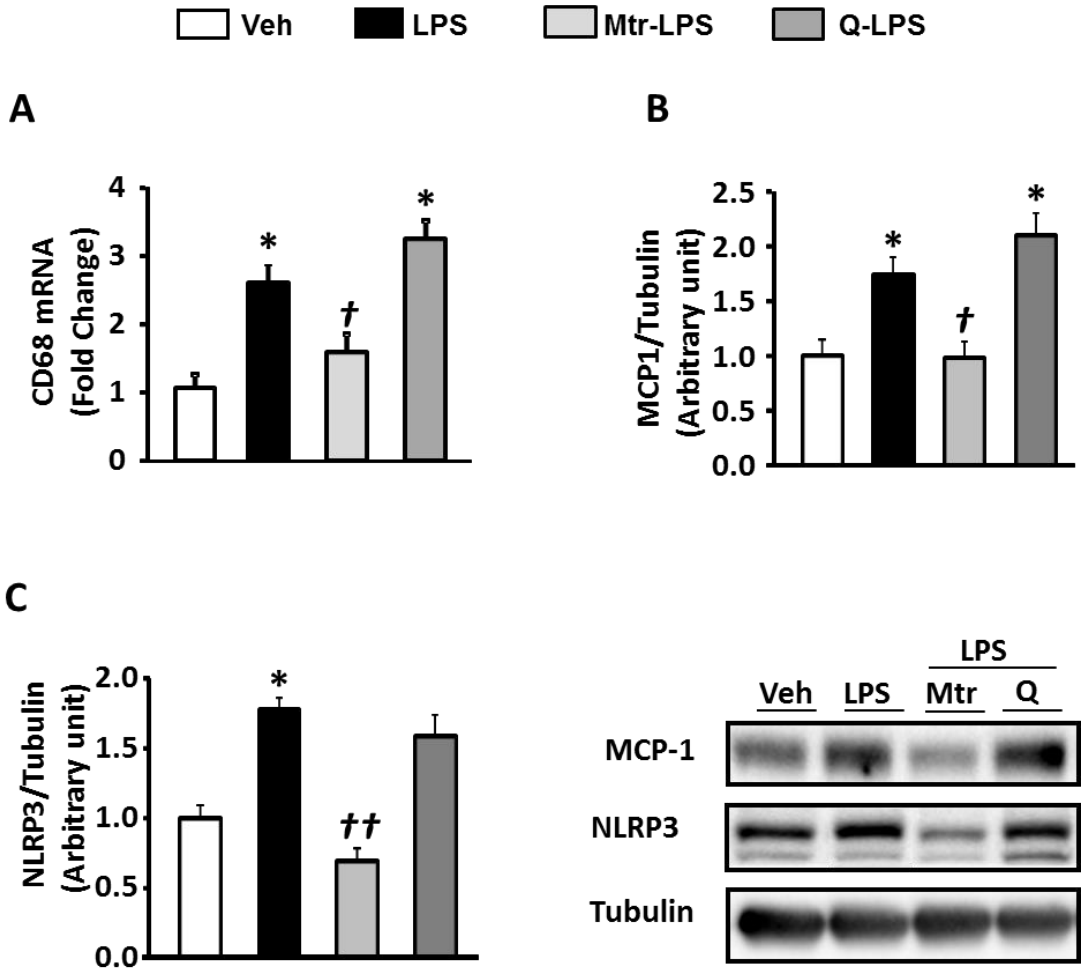

Figure 5.5 Effects of Mtr in LPS-induced inflammatory markers in the lysate of J774A.1 macrophage. Cells were pretreated with 1 μM Mtr or 50 μM quercetin for 2 h, and then treated with 3 ng/mL LPS. Quantitative RT-PCR results were normalised against 18s mRNA for (A) CD68 mRNA expression. Western blotting was analysed with densitometry for (B) MCP-1 and (C) NLRP3. Results are expressed as ±SEM and represent at least three independent experiments. **P* < 0.05 vs. Veh; *†P* < 0.05, *††P* < 0.01 vs. LPS. Veh: vehicle; Q: quercetin.

5.3.5 Effects of matrine on lipopolysaccharide-induced fibrogenic markers

The data presented in Chapter 4 showed that Mtr significantly inhibited MCD diet-induced fibrosis in the liver. To determine the potential mechanisms, the effect of Mtr on LPS-induced fibrogenic protein expression in J774A.1 cells was determined. As shown in **Figure 5.6A and B**, exposure to LPS stimulated the expression of key proteins of the fibrogenic pathway, namely collagen 1 and TGFβ (all $P < 0.01$ vs. vehicle). Mtr inhibited the increased expression of these proteins in LPS-activated J774A.1 macrophages (±55% and 56%, respectively) towards levels seen in the vehicle control. In contrast, the HSP72 inhibitor quercetin showed no effect on the increased expression of both proteins induced by LPS ($P < 0.05$ vs. vehicle). There were no significant changes in Smad3 and caspase-1 protein expression levels between groups (**Figure 5.6C and D**) during the treatment with LPS, Mtr or quercetin. These results suggest that Mtr may attenuate LPS-stimulated fibrogenic pathways and that this effect is associated with an upregulation of HSP72 as previously shown.

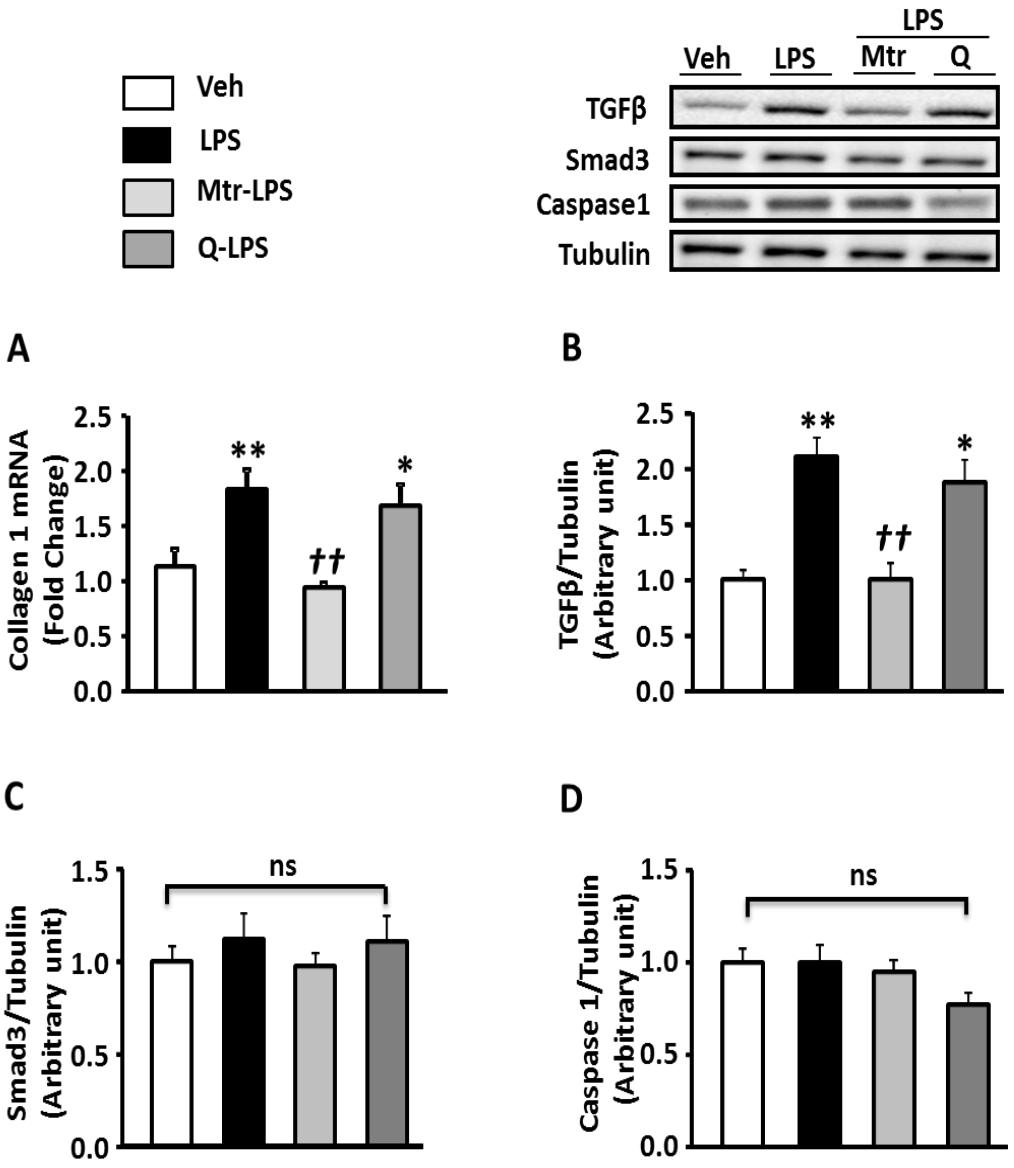

Figure 5.6 Effects of Mtr on LPS-induced fibrogenic markers in J774A.1 macrophages. Cells were pretreated with 1 μM Mtr or 50 μM quercetin for 2 h, and then treated with 3 ng/mL LPS. Quantitative RT-PCR results were normalised against 18s mRNA for (A) collagen 1 mRNA expression. Western blotting was analysed with densitometry for (B) TGFβ, (C) Smad3 and (D) caspase-1. Results are expressed as ±SEM and represent at least three independent experiments. **P* < 0.05 vs. Veh; *††P* < 0.01 vs. LPS; ns: not significant. Veh: vehicle; Q: quercetin.

5.4 Discussion

This Chapter investigated the effects of Mtr on LPS-induced activation of the pathways of inflammation and fibrogenesis at the cellular level in J774A.1 macrophages. The results showed that Mtr markedly ameliorated LPS-induced stimulation of cellular inflammatory and fibrotic activities in J774A.1 macrophages. The inhibitory effect of Mtr was associated with downregulation of mTOR and upregulation of HSP72. One consistent pattern of the effect of Mtr to inhibit LPS-induced increases in mTOR and markers of inflammatory and fibrogenic pathways was the upregulation of HSP72.

Macrophages play a major role in both inflammation and fibrosis in NASH. The macrophages present within the liver come from the activation of KCs (resident macrophages within the liver) and circulating monocyte-derived macrophages [261]. Once activated, macrophages produce inflammatory and fibrogenic cytokines to cause liver inflammation and fibrosis [262]. The results from this Chapter show that a low LPS concentration level can activates TNFα production in J774A.1 after 2 h. This is consistent with the report that stimulation of J774A.1 murine macrophages with LPS markedly increases TNFα production [263]. It has been suggested that the presence of LPS in KCs accelerates liver injury and aggravates the progression of NASH [128, 264]. The increase in TNFα production enhances inflammation and fibrogenesis in J774A.1 macrophages. Interestingly, the present study showed that low LPS concentration increased TNFα, but not IL-1β and IL-6, production. This suggests that TNFα is the major inflammatory cytokine observed after LPS stimulation. This is consistent with previous reports showing that Mtr inhibits the release of TNFα induced by KCs activation in cold ischaemia–reperfusion injury [200]. These data together

suggest that the inhibitory effect of Mtr on hepatic inflammation observed in Chapter 4 is likely to be a result, at least in part due to its effects on macrophages including KCs.

Several studies have suggested that upregulation of HSP72 is associated with the inhibition of inflammation [265, 266]. Earlier studies have indicated that upregulation of HSP72 by Mtr or other substances significantly protects against TNFα production, inhibiting inflammation [219, 267, 268]. Consistent with results from Chapters 3 and 4, the anti-TNFα effect of Mtr was associated with upregulation of HSP72 in J774A.1 cells. Given that upregulation of HSP72 might play a role in the anti-inflammatory effects of Mtr, the upregulation of this protein may be a potential cellular mechanism leading to reduction of inflammation and fibrosis. In this Chapter, protection by Mtr was correlated with quercetin, an HSP72 inhibitor, to further investigate the cellular mechanism of the anti-inflammatory effects of Mtr. These data add support to the role of HSP72 in Mtr preventing inflammation. These findings together raise the possibility that Mtr might offer distinct therapeutic effects to manifestations of NASH.

Another potential cellular target for the inhibitory effect of Mtr is mTOR. Inhibition of mTOR in experimental liver fibrosis significantly decreases fibrosis progression [164]. The results in this Chapter showed that Mtr also independently inhibited mTOR protein in J774A.1 macrophages, in agreement with the effect on mTOR in NASH mice. This is also consistent with recent clinical observations that Mtr inhibits mTOR expression in acute myelocytic leukaemia [252]. Further, the effects of Mtr on mTOR were evident even after treatment with the HSP72 blocker quercetin.

Consistent with the increased TNFα production following LPS stimulation, increased inflammatory markers including CD68, MCP-1 and NLRP3 were observed in activated J774A.1 cells. These findings are novel because there are no reports regarding the effect of Mtr on inflammation marker levels in LPS-stimulated macrophages. Further, the anti-inflammatory effects of Mtr could inhibit the inflammatory cytokines, consistent with the previous observations from Chapter 4. Quercetin however increased the expression of these proteins and exacerbated inflammation after stimulation with LPS. Blocking of HSP72 by quercetin can make cells more vulnerable to inflammatory and mTOR activity. Indeed, upregulation of HSP72 by Mtr was accompanied by inhibition of TNFα in LPS-stimulated inflammation. These results suggest that the induction of HSP72 by Mtr may confer protection against LPS-induced inflammation at least in part by inhibiting production of key inflammatory cytokines.

Another protective effect of Mtr is the prevention of the increased expression of fibrogenic pathways induced by MCD diet in mice (Chapter 4). In this Chapter, Mtr inhibited TGFβ and collagen 1–associated LPS-induced stimulation of cellular fibrogenesis, whereas quercetin further increased both cytokines after stimulation with LPS. This is consistent with previous findings that Mtr inhibits TGFβ and prevents liver fibrosis in vitro and in vivo in other animal models [189]. These results provide further support for the idea that inhibition of fibrogenic pathways by Mtr might provide a possible mechanism for its antifibrotic effects.

In summary, the results in this Chapter have revealed the possible mechanism—and promising novel anti-inflammatory and antifibrotic properties—of the beneficial effect of Mtr. Consistent with the previous Chapters, the major target of this mechanism

appears to be the mTOR-HSP72 axis. In addition, treatment with quercetin inhibited HSP72 and increased mTOR, supporting this explanation. It is likely that Mtr confers protection against LPS-induced inflammation and fibrosis at least in part by upregulating HSP72 and inhibiting mTOR. These findings suggest that the anti-inflammatory and antifibrotic effects of Mtr in macrophages are important mechanisms for the therapeutic effects in NASH as discussed in previous Chapters.

Chapter 6 General Discussion

6.1 Introduction

This Chapter will summarise the key findings from Chapters 3, 4 and 5 and discuss the potential implications and limitations of the study. It concludes by providing suggestions for further research based on the novel findings in this thesis.

6.2 Major findings

Chapter 1 reviewed literature reports on the research of NASH and current status of the treatments for NASH. Secondly, it elaborates the rationale for the selection of Mtr as a candidate for the study in this thesis to investigate its effects and mechanisms for the treatment of this disease with distinct properties different from others.

In brief, NAFLD is an umbrella term for metabolic liver disease, with a global increase in prevalence accompanied by increased metabolic diseases such as obesity and T2D. It is the most common cause of chronic liver disease and regarded as a manifestation of the metabolic syndrome in the liver. NAFLD has different stages based on its natural history and the disease pathogenesis. It has been widely recognised that excessive lipid accumulation in the liver causes the first hit. This benign stage can progress to NASH (steatohepatitis) with additional inflammation, cell damage and/or fibrosis in the liver, and may further deteriorate to cirrhosis and liver failure. However, treatment of NAFLD is currently unsatisfactory. One challenge in the study of therapeutics for NASH is the lack of a single animal model that fully reflects the pathological characteristics as presented in humans.

Current drugs used for the treatment of NAFLD are inadequate because of various adverse effects or unreliable effects on inflammation and fibrosis. Indeed, it is important to identify a novel therapeutic for NAFLD, and drug repurposing may be an effective strategy. This approach has been increasingly used in recent years because of existing knowledge of bioavailability and more reliable safety. Using this approach, this thesis selected Mtr as a candidate drug to examine its therapeutic effects for the treatment of NAFLD.

Chapter 3 investigated the potential of Mtr for the treatment of NAFLD in HFru-fed and HFD-STZ models in mice. Mtr treatment was able to attenuate hepatosteatosis and associated disorders in glucose homeostasis. Chapter 4 examined the therapeutic effects of Mtr in the treatment of hepatic inflammation and fibrosis, two other characteristics of NASH. Chapter 5 examined the therapeutic effects of Mtr on inflammation in a macrophage-like cell line and the cellular mechanism involved. These major findings are summarised in the following three sections.

6.2.1 Reduction of hepatosteatosis and associated disorders in glucose homeostasis

Chapter 3 evaluated the therapeutic effects of Mtr on hepatosteatosis and associated disorders in glucose homeostasis in HFru-fed mice. The most important finding from this study is that Mtr was effective for the treatment of hepatosteatosis and associated glucose intolerance. Several mechanisms for the antisteatotic effects of Mtr were examined. The results suggested that Mtr reduced TG accumulation in the liver, but not in muscle. This indicates that the liver is a major site for the action of Mtr and that

improved glucose tolerance is attributable to a reduction in hepatosteatosis. Further studies suggested that inhibition of hepatic DNL is likely the underlying mechanism responsible for the antisteatotic effect of Mtr in mice fed with HFru diet. Moreover, Mtr inhibited ER stress, which was associated with increased DNL, and upregulated hepatic protein expression of HSP72. Importantly, Mtr displayed a distinct mechanism in reducing hepatosteatosis associated with glucose intolerance via upregulation of HSP72. This Chapter further examined the efficacy of Mtr in hepatosteatosis-associated hyperglycaemia in a mouse model of T2D induced by HFD-STZ. The anti-hyperglycaemic effects of Mtr observed in this study were also found closely associated with a reduction in hepatosteatosis (**Figure 6.1**).

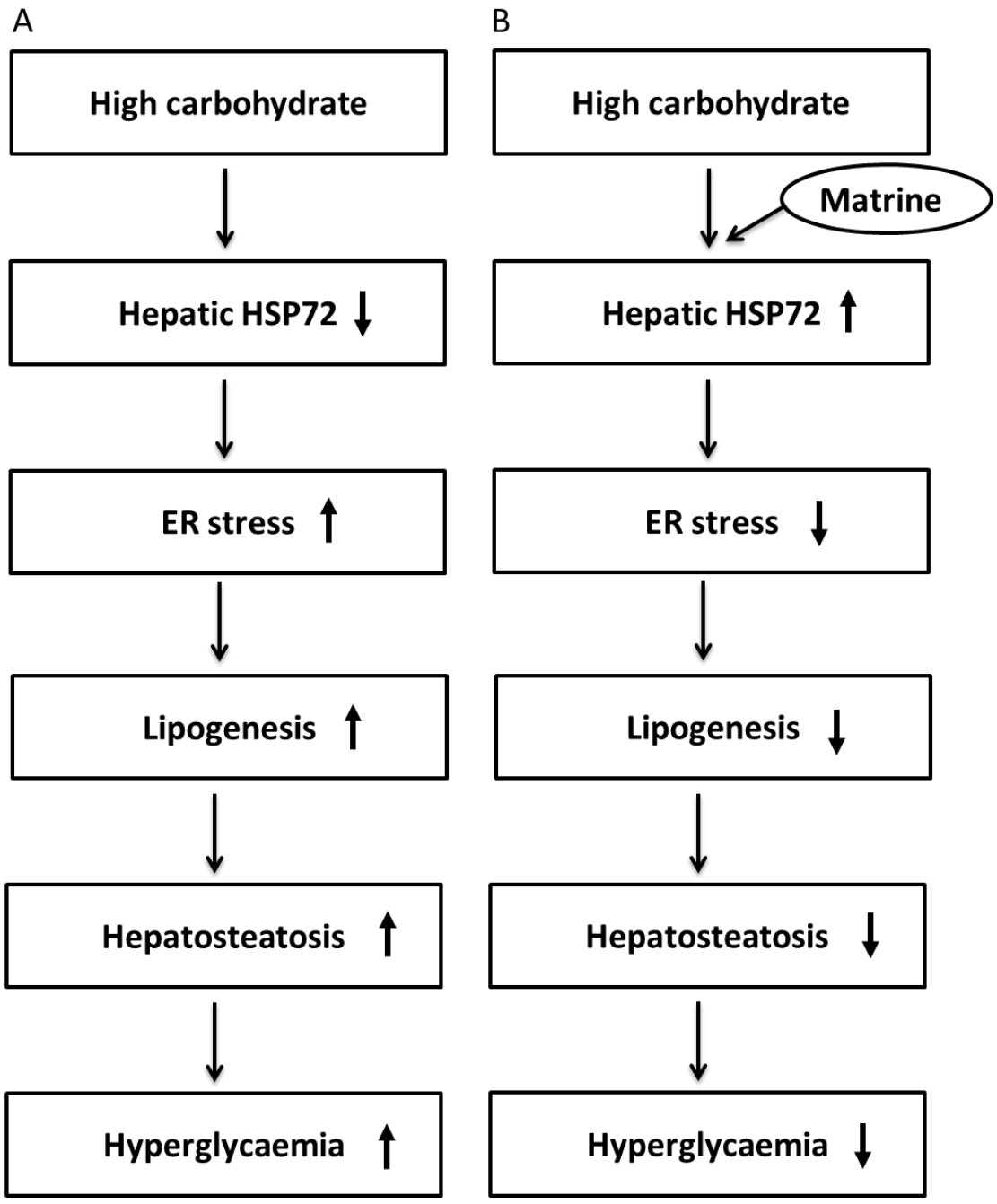

Figure 6.1 Mtr ameliorated of hepatosteatosis and associated hyperglycaemia. (A) Excess carbohydrate causes increased hepatic ER stress-DNL pathways through downregulation of HSP72. (B) Mtr exerts its effects through upregulation of HSP72, preventing hepatic ER stress-DNL pathways and associated hyperglycaemia.

In summary, Mtr treatment improved hepatosteatosis and glucose tolerance in both models, suggesting that the liver is the major target of Mtr because lipid and glucose is mainly metabolised in the liver. Upregulation of HSP72 by Mtr may suppress ER stress to inhibit DNL, and therefore hepatosteatosis, hyperglycaemia and NAFLD. The findings of upregulation of HSP72 from our present study demonstrate, for the first time, a plausible mechanism for the antisteatotic therapeutic effect of Mtr on hepatosteatosis and hyperglycaemia in mouse models of HFru feeding.

6.2.2 Amelioration of hepatic inflammation and fibrosis

The third study (Chapter 4) investigated the hepatoprotective effect including anti-inflammatory and antifibrotic effects in an MCD diet-induced mouse model of NASH. The first important finding of this study is that Mtr was able to inhibit inflammation without affecting caloric intake in MCD mice. However, Mtr treatment failed to reduce hepatosteatosis in MCD-fed mice as it does in HFD, HFru diet and T2D mice models. Because MCD diet-induced hepatosteatosis is due to the disruption of TG export, this finding suggests that Mtr does not promote TG export.

The second important finding is that Mtr exerted its antifibrotic effects at the transition stage of NASH without fibrosis to severe NASH-related fibrosis. The anti-inflammatory effect of Mtr in MCD diet-induced NASH was evidenced by marked decreases in the activation of TNFα secretion and CD68 and NLRP3 expression. This mouse model displayed mild fibrosis in the liver because of a short period of MCD diet feeding. In this short-term MCD model, Mtr reduced TGFβ and Smad3 expression and inhibited fibrosis. In addition, protein expression levels of TGFβ and caspase-1 (which

play a role in fibrosis), and Smad3 and collagen type 1 (which are associated with collagen deposition), were decreased. Overall, Mtr demonstrated therapeutic effects for the inhibition of inflammation and fibrosis in MCD diet-fed mice. Again, the anti-inflammatory and antifibrotic effects of Mtr were accompanied by upregulation of HSP72 and downregulation of mTOR pathways (**Figure 6.2**).

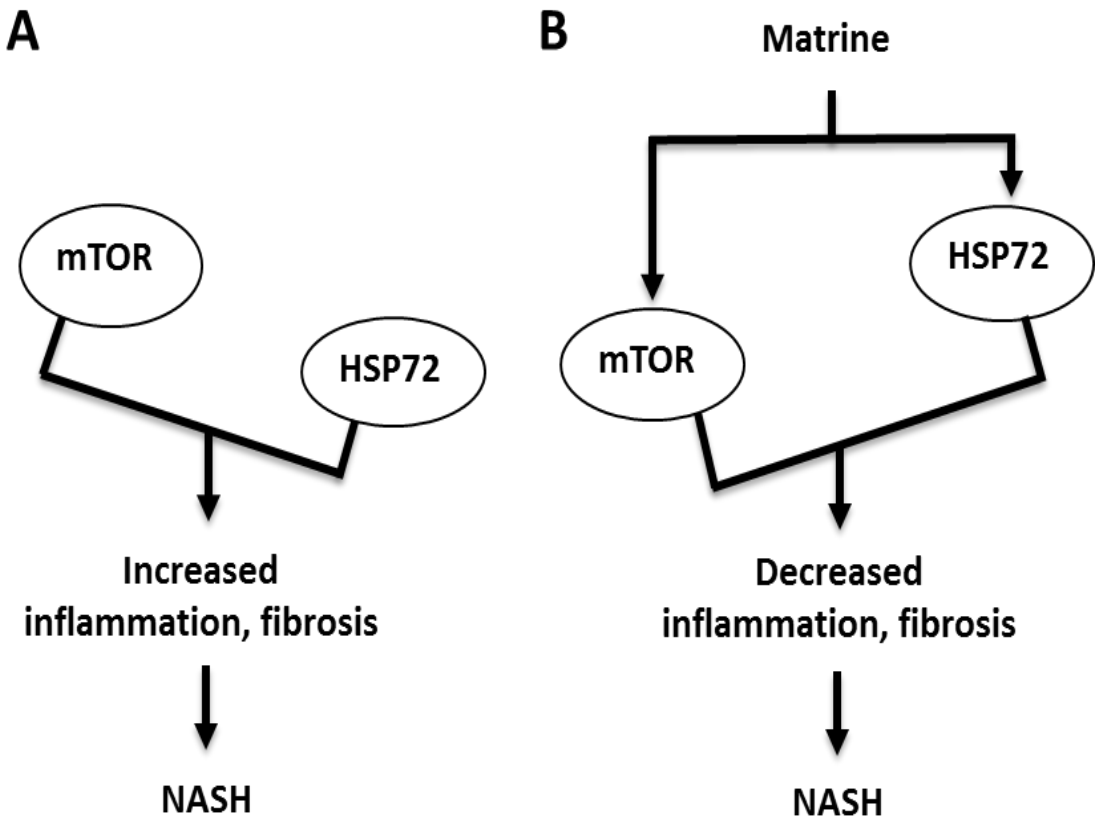

Figure 6.2 Mtr dysregulated of HSP72 and mTOR expression. (A) Hepatic inflammation and fibrosis are the major phenotypes of NASH. (B) Mtr exerts its effects through upregulation of HSP72 and downregulation of mTOR, preventing hepatic inflammation and fibrosis, and therefore protecting against the development of NASH.

6.2.3 Cellular mechanism involved in the effects of matrine

Chapter 5 investigated the mechanism of the anti-inflammatory and antifibrotic effects in macrophages, a key cell type responsible for NASH, using a well characterised murine macrophage cell line. The findings obtained in this Chapter were similar to the markers measured in Chapter 4, as a further indication of the anti-inflammatory effects of Mtr at the cellular level. The major inflammation and fibrosis markers activated by LPS in J774A.1 macrophages were inhibited by Mtr despite the low concentration of Mtr used. Notably, Mtr markedly inhibited LPS-induced increases in mTOR in J774A.1, suggesting that the therapeutic effect of Mtr may involve the inhibition of mTOR-related autophagy and inflammation in NASH, similar to the results in the MCD diet model reported in this thesis.

Overall, this thesis addressed the specific aims based on the gaps in knowledge identified by careful evaluation of the literature in Chapter 1. The relationship of the concluded studies to the specific aims are summarised in **Figure 6.3**.

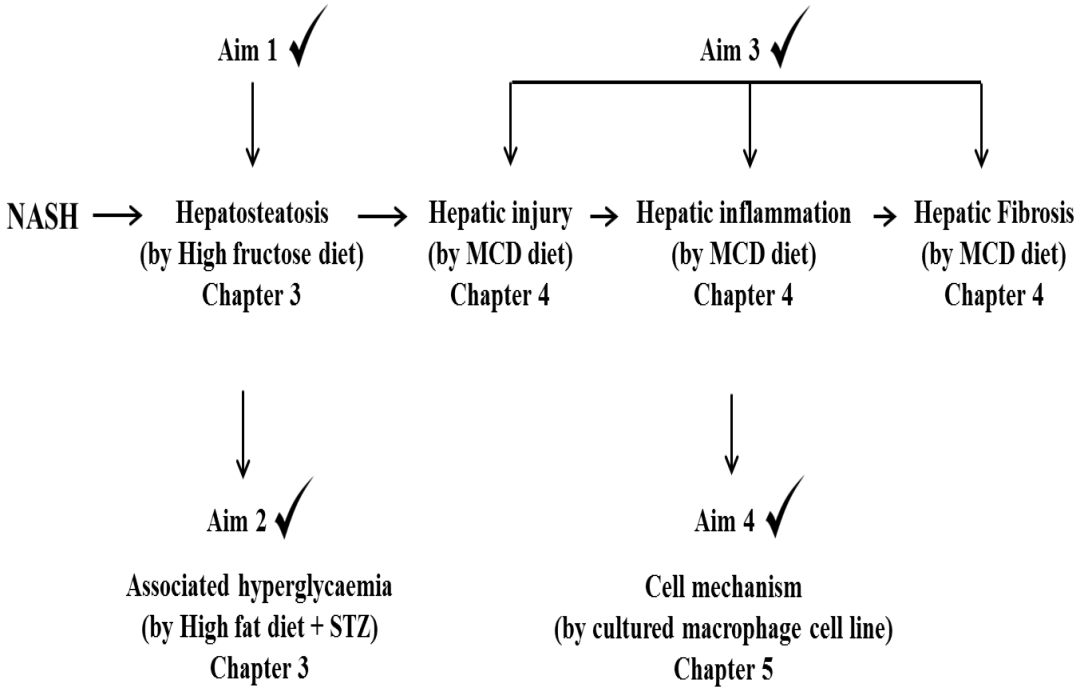

Figure 6.3 A schematic view of the findings related to the research aims in Figure 1.9.

Mtr acts as a promising antisteatotic drug by blocking the ER stress-DNL axis required for the development of hepatosteatosis. Many of the markers in this pathway, such as eIF2α, CHOP, IRE1, SREBP1c, ChREBP, SCD1 and FAS, are downregulated after Mtr treatment. Moreover, Mtr improves hyperglycaemia associated with hepatosteatosis, and attenuates hepatic inflammation and fibrosis by inhibiting inflammatory and fibrogenic pathways in NASH. The anti-inflammatory and antifibrotic effects are evidenced by blocking TNFα, NLRP3, CD68, TGFβ and collagen 1 expression. These anti-NASH effects involve upregulation of HSP72 as well as reduction in the mTOR axis. **Figure 6.4** illustrates the proposed mechanism linking the above-mentioned effects to Mtr's therapeutic properties in NAFLD and associated disorders.

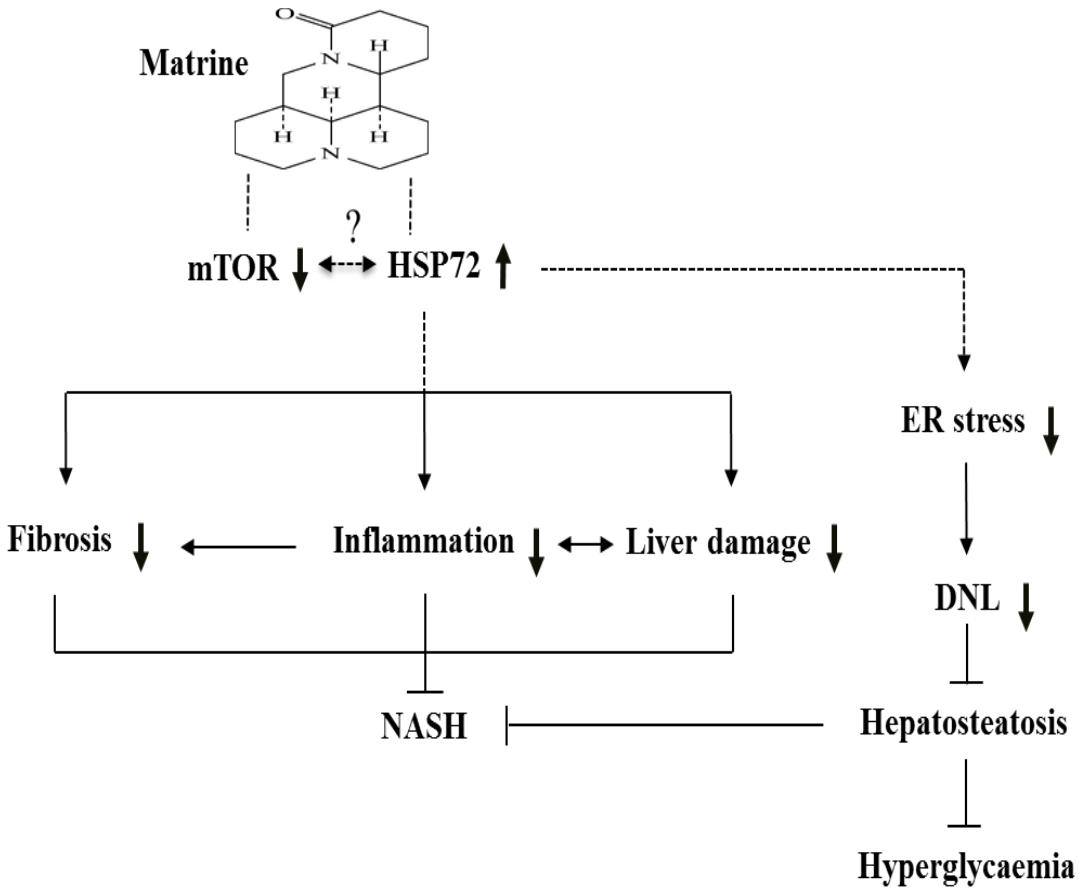

Figure 6.4 Schematic illustration of the proposed mechanism for Mtr's therapeutic effects. Mtr achieves these effects through ameliorating ER stress, DNL, and inflammatory and fibrotic signalling cascades via hepatic HSP72 upregulation and mTOR reduction. These findings suggest that Mtr may be repurposed for the treatment of NAFLD and associated diseases such as hyperglycaemia and NASH. Solid lines indicate hypothesised mechanistic links; dotted lines indicate pathways requiring future studies.

6.3 Limitations and future studies

To achieve the ultimate goal of repurposing Mtr for the treatment of NAFLD/NASH, further studies are needed in three general aspects.

6.3.1 Long-term safety for the new usage

The results in Chapter 3 showed that the antisteatotic effects of Mtr are due to decreased DNL and associated disorders in glucose metabolism. First, further evaluation of the long-term safety at the dose designed for this new therapeutic application is required. This is important because the reported safety of Mtr has not been evaluated for the metabolic condition described in this thesis. Treatments for metabolic conditions including NAFLD/NASH require long-term administration.

6.3.2 Clinical trials for the new usage

Second, additional studies are needed to fully characterise the therapeutic effects of Mtr to provide more comprehensive evidence to guide the clinical trials for its new application. According to the basic science data from this Chapter, Mtr is able to target the major components of NAFLD pathogenesis. Randomised controlled trials are the most appropriate study design to confirm the effectiveness of Mtr treatment in humans with NAFLD/NASH.

6.3.3 Precise mechanism for the molecular mode of action

6.3.3.1 Anti-hepatosteatosis

Third, the molecular mode of action and pathways involved require more detailed studies. The specific proposals for the second and third aspects are suggested below. Mtr showed a reduction in lipid accumulation in HFru and HFD-STZ mice. However, signs of hepatosteatosis were not assessed by morphological studies. One feasible approach for the assessment of lipid droplets is the use of oil red O staining [269, 270]. In future studies, histological liver sections should be performed to further assess hepatosteatosis in these nutritional models.

In addition, the mechanisms underlying the effect of Mtr on hepatosteatosis need further study. As reviewed in Chapter 3, dietary fructose has been shown to have a special tendency to induce NAFLD dependent on the activation of the ER stress pathway [44]. ER stress may be a novel mode of action for the inhibitory effect of Mtr on hepatosteatosis. Experiments using TUDCA, a classic inhibitor of ER stress, in HFru mice treated with Mtr are suggested. This will help to determine whether the amelioration of HFru-induced hepatosteatosis and associated disorders in glucose homeostasis by Mtr is due to decreased ER stress. Measuring ER stress markers including eIF2α, CHOP, IRE1 and XBP1 will help to confirm the role of ER stress in Mtr's inhibitory effects. A similar animal study may be conducted with HSP72 knockout mice to confirm the role of HSP72 in this model. The HSP72 knockdown approach may be used to provide definitive evidence to prove the hypothesised role of HSP72 in Mtr's antisteatotic effects.

6.3.3.2 Anti-inflammation

The data from Chapter 4 suggested that the anti-inflammatory effects of Mtr may be related to upregulation of hepatic HSP72 as a likely mechanism. Another possible mechanism is the inhibition of hepatic mTOR, which was downregulated in Mtr-treated MCD diet-fed mice—this will be discussed below. Using an animal model with HSP72 knockdown or knockout may provide definitive evidence to prove the hypothesised role of HSP72 in Mtr's anti-inflammatory effects. Importantly, mice with muscle-specific transgenic overexpression of HSP72 are protected against high fat-induced obesity and metabolic disorders [196]. Future studies are needed to examine the anti-inflammatory effect of Mtr by using an HSP72 knockout model. Further, the only mouse model in which mTOR is genetically altered is the 'flat-top' mutant, where incomplete and complete deletions cause failure of mTOR inhibition and shorter lifespan of mice, respectively [271].

Current data in this Chapter showed that Mtr can significantly inhibit the activation of inflammatory cytokines. This inhibition was proposed to be associated with HSP72-mTOR pathways in the liver. However, NASH features were not assessed by histological abnormalities of steatohepatitis in the liver. In future studies, the NASH activity scores of hepatic steatosis, inflammation, hepatocyte ballooning and fibrosis should be performed to further assess Mtr's efficiency for the treatment of NASH in this nutritional model [10]. This can be achieved by staining liver sections with H&E to examine macrovesicular and microvesicular steatosis, admixtures of inflammatory cells, collagen fibres and hepatocyte ballooning—features that are often observed in NASH [272].

6.3.3.3 Anti-cell injury

Hepatic cell injury has been proposed as another component of NASH features [6]. Therefore, further studies may be performed to examine the anti-cell injury of Mtr by using cell lines such as HepG2 cells, which mimic hepatocytes. First, hepatic injury may be assessed by measuring plasma ALT, a standard indication of liver injury. Hepatocyte ballooning is another indication of cell injury and a key feature required for the diagnosis of NASH. With H&E staining and microscopic examination, hepatocyte ballooning is seen as hepatocytes with fatty changes and groups of ballooned hepatocytes with enlarged, rounded, rarefied cytoplasm, some of which contain small Mallory-Denk bodies. Mtr's effects on hepatocyte ballooning can be quantified by histological grading and staging systems of NASH [10].

6.3.3.4 Anti-fibrosis

In light of these antisteatotic, anti-inflammatory and antifibrotic effects of Mtr, it may be worthwhile to investigate the cellular mechanism underlying the antifibrotic effects of Mtr in cell lines representative of HSCs. The antifibrotic effects of Mtr may be further studied using an appropriate cell line. For example, human HSCs (LX-2) can be pretreated with Mtr, and then exposed to a potent fibrotic inducer [273, 274]. Quantitative RT-PCR and western blotting can be used to measure mRNA and protein levels of fibrogenic genes.

6.4 Final conclusion and potential significance

Overall, the studies in this thesis have laid a solid base for further investigation of the cellular mechanism of the therapeutic effects of Mtr attributed to its effects on HSP72-mTOR pathways for the treatment of NASH and associated metabolic disorders. The results will serve the development of new treatments for NAFLD.

The findings from this thesis have significant implications for evaluating the therapeutic effects of Mtr in the treatment of NAFLD/NASH. The novelty of Mtr is of potential great significance for the treatment of patients suffering NAFLD.

References

1. Cohen, J.C., J.D. Horton, and H.H. Hobbs, Human fatty liver disease: old questions and new insights. Science, 2011. 332(6037): p. 1519-23.

2. Donnelly, K.L., et al., Sources of fatty acids stored in liver and secreted via lipoproteins in patients with nonalcoholic fatty liver disease. J Clin Invest, 2005. 115(5): p. 1343-51.

3. Bray, G.A. and R.M. Krauss, Overfeeding of Polyunsaturated Versus Saturated Fatty Acids Reduces Ectopic Fat. Diabetes, 2014. 63(7): p. 2222-2224.

4. He, X.X., et al., Effectiveness of Omega-3 Polyunsaturated Fatty Acids in Non-Alcoholic Fatty Liver Disease: A Meta-Analysis of Randomized Controlled Trials. PLoS One, 2016. 11(10): p. e0162368.

5. Younossi, Z., et al., Global burden of NAFLD and NASH: trends, predictions, risk factors and prevention. Nat Rev Gastroenterol Hepatol, 2018. 15(1): p. 11-20.

6. Diehl, A.M. and C. Day, Cause, Pathogenesis, and Treatment of Nonalcoholic Steatohepatitis. N Engl J Med, 2017. 377(21): p. 2063-2072.

7. Syed, G.H., Y. Amako, and A. Siddiqui, Hepatitis C virus hijacks host lipid metabolism. Trends Endocrinol Metab, 2010. 21(1): p. 33-40.

8. Westbrook, R.H., G. Dusheiko, and C. Williamson, Pregnancy and liver disease. J Hepatol, 2016. 64(4): p. 933-45.

9. Mota, M., et al., Molecular mechanisms of lipotoxicity and glucotoxicity in nonalcoholic fatty liver disease. Metabolism, 2016. 65(8): p. 1049-61.

10. Chalasani, N., et al., The diagnosis and management of non-alcoholic fatty liver disease: practice Guideline by the American Association for the Study of Liver Diseases, American College of Gastroenterology, and the American Gastroenterological Association. Hepatology, 2012. 55(6): p. 2005-23.

11. Kawano, Y. and D.E. Cohen, Mechanisms of hepatic triglyceride accumulation in non-alcoholic fatty liver disease. J Gastroenterol, 2013. 48(4): p. 434-41.

12. Rinella, M.E., Nonalcoholic fatty liver disease: a systematic review. Jama, 2015. 313(22): p. 2263-73.

13. Loomba, R., et al., Association between diabetes, family history of diabetes, and risk of nonalcoholic steatohepatitis and fibrosis. Hepatology, 2012. 56(3): p. 943-51.

14. Yamaguchi, K., et al., Inhibiting triglyceride synthesis improves hepatic steatosis but exacerbates liver damage and fibrosis in obese mice with nonalcoholic steatohepatitis. Hepatology, 2007. 45(6): p. 1366-74.

15. Suzuki, A. and A.M. Diehl, Nonalcoholic Steatohepatitis. Annu Rev Med, 2017. 68: p. 85-98.

16. Cusi, K., et al., Non-alcoholic fatty liver disease (NAFLD) prevalence and its metabolic associations in patients with type 1 diabetes and type 2 diabetes. Diabetes Obes Metab, 2017. 19(11): p. 1630-1634.

17. Farrell, G.C. and C.Z. Larter, Nonalcoholic fatty liver disease: from steatosis to cirrhosis. Hepatology, 2006. 43(2 Suppl 1): p. S99-s112.

18. LaBrecque, D.R., et al., World Gastroenterology Organisation global guidelines: Nonalcoholic fatty liver disease and nonalcoholic steatohepatitis. J Clin Gastroenterol, 2014. 48(6): p. 467-73.

19. Economics, D.A., The economic cost and health burden of liver diseases in Australia, in Gastroenterological Society of Australia and Australian Liver Association. 2012: Australia.

20. Lu, Z.Y., et al., Prevalence of and risk factors for non-alcoholic fatty liver disease in a Chinese population: An 8-year follow-up study. World J Gastroenterol, 2016. 22(13): p. 3663-9.

21. Yan, J., et al., Epidemiological survey and risk factor analysis of fatty liver disease of adult residents, Beijing, China. J Gastroenterol Hepatol, 2013. 28(10): p. 1654-9.

22. Masarone, M., et al., Liver biopsy in type 2 diabetes mellitus: Steatohepatitis represents the sole feature of liver damage. PLoS One, 2017. 12(6): p. e0178473.

23. Fattahi, M.R., et al., The Prevalence of Metabolic Syndrome In Non-alcoholic Fatty Liver Disease; A Population-Based Study. Middle East J Dig Dis, 2016. 8(2): p. 131-7.

24. Kalra, S., et al., Study of prevalence of nonalcoholic fatty liver disease (NAFLD) in type 2 diabetes patients in India (SPRINT). J Assoc Physicians India, 2013. 61(7): p. 448-53.

25. Ortiz-Lopez, C., et al., Prevalence of Prediabetes and Diabetes and Metabolic Profile of Patients With Nonalcoholic Fatty Liver Disease (NAFLD). Diabetes Care, 2012. 35(4): p. 873-878.

26. Le, M.H., et al., Prevalence of non-alcoholic fatty liver disease and risk factors for advanced fibrosis and mortality in the United States. PLoS One, 2017. 12(3): p. e0173499.

27. Sanyal, A.J., et al., Endpoints and clinical trial design for nonalcoholic steatohepatitis. Hepatology, 2011. 54(1): p. 344-53.

28. Chalasani, N., et al., The diagnosis and management of nonalcoholic fatty liver disease: Practice guidance from the American Association for the Study of Liver Diseases. Hepatology, 2018. 67(1): p. 328-357.

29. Marchesini, G., et al., Nonalcoholic fatty liver, steatohepatitis, and the metabolic syndrome. Hepatology, 2003. 37(4): p. 917-23.

30. Samuel, V.T., K.F. Petersen, and G.I. Shulman, Lipid-induced insulin resistance: unravelling the mechanism. Lancet, 2010. 375(9733): p. 2267-77.

31. Marchesini, G., et al., Nonalcoholic fatty liver disease: a feature of the metabolic syndrome. Diabetes, 2001. 50(8): p. 1844-50.

32. Wu, S., et al., Association of non-alcoholic fatty liver disease with major adverse cardiovascular events: A systematic review and meta-analysis. Sci Rep, 2016. 6: p. 33386.

33. Karpe, F., J.R. Dickmann, and K.N. Frayn, Fatty acids, obesity, and insulin resistance: time for a reevaluation. Diabetes, 2011. 60(10): p. 2441-9.

34. Samuel, V.T. and G.I. Shulman, The pathogenesis of insulin resistance: integrating signaling pathways and substrate flux. J Clin Invest, 2016. 126(1): p. 12-22.

35. Tilg, H., A.R. Moschen, and M. Roden, NAFLD and diabetes mellitus. Nat Rev Gastroenterol Hepatol, 2017. 14(1): p. 32-42.

36. Petersen, K.F., et al., Reversal of nonalcoholic hepatic steatosis, hepatic insulin resistance, and hyperglycemia by moderate weight reduction in patients with type 2 diabetes. Diabetes, 2005. 54(3): p. 603-8.

37. Samuel, V.T., et al., Mechanism of hepatic insulin resistance in non-alcoholic fatty liver disease. J Biol Chem, 2004. 279(31): p. 32345-53.

38. Oakes, N.D., et al., Mechanisms of liver and muscle insulin resistance induced by chronic high-fat feeding. Diabetes, 1997. 46(11): p. 1768-74.

39. Farese, R.V., Jr., et al., The problem of establishing relationships between hepatic steatosis and hepatic insulin resistance. Cell Metab, 2012. 15(5): p. 570-3.

40. Targher, G., F. Marra, and G. Marchesini, Increased risk of cardiovascular disease in non-alcoholic fatty liver disease: causal effect or epiphenomenon? Diabetologia, 2008. 51(11): p. 1947-53.

41. Lee, Y.H., et al., Association of nonalcoholic steatohepatitis with subclinical myocardial dysfunction in non-cirrhotic patients. J Hepatol, 2017.

42. Targher, G. and C.D. Byrne, Non-alcoholic fatty liver disease: an emerging driving force in chronic kidney disease. Nat Rev Nephrol, 2017. 13(5): p. 297-310.

43. Lozano, I., et al., High-fructose and high-fat diet-induced disorders in rats: impact on diabetes risk, hepatic and vascular complications. Nutr Metab (Lond), 2016. 13: p. 15.

44. Ren, L.P., et al., Differing endoplasmic reticulum stress response to excess lipogenesis versus lipid oversupply in relation to hepatic steatosis and insulin resistance. PLoS One, 2012. 7(2): p. e30816.

45. Chan, S.M., et al., Activation of PPARalpha ameliorates hepatic insulin resistance and steatosis in high fructose-fed mice despite increased endoplasmic reticulum stress. Diabetes, 2013. 62(6): p. 2095-105.

46. Sun, R.Q., et al., IRE1 impairs insulin signaling transduction of fructose-fed mice via JNK independent of excess lipid. Biochim Biophys Acta, 2015. 1852(1): p. 156-65.

47. Lee, A.H., et al., Regulation of hepatic lipogenesis by the transcription factor XBP1. Science, 2008. 320(5882): p. 1492-6.

48. Stanhope, K.L., et al., Consuming fructose-sweetened, not glucose-sweetened, beverages increases visceral adiposity and lipids and decreases insulin sensitivity in overweight/obese humans. J Clin Invest, 2009. 119(5): p. 1322-34.

49. Lecoultre, V., et al., Effects of fructose and glucose overfeeding on hepatic insulin sensitivity and intrahepatic lipids in healthy humans. Obesity 2013. 21(4): p. 782-5.

50. Schwarz, J.M., et al., Effect of a High-Fructose Weight-Maintaining Diet on Lipogenesis and Liver Fat. J Clin Endocrinol Metab, 2015. 100(6): p. 2434-42.

51. Ameer, F., et al., De novo lipogenesis in health and disease. Metabolism, 2014. 63(7): p. 895-902.

52. Day, C.P. and O.F. James, Steatohepatitis: a tale of two "hits"? Gastroenterology, 1998. 114(4): p. 842-5.

53. Arab, J.P., M. Arrese, and M. Trauner, Recent Insights into the Pathogenesis of Nonalcoholic Fatty Liver Disease. Annu Rev Pathol, 2018. 13: p. 321-350.

54. Tilg, H. and A.R. Moschen, Evolution of inflammation in nonalcoholic fatty liver disease: the multiple parallel hits hypothesis. Hepatology, 2010. 52(5): p. 1836-46.

55. Madan, K., et al., Oxidant stress and antioxidant status among patients with nonalcoholic fatty liver disease (NAFLD). J Clin Gastroenterol, 2006. 40(10): p. 930-5.

56. Sutti, S., et al., Adaptive immune responses triggered by oxidative stress contribute to hepatic inflammation in NASH. Hepatology, 2014. 59(3): p. 886-97.

57. Ge, C.X., et al., Betaine prevented fructose-induced NAFLD by regulating LXRalpha/PPARalpha pathway and alleviating ER stress in rats. Eur J Pharmacol, 2016. 770: p. 154-64.

58. Xiong, X., et al., Hepatic steatosis exacerbated by endoplasmic reticulum stress-mediated downregulation of FXR in aging mice. J Hepatol, 2014. 60(4): p. 847-54.

59. Ozcan, U., et al., Endoplasmic reticulum stress links obesity, insulin action, and type 2 diabetes. Science, 2004. 306(5695): p. 457-61.

60. Takahara, I., et al., Toyocamycin attenuates free fatty acid-induced hepatic steatosis and apoptosis in cultured hepatocytes and ameliorates nonalcoholic fatty liver disease in mice. PLoS One, 2017. 12(3): p. e0170591.

61. Zhang, Z., et al., Berberine prevents progression from hepatic steatosis to steatohepatitis and fibrosis by reducing endoplasmic reticulum stress. Sci Rep, 2016. 6: p. 20848.

62. Matsuzawa, N., et al., Lipid-induced oxidative stress causes steatohepatitis in mice fed an atherogenic diet. Hepatology, 2007. 46(5): p. 1392-403.

63. Moschen, A.R., S. Kaser, and H. Tilg, Non-alcoholic steatohepatitis: a microbiota-driven disease. Trends Endocrinol Metab, 2013. 24(11): p. 537-45.

64. Xue, L., et al., Probiotics may delay the progression of nonalcoholic fatty liver disease by restoring the gut microbiota structure and improving intestinal endotoxemia. Sci Rep, 2017. 7: p. 45176.

65. Kudo, H., et al., Lipopolysaccharide triggered TNF-alpha-induced hepatocyte apoptosis in a murine non-alcoholic steatohepatitis model. J Hepatol, 2009. 51(1): p. 168-75.

66. Matsushita, N., et al., Effect of Lipopolysaccharide on the Progression of Non-Alcoholic Fatty Liver Disease in High Caloric Diet-Fed Mice. Scand J Immunol, 2016. 83(2): p. 109-18.

67. Sumida, Y. and M. Yoneda, Current and future pharmacological therapies for NAFLD/NASH. J Gastroenterol, 2018. 53(3): p. 362-376.

68. Musso, G., M. Cassader, and R. Gambino, Non-alcoholic steatohepatitis: emerging molecular targets and therapeutic strategies. Nat Rev Drug Discov, 2016. 15(4): p. 249-74.

69. Younossi, Z.M., et al., The economic and clinical burden of nonalcoholic fatty liver disease in the United States and Europe. Hepatology, 2016. 64(5): p. 1577-1586.

70. Mahady, S.E., et al., Pioglitazone and vitamin E for nonalcoholic steatohepatitis: a cost utility analysis. Hepatology, 2012. 56(6): p. 2172-9.

71. Postic, C. and J. Girard, Contribution of de novo fatty acid synthesis to hepatic steatosis and insulin resistance: lessons from genetically engineered mice. J Clin Invest, 2008. 118(3): p. 829-38.

72. Schwarz, J.M., et al., Hepatic de novo lipogenesis in normoinsulinemic and hyperinsulinemic subjects consuming high-fat, low-carbohydrate and low-fat, high-carbohydrate isoenergetic diets. Am J Clin Nutr, 2003. 77(1): p. 43-50.

73. McDevitt, R.M., et al., De novo lipogenesis during controlled overfeeding with sucrose or glucose in lean and obese women. Am J Clin Nutr, 2001. 74(6): p. 737-46.

74. Ishimoto, T., et al., High-fat and high-sucrose (western) diet induces steatohepatitis that is dependent on fructokinase. Hepatology, 2013. 58(5): p. 1632-43.

75. Perry, R.J., et al., The role of hepatic lipids in hepatic insulin resistance and type 2 diabetes. Nature, 2014. 510(7503): p. 84-91.

76. Orellana-Gavalda, J.M., et al., Molecular therapy for obesity and diabetes based on a long-term increase in hepatic fatty-acid oxidation. Hepatology, 2011. 53(3): p. 821-32.

77. Rector, R.S., et al., Mitochondrial dysfunction precedes insulin resistance and hepatic steatosis and contributes to the natural history of non-alcoholic fatty liver disease in an obese rodent model. J Hepatol, 2010. 52(5): p. 727-36.

78. Jun, D.W., et al., Prevention of free fatty acid-induced hepatic lipotoxicity by carnitine via reversal of mitochondrial dysfunction. Liver Int, 2011. 31(9): p. 1315-24.

79. Morris, E.M., et al., PGC-1alpha overexpression results in increased hepatic fatty acid oxidation with reduced triacylglycerol accumulation and secretion. Am J Physiol Gastrointest Liver Physiol, 2012. 303(8): p. G979-92.

80. Li, S., et al., Dietary cholesterol induces hepatic inflammation and blunts mitochondrial function in the liver of high-fat-fed mice. J Nutr Biochem, 2016. 27: p. 96-103.

81. Begriche, K., et al., Mitochondrial adaptations and dysfunctions in nonalcoholic fatty liver disease. Hepatology, 2013. 58(4): p. 1497-507.

82. Sunny, N.E., et al., Excessive hepatic mitochondrial TCA cycle and gluconeogenesis in humans with nonalcoholic fatty liver disease. Cell Metab, 2011. 14(6): p. 804-10.

83. Minehira, K., et al., Blocking VLDL secretion causes hepatic steatosis but does not affect peripheral lipid stores or insulin sensitivity in mice. J Lipid Res, 2008. 49(9): p. 2038-44.

84. Shindo, N., et al., Involvement of microsomal triglyceride transfer protein in nonalcoholic steatohepatitis in novel spontaneous mouse model. J Hepatol, 2010. 52(6): p. 903-12.

85. Moran-Ramos, S., et al., Opuntia ficus indica (nopal) attenuates hepatic steatosis and oxidative stress in obese Zucker (fa/fa) rats. J Nutr, 2012. 142(11): p. 1956-63.

86. Raabe, M., et al., Analysis of the role of microsomal triglyceride transfer protein in the liver of tissue-specific knockout mice. J Clin Invest, 1999. 103(9): p. 1287-98.

87. Namikawa, C., et al., Polymorphisms of microsomal triglyceride transfer protein gene and manganese superoxide dismutase gene in non-alcoholic steatohepatitis. J Hepatol, 2004. 40(5): p. 781-6.

88. Zeng, X.Y., et al., Oleanolic acid reduces hyperglycemia beyond treatment period with Akt/FoxO1-induced suppression of hepatic gluconeogenesis in type-2 diabetic mice. PLoS One, 2012. 7(7): p. e42115.

89. Ferre, P. and F. Foufelle, Hepatic steatosis: a role for de novo lipogenesis and the transcription factor SREBP-1c. Diabetes Obes Metab, 2010. 12 Suppl 2: p. 83-92.

90. Guo, S., S.L. Dunn, and M.F. White, The reciprocal stability of FOXO1 and IRS2 creates a regulatory circuit that controls insulin signaling. Mol Endocrinol, 2006. 20(12): p. 3389-99.

91. Deng, X., et al., FoxO1 inhibits sterol regulatory element-binding protein-1c (SREBP-1c) gene expression via transcription factors Sp1 and SREBP-1c. J Biol Chem, 2012. 287(24): p. 20132-43.

92. Nassir, F., et al., Regulation of Mitochondrial Trifunctional Protein Modulates Nonalcoholic Fatty Liver Disease in Mice. J Lipid Res, 2018.

93. Gariani, K., et al., Inhibiting poly ADP-ribosylation increases fatty acid oxidation and protects against fatty liver disease. J Hepatol, 2017. 66(1): p. 132-141.

94. Dekker, M.J., et al., Fructose: a highly lipogenic nutrient implicated in insulin resistance, hepatic steatosis, and the metabolic syndrome. Am J Physiol Endocrinol Metab, 2010. 299(5): p. E685-94.

95. Herman, M.A. and V.T. Samuel, The Sweet Path to Metabolic Demise: Fructose and Lipid Synthesis. Trends Endocrinol Metab, 2016. 27(10): p. 719-730.

96. Miyazaki, M., et al., Stearoyl-CoA desaturase 1 gene expression is necessary for fructose-mediated induction of lipogenic gene expression by sterol regulatory element-binding protein-1c-dependent and -independent mechanisms. J Biol Chem, 2004. 279(24): p. 25164-71.

97. Dong, B., et al., High-fructose diet downregulates long-chain acyl-CoA synthetase 3 expression in liver of hamsters via impairing LXR/RXR signaling pathway. J Lipid Res, 2013. 54(5): p. 1241-54.

98. Nagai, Y., et al., Amelioration of high fructose-induced metabolic derangements by activation of PPARalpha. Am J Physiol Endocrinol Metab, 2002. 282(5): p. E1180-90.

99. Dentin, R., et al., Liver-specific inhibition of ChREBP improves hepatic steatosis and insulin resistance in ob/ob mice. Diabetes, 2006. 55(8): p. 2159-70.

100. Jegatheesan, P. and J.-P. De Bandt, Fructose and NAFLD: The Multifaceted Aspects of Fructose Metabolism. Nutrients, 2017. 9(3): p. 230.

101. Jensen, T., et al., Fructose and sugar: A major mediator of non-alcoholic fatty liver disease. J Hepatol, 2018. 68(5): p. 1063-1075.

102. Softic, S., et al., Divergent effects of glucose and fructose on hepatic lipogenesis and insulin signaling. J Clin Invest, 2017. 127(11): p. 4059-4074.

103. Postic, C., et al., ChREBP, a transcriptional regulator of glucose and lipid metabolism. Annu. Rev. Nutr., 2007. 27: p. 179-192.

104. Denechaud, P.D., et al., ChREBP, but not LXRs, is required for the induction of glucose-regulated genes in mouse liver. J Clin Invest, 2008. 118(3): p. 956-64.

105. Shimomura, I., Y. Bashmakov, and J.D. Horton, Increased levels of nuclear SREBP-1c associated with fatty livers in two mouse models of diabetes mellitus. J Biol Chem, 1999. 274(42): p. 30028-32.

106. Sekiya, M., et al., SREBP-1-independent regulation of lipogenic gene expression in adipocytes. J Lipid Res, 2007. 48(7): p. 1581-91.

107. Kammoun, H.L., et al., GRP78 expression inhibits insulin and ER stress-induced SREBP-1c activation and reduces hepatic steatosis in mice. J Clin Invest, 2009. 119(5): p. 1201-15.

108. Dentin, R., et al., Hepatic glucokinase is required for the synergistic action of ChREBP and SREBP-1c on glycolytic and lipogenic gene expression. J Biol Chem, 2004. 279(19): p. 20314-26.

109. Mao, J., et al., Liver-specific deletion of acetyl-CoA carboxylase 1 reduces hepatic triglyceride accumulation without affecting glucose homeostasis. Proc Natl Acad Sci U S A, 2006. 103(22): p. 8552-7.

110. Savage, D.B., et al., Reversal of diet-induced hepatic steatosis and hepatic insulin resistance by antisense oligonucleotide inhibitors of acetyl-CoA carboxylases 1 and 2. J Clin Invest, 2006. 116(3): p. 817-24.

111. Miyazaki, M., et al., Hepatic stearoyl-CoA desaturase-1 deficiency protects mice from carbohydrate-induced adiposity and hepatic steatosis. Cell Metab, 2007. 6(6): p. 484-96.

112. Wu, M., et al., Antidiabetic and antisteatotic effects of the selective fatty acid synthase (FAS) inhibitor platensimycin in mouse models of diabetes. Proc Natl Acad Sci U S A, 2011. 108(13): p. 5378-83.

113. Ballestri, S., et al., Nonalcoholic fatty liver disease is associated with an almost twofold increased risk of incident type 2 diabetes and metabolic syndrome. Evidence from a systematic review and meta-analysis. J Gastroenterol Hepatol, 2016. 31(5): p. 936-44.

114. Turner, N., et al., Distinct patterns of tissue-specific lipid accumulation during the induction of insulin resistance in mice by high-fat feeding. Diabetologia, 2013. 56(7): p. 1638-48.

115. Bremer, A.A., et al., Fish oil supplementation ameliorates fructose-induced hypertriglyceridemia and insulin resistance in adult male rhesus macaques. J Nutr, 2014. 144(1): p. 5-11.

116. Bennett, W.L., et al., Comparative effectiveness and safety of medications for type 2 diabetes: an update including new drugs and 2-drug combinations. Ann Intern Med, 2011. 154(9): p. 602-13.

117. Koruk, M., et al., Serum lipids, lipoproteins and apolipoproteins levels in patients with nonalcoholic steatohepatitis. J Clin Gastroenterol, 2003. 37(2): p. 177-82.

118. Walenbergh, S.M., et al., Non-alcoholic steatohepatitis: the role of oxidized low-density lipoproteins. J Hepatol, 2013. 58(4): p. 801-10.

119. Fujita, K., et al., Dysfunctional very-low-density lipoprotein synthesis and release is a key factor in nonalcoholic steatohepatitis pathogenesis. Hepatology, 2009. 50(3): p. 772-80.

120. Santhekadur, P.K., D.P. Kumar, and A.J. Sanyal, Preclinical models of non-alcoholic fatty liver disease. J Hepatol, 2018. 68(2): p. 230-237.

121. Lieber, C.S., et al., Model of nonalcoholic steatohepatitis. Am J Clin Nutr, 2004. 79(3): p. 502-9.

122. Chalasani, N., et al., Relationship of steatosis grade and zonal location to histological features of steatohepatitis in adult patients with non-alcoholic fatty liver disease. J Hepatol, 2008. 48(5): p. 829-34.

123. Sahai, A., et al., Obese and diabetic db/db mice develop marked liver fibrosis in a model of nonalcoholic steatohepatitis: role of short-form leptin receptors and osteopontin. Am J Physiol Gastrointest Liver Physiol, 2004. 287(5): p. G1035-43.

124. Malhi, H. and G.J. Gores, Cellular and molecular mechanisms of liver injury. Gastroenterology, 2008. 134(6): p. 1641-54.

125. Richardson, M.M., et al., Progressive fibrosis in nonalcoholic steatohepatitis: association with altered regeneration and a ductular reaction. Gastroenterology, 2007. 133(1): p. 80-90.

126. Hirsova, P., et al., Lipid-Induced Signaling Causes Release of Inflammatory Extracellular Vesicles From Hepatocytes. Gastroenterology, 2016. 150(4): p. 956-67.

127. Ioannou, G.N., et al., Cholesterol crystallization within hepatocyte lipid droplets and its role in murine NASH. J Lipid Res, 2017. 58(6): p. 1067-1079.

128. Baffy, G., Kupffer cells in non-alcoholic fatty liver disease: the emerging view. J Hepatol, 2009. 51(1): p. 212-23.

129. Reid, D.T., et al., Kupffer Cells Undergo Fundamental Changes during the Development of Experimental NASH and Are Critical in Initiating Liver Damage and Inflammation. PLoS One, 2016. 11(7): p. e0159524.

130. Wan, J., et al., M2 Kupffer cells promote M1 Kupffer cell apoptosis: a protective mechanism against alcoholic and nonalcoholic fatty liver disease. Hepatology, 2014. 59(1): p. 130-42.

131. Rivera, C.A., et al., Toll-like receptor-4 signaling and Kupffer cells play pivotal roles in the pathogenesis of non-alcoholic steatohepatitis. J Hepatol, 2007. 47(4): p. 571-9.

132. Luo, W., et al., Effect of modulation of PPAR-gamma activity on Kupffer cells M1/M2 polarization in the development of non-alcoholic fatty liver disease. Sci Rep, 2017. 7: p. 44612.

133. Machado, M.V. and A.M. Diehl, Pathogenesis of Nonalcoholic Steatohepatitis. Gastroenterology, 2016. 150(8): p. 1769-77.

134. Li, J., et al., Macrophage Stimulating Protein Enhances Hepatic Inflammation in a NASH Model. PLoS One, 2016. 11(9): p. e0163843.

135. Gabele, E., et al., DSS induced colitis increases portal LPS levels and enhances hepatic inflammation and fibrogenesis in experimental NASH. J Hepatol, 2011. 55(6): p. 1391-9.

136. Kita, Y., et al., Metformin prevents and reverses inflammation in a non-diabetic mouse model of nonalcoholic steatohepatitis. PLoS One, 2012. 7(9): p. e43056.

137. Kessoku, T., et al., Resveratrol ameliorates fibrosis and inflammation in a mouse model of nonalcoholic steatohepatitis. Sci Rep, 2016. 6: p. 22251.

138. El Kasmi, K.C., et al., Toll-like receptor 4-dependent Kupffer cell activation and liver injury in a novel mouse model of parenteral nutrition and intestinal injury. Hepatology, 2012. 55(5): p. 1518-28.

139. Crespo, J., et al., Gene expression of tumor necrosis factor alpha and TNF-receptors, p55 and p75, in nonalcoholic steatohepatitis patients. Hepatology, 2001. 34(6): p. 1158-63.

140. Wieckowska, A., et al., Increased hepatic and circulating interleukin-6 levels in human nonalcoholic steatohepatitis. Am J Gastroenterol, 2008. 103(6): p. 1372-9.

141. Hui, J.M., et al., Beyond insulin resistance in NASH: TNF-alpha or adiponectin? Hepatology, 2004. 40(1): p. 46-54.

142. Wree, A., M.E. Inzaugarat, and A.E. Feldstein, Transmembrane BAX Inhibitor motif-containing 1, a novel anti-inflammatory approach for nonalcoholic steatohepatitis treatment. Hepatology, 2018. 67(1): p. 438-441.

143. Satapathy, S.K., et al., Beneficial effects of tumor necrosis factor-alpha inhibition by pentoxifylline on clinical, biochemical, and metabolic parameters of patients with nonalcoholic steatohepatitis. Am J Gastroenterol, 2004. 99(10): p. 1946-52.

144. Zein, C.O., et al., Pentoxifylline improves nonalcoholic steatohepatitis: a randomized placebo-controlled trial. Hepatology, 2011. 54(5): p. 1610-9.

145. Koppe, S.W., et al., Pentoxifylline attenuates steatohepatitis induced by the methionine choline deficient diet. J Hepatol, 2004. 41(4): p. 592-8.

146. Szabo, G. and J. Petrasek, Inflammasome activation and function in liver disease. Nat Rev Gastroenterol Hepatol, 2015. 12(7): p. 387-400.

147. Wree, A., et al., NLRP3 inflammasome activation results in hepatocyte pyroptosis, liver inflammation, and fibrosis in mice. Hepatology, 2014. 59(3): p. 898-910.

148. Miura, K., et al., Toll-like receptor 2 and palmitic acid cooperatively contribute to the development of nonalcoholic steatohepatitis through inflammasome activation in mice. Hepatology, 2013. 57(2): p. 577-89.

149. Mridha, A.R., et al., NLRP3 inflammasome blockade reduces liver inflammation and fibrosis in experimental NASH in mice. J Hepatol, 2017. 66(5): p. 1037-1046.

150. Ozaki, E., M. Campbell, and S.L. Doyle, Targeting the NLRP3 inflammasome in chronic inflammatory diseases: current perspectives. J Inflamm Res, 2015. 8: p. 15-27.

151. Handa, P., et al., Differences in hepatic expression of iron, inflammation and stress-related genes in patients with nonalcoholic steatohepatitis. Ann Hepatol, 2017. 16(1): p. 77-85.

152. She, H., et al., Iron activates NF-kappaB in Kupffer cells. Am J Physiol Gastrointest Liver Physiol, 2002. 283(3): p. G719-26.

153. Fargion, S., et al., Hyperferritinemia, iron overload, and multiple metabolic alterations identify patients at risk for nonalcoholic steatohepatitis. Am J Gastroenterol, 2001. 96(8): p. 2448-55.

154. Dongiovanni, P., et al., Iron in fatty liver and in the metabolic syndrome: a promising therapeutic target. J Hepatol, 2011. 55(4): p. 920-32.

155. Schuppan, D., R. Surabattula, and X.Y. Wang, Determinants of fibrosis progression and regression in NASH. J Hepatol, 2018. 68(2): p. 238-250.

156. Tacke, F. and H.W. Zimmermann, Macrophage heterogeneity in liver injury and fibrosis. J Hepatol, 2014. 60(5): p. 1090-6.

157. Komiya, C., et al., Antifibrotic effect of pirfenidone in a mouse model of human nonalcoholic steatohepatitis. Sci Rep, 2017. 7: p. 44754.

158. Derynck, R., Y. Zhang, and X.H. Feng, Smads: transcriptional activators of TGF-beta responses. Cell, 1998. 95(6): p. 737-40.

159. Yang, L., et al., Transforming growth factor beta signaling in hepatocytes participates in steatohepatitis through regulation of cell death and lipid metabolism in mice. Hepatology, 2014. 59(2): p. 483-95.

160. Toriguchi, K., et al., Attenuation of steatohepatitis, fibrosis, and carcinogenesis in mice fed a methionine-choline deficient diet by CCAAT/enhancer-binding protein homologous protein deficiency. J Gastroenterol Hepatol, 2014. 29(5): p. 1109-18.

161. Rinella, M.E. and R.M. Green, The methionine-choline deficient dietary model of steatohepatitis does not exhibit insulin resistance. J Hepatol, 2004. 40(1): p. 47-51.

162. Rinella, M.E., et al., Mechanisms of hepatic steatosis in mice fed a lipogenic methionine choline-deficient diet. J Lipid Res, 2008. 49(5): p. 1068-76.

163. Pais, R., et al., NAFLD and liver transplantation: Current burden and expected challenges. J Hepatol, 2016. 65(6): p. 1245-1257.

164. Patsenker, E., et al., Potent antifibrotic activity of mTOR inhibitors sirolimus and everolimus but not of cyclosporine A and tacrolimus in experimental liver fibrosis. J Hepatol, 2011. 55(2): p. 388-98.

165. Lassailly, G., et al., Perspectives on Treatment for Nonalcoholic Steatohepatitis. Gastroenterology, 2016. 150(8): p. 1835-48.

166. Clark, J.M. and A.M. Diehl, Nonalcoholic fatty liver disease: an underrecognized cause of cryptogenic cirrhosis. Jama, 2003. 289(22): p. 3000-4.

167. Ascha, M.S., et al., The incidence and risk factors of hepatocellular carcinoma in patients with nonalcoholic steatohepatitis. Hepatology, 2010. 51(6): p. 1972-8.

168. Anstee, Q.M., G. Targher, and C.P. Day, Progression of NAFLD to diabetes mellitus, cardiovascular disease or cirrhosis. Nat Rev Gastroenterol Hepatol, 2013. 10(6): p. 330-44.

169. De Minicis, S., et al., HCC development is associated to peripheral insulin resistance in a mouse model of NASH. PLoS One, 2014. 9(5): p. e97136.

170. Hansen, H.H., et al., Mouse models of nonalcoholic steatohepatitis in preclinical drug development. Drug Discov Today, 2017.

171. Eccleston, H.B., et al., Chronic exposure to a high-fat diet induces hepatic steatosis, impairs nitric oxide bioavailability, and modifies the mitochondrial proteome in mice. Antioxid Redox Signal, 2011. 15(2): p. 447-59.

172. Zeng, X.Y., et al., Identification of matrine as a promising novel drug for hepatic steatosis and glucose intolerance with HSP72 as an upstream target. Br J Pharmacol, 2015. 172(17): p. 4303-18.

173. Savard, C., et al., Synergistic interaction of dietary cholesterol and dietary fat in inducing experimental steatohepatitis. Hepatology, 2013. 57(1): p. 81-92.

174. Armutcu, F., et al., Thymosin alpha 1 attenuates lipid peroxidation and improves fructose-induced steatohepatitis in rats. Clin Biochem, 2005. 38(6): p. 540-7.

175. Kohli, R., et al., High-fructose, medium chain trans fat diet induces liver fibrosis and elevates plasma coenzyme Q9 in a novel murine model of obesity and nonalcoholic steatohepatitis. Hepatology, 2010. 52(3): p. 934-44.

176. Mu, J., et al., Chronic inhibition of dipeptidyl peptidase-4 with a sitagliptin analog preserves pancreatic beta-cell mass and function in a rodent model of type 2 diabetes. Diabetes, 2006. 55(6): p. 1695-704.

177. Luo, J., et al., Nongenetic mouse models of non-insulin-dependent diabetes mellitus. Metabolism, 1998. 47(6): p. 663-8.

178. Kusakabe, T., et al., Beneficial effects of leptin on glycaemic and lipid control in a mouse model of type 2 diabetes with increased adiposity induced by streptozotocin and a high-fat diet. Diabetologia, 2009. 52(4): p. 675-83.

179. Lau, J.K., X. Zhang, and J. Yu, Animal models of non-alcoholic fatty liver disease: current perspectives and recent advances. J Pathol, 2017. 241(1): p. 36-44.

180. Sanyal, A.J., et al., Challenges and opportunities in drug and biomarker development for nonalcoholic steatohepatitis: findings and recommendations from an American Association for the Study of Liver Diseases-U.S. Food and Drug Administration Joint Workshop. Hepatology, 2015. 61(4): p. 1392-405.

181. Sanyal, A.J., et al., Pioglitazone, vitamin E, or placebo for nonalcoholic steatohepatitis. N Engl J Med, 2010. 362(18): p. 1675-85.

182. Turner, N., et al., Repurposing Drugs to Target the Diabetes Epidemic. Trends Pharmacol Sci, 2016. 37(5): p. 379-89.

183. Ashburn, T.T. and K.B. Thor, Drug repositioning: identifying and developing new uses for existing drugs. Nat Rev Drug Discov, 2004. 3(8): p. 673-83.

184. Liu, J., et al., Radix Sophorae flavescentis for chronic hepatitis B: a systematic review of randomized trials. Am J Chin Med, 2003. 31(3): p. 337-54.

185. Gong, X., et al., Effect of matrine on primary human hepatocytes in vitro. Cytotechnology, 2014: p. 1-11.

186. Yu, H.B., et al., Matrine inhibits matrix metalloproteinase-9 expression and invasion of human hepatocellular carcinoma cells. J Asian Nat Prod Res, 2011. 13(3): p. 242-50.

187. Zhang, B., et al., Antiinflammatory effects of matrine in LPS-induced acute lung injury in mice. Eur J Pharm Sci, 2011. 44(5): p. 573-9.

188. Sun, N., et al., Matrine displayed antiviral activity in porcine alveolar macrophages co-infected by porcine reproductive and respiratory syndrome virus and porcine circovirus type 2. Sci Rep, 2016. 6: p. 24401.

189. Zhang, J.P., et al., Antifibrotic effects of matrine on in vitro and in vivo models of liver fibrosis in rats. Acta Pharmacol Sin, 2001. 22(2): p. 183-6.

190. Young, J.C., et al., Pathways of chaperone-mediated protein folding in the cytosol. Nat Rev Mol Cell Biol, 2004. 5(10): p. 781-91.

191. Hartl, F.U., A. Bracher, and M. Hayer-Hartl, Molecular chaperones in protein folding and proteostasis. Nature, 2011. 475(7356): p. 324-32.

192. Kurucz, I., et al., Decreased expression of heat shock protein 72 in skeletal muscle of patients with type 2 diabetes correlates with insulin resistance. Diabetes, 2002. 51(4): p. 1102-9.

193. Sarge, K.D., S.P. Murphy, and R.I. Morimoto, Activation of heat shock gene transcription by heat shock factor 1 involves oligomerization, acquisition of DNA-binding activity, and nuclear localization and can occur in the absence of stress. Mol Cell Biol, 1993. 13(3): p. 1392-407.

194. Di Naso, F.C., et al., Obesity depresses the anti-inflammatory HSP70 pathway, contributing to NAFLD progression. Obesity (Silver Spring), 2015. 23(1): p. 120-9.

195. Flanagan, S.W., et al., Tissue-specific HSP70 response in animals undergoing heat stress. Am J Physiol, 1995. 268(1 Pt 2): p. R28-32.

196. Chung, J., et al., HSP72 protects against obesity-induced insulin resistance. Proc Natl Acad Sci U S A, 2008. 105(5): p. 1739-44.

197. Henstridge, D.C., et al., Activating HSP72 in Rodent Skeletal Muscle Increases Mitochondrial Number and Oxidative Capacity and Decreases Insulin Resistance. Diabetes, 2014. 63(6): p. 1881-1894.

198. Dokladny, K., et al., Cellular and molecular mechanisms of heat stress-induced up-regulation of occludin protein expression: regulatory role of heat shock factor-1. Am J Pathol, 2008. 172(3): p. 659-70.

199. Sookoian, S., et al., Heat Shock Protein 27 is down-regulated in Ballooned Hepatocytes of Patients with Nonalcoholic Steatohepatitis (NASH). Sci Rep, 2016. 6: p. 22528.

200. Zhu, X.H., et al., Effect of matrine on Kupffer cell activation in cold ischemia reperfusion injury of rat liver. World J Gastroenterol, 2002. 8(6): p. 1112-6.

201. Mahzari, A., et al., Repurposing matrine for the treatment of hepatosteatosis and associated disorders in glucose homeostasis in mice. Acta Pharmacol Sin, 2018.

202. McGrath, J.C., et al., Guidelines for reporting experiments involving animals: the ARRIVE guidelines. Br J Pharmacol, 2010. 160(7): p. 1573-6.

203. Kilkenny, C., et al., Animal research: reporting in vivo experiments: the ARRIVE guidelines. Br J Pharmacol, 2010. 160(7): p. 1577-9.

204. Sun, Z. and M.A. Lazar, Dissociating fatty liver and diabetes. Trends Endocrinol Metab, 2013. 24(1): p. 4-12.

205. Brun, P., et al., Increased intestinal permeability in obese mice: new evidence in the pathogenesis of nonalcoholic steatohepatitis. Am J Physiol Gastrointest Liver Physiol, 2007. 292(2): p. G518-25.

206. Li, Q., et al., Hepatitis C virus infection activates an innate pathway involving IKK-alpha in lipogenesis and viral assembly. Nat Med, 2013. 19(6): p. 722-9.

207. Iizuka, K., et al., Deficiency of carbohydrate response element-binding protein (ChREBP) reduces lipogenesis as well as glycolysis. Proc Natl Acad Sci U S A, 2004. 101(19): p. 7281-6.

208. Ye, J.M., et al., PPARdelta agonists have opposing effects on insulin resistance in high fat-fed rats and mice due to different metabolic responses in muscle. Br J Pharmacol, 2011. 163(3): p. 556-66.

209. Ye, J.M., et al., PPARalpha /gamma ragaglitazar eliminates fatty liver and enhances insulin action in fat-fed rats in the absence of hepatomegaly. Am J Physiol Endocrinol Metab, 2003. 284(3): p. E531-40.

210. Hotamisligil, G.S., Endoplasmic reticulum stress and the inflammatory basis of metabolic disease. Cell, 2010. 140(6): p. 900-17.

211. Wang, H., et al., Restoration of autophagy alleviates hepatic ER stress and impaired insulin signalling transduction in high fructose-fed male mice. Endocrinology, 2015. 156(1): p. 169-81.

212. Zhang, H.F., et al., Protective effects of matrine against progression of high-fructose diet-induced steatohepatitis by enhancing antioxidant and anti-inflammatory defences involving Nrf2 translocation. Food Chem Toxicol, 2013. 55(0): p. 70-7.

213. Gao, G. and F.C. Law, Physiologically based pharmacokinetics of matrine in the rat after oral administration of pure chemical and ACAPHA. Drug Metab Dispos, 2009. 37(4): p. 884-91.

214. Milner, K.L., et al., Chronic hepatitis C is associated with peripheral rather than hepatic insulin resistance. Gastroenterology, 2010. 138(3): p. 932-41 e1-3.

215. McPherson, S., et al., Investigation of the role of SREBP-1c in the pathogenesis of HCV-related steatosis. J Hepatol, 2008. 49(6): p. 1046-54.

216. Zeng, X.Y., et al., Screening for the efficacy on lipid accumulation in 3T3-L1 cells is an effective tool for the identification of new anti-diabetic compounds. Biochem Pharmacol, 2012. 84(6): p. 830-7.

217. Reddy, J.K., Nonalcoholic steatosis and steatohepatitis. III. Peroxisomal beta-oxidation, PPAR alpha, and steatohepatitis. Am J Physiol Gastrointest Liver Physiol, 2001. 281(6): p. G1333-9.

218. Gupte, A.A., et al., Heat treatment improves glucose tolerance and prevents skeletal muscle insulin resistance in rats fed a high-fat diet. Diabetes, 2009. 58(3): p. 567-78.

219. Gabai, V.L., et al., Hsp72 and stress kinase c-jun N-terminal kinase regulate the bid-dependent pathway in tumor necrosis factor-induced apoptosis. Mol Cell Biol, 2002. 22(10): p. 3415-24.

220. Younossi, Z.M., et al., Current and Future Therapeutic Regimens for Non-alcoholic Fatty Liver Disease (NAFLD) and Non-alcoholic Steatohepatitis (NASH). Hepatology, 2017.

221. Cheng, H., et al., Matrine improves 2,4,6-trinitrobenzene sulfonic acid-induced colitis in mice. Pharmacol Res, 2006. 53(3): p. 202-8.

222. Wu, G., et al., Matrine alleviates lipopolysaccharide-induced intestinal inflammation and oxidative stress via CCR7 signal. Oncotarget, 2017. 8(7): p. 11621-11628.

223. Leclercq, I.A., et al., CYP2E1 and CYP4A as microsomal catalysts of lipid peroxides in murine nonalcoholic steatohepatitis. J Clin Invest, 2000. 105(8): p. 1067-75.

224. Clarke, J.D., et al., Mechanism of Altered Metformin Distribution in Nonalcoholic Steatohepatitis. Diabetes, 2015. 64(9): p. 3305-13.

225. Dang, T.N., et al., The metabolism and toxicity of hemin in astrocytes. Glia, 2011. 59(10): p. 1540-50.

226. Handa, P., et al., Iron overload results in hepatic oxidative stress, immune cell activation, and hepatocellular ballooning injury, leading to nonalcoholic steatohepatitis in genetically obese mice. Am J Physiol Gastrointest Liver Physiol, 2016. 310(2): p. G117-27.

227. George, D.K., et al., Increased hepatic iron concentration in nonalcoholic steatohepatitis is associated with increased fibrosis. Gastroenterology, 1998. 114(2): p. 311-8.

228. Riemer, J., et al., Colorimetric ferrozine-based assay for the quantitation of iron in cultured cells. Anal Biochem, 2004. 331(2): p. 370-5.

229. Owen, J.E., G.M. Bishop, and S.R. Robinson, Phenanthrolines protect astrocytes from hemin without chelating iron. Neurochem Res, 2014. 39(4): p. 693-9.

230. Witek, R.P., et al., Pan-caspase inhibitor VX-166 reduces fibrosis in an animal model of nonalcoholic steatohepatitis. Hepatology, 2009. 50(5): p. 1421-30.

231. Itagaki, H., et al., Morphological and functional characterization of non-alcoholic fatty liver disease induced by a methionine-choline-deficient diet in C57BL/6 mice. Int J Clin Exp Pathol, 2013. 6(12): p. 2683-96.

232. Farrell, G.C., et al., NASH is an Inflammatory Disorder: Pathogenic, Prognostic and Therapeutic Implications. Gut Liver, 2012. 6(2): p. 149-71.

233. Tacke, F., Targeting hepatic macrophages to treat liver diseases. J Hepatol, 2017. 66(6): p. 1300-1312.

234. Han, J. and Y. Wang, mTORC1 signaling in hepatic lipid metabolism. Protein Cell, 2018. 9(2): p. 145-151.

235. Gong, Q., et al., Fibroblast growth factor 21 improves hepatic insulin sensitivity by inhibiting mammalian target of rapamycin complex 1 in mice. Hepatology, 2016. 64(2): p. 425-38.

236. Sapp, V., et al., Fructose leads to hepatic steatosis in zebrafish that is reversed by mechanistic target of rapamycin (mTOR) inhibition. Hepatology, 2014. 60(5): p. 1581-92.

237. Chen, R., et al., Protective role of autophagy in methionine-choline deficient diet-induced advanced nonalcoholic steatohepatitis in mice. Eur J Pharmacol, 2016. 770: p. 126-33.

238. Wang, Z., et al., Matrine, a novel autophagy inhibitor, blocks trafficking and the proteolytic activation of lysosomal proteases. Carcinogenesis, 2013. 34(1): p. 128-38.

239. Lunova, M., et al., Hepcidin knockout mice fed with iron-rich diet develop chronic liver injury and liver fibrosis due to lysosomal iron overload. J Hepatol, 2014. 61(3): p. 633-41.

240. Torres, D.M. and S.A. Harrison, NAFLD: Predictive value of ALT levels for NASH and advanced fibrosis. Nat Rev Gastroenterol Hepatol, 2013. 10(9): p. 510-1.

241. Liu, R., X. Pan, and P.F. Whitington, Increased hepatic expression is a major determinant of serum alanine aminotransferase elevation in mice with nonalcoholic steatohepatitis. Liver Int, 2009. 29(3): p. 337-43.

242. Omer, Z., et al., Efficacy of insulin-sensitizing agents in nonalcoholic fatty liver disease. Eur J Gastroenterol Hepatol, 2010. 22(1): p. 18-23.

243. Shields, W.W., et al., The Effect of Metformin and Standard Therapy versus Standard Therapy alone in Nondiabetic Patients with Insulin Resistance and Nonalcoholic Steatohepatitis (NASH): A Pilot Trial. Therap Adv Gastroenterol, 2009. 2(3): p. 157-63.

244. Schuster, S., et al., Triggering and resolution of inflammation in NASH. Nat Rev Gastroenterol Hepatol, 2018.

245. Tosello-Trampont, A.C., et al., Kuppfer cells trigger nonalcoholic steatohepatitis development in diet-induced mouse model through tumor necrosis factor-alpha production. J Biol Chem, 2012. 287(48): p. 40161-72.

246. Li, Z., et al., Probiotics and antibodies to TNF inhibit inflammatory activity and improve nonalcoholic fatty liver disease. Hepatology, 2003. 37(2): p. 343-50.

247. Atarashi, M., et al., Dietary Iron Supplementation Alters Hepatic Inflammation in a Rat Model of Nonalcoholic Steatohepatitis. Nutrients, 2018. 10(2).

248. Murotomi, K., et al., Involvement of splenic iron accumulation in the development of nonalcoholic steatohepatitis in Tsumura Suzuki Obese Diabetes mice. Sci Rep, 2016. 6: p. 22476.

249. Henao-Mejia, J., et al., Inflammasome-mediated dysbiosis regulates progression of NAFLD and obesity. Nature, 2012. 482(7384): p. 179-85.

250. Rodriguez-Enriquez, S., et al., Roles of mitophagy and the mitochondrial permeability transition in remodeling of cultured rat hepatocytes. Autophagy, 2009. 5(8): p. 1099-106.

251. Mao, Y., et al., Autophagy: a new target for nonalcoholic fatty liver disease therapy. Hepat Med, 2016. 8: p. 27-37.

252. Wu, J., et al., Matrine induces Akt/mTOR signalling inhibition-mediated autophagy and apoptosis in acute myeloid leukaemia cells. J Cell Mol Med, 2017. 21(6): p. 1171-1181.

253. Tang, D., et al., The anti-inflammatory effects of heat shock protein 72 involve inhibition of high-mobility-group box 1 release and proinflammatory function in macrophages. J Immunol, 2007. 179(2): p. 1236-44.

254. Bataller, R. and D.A. Brenner, Liver fibrosis. J Clin Invest, 2005. 115(2): p. 209-18.

255. Budick-Harmelin, N., et al., Triglycerides potentiate the inflammatory response in rat Kupffer cells. Antioxid Redox Signal, 2008. 10(12): p. 2009-22.

256. Jia, L., et al., Hepatocyte Toll-like receptor 4 regulates obesity-induced inflammation and insulin resistance. Nat Commun, 2014. 5: p. 3878.

257. Zhang, X., et al., Flavonoid apigenin inhibits lipopolysaccharide-induced inflammatory response through multiple mechanisms in macrophages. PLoS One, 2014. 9(9): p. e107072.

258. Poltorak, A., et al., Defective LPS signaling in C3H/HeJ and C57BL/10ScCr mice: mutations in Tlr4 gene. Science, 1998. 282(5396): p. 2085-8.

259. Hritz, I., et al., The critical role of toll-like receptor (TLR) 4 in alcoholic liver disease is independent of the common TLR adapter MyD88. Hepatology, 2008. 48(4): p. 1224-31.

260. Tsuji, H., et al., Alleviation of lipopolysaccharide-induced acute liver injury in Propionibacterium acnes-primed IFN-gamma-deficient mice by a concomitant reduction of TNF-alpha, IL-12, and IL-18 production. J Immunol, 1999. 162(2): p. 1049-55.

261. You, Q., et al., Role of hepatic resident and infiltrating macrophages in liver repair after acute injury. Biochem Pharmacol, 2013. 86(6): p. 836-43.

262. Ferluga, J. and A.C. Allison, Role of mononuclear infiltrating cells in pathogenesis of hepatitis. Lancet, 1978. 2(8090): p. 610-1.

263. Cohly, H., et al., Cell culture conditions affect LPS inducibility of the inflammatory mediators in J774A.1 murine macrophages. Immunol Invest, 2001. 30(1): p. 1-15.

264. Su, G.L., et al., Activation of human and mouse Kupffer cells by lipopolysaccharide is mediated by CD14. Am J Physiol Gastrointest Liver Physiol, 2002. 283(3): p. G640-5.

265. Ran, R., et al., Hsp70 promotes TNF-mediated apoptosis by binding IKK gamma and impairing NF-kappa B survival signaling. Genes Dev, 2004. 18(12): p. 1466-81.

266. Sheppard, P.W., et al., Overexpression of heat shock protein 72 attenuates NF-kappaB activation using a combination of regulatory mechanisms in microglia. PLoS Comput Biol, 2014. 10(2): p. e1003471.

267. Van Molle, W., et al., HSP70 protects against TNF-induced lethal inflammatory shock. Immunity, 2002. 16(5): p. 685-95.

268. Ding, X.Z., et al., Over-expression of hsp-70 inhibits bacterial lipopolysaccharide-induced production of cytokines in human monocyte-derived macrophages. Cytokine, 2001. 16(6): p. 210-9.

269. Zhang, Z.C., et al., Upregulation of miR-125b by estrogen protects against non-alcoholic fatty liver in female mice. J Hepatol, 2015. 63(6): p. 1466-75.

270. Najt, C.P., et al., Liver-specific loss of Perilipin 2 alleviates diet-induced hepatic steatosis, inflammation, and fibrosis. Am J Physiol Gastrointest Liver Physiol, 2016. 310(9): p. G726-38.

271. Hentges, K.E., et al., FRAP/mTOR is required for proliferation and patterning during embryonic development in the mouse. Proc Natl Acad Sci U S A, 2001. 98(24): p. 13796-801.

272. Brunt, E.M., et al., Nonalcoholic steatohepatitis: a proposal for grading and staging the histological lesions. Am J Gastroenterol, 1999. 94(9): p. 2467-74.

273. Shi, Y.F., et al., Effects of rhDecorin on TGF-beta1 induced human hepatic stellate cells LX-2 activation. Biochim Biophys Acta, 2006. 1760(11): p. 1587-95.

274. Huang, X., et al., Protection effect of kallistatin on carbon tetrachloride-induced liver fibrosis in rats via antioxidative stress. PLoS One, 2014. 9(2): p. e88498.

Appendix

Acta Pharmacologica Sinica

www.nature.com/aps

ARTICLE

Repurposing matrine for the treatment of hepatosteatosis and associated disorders in glucose homeostasis in mice

Ali Mazhari[1], Xiao-Yi Zeng[1], Xiu Zhou[1], Songpei Li[1], Jun Xu[2], Wen Tan[3], Ross Vlahos[1], Stephen Robinson[1] and Ji-Ming YE[1]

The present study investigated the efficacy of the hepatoprotective drug matrine (Mtr) for its new application for hepatosteatosis and associated disorders in glucose homeostasis. The study was performed in two nutritional models of hepatosteatosis in mice with various abnormal glucose homeostasis: (1) high-fructose diet (HFru) induced hepatosteatosis and glucose intolerance from hepatic, and (2) hepatosteatosis and hyperglycemia induced by high-fat (HF) diet in combination with low doses of streptozotocin (STZ). Administration of Mtr (100 mg/kg every day in diet for 4 weeks) abolished HFru-induced hepatosteatosis and glucose intolerance. These effects were associated with the inhibition of HFru-stimulated de novo lipogenesis (DNL) without altering hepatic fatty acid oxidation. Further investigation revealed that HFru-induced endoplasmic reticulum (ER) stress was inhibited, whereas heat-shock protein 72 (an inducible chaperon protein) was increased by Mtr. In a type 2 diabetic model induced by HF-STZ, Mtr reduced hepatosteatosis and improved attenuated hyperglycemia. The hepatoprotective drug Mtr may be repurposed for the treatment of hepatosteatosis and associated disorders in glucose homeostasis. The inhibition of ER stress associated DNL and fatty acid influx appears to play an important role in these metabolic effects.

Keywords: matrine; hepatosteatosis; glucose intolerance; hyperglycemic control

Acta Pharmacologica Sinica (2018) 39:1–7; https://doi.org/10.1038/s41401-018-0016-8

INTRODUCTION

The liver plays an important role in regulating whole-body lipid metabolism and glucose homeostasis. Excess accumulation of lipids (namely hepatosteatosis), either from endogenous de novo lipogenesis (DNL) and/or influx of exogenous fatty acids (FA), can disturb glucose homeostasis, increasing the risk of type 2 diabetes (T2D) [1, 2]. Although the degree of hepatosteatosis and T2D do not necessarily tightly coupled [3], inhibition of excess hepatic DNL has been shown to ameliorate hepatosteatosis and associated glucose intolerance [4]. Shulman and colleagues have also demonstrated that correction of hepatosteatosis in patients with T2D is important for hyperglycemia control [5]. In search for a new therapeutic for the treatment of hepatic steatosis from DNL, we have taken the approach of repurposing existing drugs for these conditions [6, 7].

Matrine (Mtr) is a small molecule (M_W: 248) found in Sophora and it is structurally different from the drugs currently used to treat T2D [8–10]. Mtr has been used clinically as a hepatoprotective drug for the treatment of tumors and viral hepatitis [8], where DNL is often increased [11]. A recent study from our laboratory found that Mtr is able to reduce hepatosteatosis, fasting blood glucose and glucose intolerance in high fat (HF)-fed mice [9]. However, the HF model does not exhibit the characteristics of DNL-induced hepatosteatosis and glucose intolerance because the accumulation of triglyceride (TG) in the liver is due to a direct influx of lipids into the liver from the HF diet [12, 13].

The liver is a major site of DNL production from carbohydrates [12, 14] and interestingly the inhibition of hepatic DNL reduces hepatosteatosis and hyperglycemia [4, 15]. It has been suggested that an increase in DNL is the second major source of lipid accumulation in the liver and contributes about 26% of patients with hepatosteatosis [16]. In mice, a high-fructose (HFru) diet induces hepatosteatosis as early as 1 day [17] prior to the development of glucose intolerance [12, 18, 19]. Dietary fructose is almost entirely metabolised in the liver in its first pass, and serves mainly as a substrate for DNL in both animals [13, 17, 20] and humans [19, 21–23]. HFru diets increase the expression of lipogenic transcription factors, sterol regulatory element binding protein (SREBP1c) and carbohydrate response element binding protein (ChREBP), which upregulate lipogenic genes. Upregulation of these lipogenic transcription factors can result in hepatosteatosis and glucose intolerance via promoting DNL [24, 25]. Notably, HFru-stimulated hepatic DNL via SREBP1c is dependent on the activation of the ER stress pathway [12, 26].

The primary aim of the present study was to investigate whether the hepatoprotective drug Mtr can limit the hepatosteatosis and the associated glucose intolerance that usually results from increased DNL in HFru-fed mice. If so, the second aim was to investigate whether the action of Mtr is via the ER stress pathway. Finally, we also evaluated whether Mtr assists glycemic control in a T2D mouse model generated by a combination of HF and streptozotocin (STZ) where an increased DNL via SREBP1c is also involved [27, 28].

[1]School of Health and Biomedical Sciences, RMIT University, Melbourne, VIC, Australia; [2]School of Chemical Engineering, Wuyi University, Jiangmen, China and [3]Institute of Biomedical & Pharmaceutical Sciences, Guangdong University of Technology, Guangzhou 510006, China
Correspondence: Ji-Ming YE (jiming.ye@rmit.edu.au)

Received: 18 October 2017 Accepted: 6 February 2018
Published online: 06 July 2018

MATERIALS AND METHODS

Animals and diets

C57BL/6J mice aged 10–12 weeks and weighing 21–24 g were obtained from the Animal Resource Centre Pty. Ltd. (Perth, Australia). The animals were housed in a temperature-controlled room (22 ± 1 °C) on a 12-h light/dark cycle with free access to food and water. Mice were fed ad libitum for 1 week on a normal chow diet (~70% calories from starch, ~10% calories from fat, and ~20% calories from protein; Gordon's Specialty Stock Feeds, Yanderra, Australia). Mtr (≥ 98% by HPLC) was purchased from Sigma Aldrich. The experiments described in this manuscript were approved by the Animal Ethics Committee of RMIT University (Application ID: 1012) and conducted in compliance with the guidelines of the National Health and Medical Research Council of Australia for Animal Experimentation.

Two sets of animal experiments were performed. In the first set of experiments, mice were fed a HFru diet (35% fructose, 35% starch, ~10% fat and ~20% protein) to generate hepatosteatosis. Mice were fed for 8 weeks with or without Mtr at a dose of 100 mg/kg every day as a food additive in the last 4 weeks as described previously [9, 10]. Body weight gain and food intake were measured twice a week. For blood glucose levels, blood samples were collected from the tail tip and measured using a glucometer (AccuCheck II; Roche, New South Wales, Castle Hill, Australia) after 2 weeks of Mtr treatment. In the second set of experiments, the effects of Mtr on hepatosteatosis and hyperglycemia were examined in a T2D model induced by HF feeding in combination with low doses of STZ as previously reported [28–30]. Briefly, mice were fed a HF diet (45% calorie from lard, 20% calories from protein and 35% calories from carbohydrate) for 14 weeks to induce insulin resistance. After 8 weeks of HF feeding, mice were injected with STZ at a low dose (40 mg/kg per day, ip) for 5 consecutive days to reduce the level of plasma insulin by ~50% [28–30]. One week after the last injection of STZ, fasting blood glucose was usually increased by 50%–100% (hyperglycemia, defined as T2D). The T2D mice were then divided into 2 groups: one group receiving Mtr added in the HF diet (100 mg/kg per day) for 4 weeks (T2D-Mtr) whereas the other group was fed HF alone (T2D-Con) for the same period of time. During the period of Mtr treatment, fasting blood glucose was monitored once a week. A normal control group of mice (CH-Con) was included for the same period. At the end of both sets of experiments, mice were killed by cervical dislocation and liver tissues were collected and freeze-clamped immediately for further analysis.

Assessment of the effect on hepatosteatosis

Hepatosteatosis was assessed by measuring TG content in the liver. Mice were fasted for 5–7 h before being killed; the liver was collected and freeze-clamped immediately. As described previously [13, 28] plasma and liver TG levels were determined with a Peridochrom triglyceride GPO-PAP biochemical kit (Roche diagnostics). The method of lipid extraction from liver with chloroform/methanol has been described previously [17].

Assessment of the effect on hepatic FA oxidation

FA oxidation was assessed in fresh liver tissue ex vivo as described [12, 13]. Briefly, fresh liver samples were homogenised in an isolating medium which contained 100 mM sucrose, 50 mM Tris, 100 mM KCl, 1 mM KH_2PO_4 and 0.1 mM EGTA, 0.2% FA-free BSA at pH 7.0. The liver homogenate was incubated with [^{14}C]-palmitate and [^{14}C]–CO_2 produced from the incubation was collected in 1 M sodium hydroxide. Palmitate oxidation rates were determined by counting the ^{14}C radioactivity of captured CO_2 and acid-soluble metabolites and oxidation rate were expressed as nanomoles of CO_2 per gram of wet weight per hour [12].

Assessment of the effects on DNL and ER stress

DNL and ER stress were assessed by immunoblotting with specific anti-bodies for the key proteins in the DNL, ER stress and heat shock protein (HSP) pathways based on our recent work [9, 10, 12, 13, 17]. Briefly, freeze-clamped liver was homogenized in ice-cold lysis buffer supplemented with fresh protease inhibitor and phosphatase inhibitor (Sigma Aldrich). The key proteins in the DNL pathway included SREBP-1 (Santa Cruz), ChREBP (Abcam), acetyl-CoA carboxylase (ACC, Upstate), fatty acid synthase (FAS, Abcam) and stearoyl-CoA desaturase 1 (SCD-1, Cell Signaling). The key proteins measured in the ER stress pathway included inositol-requiring kinase 1 (IRE1, Abcam), eukaryotic translation initiation factor 2α (eIF2α, Cell Signaling) and CHOP (Santa Cruz). The effect on the HSP pathway was assessed by heat shock protein 72 (HSP72, Abcam) based on our recent work [9, 10]. Proteins were quantified using a ChemiDoc and densitometry analysis was performed using Image Lab software (Bio-Rad Laboratories, USA).

Statistical analysis

All results are presented as means ± s.e.m. One-way analysis of variance was used to assess the statistical significance across all groups. When significant differences were found, the Tukey-Kramer multiple comparisons post hoc test was used to establish differences between groups. Differences at $P < 0.05$ were considered to be statistically significant and $P < 0.01$ were considered to be highly significant.

RESULTS

Effects on body weight, adiposity, hepatosteatosis and glucose tolerance in HFru-fed mice

HFru feeding is a well-defined model of hepatosteatosis, visceral adiposity and glucose intolerance resulting from increased DNL in the liver [12]. As expected, HFru feeding moderately increased the mass of epididymal fat (by 40%, $P < 0.01$) without altering body weight or food intake ($P > 0.05$; Fig. 1a–c). The TG content (indicative of hepatosteatosis) was increased dramatically in the liver (by threefold) but only moderately in muscle (~35%) (both $P < 0.01$; Fig. 1d). As shown in Fig. 1e, HFru-fed mice also showed moderate glucose intolerance.

Administration of Mtr prevented the moderate body weight gain (8%–10%) in HFru-fed mice during this period of time (Fig. 1a). It corrected HFru-induced increases in epididymal fat, liver TG content and glucose intolerance (all, $P < 0.01$ vs untreated HFru-fed mice) to the levels similar to CH-fed normal mice (Fig. 1b–e). Although not significantly reduced, muscle TG content in Mtr-treated HFru-fed mice was no longer different from the value of CH-fed normal mice (Fig. 1d).

Effects on FA oxidation and DNL in the liver of HFru-fed mice

We first examined whether Mtr treatment may promote FA oxidation in the liver of HFru-fed mice. As shown in Fig. 2a, palmitate oxidation by the liver homogenates was not affected by the treatment with Mtr, suggesting that the reduced hepatosteatosis by Mtr is not likely to be due to an increased FA oxidation in the liver. We next examined the DNL pathway because HFru-induced hepatosteatosis is believed to result from the stimulation to this pathway in the liver [13, 17, 20]. As expected, HFru-fed mice exhibited dramatic increases in DNL proteins in the liver (Fig. 2b–e), including SREBP-1c (by 2-fold), ChREBP (by 33%) ACC (by 3-fold), FAS (by 3.4-fold) and SCD-1 (by 4-fold; all $P < 0.05$). Interestingly, these lipogenic proteins except for ACC were significantly reduced by the treatment with Mtr, including SREBP-1c (by 45%, $P < 0.01$), ChREBP (by 33%, $P < 0.05$), SCD-1 (by 32%, $P < 0.01$) and FAS (by 24%, $P < 0.05$). These results suggest that the reduced TG content in the liver by Mtr can be attributed to its inhibitory effect on HFru-induced increase in hepatic DNL.

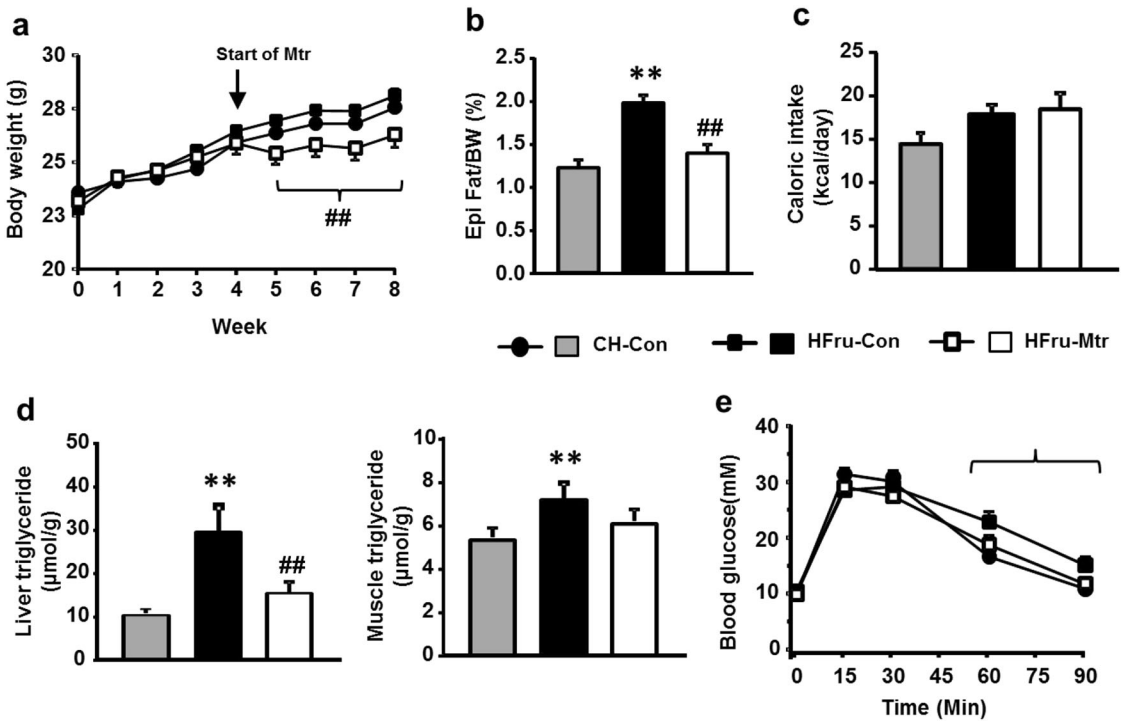

Fig. 1 Effects of Mtr on body weight gain, visceral adiposity, hepatosteatosis and glucose tolerance in HFru-fed mice. Mice were fed a high-fructose (HFru) diet for 8 weeks and matrine (Mtr, 100 mg/kg per day in diet) was administered in the last 4 weeks. A glucose tolerance test (GTT at 3 g glucose/kg BW, ip) was conducted after 2 weeks of treatment with Mtr. Epididymal (Epi) fat weight and liver TG content were determined at the end of the study. (**a**) Body weight gain, (**b**) Epididymal fat weight as a percentage of body weight, (**c**) Caloric intake, (**d**) TG content in liver and muscle. (**e**) Glucose tolerance. $^{**}P < 0.01$ vs CH; $^{\#}P < 0.05$, $^{\#\#}P < 0.01$ vs HFru ($n = 7$–8 mice/group)

Effects on ER stress and HSP72 in the liver of HFru-fed mice

By promoting DNL in the liver, the activation of ER stress represents a key step in the pathogenesis of hepatosteatosis [12, 31, 32]. As shown in Fig. 3a, HFru-fed mice exhibited marked increases of the mature form of eIF2α (by 2-fold), CHOP (by 2.3-fold) and IRE1 (by 2-fold) along with the upregulation of the DNL pathway in the liver. Treatment with Mtr markedly reduced the protein levels of these hepatic ER markers towards the levels seen in CH fed mice. These results indicate that Mtr induced-suppression of ER markers may be associated with the improvement in lipogenesis, which could account for its beneficial effects on hepatosteatosis. Recent studies indicate that HSP72 is likely to mediate the effect of Mtr on hepatosteatosis and glucose intolerance [9, 33, 34]. As shown in Fig. 3b, there was ~50% suppression of HSP72 ($P < 0.05$ vs CH fed mice) in the liver of HFru-fed mice and this reduction was reversed following treatment with Mtr ($P < 0.05$ vs untreated HFru-fed mice).

Effects on hyperglycemia in T2D mice

To investigate the relationship of the effect on hepatosteatosis with glycemic control, we examined the metabolic effects of Mtr in T2D mice generated by a HF diet in combination with low doses of STZ [9, 27, 28]. The body weight were reduced in HF-STZ induced T2D mice (by ~15%) and treatment with Mtr had no effect on the body weight (Fig. 4a), while visceral adiposity remained unchanged in T2D-Con mice compared to CH-fed mice Mtr significantly reduced epididymal fat in T2D mice ($P < 0.05$, Fig. 4b). T2D-Con mice displayed typical fasting hyperglycemia and Mtr treatment significantly reduced the degree of the hyperglycemia over the period of 4 weeks (by 20%–30%, Fig. 4c). As expected, HF-STZ-induced T2D showed severe glucose intolerance but this was not attenuated by the treatment with Mtr (Fig. 4b).

Effect on TG levels in T2D mice

Recent studies indicate that hepatosteatosis can contribute to hyperglycemia and hepatic insulin resistance [12, 35]. To determine whether the reduced hepatosteatosis by resulting from Mtr treatment is associated with the control of hyperglycemia in T2D mice, we measured the TG content in the liver. As shown in Fig. 5a, b, T2D mice exhibited hypertriglyceridemia and hepatosteatosis, however Mtr significantly reduced these conditions ($P < 0.05$). Together, these results clearly indicate that Mtr reduces the T2D-induced hepatosteatosis that is associated with hyperglycemia and this could account for its beneficial effects on the regulation of lipid metabolism.

DISCUSSION

The present study investigated whether the hepatoprotective drug Mtr can treat the hepatosteatosis and associated glucose intolerance in HFru-fed mice resulting from increased DNL. Consistent with our previous studies [13, 17, 36], HFru-fed mice developed hepatosteatosis and glucose intolerance by promoting ER stress associated DNL. Treatment of these mice with Mtr ameliorated hepatosteatosis and glucose intolerance. Within the liver, Mtr decreased the protein expression of DNL enzymes concomitant with reduced ER stress. We further examined the effects of Mtr on hepatosteatosis in relation to glycemic control in T2D mice, which display a phenotype of hyperglycemia and hepatosteatosis associated with increased DNL [27, 28]. The results showed that Mtr treatment reduced hepatosteatosis and improved hyperglycemia. Collectively, these findings suggest that Mtr has the potential to be repurposed for the treatment of hepatosteatosis resulting from increased DNL and associated disorders in glucose metabolism.

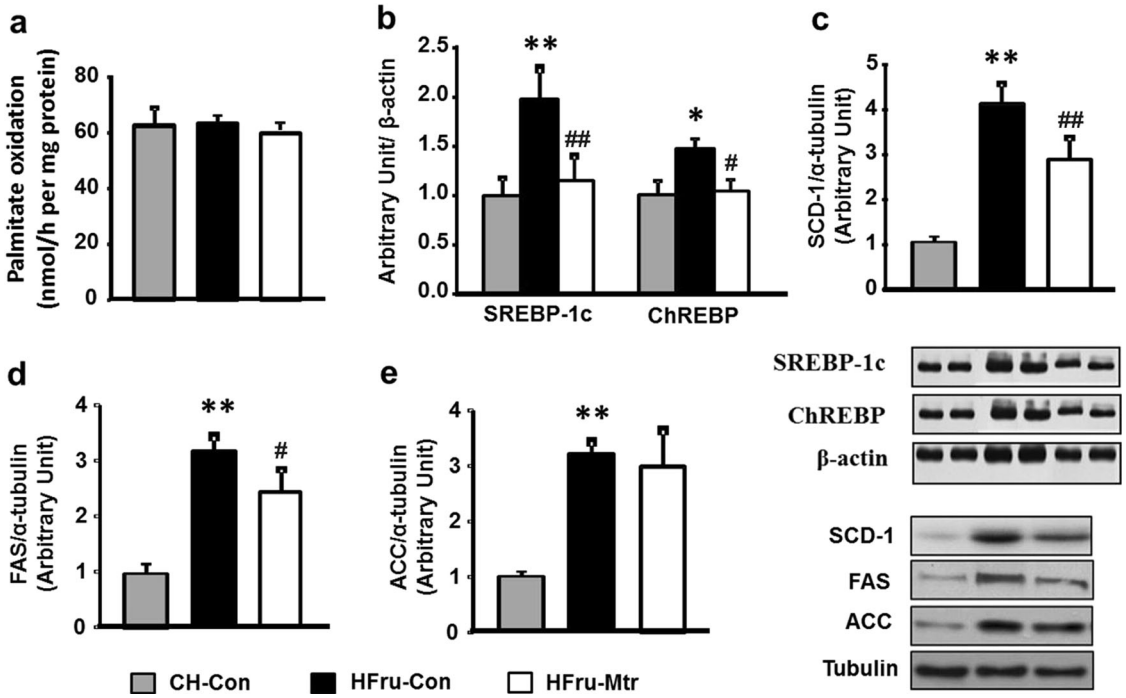

Fig. 2 Effects of Mtr on FA oxidation and DNL pathways in the liver of HFru-fed mice. FA oxidation was detected by incubating fresh liver homogenates with [^{14}C]–palmitate and DNL was assessed by the protein expression of palmitate in this pathway. (**a**) Liver lyzates from mice were immunoblotted with the mature form of SREBP-1c and ChREBP (**b**), SCD-1 (**c**), FAS (**d**) and ACC (**e**) and then quantified for statistical analysis. *$P < 0.05$, **$P < 0.01$ versus CH-Con; $^{\#}P < 0.05$, $^{\#\#}P < 0.01$ versus HFru-Con, $n = 7$–8 mice per group

Overconsumption of dietary fructose can lead to DNL and hepatosteatosis [12, 37], which in turn can result in glucose intolerance and contribute to hyperglycemia [19, 38]. Therefore, correction of hepatosteatosis is beneficial for improving glucose homeostasis in metabolic syndrome. For example, in obese patients with T2D, a reversal of hepatosteatosis can improve hepatic insulin action and glycemic control [5]. We have investigated drugs that have previously been used for the treatment of liver conditions, in order to determine whether they can be repurposed to treat hepatosteatosis [7]. One such candidate we have identified by this approach is Mtr because liver has been shown to be the major target site of Mtr [39, 40]. Indeed, our recent work has demonstrated that Mtr is able to attenuate the increased fasting blood glucose and improve glucose tolerance in insulin resistant mice induced by a HF diet [9]. The same study found that these anti-diabetic effects of Mtr appears to result from its effect in reducing hepatosteatosis without affecting HF diet induced lipid accumulation in muscle.

Mtr is clinically used for treatment of chronic liver conditions including hepatocellular carcinoma and viral hepatitis with minimal adverse effects [7–9]. Interestingly, both hepatocellular carcinoma and viral hepatitis are associated with an increase in DNL [10, 41, 42]. Indeed, our studies in 3T3L1 adipocytes have found that Mtr can reduce DNL and lipid accumulation within the cells [43]. Although our recent studies have demonstrated that Mtr is able to reduce hepatosteatosis and glucose intolerance in mice that have been fed a HF diet [9], the source of hepatosteatosis in this mouse model is from the exogenous FA due to the intake of dietary fat rather than endogenous FA from an increased DNL. Therefore, it is not clear yet whether Mtr is effective for metabolic disorders by that involve an increased hepatic DNL [12].

Several studies have demonstrated that DNL enzymes are over-expressed during the development of hepatosteatosis [24, 44]. HFru-fed mice are a well-defined animal model of DNL-induced hepatosteatosis and insulin resistance [12, 13], and DNL-induced hepatosteatosis can be observed as early as 1 day after HFru feeding [36]. Indeed, the present study showed that chronic HFru feeding resulted in hepatosteatosis (increased TG level) by promoting DNL (indicated by SREBP1c, ChREBP, acetyl-CoA carboxylase (ACC) and fatty acid synthase (FAS) and stearoyl-CoA desaturase-1 (SCD-1)) without affecting FA oxidation, as indicated by unchanged level of [^{14}C]–palmitate. However, reduced hepatic FA oxidation and mitochondrial enzyme activity has been demonstrated to occur prior to the appearance of hepatosteatosis, it has been shown that DNL is a primary cause of the development of hepatosteatosis [12, 45]. As expected, treatment with Mtr significantly reduced steatosis in the liver (not muscle because high distribution of Mtr in the liver after and oral administration [40]) and the associated glucose intolerance in these mice. We then examined the key lipogenic enzymes and found that SREBP1c, ChREBP, SCD-1 and FAS in the liver were all reduced in HFru-fed mice treated with Mtr. These results suggest that Mtr is likely to reduce hepatosteatosis via inhibition of the DNL pathway.

As an increase in FA oxidation can also attenuate hepatosteatosis [46], we next investigated whether the reduction of hepatosteatosis caused by Mtr in HFru-fed mice results from an increase in liver FA oxidation. However, Mtr did not increase the oxidation of ^{14}C-palmitate in the liver, indicating FA oxidation pathway was not activated in HFru-fed mice. This finding adds further support to our interpretation that Mtr reduces hepatosteatosis and glucose intolerance in HFru-fed mice by inhibiting DNL rather than by stimulating FA oxidation in the liver.

It has been shown that the ER stress pathway plays a critical role in HFru-induced DNL and hepatosteatosis [32, 36]. For example, an *ob/ob* mice hepatosteatosis is largely due to increased DNL as a result of hyperphagia in an ER stress-dependent manner [47]. The same study also showed that alleviation of hepatic ER stress by overexpression of GRP78 reduces hepatosteatosis and insulin resistance by inhibiting DNL. Similarly, in HFru-fed mice, inhibition of ER stress by TUDCA and Betulin suppress DNL and improve

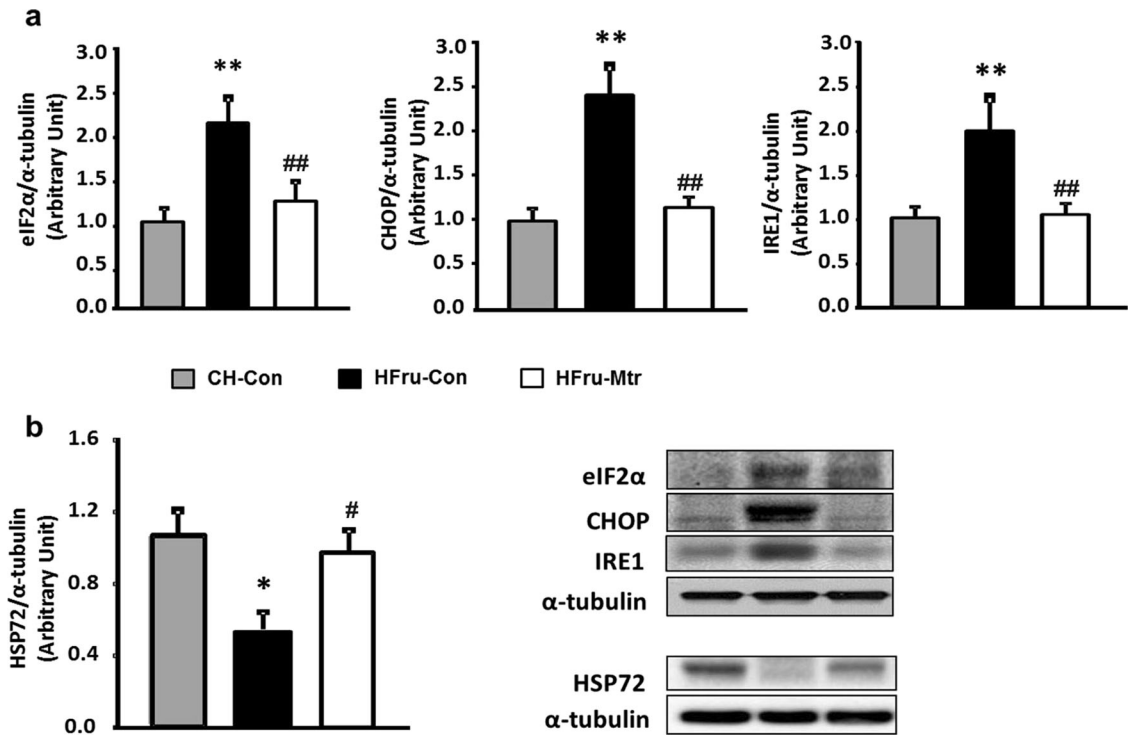

Fig. 3 Effects on ER stress and HSP72 in the liver of HFru-fed mice. Liver lyzates from mice were immunoblotted for (**a**) eIF2α, CHOP and IRE1 and (**b**) HSP72 and quantified for statistical analysis. $^{*}P < 0.05$, $^{**}P < 0.01$ versus CH-Con; $^{\#}P < 0.05$, $^{\#\#}P < 0.01$ versus HFru-Con, $n = 7$–8 mice per group

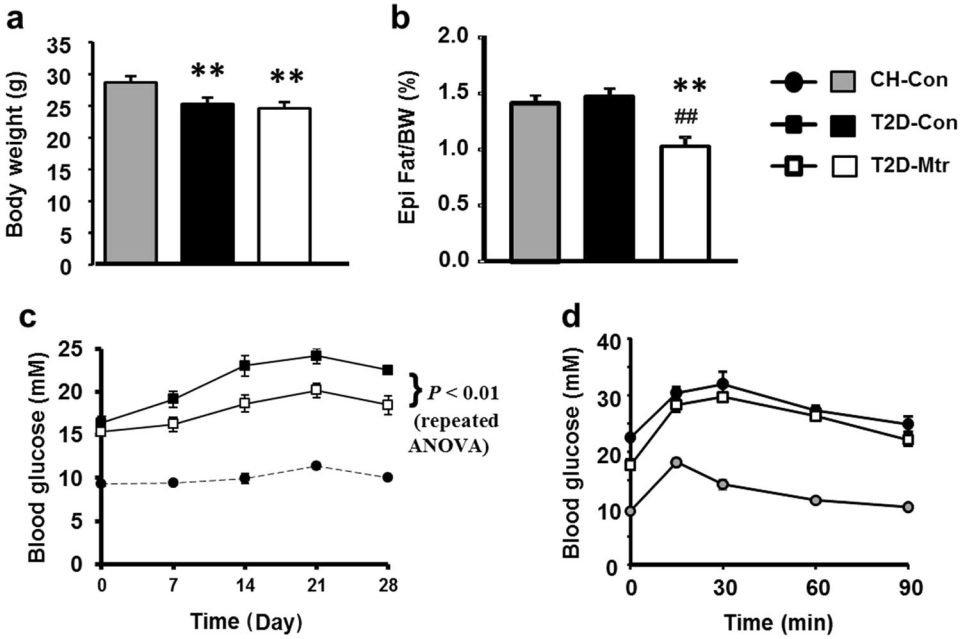

Fig. 4 Effects of Mtr on body weight, visceral adiposity, blood glucose and glucose tolerance in T2D mice. T2D was generated by a high-fat (HF) diet plus low-dose of STZ injections. After the development of hyperglycemia, Mtr (100 mg/kg per day in diet) was administered to diabetic mice for 4 weeks. Body weight at the end of the study (**a**). Epididymal (Epi) fat weight (**b**). Blood glucose levels (after 5–7 h of fasting) (**c**) were monitored once a week. An ipGTT (1.0 g glucose/g body weight) was performed after 2 weeks of treatment with Mtr (**d**). $^{**}P < 0.01$ vs CH-Con; $^{\#\#}P < 0.01$ vs T2D-Con ($n = 7$–8 mice/group)

insulin signaling in the liver [13, 17, 20]. To investigate whether the inhibition of hepatic DNL by Mtr involves the ER stress pathway, we examined the major ER stress markers in response to HFru-induced DNL. Interestingly, the results showed that HFru-induced ER stress (indicated by eIF2α, CHOP and IRE1) were all inhibited by Mtr. These findings suggest that attenuation of ER stress may be a novel mode of action for the inhibitory effect of Mtr on DNL and the resultant hepatosteatosis.

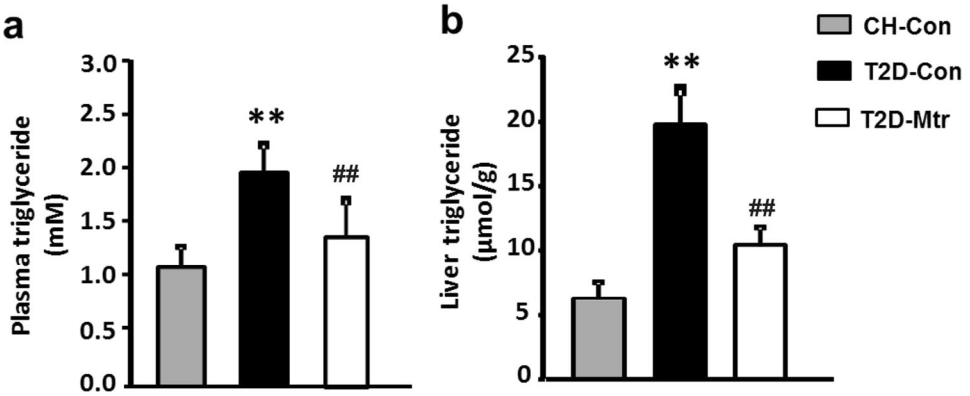

Fig. 5 Effects of Mtr on TG level in the plasma and livers of T2D mice. Plasma levels of TG were measured from blood samples collected in week 2 of the treatment (**a**). Liver TG content was determined from freeze-clamped samples obtained at the end of the study (**b**). $^{**}P < 0.01$ vs CH-Con; $^{\#\#}P < 0.01$ vs T2D-Con ($n = 7$–8 mice/group)

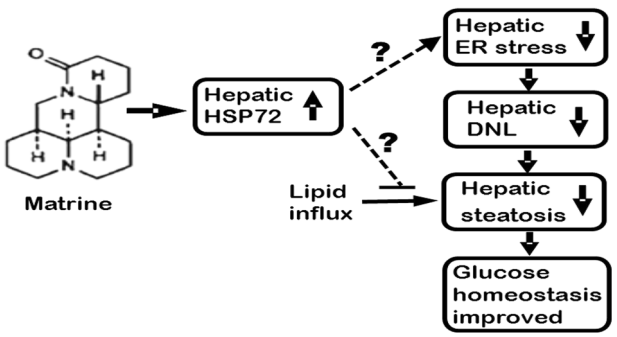

Fig. 6 Proposed hypothesis for the therapeutic effects of Mtr for hepatosteatosis and associated disorders in glucose homeostasis

In terms of the possible cellular target of Mtr, our previous work suggested that a downregulation of HSP72 may contribute to lipid accumulation in vivo [9], and in vitro [43]. We showed that Mtr is able to increase HSP72 expression and protect against lipid accumulation and glucose intolerance in the liver [9]. Consistent with this observation, the present study found that liver tissue from HFru-fed mice had significantly lower concentrations of HSP72 protein, and this reduction was prevented by Mtr treatment. HSPs have been implicated in the regulation of diverse metabolic disorders including hepatosteatosis (the major metabolic defect of non-alcoholic fatty liver disease) and insulin resistance (the major metabolic defect of T2D) [33, 48, 49]. It has been reported that an enhanced expression of HSP72 can inhibit ER stress to protect cell survival [50]. Collectively, our findings suggest that Mtr may inhibit the ER-DNL axis by up-regulating HSP72 to reduce hepatosteatosis and the associated glucose intolerance.

Hepatic DNL and hepatosteatosis also occur in transgenic diabetic mice such as *db/db* [24]. Therefore, in the present study we explored whether Mtr is able to reduce hepatosteatosis in a mouse model of T2D induced by HF-STZ [27, 28]. Our results showed that Mtr reduced epididymal fat and lowered hyperglycemia, indicating that Mtr may have the potential to control hyperglycemia in T2D. Because Mtr showed no effect on normal fasting blood glucose, glucose tolerance or liver TG content in chow-fed mice [9], the anti-diabetic effects of Mtr could be attributed to its effect in reducing hepatosteatosis.

In summary, we report here a potential novel application of the hepatoprotective drug Mtr for the treatment of hepatosteatosis and associated abnormal glucose homeostasis. This study is the first to evaluate the effect of Mtr on hepatosteatosis induced by the ER stress-DNL signaling pathway in HFru-fed mice. As suppression of ER stress can reduce hepatosteatosis by inhibiting DNL [16, 36], it is likely that Mtr may exert these beneficial effects by suppressing ER stress-induced increase in hepatic DNL. We speculate that the upregulation of the chaperon protein HSP72 may play a critical role in suppressing ER stress (as illustrated in Fig. 6) but this hypothesis requires validation by further studies using HSP72 knock-down animal model. Together with our recent findings in HF-fed mice [9], our results suggest that Mtr may be repurposed for the treatment of hepatosteatosis and associated disorders in glucose homeostasis including T2D.

ACKNOWLEDGEMENTS

This work was supported by funding from a Program Grant (535921 allocation to JMY) and a Project Grant (535930 to JMY) of the National Health and Medical Research Council of Australia. AM is supported by Al-Baha University (Ministry of Higher Education, Saudi Arabia).

AUTHOR CONTRIBUTION

J.M.Y. conceived and designed the study. A.M., S.L., X.Y.Z. and J.M.Y. performed the experiments. J.X., W.T., R.V. and S.R. provided intellectual input and participated in data analysis. J.M.Y. and J.X. contributed reagents/materials/analysis tools. A.M. and J.M.Y. prepared the manuscript. R.V. and S.R. contributed to the revision of the MS.

REFERENCES

1. Ballestri S, Zona S, Targher G, Romagnoli D, Baldelli E, Nascimbeni F, et al. Nonalcoholic fatty liver disease is associated with an almost twofold increased risk of incident type 2 diabetes and metabolic syndrome. Evidence from a systematic review and meta-analysis. J Gastroenterol Hepatol. 2016;31:936–44.
2. Cusi K, Sanyal AJ, Zhang S, Hartman ML, Bue-Valleskey JM, Hoogwerf BJ, et al. Non-alcoholic fatty liver disease (NAFLD) prevalence and its metabolic associations in patients with type 1 diabetes and type 2 diabetes. Diabetes Obes Metab. 2017;19:1630–34.
3. Sun Z, Lazar MA. Dissociating fatty liver and diabetes. Trends Endocrinol Metab. 2013;24:4–12.
4. Wu M, Singh SB, Wang J, Chung CC, Salituro G, Karanam BV, et al. Antidiabetic and antisteatotic effects of the selective fatty acid synthase (FAS) inhibitor platensimycin in mouse models of diabetes. Proc Natl Acad Sci U S A. 2011;108:5378–83.
5. Petersen KF, Dufour S, Befroy D, Lehrke M, Hendler RE, Shulman GI. Reversal of nonalcoholic hepatic steatosis, hepatic insulin resistance, and hyperglycemia by moderate weight reduction in patients with type 2 diabetes. Diabetes. 2005;54:603–8.
6. Liu JY, Hu JH, Zhu QG, Li FQ, Wang J, Sun HJ. Effect of matrine on the expression of substance P receptor and inflammatory cytokines production in human skin keratinocytes and fibroblasts. Int Immunopharmacol. 2007;7:816–23.
7. Turner N, Zeng XY, Osborne B, Rogers S, Ye JM. Repurposing Drugs to Target the Diabetes Epidemic. Trends Pharmacol Sci. 2016;37:379–89.

8. Liu J, Zhu M, Shi R, Yang M. Radix Sophorae flavescentis for chronic hepatitis B: a systematic review of randomized trials. Am J Chin Med. 2003;31:337–54.
9. Zeng XY, Wang H, Bai F, Zhou X, Li SP, Ren LP, et al. Identification of matrine as a promising novel drug for hepatic steatosis and glucose intolerance with HSP72 as an upstream target. Br J Pharmacol. 2015;172:4303–18.
10. Syed GH, Amako Y, Siddiqui A. Hepatitis C virus hijacks host lipid metabolism. Trends Endocrinol Metab. 2010;21:33–40.
11. Li Q, Pene V, Krishnamurthy S, Cha H, Liang TJ. Hepatitis C virus infection activates an innate pathway involving IKK-alpha in lipogenesis and viral assembly. Nat Med. 2013;19:722–9.
12. Ren LP, Chan SM, Zeng XY, Laybutt DR, Iseli TJ, Sun RQ, et al. Differing endoplasmic reticulum stress response to excess lipogenesis versus lipid oversupply in relation to hepatic steatosis and insulin resistance. PLoS One. 2012;7:e30816.
13. Chan SM, Sun RQ, Zeng XY, Choong ZH, Wang H, Watt MJ, et al. Activation of PPARalpha ameliorates hepatic insulin resistance and steatosis in high fructose-fed mice despite increased endoplasmic reticulum stress. Diabetes. 2013;62:2095–105.
14. Thorburn AW, Storlien LH, Jenkins AB, Khouri S, Kraegen EW. Fructose-induced in vivo insulin resistance and elevated plasma triglyceride levels in rats. Am J Clin Nutr. 1989;49:1155–63.
15. Iizuka K, Bruick RK, Liang G, Horton JD, Uyeda K. Deficiency of carbohydrate response element-binding protein (ChREBP) reduces lipogenesis as well as glycolysis. Proc Natl Acad Sci U S A. 2004;101:7281–6.
16. Donnelly KL, Smith CI, Schwarzenberg SJ, Jessurun J, Boldt MD, Parks EJ. Sources offatty acids stored in liver and secreted via lipoproteins in patients with nonalcoholic fatty liver disease. J Clin Invest. 2005;115:1343–51.
17. Sun RQ, Wang H, Zeng XY, Chan SM, Li SP, Jo E, et al. IRE1 impairs insulin signaling transduction offructose-fed mice via JNK independent of excess lipid. Biochim Biophys Acta. 2015;1852:156–65.
18. Turner N, Kowalski GM, Leslie SJ, Risis S, Yang C, Lee-Young RS, et al. Distinct patterns of tissue-specific lipid accumulation during the induction of insulin resistance in mice by high-fat feeding. Diabetologia. 2013;56:1638–48.
19. Stanhope KL, Schwarz JM, Keim NL, Griffen SC, Bremer AA, Graham JL, et al. Consuming fructose-sweetened, not glucose-sweetened, beverages increases visceral adiposity and lipids and decreases insulin sensitivity in overweight/obese humans. J Clin Invest. 2009;119:1322–34.
20. Lee AH, Scapa EF, Cohen DE, Glimcher LH. Regulation of hepatic lipogenesis by the transcription factor XBP1. Science. 2008;320:1492–6.
21. Lecoultre V, Egli L, Carrel G, Theytaz F, Kreis R, Schneiter P, et al. Effects of fructose and glucose overfeeding on hepatic insulin sensitivity and intrahepatic lipids in healthy humans. Obesity. 2013;21:782–5.
22. Schwarz JM, Noworolski SM, Wen MJ, Dyachenko A, Prior JL, Weinberg ME, et al. Effect of a high-fructose weight-maintaining diet on lipogenesis and liver fat. J Clin Endocrinol Metab. 2015;100:2434–42.
23. Ameer F, Scandiuzzi L, Hasnain S, Kalbacher H, Zaidi N. De novo lipogenesis in health and disease. Metabolism. 2014;63:895–902.
24. Shimomura I, Bashmakov Y, Horton JD. Increased levels ofnuclear SREBP-1c associated with fatty livers in two mouse models of diabetes mellitus. J Biol Chem. 1999;274:30028–32.
25. Dentin R, Benhamed F, Hainault I, Fauveau V, Foufelle F, Dyck JR, et al. Liver-specific inhibition of ChREBP improves hepatic steatosis and insulin resistance in ob/ob mice. Diabetes. 2006;55:2159–70.
26. Zheng Z, Zhang C, Zhang K. Role ofunfolded protein response in lipogenesis. World J Hepatol. 2010;2:203–7.
27. Mu J, Woods J, Zhou YP, Roy RS, Li Z, Zycband E, et al. Chronic inhibition of dipeptidyl peptidase-4 with a sitagliptin analog preserves pancreatic beta-cell mass and function in a rodent model of type 2 diabetes. Diabetes. 2006;55:1695–704.
28. Zeng XY, Wang YP, Cantley J, Iseli TJ, Molero JC, Hegarty BD, et al. Oleanolic acid reduces hyperglycemia beyond treatment period with Akt/FoxO1-induced suppression of hepatic gluconeogenesis in type-2 diabetic mice. PLoS One. 2012;7:e42115.
29. Ye JM, Tid-Ang J, Turner N, Zeng XY, Li HY, Cooney GJ, et al. PPARdelta agonists have opposing effects on insulin resistance in high fat-fed rats and mice due to different metabolic responses in muscle. Br J Pharmacol. 2011;163:556–66.
30. Ye JM, Iglesias MA, Watson DG, Ellis B, Wood L, Jensen PB, et al. PPARalpha /gamma ragaglitazar eliminates fatty liver and enhances insulin action in fat-fed rats in the absence of hepatomegaly. Am J Physiol Endocrinol Metab. 2003;284: E531–40.
31. Hotamisligil GS. Endoplasmic reticulum stress and the inflammatory basis of metabolic disease. Cell. 2010;140:900–17.
32. Ozcan U, Cao Q, Yilmaz E, Lee AH, Iwakoshi NN, Ozdelen E, et al. Endoplasmic reticulum stress links obesity, insulin action, and type 2 diabetes. Science. 2004;306:457–61.
33. Chung J, Nguyen AK, Henstridge DC, Holmes AG, Chan MH, Mesa JL, et al. HSP72 protects against obesity-induced insulin resistance. Proc Natl Acad Sci U S A. 2008;105:1739–44.
34. Kurucz I, Morva A, Vaag A, Eriksson KF, Huang X, Groop L, et al. Decreased expression of heat shock protein 72 in skeletal muscle of patients with type 2 diabetes correlates with insulin resistance. Diabetes. 2002;51:1102–9.
35. Samuel VT, Petersen KF, Shulman GI. Lipid-induced insulin resistance: unravelling the mechanism. Lancet. 2010;375:2267–77.
36. Wang H, Sun RQ, Zeng XY, Zhou X, Li S, Jo E, et al. Restoration of autophagy alleviates hepatic ER stress and impaired insulin signalling transduc-tion in high fructose-fed male mice. Endocrinology. 2015;156:169–81.
37. Herman MA, Samuel VT. The sweet path to metabolic demise: fructose and lipid synthesis. Trends Endocrinol Metab. 2016;27:719–30.
38. Perry RJ, Samuel VT, Petersen KF, Shulman GI. The role of hepatic lipids in hepatic insulin resistance and type 2 diabetes. Nature. 2014;510:84–91.
39. Zhang HF, Shi LJ, Song GY, Cai ZG, Wang C, An RJ. Protective effects of matrine against progression of high-fructose diet-induced steatohepatitis by enhancing antioxidant and anti-inflammatory defences involving Nrf2 translo-cation. Food Chem Toxicol. 2013;55:70–7.
40. Gao G, Law FC. Physiologically based pharmacokinetics of matrine in the rat after oral administration of pure chemical and ACAPHA. Drug Metab Dispos. 2009;37:884–91.
41. Milner KL, van der Poorten D, Trenell M, Jenkins AB, Xu A, Smythe G, et al. Chronic hepatitis C is associated with peripheral rather than hepatic insulin resistance. Gastroenterology. 2010;138:932–41. e1-3
42. McPherson S, Jonsson JR, Barrie HD, O'Rourke P, Clouston AD, Powell EE. Investigation of the role of SREBP-1c in the pathogenesis of HCV-related steatosis. J Hepatol. 2008;49:1046–54.
43. Zeng XY, Zhou X, Xu J, Chan SM, Xue CL, Molero JC, et al. Screening for the efficacy on lipid accumulation in 3T3-L1 cells is an effective tool for the identification of new anti-diabetic compounds. Biochem Pharmacol. 2012;84:830–7.
44. Postic C, Girard J. Contribution of de novo fatty acid synthesis to hepatic steatosis and insulin resistance: lessons from genetically engineered mice. J Clin Invest. 2008;118:829–38.
45. Rector RS, Thyfault JP, Uptergrove GM, Morris EM, Naples SP, Borengasser SJ, et al. Mitochondrial dysfunction precedes insulin resistance and hepatic steatosis and contributes to the natural history of non-alcoholic fatty liver disease in an obese rodent model. J Hepatol. 2010;52:727–36.
46. Reddy JK. Nonalcoholic steatosis and steatohepatitis. III. Peroxisomal beta-oxidation, PPAR alpha, and steatohepatitis. Am J Physiol Gastrointest Liver Physiol. 2001;281:G1333–9.
47. Kammoun HL, Chabanon H, Hainault I, Luquet S, Magnan C, Koike T, et al. GRP78 expression inhibits insulin and ER stress-induced SREBP-1c activation and reduces hepatic steatosis in mice. J Clin Invest. 2009;119:1201–15.
48. Gupte AA, Bomhoff GL, Swerdlow RH, Geiger PC. Heat treatment improves glucose tolerance and prevents skeletal muscle insulin resistance in rats fed a high-fat diet. Diabetes. 2009;58:567–78.
49. Di Naso FC, Porto RR, Fillmann HS, Maggioni L, Padoin AV, Ramos RJ, et al. Obesity depresses the anti-inflammatory HSP70 pathway, contributing to NAFLD progression. Obesity. 2015;23:120–9.
50. Gupta S, Deepti A, Deegan S, Lisbona F, Hetz C, Samali A. HSP72 protects cells from ER stress-induced apoptosis via enhancement of IRE1a-XBP1 signaling through a physical Interaction. PLoS Biol. 2010;8:e1000410.

Manuscript Details

Manuscript number	JEP_2018_1927
Title	Matrine alleviates MCD-induced steatohepatitis associated with induction of heat shock proteins and inhibition of mTOR differently from metformin
Article type	Research Paper

Abstract

Non-alcoholic steatohepatitis (NASH) is a severe stage of non-alcoholic fatty liver disease (NAFLD) characterized by steatosis, liver damage and inflammation with or without fibrosis. The present study investigated the effects of matrine (Mtr) on a methionine choline-deficient (MCD) diet-induced NASH. C57B/6J mice were fed a MCD diet for 6 weeks to induce NASH with or without the treatment of Mtr or metformin as a comparator. The results showed that Mtr treatment suppressed plasma ALT, TNFα, and hepatic fibrosis markers (TGFβ and Smad3) induced by MCD diet. Along with these effects, Mtr reversed the reduced level of HSP72 induced by MCD diet, suggesting a likely role of HSP72 in coordinating the therapeutic effects of Mtr for NASH. Metformin did not improve inflammation and had no effect on collagen 1 and caspase-1. Notably, Mtr treatment simultaneously decreased mTOR which is frequently activated in NASH. These findings suggest Mtr may be able to upregulate HSP72 and inhibit mTOR against NASH induced by MCD diet in a mechanism different from metformin.

Keywords	Matrine; NASH; inflammation; fibrosis; HSP72; mTOR; methionine choline-deficient diet
Taxonomy	Pharmaceutics, Toxicology

Corresponding Author	Ji-Ming Ye
Order of Authors	Ji-Ming Ye, Ali Mahzari, Songpei Li, Xiao-Yi Zeng, Sherouk Fouda, Xiu Zhou, Dongli Li, Majid Alhomrani, Stephen R Robinso

Matrine alleviates MCD-induced steatohepatitis associated with induction of heat shock proteins and inhibition of mTOR differently from metformin

Ali Mahzari [1], Songpei Li [1], Xiao-Yi Zeng [1], Sherouk Fouda [1], Xiu Zhou [2], Dongli Li [2], Majid Alhomrani [3], Stephen R Robinson [1] & Ji-Ming Ye [1]†.

[1] School of Health and Biomedical Sciences, RMIT University, Melbourne, VIC, Australia

[2] School of Chemical Engineering, Wuyi University, Jiangmen, Guangdong, China

[3] Centre for Inflammatory Diseases, Monash University, Clayton, VIC, Australia

† Author for correspondence:

Professor Ji-Ming Ye, PhD, MD
Lipid Biology and Metabolic Disease Laboratory
School of Health and Biomedical Sciences
RMIT University,
Melbourne, VIC 3083, Australia.
Tel: + 61-3-9925 7419; Fax: + 61-3-9925 7178.
Email: jiming.ye@rmit.edu.au

Abbreviations

Mtr, matrine; Met, metformin; MCD, methionine choline-deficient; NAFLD, non-alcoholic fatty liver disease; NASH, non-alcoholic steatohepatitis; ALT, alanine transaminase; AST, aspartate aminotransferase; TGF-β, transforming growth factor β; HSP72, heat shock protein 72; HSF1, heat shock factor 1; HSP90, heat shock protein 90; mTOR, mammalian target of rapamycin

Abstract

Ethnopharmacological relevance: Matrine has been isolated from *Sophora flavscens*, and used as a prescribed for treatment of inflammation, cancer, and liver diseases.

Aim of this study: The present study investigated the effects of matrine (Mtr) on a methionine choline-deficient (MCD) diet-induced NASH.

Materials and methods: C57B/6J mice were fed a MCD diet for 6 weeks to induce NASH with or without the treatment of Mtr or metformin as a comparator.

Results: The results showed that Mtr treatment suppressed plasma ALT, TNFα, and hepatic fibrosis markers (TGFβ and Smad3) induced by MCD diet. Along with these effects, Mtr reversed the reduced level of HSP72 induced by MCD diet, suggesting a likely role of HSP72 in coordinating the therapeutic effects of Mtr for NASH. Metformin did not improve inflammation and had no effect on collagen 1 and caspase-1. Notably, Mtr treatment simultaneously decreased mTOR which is frequently activated in NASH.

Conclusions: These findings suggest Mtr may be able to upregulate HSP72 and inhibit mTOR against NASH induced by MCD diet in a mechanism different from metformin.

Key words: Matrine; NASH; inflammation; fibrosis; HSP72; mTOR; methionine choline-deficient diet

1. Introduction

Non-alcoholic steatohepatitis (NASH) is a severe condition of non-alcoholic fatty liver disease (NAFLD), the most common chronic liver disease. It is characterized with liver steatosis, damage, inflammation and variable degrees of fibrosis by the American Association for the Study of Liver Diseases (AASL) [1]. Although the exact mechanism (s) that mediate the transition from steatosis to steatohepatitis remain unknown, hepatic inflammation is believed to play a key role in NASH pathogenesis [2]. Furthermore, it may induce hepatic fibrosis that aggravates the progression of this disease [1]. Untreated NASH with advanced fibrosis may increase the incidence rate of liver cirrhosis, hepatocellular carcinoma and liver transplantation [1]. Therefore, the major treatment of NAFLD has been focused on NASH because effective control of NASH can prevent or delay the progression to these conditions. To date, there is still no approved drug specifically for NASH [1].

Matrine (Mtr) is a small molecule (MW: 248), a natural product derived from a plant named *Sophora Flavescens* (Kushen alkaloids) [3]. The active compound Mtr has been widely prescribed as a hepatoprotective drug in China with very minimum adverse effects [4]. In addition, Mtr has several well-recognized pharmacological effects targeting the liver including anti-inflammatory, antitumor and anti-viral activities [3, 4]. One of the well-characterized anti-inflammatory effects of Mtr is inhibition of pro-inflammatory cytokines TNFα, the golden key in the pathogenesis of NASH [5]. Moreover, Mtr treatment significantly inhibits inflammation upon challenge with LPS *in vivo* and *in vitro* and liver damage in reperfusion injury of rat liver [6]. Our previous study reported the therapeutic effects of Mtr on hepatosteatosis and glucose intolerance induced by a high-fat diet in mice, with a mechanism different from metformin [7]. Given the close relationship between

metabolic syndrome and NAFLD, we are going to further investigate the effect of Mtr contained the active compound that suppress NASH with a focus on hepatic damage, inflammation and fibrosis, which are three hallmarks of NASH [1].

2. Materials and Methods

2.1. Animal care, diets and experimental design

Male C57BL/6J mice (10-week old) were purchased from the Animal Resources Centre (Perth, Australia) and acclimatized in the animal facility at RMIT University with a standard chow diet (CH diet, Specialty Feeds, Australia) for at least one week. Mice were assigned to four groups randomly: 1) fed ad libitum with a standard chow diet (CH-Con), 2) MCD alone (MCD-Con), 3) MCD treated with matrine (MCD-Mtr; Mtr: 100 mg/kg/day), and 4) MCD treated with metformin (MCD-Met; Met: 250 mg/kg/day) as a food additive for 6 weeks. Body weight and food intake were monitored daily throughout the experiment. 5-7 hours after food removal, tail vein blood was collected for glucose measurement using a glucometer (AccuCheck II; Roche, Australia). At the end of the study, plasma was also collected from the tail vein and stored at -80°C for biochemical test. A ketamine/xylazine mixture (up to 100 mg/kg body weight ketamine and 20 mg/kg body weight xylazine) is administered via intraperitoneal injection. Mice fixation was performed via transcardial perfusion with heparinized PBS (10-20 ml/mice) then perfused with 4% paraformaldehyde (PFA; 10-20 ml/mice, ProsciTech; # C007). At the completion of the paraformaldehyde perfusion, liver right lobe was dissected and immersed in 4% PFA-filled glass scintillation vials for further experiments. All experiments were approved by the Animal Ethics Committee of RMIT University (#1415) in accordance with the guidelines of the National Health and Medical Research Council of Australia.

2.2. Preparation of Matrine

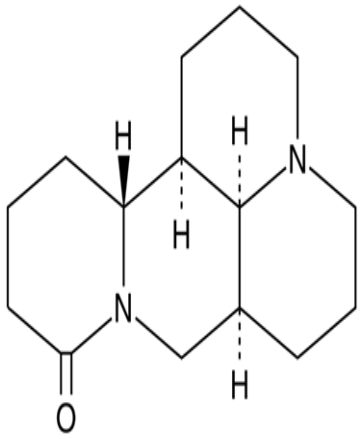

Mtr (Purity > 99.5%) was a gift from Professor Li-Hong Hu from the Shanghai Institute of Materia Medica; metformin was purchased from Sigma-Aldrich. The powders were stored at -20 °C then weighted and carefully mixed with diet at a dose of 100 mg/kg every day. **Fig. 1** shows the molecular structure of matrine.

Fig. 1 Molecular structure of matrine.

2.3. In vivo Evaluation of Total Body Fat Content

After four weeks of treatment, the total body fat content in mice was evaluated using the EchoMRI™-100H Body Composition Analyzer (Echo Medical Systems, Houston, TX, USA).

2.4. Assessment of the effect on hepatic steatosis

Hepatosteatosis was assessed by measuring hepatic TG content, which was extracted by the method of Folch and determined using a colorimetric assay kit (Triglyceride GPO-PAP; Roche Diagnostics, Australia), as described previously [8].

2.5. Assessment of the effect on liver damage

To examine the effects of Mtr on liver damage, the second component of NASH, plasma alanine aminotransferase (ALT) and aspartate aminotransferase (AST) were measured in week five using commercial kits (ALT/SGPT and AST/SGOT both Liqui-UV Kit, Boerne, USA) [9]. 5-7 hours after food removal, blood plasma was collected from the tail vein and

prepared according to the manufacturer's instructions. The absorbance was measured at 340 nm using a FlexStation (Molecular Devices, Sunnyvale, CA, USA).

2.6. Quantification of total and non-heme iron

The total iron and non-heme iron contents of liver samples were determined calorimetrically [10], because iron deposition is also regarded as a characteristic of NASH [11, 12]. As described previously [13], a fixative liver tissue was homogenized with 50 mM NaOH and incubated overnight at 75-80 degrees. To quantify the amount of total iron and non-heme iron, either reagent A (a freshly mixed solution of equal volumes of 1.4 M HCl, 4.5% [w/v] $KMnO_4$ and 40% TCA in H_2O) or reagent B (same as reagent A without $KMnO_4$) was added to samples [10].

The iron content of the sample was calculated by comparing its absorbance to that of a range of standard concentrations of equal volume. Standards (5x diluted standards) were prepared as a mixture of $FeCl_3$ in 10 mM HCl, 50 mM NaOH. Standard value was measured using lysis reagent that either contained or lacked permanganate [13]. The mixture was transferred into 96 well plate and its absorbance was measured at 550 nm.

2.7. Real-time polymerase chain reaction of liver RNA

Total RNA was isolated from mouse livers using TRIzol reagent (Invitrogen, #15596026) as previously described [14]. Real-time PCR was carried out using the IQ SYBR Green Supermix (Bio-Rad Laboratories Inc, USA) for genes of interest. Target gene expression was normalized to the housekeeping gene (18S). The primer sequence (5′ to 3′) of 18S is CGCCGCTAGAGGTGAAATTCT (sense) and CGAACCTCCG ACTTTCGTTCT (antisense); TNFα: CACAAGATGCTGGGA- CAGTGA (sense) and TCCTTGATGGTGGTGCATGA (antisense); IL-1β: CAACCAACAAGTGATATTCTCCATG (sense) and GATCCACACTCTCCAGCTGCA (antisense); CD68: TGACCTGCTCTCTCTAAGGCTACA (sense) and

TCACGGTTGCAAGAGAAACATG (antisense); Collagen 1: CTGCTGGTGAGAGAGGTGAAC (sense) and ACCAAGGTCTCCAGGAACAC (antisense).

2.8. Western Blotting

Liver lysates were resolved by SDS-PAGE and immunoblotted with specific antibodies [15]. Antibodies were diluted 1:1000 with a TBST buffer containing 1% BSA, 0.02% sodium azide (Sigma-Aldrich, #71289) and 0.0025% phenol red (Sigma-Aldrich, #32661). Antibodies for HSP72 (Catalogue No. C92F3A-5, 1:1000 dilution) and HSP90 (ADI-SPA-840HRP, 1:1000) were purchased from Enzo Life Sciences, Farmingdale, NY, USA; MCP-1 (#2027, 1:1000), HSF1 (#4356, 1:1000), TGFβ (#3709, 1:1000), Smad3 (#9523, 1:1000), mammalian target of rapamycin (mTOR), phospho^{Ser2448} mTOR (#2983, 1:1000), α-Tubulin (#3873, 1:1000) and GAPDH (#2118, 1:1000) were purchased from Cell Signaling, Danvers, MA, USA. A nod-like receptor pyrin containing 3 (NLPR3, #20B-0006-C100, 1:1000) was purchased from AdipoGen San Diego, USA. Goat Anti Mouse (#sc-2005), Goat Anti Rabbit (#sc-2004) and Goat Anti-Rat (#sc-2065) from Santa Cruz (USA). Proteins were quantified using a ChemiDoc, and densitometry analysis was performed using Image Lab software (Bio-Rad Laboratories, Australia).

2.9. Histological evaluation of liver sections

The liver samples perfused using PFA were sliced to 5 μm sections. Free-floating sections were used and stained with picrosirius red for liver fibrosis. Slides were quantified in five non-overlapping fields of view per animal using an Olympus BX41 microscope with a 20X objective lens and an Olympus DP72 digital camera (Olympus, Australia) [9, 16]. The mean of value was calculated for each experimental group using the threshold function in the ImageJ software package (NIH Image, Bethesda, MD, United States). Data are represented as percentage (%) of positive area per field.

2.10. Statistical analysis

All results are presented as means ± SEM. One-way analysis of variance was used to assess the statistical significance across all groups. When significant differences were found, the Tukey-Kramer multiple comparisons post-hoc test was used to establish differences between groups. Differences at $p \leq 0.05$ were considered statistically significant and $p \leq 0.01$ were considered highly significant.

3. Results

3.1. Effects on adiposity, hepatosteatosis and plasma glucose

MCD diet feeding is a common dietary model of NASH despite the absence of several metabolic phenotype on body weight gain and calorie intake [17, 18]. As expected, MCD diet-fed mice showed a reduced body weight, body weight gain fasting and blood glucose level despite a significant increase in calorie intake. As shown in Table 1, the excess TG accumulation, indicative of hepatosteatosis, was increased dramatically in the liver of MCD-Con mice compared with CH-Con (by 2 fold, $p < 0.01$). The difference in weight gain between chow, MCD alone and MCD with treatments was maintained throughout the 6-week treatment period.

Mtr had no effect on body weight gain and calorie intake in MCD diet-fed mice. Consistent with previous studies [18, 19], MCD diet-fed mice showed increased adiposity and hepatosteatosis but no glucose intolerance or mild hypoglycemia. There was no change in fasting blood glucose level in Mtr-treated MCD diet-fed mice compared to MCD diet-fed group. Associated with these effects, Mtr also was had no effect in reducing hepatic TG in MCD diet-fed mice (**Table 1**). Similarly, metformin did not show any effect on any of these parameters in MCD diet-fed mice.

Table 1. Effects of matrine and metformin on body weight, total food intake and liver triglyceride

	CH-Con	MCD-Con	MCD-Mtr	MCD-Met
Body weight (g)	24.3±0.2	23.5±0.2**	22.6±0.1††	22.7±0.1††
Body weight gain (g)	2.0±0.2	0.4±0.2**	0.3±0.2	0.7±0.1
Caloric intake (kcal/kg.day)	268.2±7.5	313.7±9.0	319.7±10.0	334.8±18.4
Fasting blood glucose (mM)	8.0±0.5	7.4±0.4	6.3±0.4	6.4±0.5
Liver triglyceride (μmol/g)	13.8±4.2	31.6±3.3**	28.2±2.5	31.2±3.1

Mice were fed a chow (CH-Con), or MCD alone (MCD-Con), MCD-treated with matrine (MCD-Mtr; 100mg/kg/day) or MCD-treated with metformin (MCD-Met; 250mg/kg/day). Body weight and food intake were measured twice a week. Blood glucose was performed at week 5. Plasma was collected before tissue collection at week 6 for the subsequent analysis for ALT and AST. ** $p < 0.01$ vs. CH-Con; †† $p < 0.01$ vs. MCD-Con (n = 8 mice/group).

3.2. Effects on body composition using MRI

MCD diet feeding resulted in a lack of metabolic phenotype possibly due to significantly decreased body weight (**Fig. 2A**). As illustrated in **Fig. 2B**, in spite of the reduced body weight as a result of MCD diet feeding, there was a significant increase in fat mass in MCD diet-fed mice compared to the CH-Con group. MRI also revealed that MCD diet-fed mice with or without treatment of Mtr or metformin had significant decreases in lean mas compared to the CH-Con group (**Fig. 2C**). However, Mtr and metformin had no effect on the fat mass of MCD diet-fed mice.

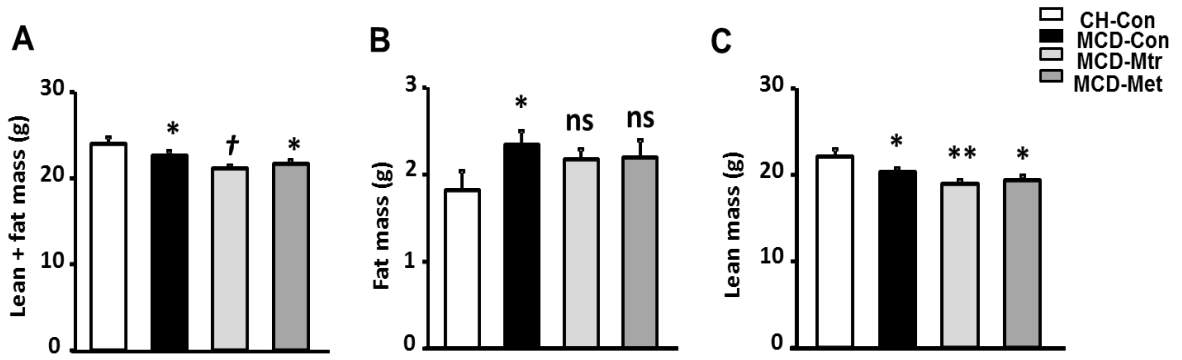

Fig. 2. Effects of Mtr on body composition in MCD mice

The body composition of CH-Con, MCD-Con, MCD-Mtr and MCD-Met was determined by EchoMRI analyzer at week 4 (**A**) Lean+fat mass; (**B**) Fat mass; (**C**) Lean mass. *$p < 0.05$, **$p < 0.01$ vs. CH-Con; †$p < 0.05$ vs. MCD-Con; ns: no significant vs. CH-Con or MCD-Con (n = 8 mice/group).

3.3. Effects on hepatic inflammation

Hepatic inflammation is critical in the progression of NASH, in which secreted pro-inflammatory cytokines produced by the Kupffer cells promote cell injury and fibrogenesis in the liver [1]. Key inflammatory cytokines, including TNFα, IL1β, MCP-1 and NLRP3, are particularly associated with liver inflammation, ultimately NASH [1, 20]. To examine the role of inflammation in MCD diet-fed mice, the protein activity or expression of these inflammatory markers were measured. As expected, MCD-diet resulted in a marked pro-inflammatory response in the liver as evidenced by increased gene expression of TNFα (2-fold increase), as well as increased protein levels of MCP1 (1.5-fold) and NLRP3 (1.5-fold). The increased expression of MCP1 coincided with an increased gene expression of CD68, suggesting recruitment and activation of the Kupffer cells, confirming the presence of hepatic

inflammation. Administration of Mtr, but not metformin, significantly decreased the expression of TNFα, CD68 (both $p < 0.05$ vs. MCD-Con mice) and MCP-1 ($p < 0.01$ vs. MCD-Con mice) (**Fig. 3 A, C and D**). However, no significant differences were detected in the expression of IL-1β amongst the experimental groups (**Fig. 3 B**). It has been suggested that NLRP3 blockade reverses advanced stage liver inflammation and fibrosis in MCD diet-induced NASH [2]. Consistent with results on the inhibition of inflammatory markers, Mtr significantly decreased the inflammasome activation in MCD diet-fed mice (**Fig. 3 E**). In contrast to Mtr, metformin had no effect on the activities or expression of these markers (**Fig. 3 A-E**).

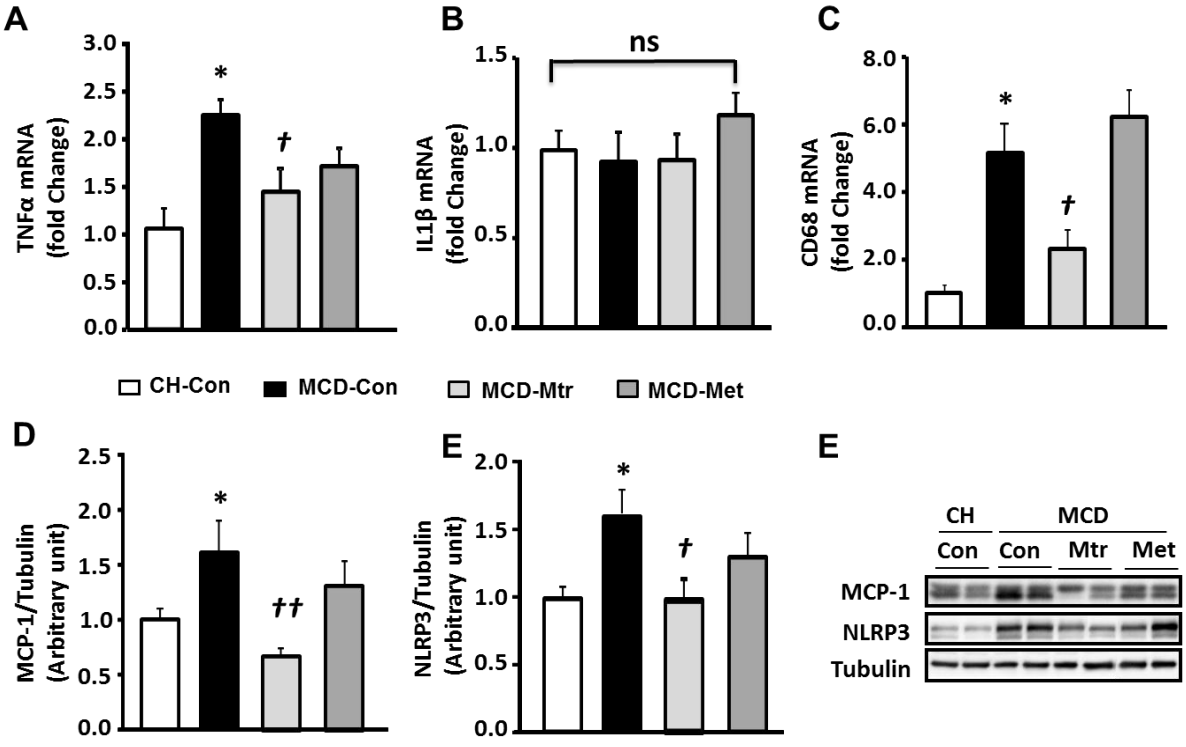

Fig. 3. Effects of Mtr on inflammation in MCD-fed mice. (**A**) TNFα mRNA, (**B**) IL1β mRNA and (**C**) CD68 mRNA. Protein expression of MCP-1 (D) and NCLP3 (E), and the corresponding representative blots (F). *p < 0.05 vs. CH-Con; †p < 0.01, ††p < 0.01 vs. MCD-Con; ns: no significant vs. CH-Con or MCD-Con (n = 7-8 mice/group).

3.4. Effects on the hepatic fibrogenesis

The effect of Mtr on hepatic fibrosis was examined, as liver fibrosis is another hallmark of advanced NASH [21, 22]. As shown in **Fig. 4 A-C**, MCD diet-fed mice exhibited marked increases in the hepatic expression of key fibrogenic proteins , namely TGFβ, collagen1 and Smad3 (p < 0.05 vs. CH-Con). Mtr treatment completely normalized the protein abundance of these fibrotic markers to the corresponding levels in CH-Con mice. Meanwhile, metformin treatment decreased these markers but less effective compared to Mtr treatment. There was no significant change in caspase-1 protein expression between groups (**Fig. 4 D**).

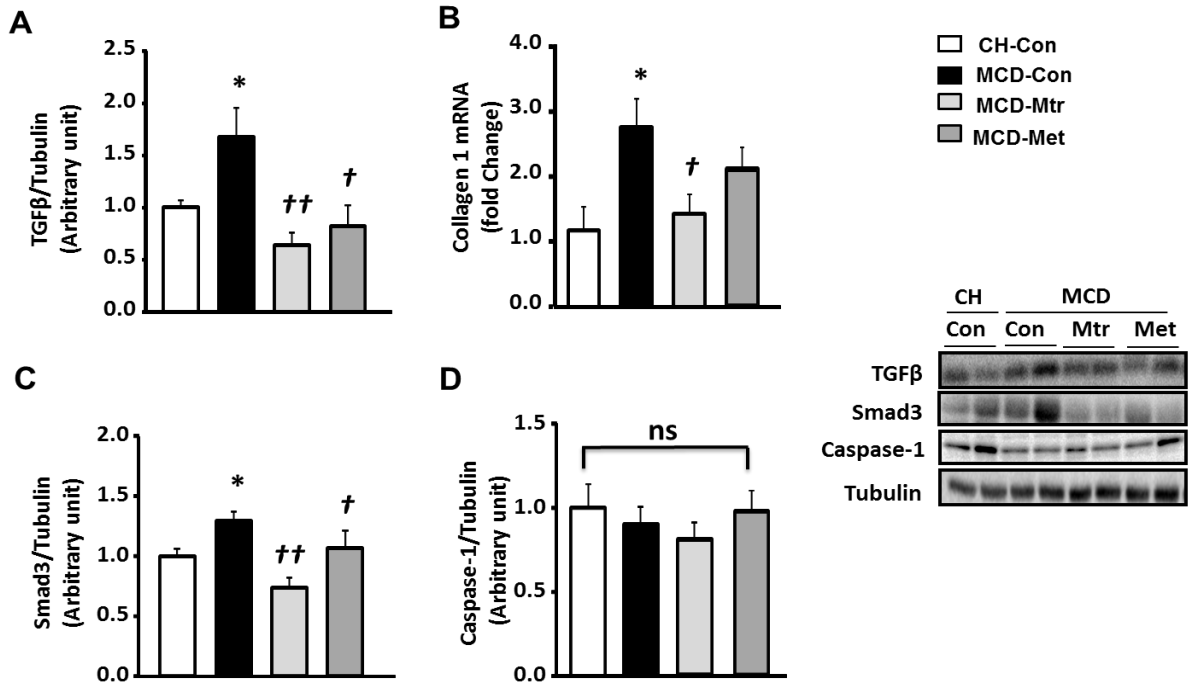

Fig. 4. Effects of Mtr on fibrosis in MCD diet-fed mice. Liver lysates from mice were immunoblotted for (**A**) TGFβ, (**C**) Smad3 and (**D**) Caspase-1 or RT-PCR for (**B**) collagen 1. *$p < 0.05$ vs. CH-Con; †$p < 0.01$, ††$p < 0.01$ vs. MCD-Con; ns: no significant vs. CH-Con or MCD-Con (n = 7-8 mice/group).

To further evaluate the effect of Mtr on hepatic fibrogenesis, liver sections were stained with picrosirius red to quantify the extent of liver fibrosis. As shown in **Fig. 5**, there was ~83% increase of liver fibrosis ($p < 0.01$ vs. CH-Con fed mice) in the liver of MCD-fed mice and this increase was reversed following treatment with Mtr (~66% reduction, $p < 0.01$ vs. MCD-Con mice). In comparison, no significant reduction of liver fibrosis was observed following metformin treatment.

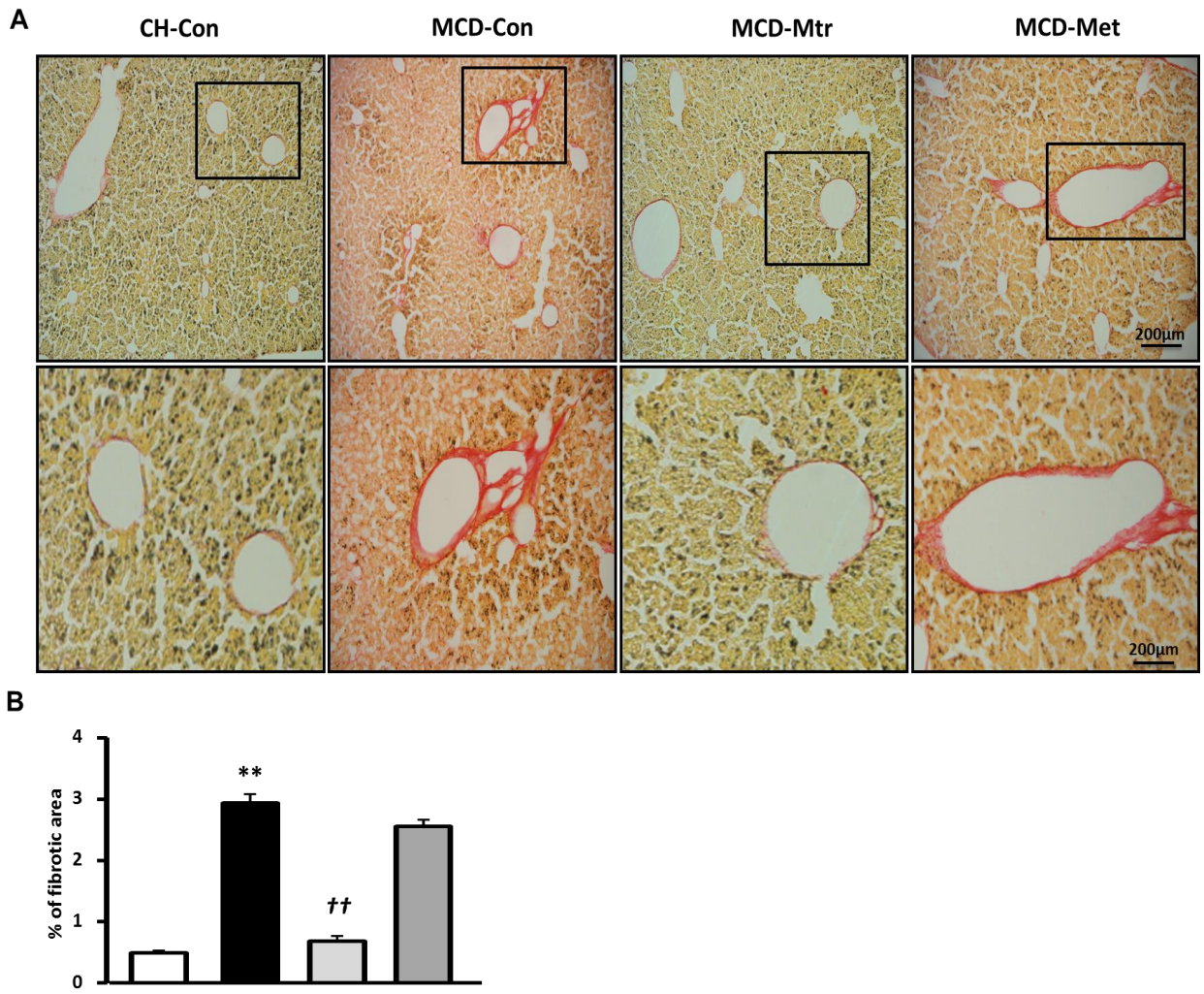

Fig. 5. Effects of Mtr on fibrosis in MCD diet-fed mice. (**A**) Representative images showing collagen staining with picrosirius red in liver sections from control and treated groups. Scale bar = 200 μm, 10, 40x magnification. (**B**) Mtr treated mice had significantly reduced fibrosis area compare to MCD-Con group. $^{**}p < 0.01$ vs. CH-Con; $^{\dagger\dagger}p < 0.01$ vs. MCD-Con (n = 7-8 mice/group).

3.5. Effects on plasma level of liver enzymes and iron deposition

Liver damage has been suggested to be an important factor that distinguishes NASH from hepatosteatosis [23]. We next examined whether Mtr treatment may alleviate liver damage in

MCD diet-fed mice. As shown in **Fig. 6 A**, MCD diet-fed mice exhibited marked increases in ALT (by 2-fold) and AST (by 1-fold) levels along with the increase of hepatosteatosis in the liver (Table 1). Mtr treatment markedly decreased both plasma ALT and AST levels, indicating Mtr may reduce liver damage. In contrast, metformin reduced the level plasma ALT, but not AST, in MCD diet-fed mice (**Fig. 6 B**). Iron overload plays an important role in the development of NASH [11]. It has been demonstrated that iron overload exacerbates inflammation and fibrosis-induced steatohepatitis in humans [24] and rodents [12, 25, 26]. We further examined the effects of Mtr on iron levels in the liver of MCD diet-fed mice. Consistent with previous reports, the hepatic level of heme or non-heme iron was elevated in mice fed a MCD diet (**Fig. 6 C and D**). However, Mtr or metformin treatment had no effect on the increased level of heme or non-heme iron in the liver of MCD diet-fed mice (**Fig. 6 C and D**).

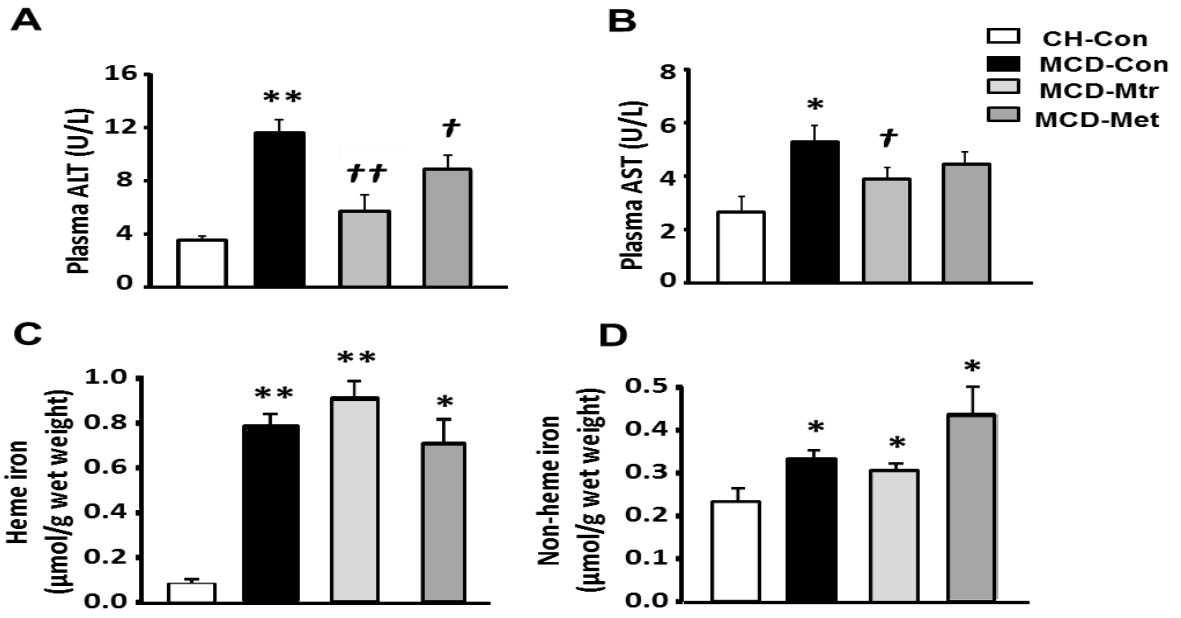

Fig. 6. Effects of Mtr on liver damage and iron level. After six weeks of feeding and drug treatment, blood sample was collected for the measurement of plasma levels of (**A**) ALT and (**B**) AST. Liver tissue was collected for the measurement of(**C**) heme and (**D**) non-heme iron. *$p < 0.05$, **$p < 0.05$ vs. CH-Con; †$p < 0.01$, ††$p < 0.01$ vs. MCD-Con (n = 7-8 mice/group).

3.6. Effects on hepatic mTOR and HSPs expression

Elevated protein expression of mTOR has been observed in NASH patients [27]. It has been reported that activation mTOR enhance hepatic inflammatory and fibrotic pathways, mTOR inhibitors decrease these pathways in HepG2 cells and rodents [27, 28]. Inhibition of mTOR has been shown to alleviate liver damage and fibrosis in a mouse model of NASH induced by MCD diet [29]. To explore whether the effect of Mtr on NASH involved the inhibition of mTOR pathway, the hepatic protein level of mTOR was assessed. Consistent with the observation in human NASH patient, MCD-Con mice had increased protein level of mTOR in the liver. Interestingly, treatment with Mtr normalized the protein level of mTOR ($p < 0.01$ vs. MCD-Con) towards the levels seen in CH-Con mice (**Fig. 7 A**). Our results suggested that Mtr treatment inhibited MCD diet-induced hepatic mTOR expression. In comparison, metformin had no effect on the hepatic mTOR level in MCD diet-fed mice.

Previous work from our laboratory has showed that the antisteatotic effects of Mtr involve the activation of HSP72 in the liver of HFD-fed mice [7]. The dissociation of HSP90 from HSF1 triggers the trimerization and activation of HSF1, which in turn initiates the expression of HSP72 [30]. To determine whether Mtr-induced improvement on NASH was associated with the upregulation of HSP72, we measured the HSP90, HSF1 and HSP72 protein expression in the liver. As shown in **Fig. 7 B-D**, HSP90 and HSP72 expression were blunted (50% reduction compared to CH-Con mice, $p < 0.05$) by MCD diet feeding, but had no significant change on the protein level of HSF1. In addition to the upregulation of hepatic HSP72 and

unchanged level of HSP90, which is consistent with our previous report [7], Mtr treatment significantly increased the hepatic HSF1 level. In comparison, metformin treatment had no effect on the expression of HSP72 and HSP90, despite of the normalization of HSF1 level. These results indicate that the therapeutic effect of Mtr on NASH is associated with inhibition of mTOR and upregulation of HSPs and, in particular, HSP72.

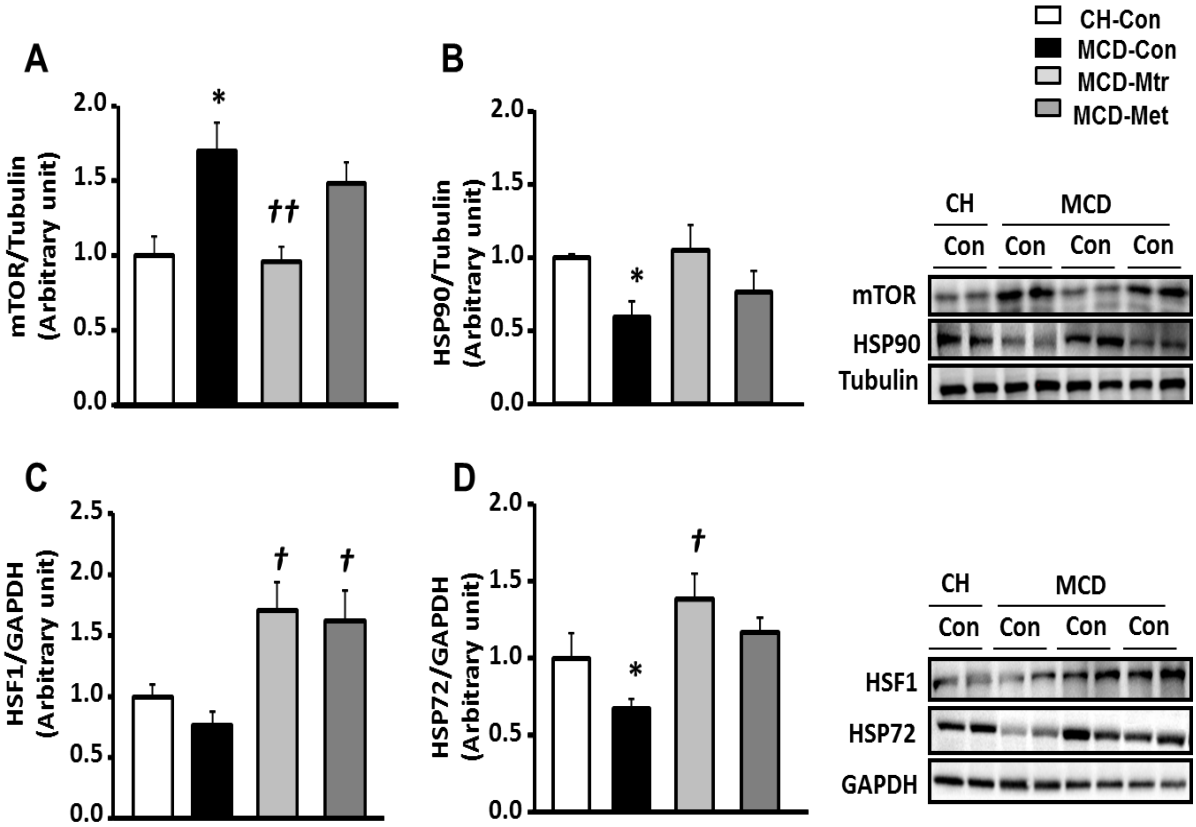

Fig. 7. Effects of Mtr on HSF1, HSP90, HSP72 and mTOR in MCD diet-fed mice. Liver lysates from mice were immunoblotted for (**A**) mTOR (**B**) HSP90, (**C**) HSF1 and (**D**) HSP72 and quantified for statistical analysis. *$p < 0.05$ vs. CH-Con; †$p < 0.01$, ††$p < 0.01$ vs. MCD -Con (n = 7-8 mice/group).

4. Discussion

Our previous studies, which focused on the metabolic effect of Mtr, have demonstrate that Mtr treatment was effective in reducing hepatosteatosis, adiposity and glucose intolerance in various diet-induced mouse models [7]. Current study further investigates the effect of Mtr on NASH, a hepatic manifestation of the metabolic syndrome [1]. This study demonstrated that Mtr markedly ameliorated hepatic damage, inflammation and fibrosis, with inhibition of mTOR and upregulation of HSP72, in a mouse model of NASH induced by MCD diet feeding. In comparison, metformin had no effect on inflammation, collagen deposition, HSP72 or mTOR.

While high-fat or high-fructose feeding results in several prominent features of metabolic syndrome (including obesity, hepatosteatosis, glucose intolerance etc.), they do not induce apparent and severe hepatic damage or fibrosis in the liver [31]. In contrast, MCD diet feeding is a well-recognized model of NASH that rapidly induces hepatic steatosis, damage, inflammation and fibrosis in mice, despite of the absence of insulin resistance and hyperglycemia [17, 18, 31]. Therefore, we evaluated the protective effects of Mtr on NASH in mice fed a MCD diet.

Consistent with previous studies, mice fed a MCD diet developed hepatic inflammation and fibrosis that reflected the natural course of NASH in human [18, 19, 32]. Mtr prevented MCD diet-induced inflammation and fibrosis in the liver after 6 weeks of treatment, as demonstrated by a Mtr-induced suppression of the increases in TNFα, CD68, MCP-1 and NLRP3, and hepatic fibrosis markers (TGFβ, Smad3 and collagen1) induced by MCD diet.

Several studies indicated that activation of inflammatory cytokines has a vital role in the progression of NASH [1, 22].The increase of pro-inflammatory cytokines production via the activation of Kupffer cells, in particular TNFα, was suggested to be the key mediator of

NASH progression [33]. Alternatively, inhibition of TNFα activity using anti-inflammatory drugs improved liver damage, inflammation and NASH [34, 35]. Furthermore, in line with increased TNFα production, the increased presence of CD68 and MCP-1 are associated with the severity of NASH [1, 9]. The results of the current study proved that Mtr significantly reduced these inflammatory targets-induced by MCD diet feeding. Another central participator in the development of NASH is the activation of the NLRP3 inflammasome [20, 36]. It has been recently reported that blockage NLRP3 activation reduced liver inflammation and fibrosis in MCD diet-fed mice [2]. It generally believes that the anti-inflammatory activities of Mtr are largely due to its ability to scavenge airway inflammation and hepatic inflammation [6]. The result of Mtr-induced attenuation of hepatic inflammation, through inhibiting the activity of TNFα and suppressing several inflammatory proteins and chemokines (including CD68, MCP-1 and NLRP3) in the MCD diet-fed mice, supported the notion that Mtr is likely to reduce NASH via inhibition of the inflammation pathway.

Consistent with elevated levels of pro-inflammation cytokines and exacerbated fibrosis, MCD-diet feeding resulted in hepatic fibrosis, is also known as another hallmark of NASH [1, 18], and it is considered as a result of repetitive inflammation events [22]. In NASH, fibrosis closely correlates with the degree of inflammation and severity of the disease [21, 22]. While Mtr prevents liver fibrosis (TGFβ and collagen production) induced by carbon tetrachloride (CCl_4) in rats [37], whether Mtr inhibit fibrosis in a NASH model without the involvement of chemical toxicity remains unclear. To investigate whether the inhibition of hepatic inflammation by Mtr involves the inhibition of fibrosis signaling and collagen production [20, 38]; we examined the effect of Mtr on fibrosis in a mouse NASH model induced by MCD diet. Consistent with the reduction in inflammation, our data indicated that Mtr inhibited the activation of fibrosis by suppression of TGFβ, Smad3 and collagen 1

synthesis in the liver of MCD diet-fed mice. The effect of Mtr in alleviating fibrosis was further support by the histological data revealing a significant reduction in the number of collagen proportionate area in MCD diet-fed mice after Mtr treatment.

Consistent with elevated levels of pro-inflammation cytokines and exacerbated fibrosis, MCD-diet feeding resulted in severe liver damage as indicated by the elevated plasma level of liver enzymes, particularly ALT, which has been considered as a requisite in the diagnosis of NASH [1, 39]. Treatment with Mtr significantly decreased the elevated plasma levels of ALT and AST, indicating a less extent of liver damage, which is in line with the effect of Mtr on hepatic inflammation and fibrosis.

After demonstrating the effect of Mtr in improving inflammation, fibrosis and liver damage in MCD diet-induced NASH, we next investigated the possible molecular mechanism involved. Our previous work suggested that upregulation of HSP72 may contribute to hepatosteatosis induced by HFD or HFru feeding in mice [7]. Another study from our lab showed that Mtr could reduce glucose intolerance in mice caused by an increase in *de novo* lipogenesis (DNL) in HFru diet-fed mice (accepted data). Consistent with this observation, the present study found that liver tissue mice fed with MCD diet had significantly lower concentrations of HSP72 and HSP90 protein, and this reduction was rescued by Mtr treatment. Heat shock protein 72 (HSP72) is the major inducible heat shock protein, exerts cytoprotective effects by assisting in protein folding, protein degradation, signal transduction and translocation of client proteins across membranes [40]. It is been suggested that HSP72 expression is progressively suppressed in the liver and muscle of obese and NAFLD patients [41], and in skeletal muscle of T2D patients [42]. An elevation in HSP72 is associated with the reduction in JNK phosphorylation and attenuation of insulin resistance [43]. These results

suggest the anti-inflammatory effects of Mtr, at least in part, involving the activation of HSP72 in the liver.

It is worthwhile noting that Mtr also inhibited MCD-induced increase in mTOR. This is interesting because overexpression of mTOR contributes to NAFLD progression [27]. It has been suggested to play an important role in the development of NASH by activating inflammation and fibrosis in mice fed with choline-deficient diet-induced steatohepatitis [29]. In comparison, metformin showed no effect on MCD-induced increase in mTOR or NASH phenotype. These data suggest that the suppressed mTOR by Mtr may also contribute to its therapeutic effects for NASH. However, studies are required to determine the molecular mechanism involved and how the HSP pathway may interact with the mTOR pathway to medicate the therapeutic effects of Mtr for NASH.

In conclusion, the present study suggests that Mtr, a hepatoprotective drug, might offer protective effects against NASH via suppression of hepatic inflammation, fibrosis and damage, possibly via the upregulation of HSP72 and the reduction of mTOR (**Fig. 8**). Future work involving the use of HSP72 and/or mTOR liver-specific knock-out model is required to further confirm the exact molecular regulator of the effect of Mtr.

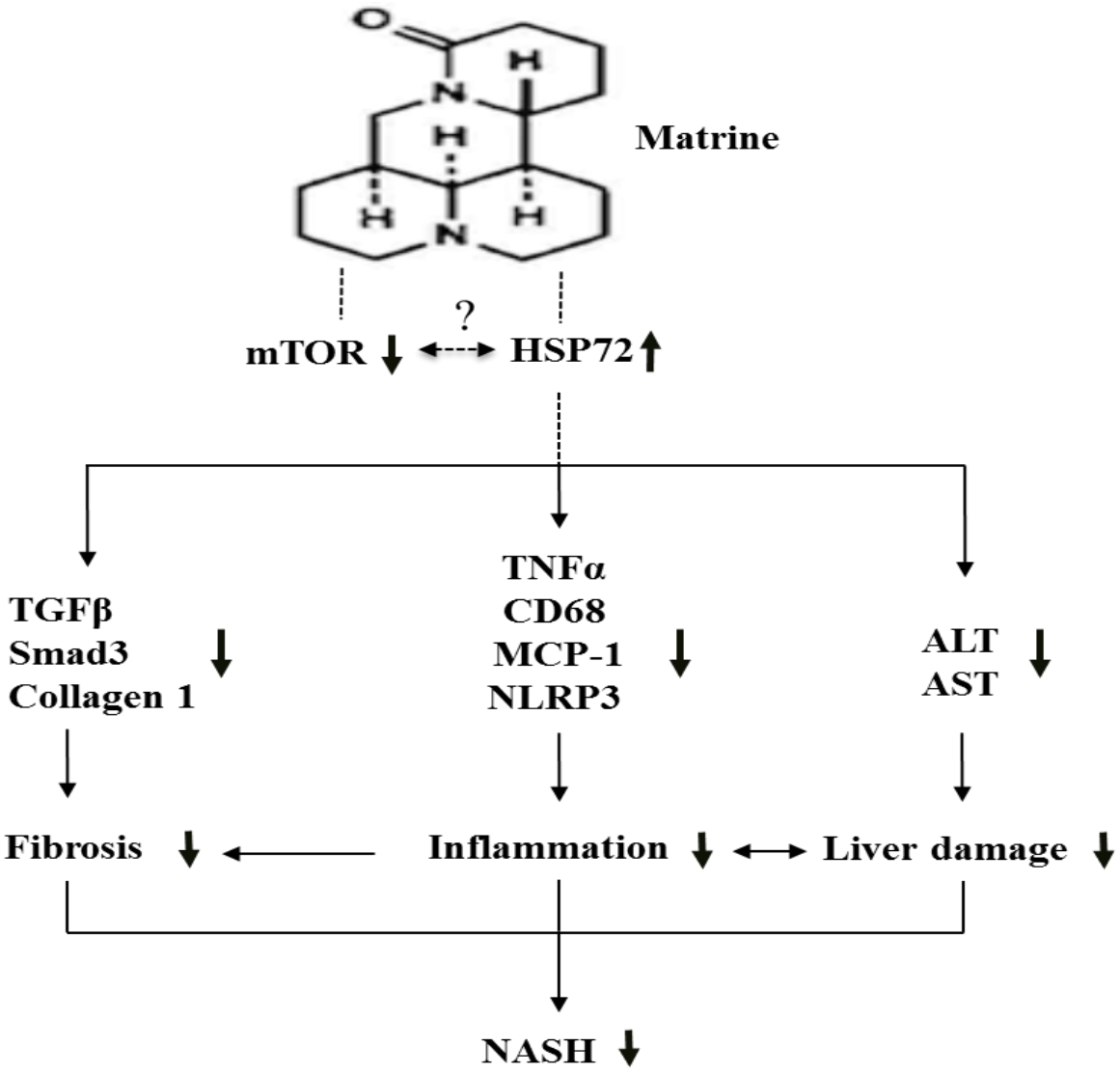

Fig. 8. A Schematic diagram illustrating the proposed mechanism underlying the effects of Mtr against MCD diet-induced NASH

ACKNOWLEDGEMENTS

The authors would like to acknowledge the assistance from Dr Stanley MH Chan and Dr Wala Alzahrani for this study. This work was supported by the National Health and Medical Research Council of Australia (Project Grant 535930 to JMY), Bureau for Foreign Experts Grant of China (SYSUPCS2014 to JMY) and Education Department of Guangdong (2017KSYS010). AM was supported by Al-Baha University and Ministry of Higher Education of Saudi Arabia and MA was a recipient of the scholarship of the Taif University of Saudi Arabia.

AUTHOR CONTRIBUTIONS

JMY and DL conceived the study. JMY, XYZ and XZ designed the experiments. AM, SL, XYZ, MA, XZ performed the experiments. SRR supervised the heme assay and histological studies, SF contributed to the histologic studies. AM and XYZ prepared the manuscript. JMY and SRR revised the manuscript.

CONFLICT OF INTEREST STATEMENT

The authors declare that there is no any conflict of interest to disclose for this study.

References

[1] A.M. Diehl, C. Day, Cause, Pathogenesis, and Treatment of Nonalcoholic Steatohepatitis, N Engl J Med 377(21) (2017) 2063-2072.

[2] A.R. Mridha, A. Wree, A.A.B. Robertson, M.M. Yeh, C.D. Johnson, D.M. Van Rooyen, F. Haczeyni, N.C. Teoh, C. Savard, G.N. Ioannou, S.L. Masters, K. Schroder, M.A. Cooper, A.E. Feldstein, G.C. Farrell, NLRP3 inflammasome blockade reduces liver inflammation and fibrosis in experimental NASH in mice, J Hepatol 66(5) (2017) 1037-1046.

[3] H. Cheng, B. Xia, L. Zhang, F. Zhou, Y.X. Zhang, M. Ye, Z.G. Hu, J. Li, J. Li, Z.L. Wang, C. Li, Q.S. Guo, Matrine improves 2,4,6-trinitrobenzene sulfonic acid-induced colitis in mice, Pharmacological research 53(3) (2006) 202-8.

[4] J. Liu, M. Zhu, R. Shi, M. Yang, Radix Sophorae flavescentis for chronic hepatitis B: a systematic review of randomized trials, Am J Chin Med 31(3) (2003) 337-54.

[5] S.K. Satapathy, S. Garg, R. Chauhan, P. Sakhuja, V. Malhotra, B.C. Sharma, S.K. Sarin, Beneficial effects of tumor necrosis factor-alpha inhibition by pentoxifylline on clinical, biochemical, and metabolic parameters of patients with nonalcoholic steatohepatitis, Am J Gastroenterol 99(10) (2004) 1946-52.

[6] X.H. Zhu, Y.D. Qiu, H. Shen, M.K. Shi, Y.T. Ding, Effect of matrine on Kupffer cell activation in cold ischemia reperfusion injury of rat liver, World J Gastroenterol 8(6) (2002) 1112-6.

[7] X.Y. Zeng, H. Wang, F. Bai, X. Zhou, S.P. Li, L.P. Ren, R.Q. Sun, C.C. Xue, H.L. Jiang, L.H. Hu, J.M. Ye, Identification of matrine as a promising novel drug for hepatic steatosis and glucose intolerance with HSP72 as an upstream target, British journal of pharmacology 172(17) (2015) 4303-18.

[8] L.P. Ren, S.M. Chan, X.Y. Zeng, D.R. Laybutt, T.J. Iseli, R.Q. Sun, E.W. Kraegen, G.J. Cooney, N. Turner, J.M. Ye, Differing endoplasmic reticulum stress response to excess lipogenesis versus lipid oversupply in relation to hepatic steatosis and insulin resistance, PloS one 7(2) (2012) e30816.

[9] S. Li, X.Y. Zeng, X. Zhou, H. Wang, E. Jo, S.R. Robinson, A. Xu, J.M. Ye, Dietary cholesterol induces hepatic inflammation and blunts mitochondrial function in the liver of high-fat-fed mice, J Nutr Biochem 27 (2016) 96-103.

[10] T.N. Dang, G.M. Bishop, R. Dringen, S.R. Robinson, The metabolism and toxicity of hemin in astrocytes, Glia 59(10) (2011) 1540-50.

[11] D.K. George, S. Goldwurm, G.A. MacDonald, L.L. Cowley, N.I. Walker, P.J. Ward, E.C. Jazwinska, L.W. Powell, Increased hepatic iron concentration in nonalcoholic steatohepatitis is associated with increased fibrosis, Gastroenterology 114(2) (1998) 311-8.

[12] K. Murotomi, S. Arai, S. Uchida, S. Endo, H. Mitsuzumi, Y. Tabei, Y. Yoshida, Y. Nakajima, Involvement of splenic iron accumulation in the development of nonalcoholic steatohepatitis in Tsumura Suzuki Obese Diabetes mice, Sci Rep 6 (2016) 22476.

[13] J. Riemer, H.H. Hoepken, H. Czerwinska, S.R. Robinson, R. Dringen, Colorimetric ferrozine-based assay for the quantitation of iron in cultured cells, Anal Biochem 331(2) (2004) 370-5.

[14] X.Y. Zeng, Y.P. Wang, J. Cantley, T.J. Iseli, J.C. Molero, B.D. Hegarty, E.W. Kraegen, Y. Ye, J.M. Ye, Oleanolic acid reduces hyperglycemia beyond treatment period with Akt/FoxO1-induced suppression of hepatic gluconeogenesis in type-2 diabetic mice, PloS one 7(7) (2012) e42115.

[15] S.M. Chan, R.Q. Sun, X.Y. Zeng, Z.H. Choong, H. Wang, M.J. Watt, J.M. Ye, Activation of PPARalpha ameliorates hepatic insulin resistance and steatosis in high fructose-fed mice despite increased endoplasmic reticulum stress, Diabetes 62(6) (2013) 2095-105.

[16] R.P. Witek, W.C. Stone, F.G. Karaca, W.K. Syn, T.A. Pereira, K.M. Agboola, A. Omenetti, Y. Jung, V. Teaberry, S.S. Choi, C.D. Guy, J. Pollard, P. Charlton, A.M. Diehl, Pan-caspase inhibitor VX-166 reduces fibrosis in an animal model of nonalcoholic steatohepatitis, Hepatology (Baltimore, Md.) 50(5) (2009) 1421-30.

[17] L. Hebbard, J. George, Animal models of nonalcoholic fatty liver disease, Nat Rev Gastroenterol Hepatol 8(1) (2011) 35-44.

[18] M.E. Rinella, R.M. Green, The methionine-choline deficient dietary model of steatohepatitis does not exhibit insulin resistance, J Hepatol 40(1) (2004) 47-51.

[19] M.V. Machado, G.A. Michelotti, G. Xie, T. Almeida Pereira, J. Boursier, B. Bohnic, C.D. Guy, A.M. Diehl, Mouse models of diet-induced nonalcoholic steatohepatitis reproduce the heterogeneity of the human disease, PloS one 10(5) (2015) e0127991.

[20] A. Wree, A. Eguchi, M.D. McGeough, C.A. Pena, C.D. Johnson, A. Canbay, H.M. Hoffman, A.E. Feldstein, NLRP3 inflammasome activation results in hepatocyte pyroptosis, liver inflammation, and fibrosis in mice, Hepatology (Baltimore, Md.) 59(3) (2014) 898-910.

[21] T. Tsuchida, S.L. Friedman, Mechanisms of hepatic stellate cell activation, Nat Rev Gastroenterol Hepatol 14(7) (2017) 397-411.

[22] D. Schuppan, R. Surabattula, X.Y. Wang, Determinants of fibrosis progression and regression in NASH, J Hepatol 68(2) (2018) 238-250.

[23] D.T. Reid, J.L. Reyes, B.A. McDonald, T. Vo, R.A. Reimer, B. Eksteen, Kupffer Cells Undergo Fundamental Changes during the Development of Experimental NASH and Are Critical in Initiating Liver Damage and Inflammation, PloS one 11(7) (2016) e0159524.

[24] S. Fargion, M. Mattioli, A.L. Fracanzani, M. Sampietro, D. Tavazzi, P. Fociani, E. Taioli, L. Valenti, G. Fiorelli, Hyperferritinemia, iron overload, and multiple metabolic alterations identify patients at risk for nonalcoholic steatohepatitis, Am J Gastroenterol 96(8) (2001) 2448-55.

[25] M. Atarashi, T. Izawa, R. Miyagi, S. Ohji, A. Hashimoto, M. Kuwamura, J. Yamate, Dietary Iron Supplementation Alters Hepatic Inflammation in a Rat Model of Nonalcoholic Steatohepatitis, Nutrients 10(2) (2018).

[26] P. Handa, V. Morgan-Stevenson, B.D. Maliken, J.E. Nelson, S. Washington, M. Westerman, M.M. Yeh, K.V. Kowdley, Iron overload results in hepatic oxidative stress, immune cell activation, and hepatocellular ballooning injury, leading to nonalcoholic steatohepatitis in genetically obese mice, Am J Physiol Gastrointest Liver Physiol 310(2) (2016) G117-27.

[27] C. Wang, L. Hu, L. Zhao, P. Yang, J.F. Moorhead, Z. Varghese, Y. Chen, X.Z. Ruan, Inflammatory stress increases hepatic CD36 translational efficiency via activation of the mTOR signalling pathway, PloS one 9(7) (2014) e103071.

[28] E. Patsenker, V. Schneider, M. Ledermann, H. Saegesser, C. Dorn, C. Hellerbrand, F. Stickel, Potent antifibrotic activity of mTOR inhibitors sirolimus and everolimus but not of cyclosporine A and tacrolimus in experimental liver fibrosis, J Hepatol 55(2) (2011) 388-98.

[29] Q. Gong, Z. Hu, F. Zhang, A. Cui, X. Chen, H. Jiang, J. Gao, X. Chen, Y. Han, Q. Liang, D. Ye, L. Shi, Y.E. Chin, Y. Wang, H. Xiao, F. Guo, Y. Liu, M. Zang, A. Xu, Y. Li, Fibroblast growth factor 21 improves

hepatic insulin sensitivity by inhibiting mammalian target of rapamycin complex 1 in mice, Hepatology (Baltimore, Md.) 64(2) (2016) 425-38.

[30] J. Anckar, L. Sistonen, Regulation of HSF1 function in the heat stress response: implications in aging and disease, Annu Rev Biochem 80 (2011) 1089-115.

[31] P.K. Santhekadur, D.P. Kumar, A.J. Sanyal, Preclinical models of non-alcoholic fatty liver disease, J Hepatol 68(2) (2018) 230-237.

[32] M.E. Rinella, M.S. Elias, R.R. Smolak, T. Fu, J. Borensztajn, R.M. Green, Mechanisms of hepatic steatosis in mice fed a lipogenic methionine choline-deficient diet, J Lipid Res 49(5) (2008) 1068-76.

[33] A.C. Tosello-Trampont, S.G. Landes, V. Nguyen, T.I. Novobrantseva, Y.S. Hahn, Kuppfer cells trigger nonalcoholic steatohepatitis development in diet-induced mouse model through tumor necrosis factor-alpha production, J Biol Chem 287(48) (2012) 40161-72.

[34] Z. Li, S. Yang, H. Lin, J. Huang, P.A. Watkins, A.B. Moser, C. Desimone, X.Y. Song, A.M. Diehl, Probiotics and antibodies to TNF inhibit inflammatory activity and improve nonalcoholic fatty liver disease, Hepatology (Baltimore, Md.) 37(2) (2003) 343-50.

[35] S.W. Koppe, A. Sahai, P. Malladi, P.F. Whitington, R.M. Green, Pentoxifylline attenuates steatohepatitis induced by the methionine choline deficient diet, J Hepatol 41(4) (2004) 592-8.

[36] J. Henao-Mejia, E. Elinav, C. Jin, L. Hao, W.Z. Mehal, T. Strowig, C.A. Thaiss, A.L. Kau, S.C. Eisenbarth, M.J. Jurczak, J.P. Camporez, G.I. Shulman, J.I. Gordon, H.M. Hoffman, R.A. Flavell, Inflammasome-mediated dysbiosis regulates progression of NAFLD and obesity, Nature 482(7384) (2012) 179-85.

[37] J.P. Zhang, M. Zhang, J.P. Zhou, F.T. Liu, B. Zhou, W.F. Xie, C. Guo, Antifibrotic effects of matrine on in vitro and in vivo models of liver fibrosis in rats, Acta pharmacologica Sinica 22(2) (2001) 183-6.

[38] H. Itagaki, K. Shimizu, S. Morikawa, K. Ogawa, T. Ezaki, Morphological and functional characterization of non-alcoholic fatty liver disease induced by a methionine-choline-deficient diet in C57BL/6 mice, Int J Clin Exp Pathol 6(12) (2013) 2683-96.

[39] D.M. Torres, S.A. Harrison, NAFLD: Predictive value of ALT levels for NASH and advanced fibrosis, Nat Rev Gastroenterol Hepatol 10(9) (2013) 510-1.

[40] F.U. Hartl, A. Bracher, M. Hayer-Hartl, Molecular chaperones in protein folding and proteostasis, Nature 475(7356) (2011) 324-32.

[41] F.C. Di Naso, R.R. Porto, H.S. Fillmann, L. Maggioni, A.V. Padoin, R.J. Ramos, C.C. Mottin, A. Bittencourt, N.A. Marroni, P.I. de Bittencourt, Jr., Obesity depresses the anti-inflammatory HSP70 pathway, contributing to NAFLD progression, Obesity (Silver Spring, Md.) 23(1) (2015) 120-9.

[42] I. Kurucz, A. Morva, A. Vaag, K.F. Eriksson, X. Huang, L. Groop, L. Koranyi, Decreased expression of heat shock protein 72 in skeletal muscle of patients with type 2 diabetes correlates with insulin resistance, Diabetes 51(4) (2002) 1102-9.

[43] J. Chung, A.K. Nguyen, D.C. Henstridge, A.G. Holmes, M.H. Chan, J.L. Mesa, G.I. Lancaster, R.J. Southgate, C.R. Bruce, S.J. Duffy, I. Horvath, R. Mestril, M.J. Watt, P.L. Hooper, B.A. Kingwell, L. Vigh, A. Hevener, M.A. Febbraio, HSP72 protects against obesity-induced insulin resistance, Proc Natl Acad Sci U S A 105(5) (2008) 1739-44.